CHARACTERIZING THE ROLE OF OXYGEN IN BEEF DISCOLORATION

By

MORGAN DENZER

Bachelor of Science in Food Science
Iowa State University
Ames, Iowa
2018

Master of Science in Food Science
Oklahoma State University
Stillwater, Oklahoma
2020

Submitted to the Faculty of the
Graduate College of the
Oklahoma State University
in partial fulfillment of
the requirements for
the Degree of
DOCTOR OF PHILOSOPHY
May 2023

CHARACTERIZING THE ROLE OF OXYGEN IN BEEF DISCOLORATION

Dissertation Approved:

Dr. Ranjith Ramanathan

Dissertation Adviser

Dr. Gretchen Mafi

Dr. Morgan Pfeiffer

Dr. Daching Piao

ACKNOWLEDGEMENTS

During my time at Oklahoma State University, there has been many influential people who helped me on my journey. First, I would like to thank my advisor, Dr. Ramanathan, for taking me in as a graduate student. Dr. Ramanathan. Thank you for allowing me to continue my time here at OSU and encouraging me to expand my knowledge. Your guidance has pushed me to new levels and helped me to explore outside of my comfort zone. Furthermore, you have helped my growth personally and professionally beyond anything I could imagine. You continued to challenge me to expand my research knowledge but also attempt new experiences. You have helped me grow so much as a person. Thank you for always being in a good mood and keeping me grounded. Dr. Mafi, your guidance has been unparalleled during my time at OSU. Your knowledge and experience has been invaluable. I am unbelievable grateful to have been able to work with you. Thank you Dr. Piao for challenging my knowledge of myoglobin and understanding of color analysis. I am grateful for you always being willing to collaborate, share ideas, and explain concepts. Dr. Pfeiffer, it has been amazing to have you as a mentor during my master's and now a committee member during my PhD. You have provided unparalleled support in the endeavors of graduate school. I am so grateful to have you back at OSU! Thank you for being an amazing mentor, and I know you will continue to be a great asset to the meat science program.

My fellow graduate students! Wow, it has been an amazing experience being at

OSU with you. I would not have been able to do this without all of you. Each and every one of you has provided me guidance and support throughout my time here. Thank you for all your willingness to help no matter the situation or project. We have pushed each other and pushed the research we thought we could do. I know we have had some very long days, but I have truly appreciated getting to know and guide many of you during your time here. I could not imagine this experience without all of you, and I am grateful to have shared this experience with you. To the undergraduate student workers and researchers, I thank you so much for trusting me to mentor you and guide you during your time at OSU. It has been an amazing time getting to know all of you and help you in your future endeavors. Thank you for being there for all the projects with excitement and passion for our research.

Jake, you moved on early in my PhD, but I am so grateful for the time you were here and the knowledge you passed on. Aaron, it has been amazing to get to know you! You have been such an amazing problem solver and always willing to help. To the FAPC group, thank you for everything you do and always willing to help and clean up. To Mellissa, Cindy, Kathy, Kristy, and Glynna, thank you for always answering my questions, guiding me, and providing candy/snacks when needed.

To my family, you are the biggest support system, and I thank you for everything you have done for me and will continue to do. To my parents, Pam and Steve, thank you for always being a phone call away to listen to me and provide guidance. Thank you for the countless adventures here in Oklahoma and the heat. I am so grateful for all the time you have taken to support me here. To my brother, thank you for your time and support. You have been an amazing example of perseverance and fighting for what you want in

life. To my friends, thank you for being encouraging on my journey here at OSU. Thank you for always answering my phone calls, texts, or emails. I appreciate all of you! Kate, thank you for your unwavering guidance during my time in graduate school. You have always been willing to chat, answer questions, and edit my CV. Thank you!

Finally, a huge thank you to everyone at Oklahoma State University and the Animal and Food Science Department. There are so many faculty and staff that have been a helping hand or a smiling face. I greatly appreciate each one of you. For anyone that has helped me along the way, thank you!

Name: MORGAN DENZER

Date of Degree: MAY 2023

Title of Study: CHARACTERIZING THE ROLE OF OXYGEN IN BEEF DISCOLORATION

Major Field: FOOD SCIENCE

Abstract: The objective of this research was to characterize the role of oxygen in beef discoloration. Limited studies have evaluated the discoloration of the interior of steaks during retail display in association with the development of metmyoglobin. A recent approach in our laboratory has characterized interior color changes by means of needle-probe based single-fiber reflectance (SfR) spectroscopy. The *a** values of steaks decreased ($P < 0.05$) with display time. Metmyoglobin at all depths from 1 mm to 5 mm estimated by the needle-probe SfR increased during display while showing greater metmyoglobin at a depth of 1-mm compared to the depths of 2 – 5 mm. Metmyoglobin estimated at 1 mm depth by the needle-probe SfR and the retail surface by HunterLab spectrophotometer were strongly negatively ($P < 0.05$) correlated with *a** values during retail display. Therefore, internal metmyoglobin formation negatively influences surface color. Furthermore, the display surface was considered as oxygen exposed (OE), while the interior of the steak was denoted as not exposed to oxygen (NOE). NOE steak surface had greater ($P < 0.05$) metmyoglobin reducing ability compared with OE surfaces on d 6 of display. Oxygen exposure affected the oxygen consumption of the steaks, with the OE surfaces having lower ($P < 0.05$) oxygen consumptioncompared to NOE surfaces on d 6 of display. The loss of succinate from d 0 to d 6 of retail display reinforced the decline in color during display. Greater alpha-tocopherol in the NOE surface supported less oxidative changes compared to the OE surface during retail display. These results indicate the presence of oxygen can influence metabolite profile and negatively influence metmyoglobin reducing ability and color. In conclusion, the presence of oxygen can negatively impact the shelf life of steaks; however, the non-exposed interior of muscle remains more biochemically active.

TABLE OF CONTENTS

Chapter Page

Chapter Page

LIST OF TABLES

Table Page

Table Page

Table Page

Table Page

LIST OF FIGURES

Figure Page

Figure Page

CHAPTER I

INTRODUCTION

Oxidative stress is the greater influx of prooxidants, such as reactive oxygen species, in comparison to antioxidants in the body (Cecarini et al., 2007). Reactive oxygen species include compounds such as the superoxide anion, hydroxyl radical, and hydrogen peroxide, which have been reported to increase the oxidation of proteins and lipids (Cui, Kong, & Zhang, 2012; Sastre, Pallardó, & Viña, 2003). In humans, oxidative stress research has increased with time (Giustarini, Dalle-Donne, Tsikas, & Rossi, 2009). Oxidative stress has been linked to Wilson's disease and speculated to play a role in aging in humans (Giustarini et al., 2009). Oxidative stress in cattle can occur for a multitude of reasons leading to a negative impact on animal health (Celi, 2011; Celi & Gabai, 2015). In the body, the mitochondria have been linked to the production of reactive oxygen species by means of aerobic respiration (Cui et al., 2012; Sastre et al., 2003). While research on oxidative stress has focused primarily on human health (Lenaz, 1998; Sastre et al., 2003), the presence of active mitochondria postmortem indicates oxidative stress could play a significant role in oxidative changes in muscle postmortem.

In skeletal muscle, oxidative changes and mitochondrial respiration are the main sources of free radicals (Bekhit, Hopkins, Fahri, & Ponnampalam, 2013; Ramanathan,

Suman, & Faustman, 2020a). Upon slaughter, there is a loss of homeostasis and a decrease in antioxidant mechanisms (Ke et al., 2017; Ramanathan et al., 2020a). As a result, postmortem mitochondria begin to degenerate, leading to less mitochondrial content and decreased mitochondrial activity (Ke et al., 2017; Mancini & Ramanathan, 2014; Mitacek et al., 2019). From the degradation of the mitochondria, more reactive oxygen species form postmortem with greater time (Ke et al., 2017; Ramanathan et al., 2020a). Hence, an accumulation of reactive oxygen species can occur in muscle postmortem resulting in oxidative changes, which can be detrimental to meat quality (Ke et al., 2017; Ramanathan et al., 2020a). Therefore, the postmortem mechanisms in response to oxidative stress can influence meat quality characteristics, specifically meat color.

Meat color has a large influence on consumer purchasing decisions due to consumers' perceptions of specific colors (Holman, van de Ven, Mao, Coombs, & Hopkins, 2017). Consumers view bright-cherry red oxymyoglobin as wholesome and fresh, while brown discoloration is negatively perceived by consumers (Carpenter, Cornforth, & Whittier, 2001). Discoloration begins below the surface through the oxidation of the pigment forming protein myoglobin (Limsupavanich et al., 2004, 2008). Brown metmyoglobin forms below the surface oxymyoglobin due to low oxygen partial pressure in steaks (Limsupavanich et al., 2004, 2008). Research measuring the subsurface metmyoglobin and interior deoxymyoglobin has been limited, and popular spectrophotometers only measure surface myoglobin. However, the penetration of oxygen and the development of subsequent layers has been correlated with color stability (Limsupavanich et al., 2004, 2008; O'Keeffe & Hood, 1982). Metmyoglobin reducing

ability and oxygen consumption are two parameters to demonstrate color stability in retail. Research on the influence of subsurface metmyoglobin due to oxygen exposure on metmyoglobin reducing ability and oxygen consumptionis limited. Therefore, a better understanding of the layer development during retail and the impact of oxygen on the attributes related to color stability is important to evaluate metmyoglobin.

The muscle type influences the color stability in retail display, with oxidative muscles categorized as color labile and glycolytic muscles considered color stable (McKenna et al., 2005; O'Keeffe & Hood, 1982). The difference in primary metabolism impacts the metabolome and proteome, which can directly impact color stability (Abraham, Dillwith, Mafi, VanOverbeke, & Ramanathan, 2017; Joseph, Suman, Rentfrow, Li, & Beach, 2012). In addition, oxygen penetration is influenced by the muscle type, with the *psoas major* having smaller penetration compared to the *longissimus* muscle (Limsupavanich et al., 2004, 2008; O'Keeffe & Hood, 1982). The impact of the muscle metabolome on the differences in oxygen penetration is unclear. Research has speculated the difference may be due to differences in mitochondrial oxygen consumptionbased on muscle type (Ke et al., 2017). In addition, the *psoas major* muscle has been reported to have greater number of radical oxygen species and increased oxidative stress than the *longissimus* (Yu, Tian, Shao, Li, & Dai, 2020), which may impact the response to oxygen penetration and subsequently influence color stability. However, the connection between oxygen penetration and subsequent differences in metabolism is not clear. Therefore, the role of oxygen in oxidative stress in different muscles is important to understand in relation to color stability.

CHAPTER II

REVIEW OF LITERATURE

Protein oxidation

Protein oxidation has been connected to decreased tenderness through structural changes (Lund, Heinonen, Baron, & Estévez, 2011). Crosslinking of myosin and titin has been reported during storage of beef steaks (Kim, Huff-Lonergan, Sebranek, & Lonergan, 2010). The HiOx-MAP has increased protein oxidation and subsequent crosslinking of myosin (Bao & Ertbjerg, 2015; Bao, Puolanne, & Ertbjerg, 2016; Kim et al., 2010; Moczkowska, Poltorak, Montowska, Pospiech, & Wierzbicka, 2017). Therefore, crosslinking has been influenced by oxygen conditions and is a product of protein oxidation. Crosslinking from protein oxidation can negatively impact tenderness. In support, research has reported increased toughness in beef (Kim et al., 2010; Lagerstedt, Lundstrom, & Lindahl, 2011) and pork (Bao & Ertbjerg, 2015; Lund, Lametsch, Hviid, Jensen, & Skibsted, 2007) stored in an oxidative environment such as high-oxygen modified atmospheric packaging (HiOx-MAP). Furthermore, water holding capacity has been negatively influenced by protein oxidation which can impact palatability (Lund et al., 2007). Greater protein oxidation has been reported to increase shear force values and results in less degradation of key structural proteins such as troponin T and desmin (Rowe, Maddock, Lonergan, & Huff-Lonergan, 2004). Postmortem proteolysis occurs

through calpains which require calcium and reducing environments to be activated (Guttmann & Johnson, 1998; Rowe et al., 2004). μ-Calpain activity decreased in the presence of protein oxidation, whereas calpastatin activity increased or was unaffected (Guttmann & Johnson, 1998; Rowe et al., 2004). Hence, oxidative conditions lead to less proteolysis and increased inhibition of μ-Calpain increasing shear force. However, the oxidation of proteins occurs through reactive oxygen species formation of free radicals and propagation similarly to lipid oxidation (Lund et al., 2011). During postmortem aging, reactive oxygen species increased, and apoptosis factors in mitochondria and muscle increased (Chen et al., 2020). The associated oxidative stress and subsequent apoptosis result in increased tenderness of beef (Chen et al., 2020). Therefore, the oxidation of proteins negatively influences the proteolysis and structure of meat, but reactive oxygen species and subsequent oxidative stress can positively influence tenderness.

Myoglobin oxidation

Myoglobin is the primary protein responsible for meat color due to the presence of a porphyrin ring containing a heme group. Oxymyoglobin is a red pigment with oxygen bond to myoglobin which consumers prefer to see in retail cases (Carpenter et al., 2001). Oxidation of myoglobin directly impacts the appearance of meat products in retail by forming surface discoloration or metmyoglobin (Carpenter et al., 2001). Recently, a study evaluated the economics of discoloration and determined discoloration of steaks costs approximately $3.73 billion annually and results in the waste of almost 780,000 animals (Ramanathan et al., 2022a). Therefore, limiting metmyoglobin formation during retail display can help to reduce food waste and provide value back to the meat industry.

Initially, metmyoglobin forms below the surface and under the oxymyoglobin layer (Limsupavanich et al., 2004, 2008). In steaks, low oxygen partial pressure (5-7 mmHg) increases the oxidation of myoglobin (Ledward, 1970). As retail display time increased, the metmyoglobin layer increases in size while the oxymyoglobin decreases in size (Limsupavanich et al., 2004, 2008). As the metmyoglobin layer increases, the metmyoglobin appears on the surface of steaks. Therefore, the myoglobin oxidation increases with time internally, indicative of oxidative changes in steaks. As there is a connection between myoglobin and lipid oxidation (Faustman, Sun, Mancini, & Suman, 2010), understanding the oxidative changes in muscle due to oxidative conditions is important. Reactive oxygen species can lead to oxidation (Faustman et al., 2010). Therefore, oxygen plays a key role in postmortem muscle changes, as oxygen can lead to the formation of oxymyoglobin and the oxidation of metmyoglobin. In muscle, the interior remains deoxygenated myoglobin or deoxymyoglobin (Limsupavanich et al., 2004, 2008). Mitochondrial oxygen consumption leads to the formation of deoxymyoglobin by lowering the oxygen partial pressure (Tang, Faustman, Hoagland, et al., 2005a). However, postmortem changes to mitochondria can lead to reactive oxygen species production (Ke et al., 2017). As mitochondrial oxygen consumption is muscle specific, oxygen consumption will influence the oxidative state of myoglobin and the oxidative changes occurring.

Lipid oxidation

As lipid oxidation compounds in postmortem muscle negatively influence palatability by developing rancid flavor (Legako et al., 2015), understanding the occurrence of lipid oxidation may improve meat quality via extended shelf life. Research

has reported an increase in lipid oxidation with greater display time (Ke et al., 2017; Mitacek et al., 2019). Early postmortem, the body attempts to reestablish homeostasis through the production of adenosine triphosphate (ATP) (Yu, Tian, Shao, Li, & Dai, 2019). As ATP is depleted, fatty acid metabolism can increase due to the energy depletion in postmortem muscle (Consolo et al., 2021). As fatty acids are metabolized, lipid oxidation increases, which can have negative implications on palatability. Research has reported enhancing meat with metabolites can influence lipid oxidation. Lipid oxidation was lower in steaks enhanced with pyruvate and lactate while packaged in polyvinyl chloride (PVC) and HiOx-MAP. In PVC and HiOx-MAP, lower lipid oxidation was reported in ground beef patties with succinate (Mancini, Ramanathan, Suman, Dady, & Joseph, 2011). Thus, the addition of tricarboxylic acid (TCA) cycle metabolites limit lipid oxidation by minimizing myoglobin oxidation. Therefore, understanding postmortem metabolome changes may provide insight into lipid and protein oxidation from oxidative stress postmortem.

Metmyoglobin formation – extrinsic factors

Metmyoglobin formation can be impacted by a variety of extrinsic factors, including temperature, aging, oxygen partial pressure, and packaging.

Oxygen partial pressure

Lower oxygen partial pressure increased the rate of oxymyoglobin oxidation *in vitro* (George & Stratmann, 1952). In steaks, the oxidation of myoglobin occurred most readily at an oxygen partial pressure of 5-7 mm Hg (Ledward, 1970). Therefore, oxygen levels present in steaks will influence the myoglobin forms. An example would be the

formation of deoxymyoglobin in anaerobic systems. Mitochondrial oxygen consumption led to the formation of deoxymyoglobin by lowering the oxygen partial pressure (Tang et al., 2005a). Therefore, low oxygen partial pressure could be formed in steaks due to oxygen consumption. Higher oxygen consumption has been reported to have lower oxygen penetration (McKenna et al., 2005; O'Keeffe & Hood, 1982). For example, muscles such as the *psoas major* have been reported to have greater oxygen consumption and smaller oxygen penetration than the *longissimus* (McKenna et al., 2005; O'Keeffe & Hood, 1982). Therefore, greater oxygen consumption led to little penetration of oxygen and a smaller oxymyoglobin layer in steaks (Limsupavanich et al., 2004, 2008). Subsequently, the metmyoglobin layer has been reported to be larger in muscles with greater oxygen consumption (Limsupavanich et al., 2004, 2008), supporting the influence of oxygen consumption on oxidation by low oxygen partial pressure. Therefore, oxygen content in intact muscles and subsequent oxygen consumption greatly influence the development of metmyoglobin and color stability in retail.

Packaging

Packaging type will influence color stability and metmyoglobin formation. Packaging types are categorized by their atmospheric conditions, including anaerobic, aerobic (20% oxygen), and high oxygen (80% oxygen). Anaerobic packaging can include vacuum packaging or carbon monoxide-modified atmosphere packaging (MAP). Vacuum packaging will be the primary anaerobic packaging discussed in relation to oxygen and metmyoglobin formation. In MAP, increasing oxygen concentration increased color stability and decreased metmyoglobin formation of steaks (Lu, Cornforth, Carpenter, Zhu, & Luo, 2020). Specifically, HiOx-MAP conditions have improved color stability of

steaks (Seyfert, Mancini, Hunt, Tang, & Faustman, 2007) and ground beef (Jayasingh, Cornforth, Brennand, Carpenter, & Whittier, 2002) compared to aerobic conditions. The increased color stability may be due to oxygen penetration. With greater oxygen concentration, there was deeper oxygen penetration in steaks stored in MAP systems (Lu et al., 2020; Taylor & MacDougall, 1973). An aerobic MAP system achieved maximal penetration at day 4 remained constant then declined (Lu et al., 2020). Higher oxygen concentrations reached maximum penetration on day 7 and then declined (Lu et al., 2020). In support, dark-cutting steaks in HiOx-MAP had greater oxygen penetration compared to aerobic oxygen concentrations and increased color stability (Yang et al., 2022). Oxygen consumption of the non-oxygen exposed (NOE) surface of dark-cutting steaks decreased at a faster rate in HiOx-MAP conditions compared to aerobic MAP conditions (Yang et al., 2022). This supports a lower oxygen consumption leading to greater penetration of oxygen into steaks and increased color stability. A greater decrease in oxygen consumption was reported in extended aged steaks in HiOx-MAP compared to steaks in traditionally PVC (English, Mafi, VanOverbeke, & Ramanathan, 2016). With a greater oxygen penetration, the metmyoglobin layer would form deeper, leading to masking of the discoloration by a larger oxymyoglobin layer extending color stability. Therefore, the oxygen concentration in packaging increases the depth of oxygen penetration by influencing oxygen consumption.

Metmyoglobin reducing ability is influenced by the oxygen conditions of packaging. Using the non-oxygen exposed (NOE) surface, steaks in vacuum packaging had higher metmyoglobin reducing ability compared to steaks packaged in HiOx-MAP and PVC (Ramanathan, Mancini, & Dady, 2011). In addition, ground beef patties

packaged in PVC had greater metmyoglobin reducing ability compared to HiOx-MAP patties (Ramanathan, Mancini, Van Buiten, Suman, & Beach, 2012a). A similar decline in NOE metmyoglobin reducing ability was reported in extended-aged steaks packaged in HiOx-MAP over PVC-packaged steaks (English et al., 2016a). HiOx-MAP had lower metmyoglobin reducing ability compared to steaks packaged in PVC for the NOE and oxygen exposed (OE) surfaces (Mancini, Seyfert, & Hunt, 2008). High oxygen conditions also decreased the metmyoglobin reducing ability of the OE surface of dark-cutting steaks during retail (Yang et al., 2022). A greater oxygen concentration within packaging resulted in lower metmyoglobin reducing ability, which could influence color stability as metmyoglobin rises to the surface in higher oxygen conditions.

Oxygen concentration in packaging can also influence the lipid oxidation of the system. Greater oxygen concentration in a MAP system increases lipid oxidation of dark-cutting steaks during retail display, impacting the oxidation of myoglobin (Lu et al., 2020). On the other hand, Łopacka, Półtorak, and Wierzbicka (2017) reported no effect of oxygen concentration on lipid oxidation during the storage of steaks. Lipid oxidation has been greater in steaks packaged in HiOx-MAP compared to vacuum packaging (Kim et al., 2010). In support, English et al. (2016b) reported greater lipid oxidation in HiOx-MAP than PVC packaged steaks after extended aging. Furthermore, proteomic analysis has reported lower antioxidant capacity in steaks packaged in HiOx-MAP conditions compared to those in CO-MAP, which may indicate the negative influence of oxygen on oxidative stability (Yang et al., 2018). These results support the negative influence of high oxygen conditions on oxidative conditions in the meat. Overall, packaging type and

subsequent oxygen presence influence color stability through impacts on oxygen penetration, oxygen consumption, metmyoglobin reducing ability, and lipid oxidation.

Temperature

Oxidation of myoglobin *in vitro* occurs more rapidly at higher temperatures compared to temperatures of meat storage (Brown & Mebine, 1969; Snyder & Ayres, 1961). Furthermore, metmyoglobin content increased with higher storage temperature during dark storage (Hood, 1980). A higher temperature during storage decreases color stability of beef (Jeremiah & Gibson, 2001; Limbo, Torri, Sinelli, Franzetti, & Casiraghi, 2010; Mancini & Ramanathan, 2014). However, electron transport chain (ETC)-mediated metmyoglobin reduction occurs more readily at higher temperatures (Tang, Faustman, Mancini, Seyfert, & Hunt, 2005b), indicating that physiological temperatures allow for more metmyoglobin reduction. Furthermore, the use of malate dehydrogenase system increased in reduction at a temperature closer to physiological temperature (Mohan, Muthukrishnan, Hunt, Barstow, & Houser, 2010a). Postmortem storage temperature of meat can slow the oxidation of myoglobin but also limits some of the metmyoglobin reducing pathways to be more active in physiological conditions.

Aging

Wet aging in vacuum packaging is a common practice in the meat industry to improve tenderness and flavor. Improved eating quality is negated by lower color stability. Increased aging time led to greater metmyoglobin formation and decreased a^* values during storage (English et al., 2016a; Mancini & Ramanathan, 2014; Mitacek et al., 2019; Nair, Li, Beach, Rentfrow, & Suman, 2018). In addition, bloom development decreased with increased aging time (English et al., 2016a; Mitacek et al., 2019). With

increased time postmortem, there is a decrease in oxygen consumption (English et al., 2016a; Mancini & Ramanathan, 2014; Mitacek et al., 2019) which can influence oxygen penetration. A greater oxygen penetration has been reported when there is lower oxygen consumption (O'Keeffe & Hood, 1982). Therefore, aging could increase penetration, but color stability would be limited by the decline in metmyoglobin reducing ability (English et al., 2016a; Mitacek et al., 2019). One such example would be aged dark-cutting beef. With greater aging time, dark-cutting beef has less deoxymyoglobin formation and improved *L** values, possibly due to muscle structure breakdown through proteolysis and greater oxygen penetration (English et al., 2016b). However, increased aging decreased metmyoglobin reducing ability of dark-cutting beef (English et al., 2016b), which can negatively influence color stability. Therefore, the aging process used in industry can lead to detrimental effects on metmyoglobin formation and color stability.

Metmyoglobin formation – intrinsic factors

Metmyoglobin formation can be impacted by a variety of intrinsic factors, including pH, lipid and protein oxidation, muscle fiber type, muscle metabolism, and mitochondrial oxygen consumption.

pH

Oxidation of proteins such as myoglobin is influenced by pH. Brown and Mebine (1969) reported greater oxidation of myoglobin occurs at a lower pH compared to physiological pH. In steaks, dark-cutting beef (pH > 6.0) shows slower discoloration formation than normal-pH beef during retail display (Ramanathan et al., 2022b; Sawyer, Apple, Johnson, Baublits, & Yancey, 2009; Wills et al., 2017). Myoglobin is stabilized

by distal and proximal histidines, which can be impacted by pH. The distal histidine hydrogen bonds with oxygen of oxymyoglobin to stabilize myoglobin (Richards, 2013). Protonation of the distal histidine occurs at lower pH levels leading to less stability of oxygen through a weakened hydrogen bond and increased oxidation to occur (Richards, 2013). In addition, protonation of the proximal histidine will contribute further to promoting oxidation due to decreased stability of the heme linkage with the proximal histidine (Richards, 2013). At lower pH conditions, there was less oxygen affinity for myoglobin reducing oxymyoglobin formation (Nerimetla et al., 2017). In addition, a postmortem pH level had lower metmyoglobin reduction compared to a physiological pH level (Mohan et al., 2010a; Nerimetla et al., 2017; Ramanathan et al., 2012a; Tang et al., 2005b). All these factors indicate the greater susceptibility of myoglobin oxidation in postmortem meat from a lower pH.

Lipid and protein oxidation

Protein and lipid oxidation are linked, and protein oxidation is believed to proceed in a similar manner as lipid oxidation (Faustman et al., 2010). Metmyoglobin formation has been increased by the presence of lipid oxidation products (Faustman et al., 2010; Lynch & Faustman, 2000). Specifically, 4-hydroxy-2-nonenal (HNE) has been reported to increase metmyoglobin formation *in vitro* (Ramanathan, Mancini, Suman, & Cantino, 2012b). Higher lipid oxidation during retail display has been significantly correlated with lower *a** values and greater surface discoloration (Ma et al., 2017). The secondary lipid oxidation product HNE has been reported to decrease ETC-mediated metmyoglobin reduction, NADH-dependent reductase activity, and LDH activity (Ramanathan,

Mancini, Suman, & Beach, 2014; Zhai, Peckham, Belk, Ramanathan, & Nair, 2019a) influencing metmyoglobin formation.

Lipid and protein oxidation can be influenced by the packaging used during storage. In previous studies, PVC-packaged *longissimus* steaks had greater lipid oxidation than vacuum packaging with greater display time (Fu, Molins, & Sebranek, 1992; Ramanathan et al., 2011; Reyes et al., 2022). Furthermore, steaks packaged in HiOx-MAP reported an increase in lipid oxidation compared to vacuum packaging (Ramanathan et al., 2011; Yang et al., 2016; Zakrys, Hogan, O'Sullivan, Allen, & Kerry, 2008). Higher protein oxidation has been reported in HiOx-MAP steaks compared to vacuum-packaged steaks during storage (Moczkowska et al., 2017; Yang et al., 2016). A similar trend was reported in pork chops packaged in HiOx-MAP (Spanos, Tørngren, Christensen, & Baron, 2016) and 20% oxygen conditions (Bao & Ertbjerg, 2015). Therefore, the presence and level of oxygen negatively impacts of the oxidative state of the system.

Enhancement with metabolites can influence the amount of lipid oxidation during storage. Enhancement with lactate and pyruvate decreased lipid oxidation of steaks packaged in PVC and HiOx-MAP (Ramanathan et al., 2011). In addition, lipid oxidation was lower with pyruvate addition to ground beef patties in PVC and HiOx-MAP (Ramanathan et al., 2012a). Succinate decreased lipid oxidation of ground beef patties in PVC and HiOx-MAP (Mancini et al., 2011). The addition of these TCA cycle metabolites may limit lipid oxidation by limiting myoglobin oxidation. Therefore, the presence of metabolites in steaks could influence lipid oxidation and, thereby, metmyoglobin formation.

Muscle types

Muscles have specific meat quality characteristics influenced by metabolism differences. Type I or red fibers have a greater oxidative metabolism compared to type IIb or white fibers (Hunt & Hedrick, 1977; Kirchofer, Calkins, & Gwartney, 2002). For example, the *psoas major* has more oxidative fibers, while the *longissimus* and *semitendinosus* muscles have more glycolytic fibers (Hunt & Hedrick, 1977; Yu et al., 2019). A greater oxidative metabolism has been shown to be less color stable than muscles that have greater glycolytic metabolism (McKenna et al., 2005; O'Keeffe & Hood, 1982). In addition, oxidative muscles such as the *psoas major* have greater mitochondrial content compared to glycolytic muscles such as the *longissimus* (Ke et al., 2017). As the mitochondria are the main source of reactive oxygen species in muscle, the greater abundance of mitochondria negatively impacts the oxidative stability of the *psoas major* muscle (Liu et al., 2022). Furthermore, the *psoas major* in chickens was more susceptible to oxidative stress than the *gastrocnemius* (Liu & Xiong, 2015). These differences in muscle type can result in differences in oxidation.

In terms of protein oxidation, there are muscle-specific implications on appearance. Both the *longissimus* and *semitendinosus* muscles were reported as color stable, while the *psoas major* muscle was categorized as color labile (McKenna et al., 2005; Seyfert et al., 2007). During storage, the *longissimus* and *semitendinosus* muscles had greater redness compared to the *psoas major* muscle (McKenna et al., 2005; Nair et al., 2018). Furthermore, a more rapid decrease in *a** values and chroma and an increase in metmyoglobin was reported in the *psoas major* compared to thelongissimus lumborum muscle (Joseph et al., 2012; Kim, Keeton, Smith, Berghman, & Savell, 2009). The *psoas*

major muscle has greater lipid oxidation than the *longissimus* muscle (Canto et al., 2016; Joseph et al., 2012; Ke et al., 2017) and *semitendinosus* (McKenna et al., 2005), contributing to the oxidation of myoglobin. A lower metmyoglobin reducing ability was reported in the *psoas major* compared to the *longissimus* muscle (Abraham et al., 2017; Joseph et al., 2012; Ke et al., 2017; McKenna et al., 2005) and the *semitendinosus* muscle (Nair et al., 2018). The lower reducing capacity would negatively influence the oxidative state of myoglobin, resulting in more myoglobin oxidation. However, McKenna et al. (2005) reported no difference in metmyoglobin reducing ability between the *semitendinosus* and *psoas major* muscles after storage. Furthermore, oxygen consumptiondecreased at a greater rate in the *psoas major* than thelongissimus lumborum during retail display (Abraham et al., 2017; Ke et al., 2017). The differences in fiber type resulted in differences in lipid oxidation, oxygen consumption, and metmyoglobin reducing ability, influencing color stability. Recent research has focused on the specific metabolite and protein differences between muscles that could be connected to color stability.

Metabolomic and proteomic effects

Several studies have evaluated the differences in metabolome and proteome between the *psoas major* and *longissimus,* while there has been limited research on the metabolome and proteome of the *semitendinosus.* Early postmortem evaluation reported more glycolytic enzymes in thelongissimus lumborum muscle than the *psoas major* muscle (Yu et al., 2019; Yu et al., 2018). Joseph et al. (2012) reported more glycolytic enzymes in the *longissimus* during retail display compared to the *psoas major* muscle. Similar results were reported by Nair et al. (2018) whereas the *semitendinosus*

andlongissimus lumborum muscles had a greater abundance of glycolytic enzymes than the *psoas major* muscle. In support, glycolytic metabolites have been reported to be greater in thelongissimus lumborum during retail display compared to *psoas major* supporting glycolytic muscles having greater color stability in retail display (Abraham et al., 2017). Furthermore, oxidative phosphorylation enzymes were reported to be greater in the *psoas major* muscle than the *longissimus* muscle (Yu et al., 2019, 2020; Zhai et al., 2020). The presence of glycolytic metabolites and enzymes in predominantly glycolytic muscles may support the limited oxidative changes reported in the *longissimus* compared to the *psoas major*. In addition, glycolytic enzymes can lead to the production of reduced nicotinamide adenine dinucleotide (NADH), and NADH can be used for metmyoglobin reduction, indicating a greater capacity for metmyoglobin reduction in glycolytic muscles. Producers of reactive oxygen species were more abundant in the *psoas major* muscle than in the *longissimus* muscle (Zhai et al., 2020). More reactive oxygen species indicates more oxidative stress in the *psoas major* muscle than the *longissimus* muscle, and thereby, lower color stability and greater myoglobin oxidation. Furthermore, research has reported the *psoas major* muscle has a loss of membrane potential and increased mitochondrial dysfunction due to changes in the proteome early postmortem which could further the production of reactive oxygen species and oxidative stress (Liu et al., 2022).

The presence of specific metabolites and enzymes supports the muscle-specific reduction capacity and oxidative stress response. The *longissimus* muscle has greater succinic acid content than the *psoas major* during retail display (Abraham et al., 2017). The role of succinate in ETC-mediated metmyoglobin reduction supports the greater color stability of the *longissimus* over the *psoas major* muscle. Metmyoglobin reduction

has also been reported through the use of lactate dehydrogenase (Kim et al., 2009) and malate dehydrogenase (Mohan et al., 2010a). Lactate dehydrogenase was more abundant in the *psoas major* than the *semitendinosus* muscle (Nair et al., 2018) and more active in the *psoas major* than the *longissimus* muscle (Kim et al., 2009). Malate dehydrogenase was more abundant in the *longissimus* and *semitendinosus* muscles compared to the *psoas major* and could be used to reduce metmyoglobin and extend color stability (Nair et al., 2018). In support, muscle extracts from the *longissimus* and *semitendinosus* had greater reduction compared to the *psoas major* in the presence of NAD and malate (Mohan et al., 2010a). The substrate malate can be formed from carnitines which have been reported to be greater in the *longissimus* than the *psoas major* muscle (Ma et al., 2017). Alternatively, Abraham et al. (2017) reported the *psoas major* muscle with a greater abundance of carnitines due to the increased mitochondrial content. Variations in metabolites and proteins influence the capacity for myoglobin oxidation and subsequent reduction.

Antioxidant proteins play a large role in limiting oxidative stress by reducing reactive oxygen species. Joseph et al. (2012) reported greater antioxidant capacity in the *longissimus* muscle than in the *psoas major* muscle. Specifically, there was a greater abundance of antioxidant proteins such as peroxiredoxin-2 and peptide methionine sulfoxide reductase in the *longissimus* muscle than in the *psoas major* muscle (Joseph et al., 2012). Both enzymes could be used to limit the negative effects of reactive oxygen species in postmortem muscle (Joseph et al., 2012). Peroxiredoxin-6 increased during storage of the *psoas major* muscle, whereas peroxiredoxin-1 increased in the *longissimus* muscle (Wu et al., 2016). As an antioxidant protein, peroxiredoxin-6 may prevent or limit

myoglobin and lipid oxidation in addition to their activation from cellular stress (Gagaoua et al., 2020). Peroxiredoxin-1 was positively correlated with *a** values during retail display of the *longissimus*, indicating the potential for peroxiredoxin-1 to play an antioxidant role in preventing oxidative changes (Wu et al., 2016). Superoxide dismutase removes reactive oxygen species and could prevent the free radical damage and oxidation of proteins and lipids (Malheiros et al., 2019). Therefore, superoxide dismutase may act as an antioxidant defense mechanism from oxidative stress in the *psoas major* muscle. Superoxide dismutase was reported to be higher in the *psoas major* than the *semitendinosus* during storage (Nair et al., 2018). The same enzyme was reported to be lower in the *psoas major* compared to the *longissimus* muscle (Wu et al., 2016). Furthermore, superoxide dismutase had greater oxidative damage in tender *longissimus* steaks over tough *longissimus* steaks (Malheiros et al., 2019). In support, other antioxidant proteins such as peroxiredoxin-1 and -2 also reported greater oxidative damage in tender *longissimus* compared with tougher *longissimus* (Malheiros et al., 2019). Therefore, the increase in oxidative damage may lead to tender meat as oxidative changes occur. Mitochondrial aconitase can utilize citrate and was reported to be more abundant in the *psoas major* than in the *longissimus* muscle (Joseph et al., 2012; Yu et al., 2017). In support, citric acid was greater in the *longissimus* at the end of retail display than in the *psoas major* (Abraham et al., 2017). The difference in citrate content could be due to the greater mitochondrial content in the *psoas major* muscle (Abraham et al., 2017). The mitochondrial aconitase enzyme could increase free radical-induced lipid oxidation and, thereby, myoglobin oxidation. Therefore, a lower abundance of the enzyme mitochondrial aconitase enzyme and a greater abundance of citrate could indicate

less oxidative changes in the *longissimus* muscle than in the *psoas major* muscle. However, there has not been a direct connection between citrate and lower myoglobin or lipid oxidation. These antioxidant mechanisms may influence myoglobin oxidation and, therefore, reducing capacity of different muscles.

Enzymes involved in fatty acid degradation can vary based on muscle type. In early postmortem muscle, the *psoas major* muscle had a greater abundance of fatty acid degradation enzymes compared to the *longissimus* muscle (Zhai et al., 2020). Furthermore, research supports greater fatty acid degradation in the *psoas major* than the *longissimus* based on abundant enzymes, which would promote lipid oxidation induced pigment oxidation (Yu et al., 2019; Yu et al., 2018). Therefore, the greater enzyme content and thereby degradation of fatty acids would support greater lipid oxidation in the *psoas major* compared to the *longissimus* postmortem (Canto et al., 2016; Joseph et al., 2012; Ke et al., 2017). In live animals, vitamin E supplementation has been reported to limit oxidation of myoglobin in postmortem muscle (Faustman, Chan, Schaefer, & Havens, 1998). More specifically, Zhai et al. (2019b) reported a lower abundance of NADH dehydrogenase, which forms reactive oxygen species in vitamin E-supplemented cattle. Therefore, the presence of dietary vitamin E decreased the enzymes which promote oxidative stress by the production of reactive oxygen species. This proteome changes support the limited lipid and myoglobin oxidative changes previously reported in vitamin-E-supplemented beef postmortem (Faustman et al., 1998). Overall, the promotion of fatty acid degradation negatively influences the oxidative conditions in postmortem muscle and can be influenced by live animal conditions.

Other differences in proteome between the *longissimus lumborum* and *psoas major* muscles include differences in heat shock proteins. Heat shock protein 71 was reported to increase during extended storage of the *psoas major* muscle (Wu et al., 2016). In the *longissimus* muscle, heat shock protein 71 increased with greater storage as well as the *longissimus* muscle had a greater abundance of heat shock protein 71 compared to the *psoas major* and *semitendinosus* (Nair et al., 2018). Similarly, heat shock protein 70 was reported in greater abundance in the *longissimus lumborum* compared to the *psoas major* during retail display (Joseph et al., 2012). Heat shock protein 27 was reported to increase in the *longissimus* early postmortem (Jia et al., 2006). Furthermore, the *longissimus* muscle had a greater abundance of heat shock 27 compared to the *psoas major* muscle (Joseph et al., 2012). Heat shock protein 20 was higher in the *longissimus* compared to the *psoas major* (Zhai et al., 2020). Several heat shock proteins have been reported to decrease in the *psoas major* early postmortem (Liu et al., 2022). The decline in heat shock proteins could result in changes in mitochondrial morphology and subsequent release of reactive oxygen species (Liu et al., 2022). Therefore, the loss of heat shock proteins in the *psoas major* could indicate oxidative stress in the muscle with the heat shock proteins acting as part of the response (Liu et al., 2022). Greater oxidative damage of heat shock proteins 70 and 20 were reported in tender meat (Malheiros et al., 2019). The loss of heat shock proteins may prevent a decline in proteolysis and lead to increased tenderness, which aligns with the tender *psoas major* losing heat shock proteins 70 and 20 compared to the *longissimus* muscle (Malheiros et al., 2019). This may be due to the protection heat shock proteins can provide against stress-induced denaturation (Gagaoua et al., 2020). Positively correlated heat shock protein 60 was reported to decrease during

storage with a decrease in the *a** values of the *longissimus* (Wu et al., 2016). Early postmortem, the same protein was reported to increase in the *longissimus* muscle (Jia et al., 2006). Furthermore, heat shock protein 60, a mitochondrial protein, was reported to be higher in the *psoas major* than the *longissimus* early postmortem (Zhai et al., 2020) and with aging (Nair et al., 2018). The *semitendinosus* muscle also reported a lower abundance of heat shock protein 60 compared to the *psoas major* (Nair et al., 2018). Therefore, the greater abundance of mitochondria in the *psoas major* muscle compared to the *semitendinosus* and *longissimus* may influence the changes in heat shock protein 60 and impacts its presence in oxidative stress compared to other heat shock proteins. Therefore, the location of the protein and muscle type could influence the response and changes of the heat shock proteins. The varying changes in heat shock proteins in response to oxidative stress in different muscle types may indicate muscle-specific biomarkers for oxidative stress.

Mitochondrial influence

Postmortem mitochondria remain active consuming oxygen and competing with myoglobin for oxygen in meat (Tang et al., 2005a). Furthermore, as mitochondria respire, reactive oxygen species can be produced (Cecarini et al., 2007). The *psoas major* muscle has greater mitochondrial oxygen consumption and mitochondrial content than the *longissimus*, with a more rapid decrease in mitochondrial oxygen consumption during retail display (Ke et al., 2017). A greater mitochondrial content and oxygen consumption can lead to a greater number of radical oxygen species and increased oxidative stress, which can lead to faster myoglobin oxidation and apoptosis in the *psoas major* compared to the *longissimus* (Yu et al., 2020). Furthermore, the *psoas major* muscle had lower

mitochondrial membrane permeability of the mitochondria than the *longissimus* (Yu et al., 2020). Therefore, the mitochondrial damage was greater in the *psoas major* than in *longissimus.* This damage can lead to greater oxidative changes and stress in the *psoas major* than in the *longissimus.* In support, the *psoas major* has greater lipid oxidation than the *longissimus* muscle during retail display (Joseph et al., 2012; Ke et al., 2017). The differences in mitochondrial oxygen consumption and oxidative changes influence the oxidative state of myoglobin in muscle.

With increased time postmortem, mitochondria will degenerate and degrade, decreasing activity. Aging decreased mitochondrial oxygen consumption (Mancini & Ramanathan, 2014; Mitacek et al., 2019; Tang et al., 2005a) as well as mitochondrial protein content (Mitacek et al., 2019). Degeneration leads to mitochondrial damage and increased reactive oxygen species, which can negatively impact oxidative conditions (Ke et al., 2017; Yu et al., 2018). With aging, there was an increase in myoglobin oxidation in steaks (English et al., 2016a; Mitacek et al., 2019) and lower NADH content important for metmyoglobin reduction (Mitacek et al., 2019). The decrease in mitochondrial activity and subsequent degradation can influence the oxidative stress in steaks. Therefore, the presence of active mitochondria and mitochondrial substrates in muscle is important to oxidative stability.

Oxygen penetration depth is also influenced by oxygen consumption. The *psoas major* has less oxygen penetration compared to the *longissimus* (McKenna et al., 2005; O'Keeffe & Hood, 1982), which is influenced by the mitochondrial oxygen consumptionalong with oxygen diffusion. With the higher mitochondrial content and oxygen consumptioninitially, the *psoas major* has lower oxymyoglobin depth formed at

the surface compared to a deeper penetration reported in the *longissimus* (Limsupavanich et al., 2004, 2008). This smaller penetration has been associated with less color stability of the *psoas major* and greater metmyoglobin formation during display due to the low partial pressure oxygen area being closer to the surface of meat (Limsupavanich et al., 2004, 2008). Similar effects reported in *psoas major* are reported in dark-cutting beef. Dark-cutting beef has greater mitochondrial activity (Ashmore, Parker, & Doerr, 1972; Ramanathan & Mancini, 2018) and greater oxygen consumption (Kiyimba et al., 2021; Ramanathan, Kiyimba, Gonzalez, Mafi, & DeSilva, 2020b; Ramanathan & Mancini, 2018). More deoxymyoglobin formation has been reported on the surface compared to normal-pH beef (English et al., 2016b). Higher deoxymyoglobin formation is supported by smaller oxygen penetration reported in dark-cutting beef compared to normal-pH beef (Lu et al., 2020). This limited penetration also leads to a decrease in bloom in dark-cutting beef with less myoglobin oxygenation (English et al., 2016b). Less bloom or muscle darkening is also reported in lactate-enhanced beef due to increased mitochondrial oxygen consumption (Ramanathan, Mancini, Joseph, & Suman, 2013; Ramanathan, Mancini, & Konda, 2009; Ramanathan, Mancini, & Maheswarappa, 2010) and less myoglobin oxygenation (Ramanathan, Mancini, & Konda, 2010). Lactate-enhanced steaks had lower oxygen penetration compared to unenhanced steaks (Ramanathan, Mancini, & Konda, 2010), supporting the increase in oxygen consumption decreases the penetration of oxygen into the muscle. Therefore, differences in mitochondrial content and oxygen consumption can influence the oxygen penetration and, thereby color stability of the muscle.

In terms of the relationship between metabolites and mitochondria, research has reported the influence of metabolites in mitochondrial oxygen consumption and subsequent lipid and myoglobin oxidation. Succinate has been reported as a substrate for mitochondrial oxygen consumption (Ramanathan & Mancini, 2010; Ramanathan et al., 2009; Tang et al., 2005b; Zhu, Liu, Li, & Dai, 2009) and was reported as part of ETC-mediated metmyoglobin reduction (Tang et al., 2005b). Pyruvate addition to mitochondria results in oxygen consumption of heart muscle (Ramanathan & Mancini, 2010; Ramanathan et al., 2009) and metmyoglobin reduction (Ramanathan & Mancini, 2010). In PVC and HiOx-MAP, succinate decreased lipid oxidation of ground beef patties (Mancini et al., 2011). In addition, metabolites can influence myoglobin oxygenation due to mitochondrial oxygen consumption competing for oxygen with myoglobin. Lactate addition has been reported to darken the *longissimus* muscle (Kim et al., 2006; Ramanathan et al., 2011; Ramanathan et al., 2009) and decrease myoglobin oxygenation (Ramanathan, Mancini, & Konda, 2010). The decrease in myoglobin oxygenation could be due to increased mitochondrial oxygen consumption via the lactate-lactate dehydrogenase-NAD system (Ramanathan et al., 2013; Ramanathan et al., 2009; Ramanathan, Mancini, & Maheswarappa, 2010). The *psoas major* has been reported to have lower lactate dehydrogenase activity and NADH content compared to the *semimembranosus* and *longissimus* muscles which could contribute to the increased myoglobin oxidation reported in the *psoas major* muscle (Kim et al., 2009). Enhancement with lactate decreased lipid oxidation of steaks packaged in PVC and HiOx-MAP (Ramanathan et al., 2011). The presence of these metabolites could influence oxygenation of myoglobin and reducing capacity through mitochondrial oxygen

consumption. The products of lipid oxidation can influence mitochondrial oxygen consumption. Lipid oxidation products such as HNE have been reported to decrease mitochondrial oxygen consumption and increase myoglobin oxidation (Ramanathan et al., 2012b). In addition, mitochondria treated with HNE changed their morphology (Ramanathan et al., 2012b). Specifically, at pH 5.6, mitochondria with HNE were shrunken, and the membrane was less permeable (Ramanathan et al., 2012b). Decreased membrane permeability indicated oxidative stress and can negatively impact the oxidative state of myoglobin and other proteins (Ramanathan et al., 2012b). Lipid oxidation products can negatively influence mitochondrial oxygen consumption and increase myoglobin oxidation.

Oxygen consumption

Oxygen consumption is the use of oxygen by myoglobin, oxygen consumption enzymes, microbes, lipids, and mitochondria (Baron & Andersen, 2002; Faustman & Cassens, 1990; Tang et al., 2005a). Most oxygen consumption evaluated in meat is considered oxygen used through the mitochondria and oxygen consuming enzymes. Mitochondria is considered important to oxygen consumption in muscle because it is the main organelle responsible for oxygen consumption (Ouali et al., 2013). Oxygen is consumed by the mitochondria at Complex IV as oxygen acts as the final electron acceptor. Mitochondria compete with myoglobin for oxygen, which influences meat color (Ramanathan & Mancini, 2018; Tang et al., 2005a). Enzymes involved in consumption of oxygen are primarily involved in the Krebs cycle (King et al., 2023).

Muscle oxygen consumption can be evaluated by a variety of different methods, including Waring Flask, Clark Electrode, Spectrophotometry, and Oxygen Headspace

analysis. These methods provide insight into muscle oxygenation; however, most cannot be done in real-time and are invasive (Mohan, Hunt, Barstow, Houser, & Hueber, 2010b). The oxygen consumption method of focus in the present review is evaluating oxygen consumption on whole muscle. This method focuses on forming oxymyoglobin through bloom and then subsequent anaerobic storage at an elevated temperature to decrease oxymyoglobin content through oxygen consumption. Therefore, most studies use a freshly cut interior portion of muscle to evaluate whole muscle oxygen consumption. To calculate oxygen consumption, the percentage or $\frac{K}{S}$ ratio of oxymyoglobin or deoxymyoglobin is determined before and after incubation (King et al., 2023). Many studies report the change in deoxymyoglobin or oxymyoglobin as the oxygen consumption.

Oxygen consumption of intact muscle has been reported to indicate color stability (O'Keeffe & Hood, 1982; Sammel, Hunt, Kropf, Hachmeister, & Johnson, 2002). Sammel et al. (2002) reported an intermediate oxygen consumption would be beneficial to color stability which was supported by several reviews (Ramanathan et al., 2020c; Ramanathan, Nair, Hunt, & Suman, 2019). Based on the information provided, high oxygen consumption can result in decreased oxygen penetration, decreased color stability, and increased deoxymyoglobin formation. With low oxygen consumption from mitochondrial damage, there is increased oxidative stress and less reduction due to limited NADH and decreased reducing activity. Therefore, there needs to be a balance in the oxygen consumption, with a moderate level of oxygen consumption being representative of color stability. An example of this system would be the *longissimus* compared to the *psoas major*. In the *longissimus*, there is greater oxygen penetration

(Limsupavanich et al., 2004, 2008; McKenna et al., 2005; O'Keeffe & Hood, 1982), smaller loss of oxygen consumption during storage (Abraham et al., 2017; Ke et al., 2017), slower degeneration of mitochondria (Ke et al., 2017; Yu et al., 2020), and increased color stability (Abraham et al., 2017; McKenna et al., 2005; O'Keeffe & Hood, 1982) compared to the *psoas major*. Therefore, an intermediate level of oxygen consumption would allow for better color stability.

Oxygen consumption can be influenced by a variety of factors. A higher temperature increases mitochondrial and enzymatic activity and, therefore, oxygen consumption (Tang et al., 2005a). A pH closer to physiological pH increases mitochondrial and enzyme activity and thereby increases oxygen consumption. Dark-cutting beef has a higher pH and higher mitochondrial activity (Ashmore et al., 1972; Ramanathan & Mancini, 2018) and greater oxygen consumption (Kiyimba et al., 2021; Ramanathan et al., 2020b; Ramanathan & Mancini, 2018) resulting in more deoxymyoglobin on the surface than normal-pH beef (English et al., 2016b). Muscle type influences the oxygen consumption, as previously discussed. The *psoas major* has more oxidative metabolism and increased mitochondrial content, which will lead to increased oxygen consumption over the *longissimus* at the beginning of storage (Abraham et al., 2017; Ke et al., 2017; O'Keeffe & Hood, 1982), and the mitochondria of the *psoas major* muscle deteriorates faster losing oxygen consumption faster than *longissimus* (Abraham et al., 2017; Ke et al., 2017; O'Keeffe & Hood, 1982). Tricarboxylic acid cycle metabolites influence mitochondrial oxygen consumption impacting the oxygen consumption of intact muscle and ground beef (Kim et al., 2006; Ramanathan et al., 2011; Ramanathan et al., 2009; Ramanathan et al., 2012a). Oxygen conditions impact the

oxygen consumption such as HiOx-MAP conditions decreasing oxygen consumption compared to aerobic packaging systems in ground beef (Ramanathan et al., 2012a) and aged steaks (English et al., 2016a). However, limited research has evaluated the impact of retail oxygen exposure on the oxygen consumption of intact muscle since oxygen consumption has been based on freshly cut surfaces.

Metmyoglobin reduction

Pathways of metmyoglobin reduction

There are three pathways by which metmyoglobin can be reduced and limit the accumulation of surface discoloration. The pathways to reduce metmyoglobin include electron-transport metmyoglobin reducing ability (Tang et al., 2005b), enzymatic reduction (Arihara, Cassens, Greaser, Luchansky, & Mozdziak, 1995), and non-enzymatic reduction (Brown & Snyder, 1969). Electron-transport metmyoglobin reducing ability is mediated by the mitochondria (Tang et al., 2005b). In Tang, Faustman, Mancini, et al. (2005), the electron-mediated metmyoglobin reducing ability mechanism was reported. Complex II uses succinate to contribute electrons to the ETC, and the electrons come to cytochrome *c* between complexes III and IV. Cytochrome *c* acts as an electron carrier to transport electrons from the ETC to metmyoglobin. This occurs through transporting electrons from the inner membrane, where the ETC is located to the outer membrane of the mitochondria. Cytochrome *c* can move into the intermembrane space in addition to the cytochrome *c* present in the intermembrane space. At the outer membrane of the mitochondria, cytochrome *c* can transport the electrons to the outer membrane cytochrome *b5* which can provide electrons to reduce metmyoglobin to deoxymyoglobin. A greater pH and temperature resulted in an increase in electron-mediated metmyoglobin

reducing ability, indicating the role of the pathway in the physiological conditions found in skeletal muscle and aligning with the increase in myoglobin oxidation at postmortem pH levels. Anaerobic conditions allow for more electrons available for reduction as electrons do not pass to complex IV and can accumulate at complex III. Therefore, mitochondrial stability and interaction with oxygen in postmortem muscle influence color stability through metmyoglobin reduction.

Enzymatic reduction involves the enzyme NADH-cytochrome b5 reductase (Arihara et al., 1995). The enzyme is located in the outer membrane of mitochondria and can act to reduce metmyoglobin to deoxy/oxymyoglobin through electrons. These electrons come from NADH, and the enzyme mediates the reduction through cytochrome *b5*, which is also on the outer membrane of the mitochondria. The electron transfer to cytochrome *b5* leads to the reduction of cytochrome *b5*. Reduced cytochrome *b5* transfers electrons to metmyoglobin with the use of NADH-cytochrome b5 reductase, forming reduced myoglobin and oxidized cytochrome *b5*. The enzymatic reduction was higher at a higher temperature and lower pH (Mikkelsen & Skibsted, 1992). Oxygen conditions can influence enzymatic reduction as oxygen competes with metmyoglobin for the electrons at reduced cytochrome *b5* (Mikkelsen & Skibsted, 1992). Therefore, oxygen exposure during storage can influence enzymatic reduction.

Non-enzymatic reduction takes place using electron carriers such as cytochrome *c*, quinone, or methylene blue (Brown & Snyder, 1969; Denzer et al., 2020). The electrons can come from NADH and are transferred through an electron carrier to metmyoglobin for subsequent reduction. Through this pathway, the electron carrier is reduced and subsequently oxidized to reduce the heme iron of myoglobin from ferric to

ferrous state. Nonenzymatic reduction has been reported to occur at postmortem muscle pH and temperature conditions (Denzer et al., 2020). Koizumi & Brown (1972) determined aerobic conditions increased metmyoglobin reduction nonenzymatically. Therefore, oxygen conditions at retail could positively impact the non-enzymatic pathway. Reverse electron transport can help to form NADH at Complex I of the ETC, which can be used to reduce metmyoglobin through enzymatic and non-enzymatic mechanisms (Belskie, Van Buiten, Ramanathan, & Mancini, 2015). Consequently, metabolites used by the mitochondria and in the TCA cycle play an important role in metmyoglobin reduction.

Metabolites in metmyoglobin reduction

Electrons for the metmyoglobin reduction can be provided through various metabolites of the TCA cycle forming NADH. The enhancement of loins with pyruvate, succinate, and lactate has been reported to have higher *a** values and lower metmyoglobin after 13 d of dark storage in PVC and HiOx-MAP compared to unenhanced steaks (Ramanathan et al., 2011). Similarly, malate, lactate, and pyruvate have been reported to slow metmyoglobin formation in meat homogenates (Mohan, Hunt, Barstow, Houser, & Muthukrishnan, 2010c). Malate and lactate were reported to improve color stability of meat homogenates compared to pyruvate (Mohan et al., 2010c). An improvement in *a** values and reduction of metmyoglobin was reported in ground beef patties containing pyruvate stored in PVC and HiOx-MAP (Ramanathan et al., 2012a). Succinate and lactate improved the metmyoglobin reducing ability of the steaks (Ramanathan et al., 2011), while pyruvate decreased metmyoglobin reducing ability in steaks (Ramanathan et al., 2011) and patties (Ramanathan et al., 2012a). A similar

improvement in metmyoglobin reducing ability and color stability by lactate enhancement was reported by Kim et al. (2006). Therefore, reduction of metmyoglobin by substrate addition is dependent on the metabolite added.

Lactate in the presence of lactate dehydrogenase and NAD increased the formation of NADH (Kim et al., 2006; Ramanathan, Mancini, & Maheswarappa, 2010). Metmyoglobin reduction by ETC-mediated pathway was increased by the addition of lactate and further improved by the addition of lactate-lactate dehydrogenase-NAD system (Ramanathan, Mancini, & Maheswarappa, 2010). Enzymatic metmyoglobin reduction was increased using the lactate-lactate dehydrogenase-NAD system (Ramanathan, Mancini, & Maheswarappa, 2010), and reduction was increased in a muscle extract system containing lactate and NAD (Rodríguez, Kim, Faget, Rosazza, & Keeton, 2011). Without the presence of lactate dehydrogenase or reductase, the NADH formed cannot reduce metmyoglobin (Ramanathan, Mancini, & Maheswarappa, 2010). Therefore, NADH can be produced by the addition of lactate to meat products leading to the use of NADH for metmyoglobin reduction through ETC-mediated or enzymatic reduction.

Malate dehydrogenase, with the addition of malate and nicotinamide adenine dinucleotide (NAD+) lead to the formation of NADH and subsequent reduction of metmyoglobin (Mohan et al., 2010c). Using muscle homogenates paired with horse metmyoglobin reductase, NADH production, and metmyoglobin reduction were increased in the presence of malate and NAD+. The system proposed could use malate dehydrogenase to form NADH and subsequently reduce metmyoglobin through enzymatic and non-enzymatic means.

As previously mentioned, succinate plays a large role in the ETC-mediated reduction of metmyoglobin (Tang et al., 2005b). Succinate improved stability of *a** values in beef steaks (Ramanathan et al., 2011) and patties (Gao, Wang, Tang, Ma, & Dai, 2014; Zhu et al., 2009). There was an increase in nitrite-induced metmyoglobin reduction in steaks (Ramanathan et al., 2011) and in patties (Mancini et al., 2011) with succinate addition. Enzymatic metmyoglobin reduction was not impacted by succinate in patties (Gao et al., 2014). Therefore, succinate can improve color stability through ETC-mediated reduction. Pyruvate can be used in the TCA cycle and then used to produce NADH in the mitochondria, which has been reported to increase metmyoglobin reduction in bovine heart (Ramanathan & Mancini, 2010). However, the reduction occurring by pyruvate has been reported to be lower than by succinate (Ramanathan & Mancini, 2010). Overall, TCA cycle metabolites have been reported to contribute to color stability and metmyoglobin reduction pathways.

Measurement of metmyoglobin reducing abilitymetmyoglobin reducing ability

Sammel et al. (2002) evaluated different procedures for metmyoglobin reducing ability in the *semimembranosus* muscle. These researchers determined the nitric oxide metmyoglobin assay had high correlation with *a** values after display and would be a good assay for evaluating metmyoglobin reducing ability at differing stages of discoloration. Nitric oxide metmyoglobin metmyoglobin reducing ability is one of the most common procedures used to evaluate metmyoglobin reducing ability (King et al., 2023). The procedure uses nitrite to induce the formation of metmyoglobin on the surface of a sample. The sample is incubated to increase metmyoglobin reduction. To evaluate the metmyoglobin reducing ability, a spectrophotometer is used to evaluate the amount of

metmyoglobin after induction and after incubation. From the spectra, the metmyoglobin reducing ability can be determined several different ways including the change in percent metmyoglobin or change in the $\frac{K}{S}$ ratio of metmyoglobin. The American Meat Science Association (2012) recommends calculating the metmyoglobin reducing ability by the change in percent metmyoglobin which requires the creation of 100% forms of oxymyoglobin, deoxymyoglobin, and metmyoglobin. These standards are important when comparing different muscles, but they can increase the error and decrease the accuracy. The calculations used for metmyoglobin reducing ability in research include initial metmyoglobin, post incubation metmyoglobin, change in metmyoglobin, and change in metmyoglobin relative to initial metmyoglobin. This procedure and calculations were evaluated more in-depth by Mancini et al. (2008). In their research, the location of analysis was evaluated with interior/subsurface metmyoglobin reducing ability compared to exterior/surface metmyoglobin reducing ability. The surface metmyoglobin reducing ability tended to have higher correlations with color attributes of the *longissimus lumborum*, *psoas major*, and *semimembranosus* muscles compared to the subsurface metmyoglobin reducing ability. Instrumental color is evaluated on the oxygen exposed surface and metmyoglobin reducing ability on the same surface best aligns with the color during retail. In addition, the calculation of metmyoglobin reducing ability was evaluated in relation to retail color stability. Mancini et al. (2008) calculated metmyoglobin reducing ability in four methods paralleling with calculations used in various journal articles. The measurements were based on percentage and included initial metmyoglobin formation (IMF), post-reduction metmyoglobin (PRM), change in metmyoglobin (absolute metmyoglobin reducing ability), and change in metmyoglobin

relative to initial metmyoglobin (relative metmyoglobin reducing ability). For the *longissimus lumborum* muscle, the IMF metmyoglobin reducing ability was highly correlated with color stability during retail display, whereas the other metmyoglobin reducing ability calculations were not well correlated. The IMF metmyoglobin reducing ability of the *psoas major* muscle was more correlated with visual color changes than other forms of metmyoglobin reducing ability. However, the instrumental color analysis had limited correlation with IMF metmyoglobin reducing ability of the *psoas major* muscle. There may be differences in metmyoglobin reducing ability analysis depending on the muscle. Overall, the IMF and PRM metmyoglobin reducing ability were most indicated as useful in relating to color stability no matter the muscle. The IMF metmyoglobin reducing ability reported a lower value for more color stable muscles indicating a greater resistance to metmyoglobin formation. These results support the use of IMF metmyoglobin reducing ability as a more appropriate evaluation of display-color stability. The methodology for the evaluation of metmyoglobin reducing ability should be objective and muscle-specific to ensure an accurate understanding of metmyoglobin reducing ability in relation to color stability.

Color and myoglobin evaluation

Research has reported a variety of colorimeters to evaluate meat color. The most used colorimeters are the Minolta and the HunterLab (Tapp, Yancey, & Apple, 2011). Both colorimeters evaluate the instrumental color in terms of *L*, a*,* and b* values as well as calculated chroma and hue (Tapp et al., 2011). The American Meat Science Association Meat Color Guidelines (King et al., 2023) recommends using the illuminant A for greater sensitivity to redness and more closely aligned with visual color (Tapp et

al., 2011). This illuminant is only available in HunterLab colorimeters (Tapp et al., 2011). Both Minolta and HunterLab spectrophotometers report the reflectance spectra from 400 – 700 nm every 10 nm. The reflectance can be used to determine the percentage of each myoglobin forms on the surface of a meat sample using Kubelka-Munk theory (King et al., 2023). To quantify forms, reflectance at 474, 525, 572, and 610 nm is converted to $\frac{K}{S}$ ratios. By converting to the $\frac{K}{S}$ ratios, both the scattering (S) and absorption (K) properties of meat is accounted for. To accurately determine the forms, 100% myoglobin forms must be created as standards. Deoxymyoglobin is determined based on ratio at 474 nm, metmyoglobin at 572 nm, and oxymyoglobin at 610 nm, which are all normalized based on 525 nm. In addition, myoglobin forms can be determined based on the reflectance at selected wavelengths of 473, 525, 572, and 730 nm. From the reflectance, the reflex attenuance is determined, which is used to determine the contents of metmyoglobin and deoxymyoglobin. Oxymyoglobin is determined by subtraction to result in combined percentages of 100%. Using the selected wavelengths method, no standards are required. Both reflectance-based methods evaluate surface myoglobin forms and have limited penetration into the sample (Piao, Denzer, Mafi, & Ramanathan, 2022). In addition, the methods using spectrophotometers focus on four wavelengths in the visible spectra range, and with more wavelengths evaluated, the accuracy could be increased.

An important part of color evaluation is the form of myoglobin present in the product. Krzywicki's equations were established to determine the myoglobin forms present in extracts (Krzywicki, 1982). These equations were modified by Tang, Faustman, and Hoagland (2006). The equations are based on absorbance values at 503,

525, 557, and 582 nm. The wavelengths of 503, 557, and 582 nm are selected as the peak absorptions of metmyoglobin, deoxymyoglobin, and oxymyoglobin, respectively, and the absorbances are normalized to the isosbestic point of myoglobin at 525 nm. This methodology determines myoglobin forms in extracts and purified solutions which can be less reliable due to extraction will influence the forms present (King et al., 2023). While the equations reduced the number of negative values, there still can be negative values determined, and the total percentage can be over 100% (Tang et al., 2006). In addition, Krzywicki's method detected less differences than the K/S method employed when using a spectrophotometer (Hawkins et al., 2021). Furthermore, an extraction method can provide more insight into myoglobin forms throughout a steak compared to the surface evaluation used with a spectrophotometer (Piao et al., 2022).

Novel techniques to evaluate myoglobin oxygenation and determine myoglobin forms

The Nix Pro Color Sensor has been researched to evaluate meat color during storage and compared to the HunterLab spectrophotometer. Research has demonstrated the ability to use the Nix Pro Color Sensor to evaluate pork color (Xiong, Chen, Warner, & Fang, 2020), lamb color (Holman, Diffey, Logan, Mortimer, & Hopkins, 2021), and beef color (Holman, Collins, Kilgannon, & Hopkins, 2018; Holman & Hopkins, 2019). The Nix is lighter, cost-effective, and smaller option compared to the HunterLab spectrophotometer making the Nix a viable industry option for evaluating color (Nix Color Sensor, 2022; HunterLab). The aperture size of the Nix is smaller, leading to more surface measurements being required to match the sensitivity of the HunterLab spectrophotometer (Holman et al., 2018; Holman et al., 2021). In addition, the Nix is

calibrated by calibration software in the app without standardizing using colored tiles compared to the HunterLab, which is calibrated by the company annually and standardized before every use (Nix Color Sensor, 2022; HunterLab). The Nix Pro Color Sensor can be used in place of the HunterLab spectrophotometer while keeping in mind some of the limitations of the Nix instrument in terms of sensitivity and standardization.

Nuclear magnetic resonance (NMR) has been used to evaluate meat quality in pork and beef. In pork, NMR has been used to evaluate water holding capacity in relation to pork color (Bertram & Andersen, 2007; Brown et al., 2000). Research has found correlation between the water holding capacity and postmortem pH of pork relating to the appearance (Bertram & Andersen, 2007; Brown et al., 2000). Moreover, Brown et al. (2000) found a correlation between water holding capacity and L^* values of pork chops indicating the use of NMR technology for determining meat color changes based on pH. In beef, time-domain NMR has been used to predict beef color and has reported a high correlation between beef color and NMR results (Moreira et al., 2016). However, NMR can be an expensive technology and is limited to application on small samples only (Moreira et al., 2016). Time-domain NMR has some benefits to increasing frequency and lowering the cost in comparison to other NMR methods (Moreira et al., 2016). The NMR method does not provide an indication of the myoglobin state present limiting application in more myoglobin focused studies.

Raman spectroscopy has been used for molecular spectroscopy and in biosciences by using laser light to excite and shift wavelengths of scattered light from proteins. Raman spectroscopy has been used to evaluate hemoglobin oxygenation and myoglobin structural changes (Filho et al., 2016; Wackerbarth, Kuhlmann, Tintchev, Heinz, &

Hildebrandt, 2009; Wrobel et al., 2018). This technique can be used as a noninvasive procedure to evaluate oxygenation of tissues (Filho et al., 2016) as well as determine prehypertensive status based on different states of hemoglobin oxygenation (Wrobel et al., 2018). While changes in myoglobin structure have been documented in pork chops (Wackerbarth, Kuhlmann, Tintchev, Heinz, & Hildebrandt, 2009), there has been limited research on using Raman spectroscopy in relation to myoglobin oxygenation in meat.

An Ocean Optics Neofox Oxygen Sensing System probe uses light to quantify oxygen content of a liquid or gas sample (Ocean Insights). The NeoFox sensor evaluates the parts per million of oxygen present in gas or liquid. With the Neofox sensor, oxygen consumption was determined over time of a steak using the measurement of oxygen in the headspace (Lawson et al., 2020). This system provided information about the amount of oxygen consumed from a flushed anaerobic system and was more sensitive than the HunterLab spectrophotometer oxygen consumption determined by change in myoglobin forms (Lawson et al., 2020). However, myoglobin oxygenation could not be determined with the sensor system. In addition, the Neofox sensor cannot interact directly with protein (Ocean Insights) limiting its application to oxygen consumed in a meat product.

Multispectral imaging is a technique that has been used to evaluate the myoglobin forms below the surface of steaks (Sáenz, Hernández, Alberdi, Alfonso, & Diñeiro, 2008). Multispectral imaging gathers a sequence of images, with each image corresponding to a spectral band. In this study, the spectral bands evaluated were at 474, 525, 572, and 610 nm to evaluate the myoglobin forms present in the steaks. The results indicated that oxymyoglobin increased with bloom time while metmyoglobin formed below the surface of the steaks. The metmyoglobin present at the surface increased with

time. Oxymyoglobin and deoxymyoglobin decreased with time, and the deoxymyoglobin layer was deeper with time. This method supported the development of bloom and subsequent layers within the steaks over time. The benefits of this method were the ability to evaluate myoglobin forms in the depths of the tissue and evaluate small features that the larger port of colorimeters may not be sensitive to. The setup required the sample to be pressed between two plates immediately after cutting for the images to be taken and layers evaluated. Therefore, the setup of the method may prevent analysis in different packages or storage conditions. In addition, the changes demonstrated were not real-time changes in a steak during display.

A near-infrared (NIR)-based oxygen sensor called MOXY has been used in past research to evaluate the oxygenated myoglobin or hemoglobin in muscle (Lawson et al., 2020; England et al., 2018) and blood systems (Wilson et al., 1989). In blood, hemoglobin blood saturation had a linear relationship with the NIR system indicating changes in hemoglobin oxygenation in tissues could be identified (Wilson et al., 1989). Lawson et al. (2020) reported the MOXY system as a viable method for determining oxygen consumption of a steak. Although the MOXY sensor was more sensitive, the MOXY had greater variance compared to the oxygen consumption determined from the HunterLab spectrophotometer (Lawson et al., 2020). Myoglobin oxygenation was determined using the MOXY in early postmortem skeletal muscle (England et al., 2018). In comparison to a myoglobin extraction method, the amount of oxygenated myoglobin was similar using the MOXY system. The MOXY system measures below the surface of the muscle, which resulted in differences between the oxygenated myoglobin determined by MOXY and the a^* values in various packaging systems (England et al., 2018). The

research supports the use of MOXY to evaluate oxygenated myoglobin with some limitations in terms of variability and alignment with retail color.

An oximeter uses frequency domain NIR spectroscopy and has been used to document changes in myoglobin oxygenation during retail display (Mohan, Hunt, Barstow, Houser, Bopp, et al., 2010d; Mohan et al., 2010b). The oximeter has been used in exercise physiology and biomedical applications to evaluate the saturation of oxygen to myoglobin in skeletal muscle. To determine the oxygenation of myoglobin, the oximeter uses two wavelengths (690 and 830 nm) in the spectra (690 and 830 nm) in the spectra (Mohan et al., 2010b) compared to the four wavelengths (474, 525, 572, and 610 nm) used from the KM theory as previously mentioned. From changes in absorption, the content of deoxymyoglobin and oxymyoglobin were determined. Metmyoglobin was determined by subtraction because the oximeter can only evaluate oxygenated and deoxygenated myoglobin forms. When using the oximeter, the depth of measurement can be a couple of centimeters which increases the size of the steak to be thicker than most articles report using. Mohan et al., (2010b) evaluated the use of the oximeter to determine differences in muscles in aerobic and anaerobic packaging during display. These researchers reported greater oxymyoglobin in aerobic packages compared to anaerobic packages for the *longissimus lumborum*, *psoas major,* and *semitendinosus* muscles using the oximeter. In PVC packaging, oxymyoglobin decreased for all three muscles during display, paralleling with spectrophotometer results. At the end of display, the oxymyoglobin content determined by the oximeter in each muscle was as follows *longissimus* > *semitendinosus* > *psoas major* while the spectrophotometer reported no differences between the *longissimus* and *semitendinosus* muscles. Both instruments

reported metmyoglobin increasing in all three muscles during display with the greatest content found in the *psoas major*. There was a strong correlation between the two instruments measuring oxymyoglobin and deoxymyoglobin after d 0 of retail display while the correlation was lower for metmyoglobin content. Instrumental color corresponded well with the oximeter data, and from this study, the oximeter was shown to report and find differences between muscles with different color stability. Further studies with the oximeter focused on the influence of fiber orientation and storage time impacts on the quantification of myoglobin forms (Mohan et al., 2010d). Fiber orientation impacts the oxygenation of myoglobin evaluated using the oximeter. A perpendicular analysis led to greater quantities of oxymyoglobin and less deoxymyoglobin in aerobic packages during display compared to parallel fiber orientation. Using a HunterLab spectrophotometer, the fiber orientation had less impact early in the display, while at the end of display, perpendicular fibers had greater oxymyoglobin compared to parallel. These results paralleled with the higher *a** values reported in perpendicular fibers compared to parallel fibers at the beginning of display and greater color stability of perpendicular fibers. Both methods reported a decrease in oxymyoglobin with retail display. The oximeter has several benefits from this study, such as being a noninvasive method measuring at greater depths in the muscle than a spectrophotometer. In addition, the oximeter had similar results to instrumental color and spectrophotometer oxymyoglobin content. However, the oximeter cannot directly determine metmyoglobin and with a larger depth of measurement, fiber orientation plays a larger role in color analysis.

Several other NIR probes have also been used to evaluate different tissues to act as a minimally invasive or noninvasive technique to sense differences in tissue optical properties. These NIR probes evaluate the changes of light from differences in biochemical tissue composition and micromorphology changes in tissues (Piao, McKeirnan, Jiang, Breshears, & Bartels, 2012). Single-fiber reflectance spectroscopy accumulates reflected light or scattered light returning to the single fiber which emitted the light (Piao et al., 2012). A single-fiber probe has not been used in a meat system. However, there has been research demonstrating its use in evaluating intervertebral disc disease in the canines (Piao et al., 2012). This fiber system used differences in scattering intensity to determine degenerated discs. Meat systems contain absorbed and scattered light (King et al., 2023). Therefore, the single fiber system could be used to evaluate changes in myoglobin forms based on changes in the NIR spectral changes. Previous research using NIR diffuse reflectance spectroscopy (DRS) with a two-fiber optical probe system evaluated meat color changes on the surface of a steak throughout retail display (Piao et al., 2022). This two-fiber system varies from a single fiber as one fiber acts as an applicator and the other the illumination fiber. The distance from the two fibers influences the depth inside the meat sample evaluated, and in Piao et al. (2022), the system was used on the surface of the steaks with an approximate sampling depth of 1.5 mm. This depth was smaller in compared to the oximeter and more comparable to the limited depth when using the HunterLab spectrophotometer. In addition, the DRS NIR probe used a range of wavelengths compared to the four for the HunterLab spectrophotometer and the two used in the calculations of the NIR oximeter. From this study, there was high correlation between the HunterLab spectrophotometer and the

probe system for metmyoglobin. The loss of oxymyoglobin was slower in the probe system compared to the spectrophotometer resulting in moderate correlation between the two. This may be due to differences in accuracy between the two systems. The two-fiber system demonstrated viability in evaluating meat color with comparable results to the HunterLab spectrophotometer.

Conclusion

Meat color can be influenced by various factors and can be analyzed by several instruments. Improving color stability and limiting metmyoglobin formation is key to extending shelf life, limiting food waste, and decreasing profit loss. To determine shelf life, metmyoglobin reduction and oxygen consumption play a role in evaluating color stability. Oxygen is a key influencer in retail settings and understanding the impact of oxygen on metmyoglobin formation and subsequent color stability attributes. Metmyoglobin formation occurs below the surface and determining the changes in myoglobin subsurface where oxygen partial pressure is low can provide insight into color stability during retail.

CHAPTER III

NOVEL NEEDLE-PROBE SINGLE-FIBER REFLECTANCE SPECTROSCOPY TO QUANTIFY SUB-SURFACE MYOGLOBIN FORMS ON BEEF *PSOAS MAJOR* STEAKS DURING RETAIL DISPLAY

ABSTRACT

Meat discoloration starts between the interface of the bright red oxymyoglobin layer and the interior deoxymyoglobin layer. Currently, limited tools are available to characterize myoglobin forms formed within the sub-surface of meat. The objective was to demonstrate a needle-probe based single-fiber reflectance (SfR) spectroscopy approach for characterizing sub-surface myoglobin forms of beef *psoas major* muscles during retail storage. A 400-µm fiber was placed in a 17-gauge needle that was inserted into the muscle at five depths of 1 mm increment and 1 cm lateral shift. Metmyoglobin content increased during display from 1 mm to 5 mm depth. Metmyoglobin at a depth of 1 mm was greater compared to that of 2 – 5 mm depth. The sub-surface formation of metmyoglobin aligns with changes in a^* values during retail display and decrease in deoxymyoglobin content. In summary, the results suggest that needle-probe SfR spectroscopy can determine interior myoglobin forms and understand meat discoloration.

INTRODUCTION

Consumers discriminate against surface discoloration resulting in meat products being discounted or removed from the retail case. A recent study estimates surface discoloration costs the US beef industry approximately $3.73 billion annually (Ramanathan et al., 2022a). Interestingly, meat discoloration starts between the bright-red oxymyoglobin (OxyMb) layer and the interior deoxymyoglobin (DeoxyMb), where oxygen partial pressure is not enough to oxygenate all deoxymyoglobin molecules (King et al., 2023). More specifically, myoglobin is more prone to oxidation at a lower oxygen partial pressure (Ledward, 1970). After animal harvest, oxygen diffusion from the surface is the primary source of oxygen. Various factors, such as pH, fiber type, and mitochondrial activity, can influence oxygen diffusion into the interior. Diffusion of oxygen beneath the surface creates an oxygen gradient with greater oxygen at the surface and lower oxygen partial pressure in the interior of meat. The sub-surface oxygen partial pressure creates an ideal situation for metmyoglobin formation when metmyoglobin reducing capacity decreases. Since interior discoloration may precede surface discoloration, measuring sub-surface myoglobin forms helps to characterize meat color changes. Nevertheless, limited techniques are currently available to study the interior discoloration of intact meat. Various techniques have been used to evaluate the surface color of steaks during storage. The most common instrument for surface color evaluation is portable spectrophotometers such as HunterLab MiniScan or Minolta (Tapp, Yancey, & Apple, 2011). However, handheld spectrophotometers' light penetration is insufficient to quantify localized interior discoloration.

Sub-surface evaluation of myoglobin forms has been more limited due to technological inadequacies. The near-infrared (NIR) oximeter has been used in steaks to determine oxymyoglobin (OxyMb) and deoxymyoglobin (DeoxyMb) forms (Mohan et al., 2010d; Mohan et al., 2010b). The depth of myoglobin quantified corresponded to the approximate depth of layer that could be sampled by a surface applicator probe configured by an illumination channel and a light-collection channel approximately 2 cm apart. However, it is worth noting that the volume of sampling by the surface applicator stretched widely between the illumination and collection channels. Hence, the signal acquired by the surface probe would be affected at a much greater degree by the myoglobin concentration near the surface than by the same concentration at the 1 cm depth. As a result, the information obtained by the surface application did not represent the local metmyoglobin formed interior. A recent study reported using near-infrared diffuse reflectance spectroscopy (NIR-DRS) with a surface probe of a 3 mm illumination-collection distance allowing sampling myoglobin forms at a depth of approximately 1.5 mm (Piao et al., 2022). The metmyoglobin information obtained within the depth of 1.5 mm was certainly much more confined than that obtained within a depth of 10 mm. However, the measurement was not localized to the specific depth or in other words, the instrument-evaluated condition for the depth was not dissociated with the surface condition of metmyoglobin. This is because the path of the surface probed light in muscle while propagating between the illumination channel and the detection channel interrogates myoglobin distributed in all layers from the surface to the depth. A single-fiber probe that has the illumination channel overlap with the light-collection channel could significantly reduce the size of tissue being sampled in comparison to that by

surface probes of displaced illumination channel and light-collection channel. Introducing the single-fiber probe at a greater depth than the dimension of the sampling volume would allow the metmyoglobin localized to the probe's tip to be sampled. In this research, a needle-probe single-fiber reflectance (SfR) system based on a 400 μm fiber probe was developed to evaluate myoglobin forms at depths of 1 mm to 5 mm within the *psoas major* steaks during retail display.

MATERIALS AND METHODS

Raw materials and retail display

Seven United States Department of Agriculture (USDA) Select *psoas major* muscles (Institutional Meat Purchasing Specification (IMPS) #190A) were transported from a local processing facility on 5 d postmortem to the Oklahoma State University Robert Kerr Food and Agricultural Products Center. pH was measured at three random locations across each tenderloin with a pH probe (Handheld HI 99163; probe FC232; Hanna Instruments). Muscles were sliced into 2.54-cm thick steaks, and one steak from the anterior end was selected for analysis using the needle-probe SfR spectroscopy and HunterLab MiniScan color measurements (the same steaks were used for needle-probe and HunterLab MiniScan color measurements). The remaining steaks were randomly assigned to analysis on d 0 or d 3 of the display, and used to measure metmyoglobin reducing ability, oxygen penetration, and oxygen consumption. Steaks selected for retail display were packaged in white polystyrene PVC overwrap (15,500-16,275 cm^3 $O_2/m^2/24$ h at 23°C, E-Z Wrap Crystal Clear Polyvinyl Chloride Wrapping Film, Koch Supplies, Kansas City, MO) Styrofoam™ trays. All steaks were placed in a coffin-style retail

display case for 5 d at 2 ± 1°C. There was continuous LED lighting (Philips LED lamps, 12 watts, 48 inches, color temperature = 3,500°K, 54 Phillips, China) throughout the retail display.

Surface color measurement by using HunterLab MiniScan spectrophotometer

During retail display, surface color was evaluated using a HunterLab 4500L MiniScan EZ portable spectrophotometer (2.5-cm aperture, illuminant A, and 10° standard observer angle, HunterLab Associates, Reston, VA) three times before the needle-probe SfR spectroscopy measurements. The same steaks were repeatedly used to measure color on d 0, 3, and 5. The steaks assigned to surface color were utilized for both the HunterLab MiniScan portable spectrophotometer and the needle-probe SfR spectroscopy. The CIE a^* and b^* values were used to calculate the chroma $\left[\sqrt{(a^{*^2} + b^{*^2})}\right]$ and hue $[\tan^{-1}(\frac{b^*}{a^*})]$. A larger hue value indicated greater discoloration, while a larger chroma represented greater color intensity. The reflectance spectral profile acquired by HunterLab MiniScan spectrophotometer from 400 to 700 nm at a 10nm spectral interval was used to calculate four isobestic wavelengths of $\lambda = 474$, 572, and 610 nm to calculate OxyMb, DeoxyMb, and MetMb (King et al., 2023).

Needle-probe based single-fiber-reflectance spectroscopy device

Single-fiber-reflectance spectroscopy system implementing a needle-probe for locally assessing the myoglobin composition of muscle below the surface

The SFR spectroscopy device fitted with a 400 µm fiber in a needle-probe for assessing the myoglobin composition below the surface to a depth up to 5 mm is illustrated in Figure 3.1. The device was modified from a lab-on-a-crate unit developed in

the laboratory (Piao, Borron, Hawxby, Wright, & Rubin, 2018). Specifically, the output of a Halogen light source (Cuda I-150, Jacksonville, FL) through a fiber-optical light conduit of 6-mm in diameter was coupled by a 40× objective lens (Olympus RMS40X, Thorlabs Inc, Newton, NJ) onto one of two 400 μm branching fibers of a bifurcated fiber cable (BIF400-VIS/NIR, Ocean Optics, Orlando, FL). The bundled terminal of the bifurcated fiber cable was coupled to a low-OH 400 μm fiber used for percutaneous laser disk ablation (PLDA), which was positioned in a 17-gauge spinal needle as the probe for inserting into muscle. The other bifurcated terminal of the fiber cable was connected to a compact VIS-NIR spectrometer (BRC111A-USB-VIS, Edmund Optics, Barrington, NJ) having a 16-bit data resolution (0-65535) controlled by a laptop computer (Dell Model PP17L, Dell Inc., Round Rock, TX) via a vendor-provided user interface. The acquired raw spectral profile was saved to a text format compatible with EXCEL for off-line processing in a MATLAB environment. The effective spectral response of the system, as was constrained by the spectral profile of the light source, was approximately 450 - 700 nm. Within the effective spectral range, the spectrum over 480 - 650 nm was utilized for the assessment of myoglobin composition in consideration of the usability of the spectral absorbance of OxyMb, DeoxyMb, and MetMb.

The single-fiber needle-probe and the method to control the depth of probe insertion into the muscle

The single-fiber needle probe, which held the 400-μm PLDA fiber applicator in a fixed position, was developed by using a 17-gauge 2.5-inch myelographic needle. After retracting the stylet of the needle, the 400-μm PLDA fiber cleaved straightly was inserted through the needle. The fiber was held in position by using a spiral wire strain squeezed

into the barrel chamber of the needle. The squeezing of the spiral wire by the barrel of the needle caused the spiral wire strain to press circumferentially on the protecting sleeve of the fiber to maintain the longitudinal position of the fiber in the needle. The fiber was fixed at a length of extruding approximately 0.5 mm beyond the beveled tip of the needle. A small platform made of machine-grade plastic was developed to place the fiber-fixated needle-probe vertically into the muscle at a preset depth. Six holes of 1.5 mm in diameter were drilled along a line in the middle section of the platform at a spacing of 10 mm to allow the needle-probe to be inserted and set perpendicular to the bottom plane of the platform, contacting the muscle wrapped in plastic film. A staircase structure of 6 stairs that receded at a step of 1 mm after each lateral displacement of 10 mm was fabricated onto the middle section of the platform to allow the fiber-probe to be placed at depths of 1 mm difference. The position of the needle-probe at the reference depth, the 0-mm depth or in alignment with the under-surface of the platform, was set visually by controlling the length of a heat-shrinking tube sleeved to the needle as a spacer. The placement of the needle-probe in the other 5 holes would then make the tip of the needle-probe to extrude 1 mm to 5 mm beyond the bottom surface of the positioning platform.

The daily measurement of the muscle by using the needle-probe SfR spectroscopy device was performed at near 24 h intervals from d 0 to d 5 of the display. At each time of the day for daily measurement, the needle-probe SfR spectroscopy system was turned on to warm up for approximately 10 min. Reference needle-probe SfR spectroscopy measurements were acquired from distilled water filled in a black bottle (250 mL) as the baseline spectral reflection occurring at the fiber-water interface for water-immerged fiber, as would be needed for post-processing. Each steak was then brought to be placed

in hands-free contact with the applicator probe. The fiber-probe holder was stabilized in contact with the muscle by its own weight. The measurements on each *psoas major* muscle were performed at depths of 1 mm to 5 mm at a depth interval of 1 mm and lateral spacing of 10 mm. The procedures contained pressing the needle-probe positioning module on the unwrapped muscle slightly, then inserting the needle-probe into one positioning hole, completing the reading, the raw spectra acquisition on the spectrometer, then repositioning the needle-probe in another hole resulting in insertion into the muscle at 1 mm depth than the previous location and at a position laterally shifted for 10 mm. All needle-probe SfR raw spectra were acquired at an acquisition time of 150 ms and averaged over 5 acquisitions at each depth.

The raw needle-probe SFR spectral profile from the muscle was post-processed to remove the effect of source-spectral variation as well as baseline noise. The noise-deducted spectral reflectance from the muscle was then normalized with respect to the noise-deducted spectral reflectance acquired from water that informs the native spectrum of the light source as is routine to reflectance spectroscopy of similar principle. The normalized spectral reflectivity of muscle was fitted by a model of single-fiber reflectance (Sun et al., 2021, Sun & Piao, 2022). The muscle scattering was assumed to be wavelength invariant over the spectrum of interest (480 - 650 nm) (Schmitt & Kumar, 1998). The muscle's spectral absorption was assumed to be dominated by the three redox forms of myoglobin: OxyMb, DeoxyMb, and MetMb (de Groot, Zuurbier, & van Beek, 1999; Mohan et al., 2010d). The absorption of each myoglobin form was the product of the molar extinction coefficient and the molar concentration. In this work, we modeled the needle-probe SfR spectra at 18 wavelengths, from 480 – 650 nm at a wavelength

interval of 10 nm, to resolve the three redox forms of myoglobin. The absorbances of myoglobin redox forms at a 10-nm spectral interval over 480 - 650 nm followed the numbers available in (Piao et al. 2022), which were developed by using a set of data published by Tang, Faustman, & Hoagland (2006) containing the absorbance of OxyMb, DeoxyMb, and MetMb measured over a 1-cm transmission pathlength over a spectral range of approximately 475 - 650 nm.

Proximate analysis

From the posterior portion of each tenderloin, 200 g of steak was coarse ground with a table-top grinder (Big Bite Grinder, 4.5 mm, fine grind, LEM). A benchtop near-infrared spectrophotometer (FoodScan Lab Analyzer, Foss, NIRsystem Inc.; Slangerupgrade, Denmark) was used to determine the percent moisture, fat, and protein on d 0 of the display.

Metmyoglobin reducing ability and oxygen consumption

Steak assigned to metmyoglobin reducing abilitymetmyoglobin reducing ability and oxygen consumption was bisected perpendicular to the retail surface and resulted in two equal sections. The first section was used for metmyoglobin reducing ability, and the second section was used for oxygen consumption analysis on d 0, 3, and 5.

Steaks were cut in half parallel to the retail surface, resulting in two surfaces – surface exposed to oxygen/retail surface and surface not exposed to oxygen or interior. Both retail and interior surfaces were used for metmyoglobin reducing ability analysis. Both retail surface and interior sections were submerged in 0.3% sodium nitrite for 20 min, and subsequently, samples were removed and patted dry. With a HunterLab MiniScan spectrophotometer, samples were analyzed three times to quantify initial

MetMb formation. The reflectance spectra were used to calculate the absorption- (K) and scattering coefficient (S). The metmyoglobin reducing ability determined by the K/S ratio of $\left[\frac{K}{S}(572)\right]/\left[\frac{K}{S}(525)\right]$ was used to determine the amount of MetMb formed after submersion (Mancini et al., 2008). A greater number indicates a greater metmyoglobin reducing ability.

The remaining half of the steak was cut in half parallel to the retail surface to evaluate oxygen consumption. Both the retail surface and interior surface were used for oxygen consumption. Samples were allowed to bloom for 1 h at 4ºC, vacuum packaged and incubated at 30ºC for 30 min. Samples were read using the HunterLab MiniScan spectrophotometer at 0 and 30 min of incubation. Oxygen consumption was calculated by the change in $\left[\frac{K}{S}(610)\right]/\left[\frac{K}{S}(525)\right]$ from pre-incubation to post-incubation. A greater number indicates greater oxygen consumption.

Oxygen penetration during retail display

The depth of OxyMb and MetMb layers was used to indicate oxygen penetration. The oxygen penetration was measured using a handheld caliper. Steaks were cut perpendicular to the retail surface, and the OxyMb and MetMb layer was measured three times across the cut surface perpendicular to the retail surface. Surface layer depth was converted to a percentage by determining the depth of the layers relative to the width of the piece.

Statistical analysis

The experimental design was a completely randomized block design for analysis of retail color (n = 7 replications). The data were analyzed using the PROC GLIMMIX

procedure of SAS (SAS 9.4, SAS Institute Inc., Cary, NC). Each loin served as a block and was considered a random effect. Repeated measures were used to analyze the retail color of the steaks used for the SfR. Based on the AICC values, the covariance structure of the repeated measures was first-order autoregressive. Degrees of freedom were determined using the Kenwood-Roger method.

Simple linear regression analysis and Pearson's correlation were used to evaluate the relationship between the myoglobin forms determined from the needle-probe SfR spectroscopy and HunterLab MiniScan *a** values and myoglobin forms calculated from HunterLab MiniScan reflectance values and HunterLab MiniScan *a** values. Using PROC Corr (SAS 9.4, SAS Institute Inc., Cary, NC), data were analyzed for correlation, with significant correlations having a $P < 0.05$. Simple linear regression analysis was completed using the PROC Reg procedure in SAS (SAS 9.4, SAS Institute Inc., Cary, NC). Significant linear regression values were considered with a $P < 0.05$.

RESULTS

Proximate and pH analysis

Proximate analysis results and pH indicate normal pH and typical values for the *psoas major* (Table 3.1).

Color measurement by using HunterLab MiniScan Spectrophotometer

There was a significant day effect on the retail color (Table 3.2). As retail time increased, steaks appeared darker and less red with lower *a** and chroma values. Furthermore, there was an increase ($P < 0.05$) in hue angle with retail display, indicating greater discoloration. The percent myoglobin forms calculated from the HunterLab MiniScan spectrophotometer significantly changed with retail display (Figure 3.2). The

OxyMb decreased ($P < 0.05$) with retail display, while MetMb increased ($P < 0.05$). The DeoxyMb significantly increased from d 0 to d 1 on the surface and then was stable ($P > 0.05$) till d 4 of retail display.

Needle-probe single-fiber reflectance spectroscopy for measuring myoglobin forms up to 5 mm depth

The SfR system evaluated the subsurface forms of myoglobin from 1 – 5 mm of depth in the muscle (Figure 3.2). OxyMb at 1- and 2-mm depth increased from d 0 to d 1, and after d 1, OxyMb decreased with retail display time. These results align with the decrease in the OxyMb reported using HunterLab MiniScan spectrophotometer readings at the surface. There were minimal changes in OxyMb through retail display with increasing depth from 3 mm to 5 mm. At 2 mm, there was slightly greater OxyMb than 3-, 4-, and 5-mm depths during retail display. In support, the surface oxygen penetration depth (depth of OxyMb and MetMb) was reported to be 1.7 mm, 3.5 mm, and 3.5 mm on d 0, d 3, and d 5, respectively. This change in surface layer depth aligns with the minimal changes in OxyMb at greater depths based on SfR.

The MetMb content tended to increase during retail display at 1-mm and 2-mm depths aligned with the HunterLab MiniScan spectrophotometer measurements. At depths 3 mm, 4 mm, and 5-mm, MetMb increased from d 0 to d 5. However, there was more variation in the MetMb at 2 – 5 mm depths compared to the 1 mm depth evaluated by the SfR probe. The lowest change in MetMb through retail display was reported at 5-mm depth. The increase in MetMb at various depths parallels the decrease reported in DeoxyMb.

With increased depth, there was a greater percentage of DeoxyMb determined with the SfR throughout the display. Furthermore, the DeoxyMb tended to decrease during retail display at depths 2 - 5 mm. The loss of DeoxyMb parallels the increase in MetMb during retail display reported by the SfR probing. The results indicated the oxidation of DeoxyMb would lead to the formation of MetMb. Furthermore, internal (2 - 5 mm) DeoxyMb determined with the SfR was greater than the reported DeoxyMb at the surface by the HunterLab spectrophotometer. The HunterLab spectrophotometer cannot evaluate the subsurface myoglobin, and therefore, the HunterLab spectrophotometer would not expect to align with interior myoglobin analysis by the SfR probe.

Relationship between the myoglobin forms determined on the surface by HunterLab spectrophotometer and in depths estimated by SfR spectroscopy

The correlation and regression between *a** values and the HunterLab spectrophotometer and SfR spectroscopy for DeoxyMb, OxyMb, and MetMb are presented in Tables 3.3 and 3.4. OxyMb and MetMb forms calculated from HunterLab MiniScan reflectance values had a greater relationship with *a** values (based on correlation and regression coefficient). However, DeoxyMb had a moderate relationship with surface *a** values. Both Deoxy and OxyMb values calculated from needle-probe SfR reflectance had a moderate relationship with surface *a** values. Nevertheless, MetMb calculated from needle-probe SfR spectroscopy had a greater relationship with surface *a** values. With all forms, the relationship with surface *a** values decreased with an increase in depth, indicating a need for developing tools to characterize interior myoglobin forms.

Metmyoglobin reducing ability

The metmyoglobin reducing ability was evaluated on the retail and interior surfaces during retail display (Table 3.5). For retail surface, metmyoglobin reducing ability decreased ($P < 0.05$) during retail display, while the interior surface was unchanged ($P > 0.05$). The retail surface had lower ($P > 0.05$) metmyoglobin reducing ability compared to the interior surface on d 3 and d 5 of retail display.

Oxygen consumption

There was a significant retail display day × oxygen exposure interaction for oxygen consumption (Table 3.6). Oxygen consumption for the interior surface increased ($P < 0.05$) with retail display day, while the oxygen consumption of retail surface decreased ($P < 0.05$) in oxygen consumption. Oxygen consumption of the retail surface was lower ($P < 0.05$) than the interior surface at d 3 and d 5 of retail display.

Oxygen penetration

There was a significant retail day effect on surface layer depth (Table 3.7). From d 0 to d 3 of display, the surface layer of MetMb and OxyMb increased ($P < 0.05$), indicating a greater oxygen penetration. There were no differences ($P > 0.05$) between d 3 and d 5 surface layer depth. As the surface layer was measuring both OxyMb and MetMb, the changes in the two forms may not lead to differences in oxygen penetration depth.

DISCUSSION

The overall goal of this study was to develop tools to understand the basic concept or steps in meat discoloration within a steak. Using needles to measure color on steaks in

retail conditions is not feasible due to food safety concerns. Hence, this tool cannot be used in industry settings. However, this is the first report of characterizing sub-surface myoglobin forms and can be used to study the impact of muscle-specific, packaging, or antioxidant effects on discoloration.

Intact muscle measurements using portable spectrophotometers may quantify only surface meat color changes. In the current research, we utilized an economically important color labile, *psoas major*, muscle to characterize interior and surface color changes. Various studies also reported short color stability of the *psoas major* muscle (McKenna et al., 2005; O'Keeffe & Hood, 1982; Abraham, Dillwith, Mafi, VanOverbeke, & Ramanathan, 2017; Joseph, Suman, Rentfrow, Li, & Beach, 2012; Ke et al., 2017; McKenna et al., 2005).

Surface MetMb content determined by HunterLab MiniScan spectrophotometer (Ke et al., 2017; McKenna et al., 2005; Mohan et al., 2010b) and extraction method (Jeong et al., 2009) noted greater discoloration with increased display time (Jeong et al., 2009; Ke et al., 2017; McKenna et al., 2005). Almost all reflectance spectroscopy technologies rely upon comparing the spectral change of the light after interacting with tissue with respect to the innate spectrum of light introduced into the medium over a spectral range wherein the targeted molecules (e.g., OxyMb, DeoxyMb, and MetMb), preferably have high spectral contrast over other molecules (referred to as spectrally significant). The spectral attenuation of the light over a reasonably well-defined light-pathlength, when interacting with the medium, is computed with a mathematical model of the light-tissue interaction that is always custom to the configuration of the applicator to resolve the concentrations of the individual spectral significant components such as

OxyMb, DeoxyMb, and MetMb. The HunterLab MiniScan, due to its blanketed light illumination and detection needed for being compatible with the underlying algorithm of spectral approximation, limits the sensitivity to the metmyoglobin content near the surface (Piao et al., 2022). Hence, the interior discoloration cannot be determined using a HunterLab MiniScan. The extraction procedure leads to over-estimation of MetMb due to oxidation during the extraction procedure and under-estimation of DeoxyMb due to rapid interconversion when exposed to air. In the current research, needle-probe SfR spectroscopy was able to detect increased MetMb with greater depth and storage time. The needle-probe allowed the introduction of the single-fiber to locally sample the myoglobin. SfR spectroscopy, due to its extremely small profile, has been utilized in assessing tissues via invasive or minimally invasive procedures that are otherwise difficult to access. For example, SfR probe was introduced via the instrument channel of an endoscopic probe to assess tissue in the lung for fine-needle aspiration (Kanick et al., 2010). SfR probe was introduced percutaneously to the intervertebral disk to assess the mineralization condition subjected to laser disk ablation (Piao et al., 2014). SfR was also used via needle-probe to assess lipid deposition *in vivo* in rat liver developed as a model of hepatic steatosis (Piao et al., 2015). The 400 μm fiber used in this work would sample tissue of a volume with a diameter approximately the size of the fiber (Piao et al., 2012). This made the measurements at a depth interval of 1mm to be more specific to the depth to make it locally informative.

Internal myoglobin changes have been reported using an oximeter at approximately 1 cm depth, NIR DRS at approximately 1.5 mm depth, and multispectral imaging. With an oximeter, there has been a decrease in the OxyMb content of the *psoas*

major muscle during retail display (Mohan et al., 2010b). There was a numerical increase in MetMb content of the *psoas major* reported when determining OxyMb and DeoxyMb with an oximeter (Mohan et al., 2010b). The results reported by the oximeter align with the changes reported for OxyMb at the surface from the spectrophotometer and at 1- and 2-mm depths using the SfR in the present study. With NIR-DR spectroscopy, the OxyMb content decreased, whereas the MetMb content increased for the *longissimus* muscle during retail display (Piao et al., 2022). The NIR-DR spectroscopy reported changes reaching up to 1.5-mm depth and aligned with changes of OxyMb and MetMb at 1- and 2-mm depths in the *psoas major* muscle demonstrated with the SfR in the current study. Mohan et al. (2010b) reported an initial loss of DeoxyMb content in the *psoas major* from d 0 to d 2 of retail display with no subsequent changes in DeoxyMb using an oximeter. Similarly, DeoxyMb content reported little change when determined using a NIR-DRS (Piao et al., 2022). These results align with the changes reported in DeoxyMb at the surface by the HunterLab spectrophotometer and at 1-mm depth by the SfR. Furthermore, multispectral imaging reported the greatest DeoxyMb content deeper than 2 mm in the *longissimus* muscle (Sáenz et al., 2008) in support of the SfR results. As OxyMb content determined by the SfR remained constant between 3 - 5 mm, the decline in DeoxyMb content and increase in MetMb content was rapid between 3 - 5 mm. These results support the oxidation of DeoxyMb to MetMb internally. Limited studies have reported the conversion in the sub-surface in intact steaks. Therefore, using the SfR allowed the determination of the sub-surface changes in MetMb, DeoxyMb, and OxyMb.

Myoglobin is prone to oxidation at low oxygen partial pressure conditions (Brantley, Smerdon, Wilkinson, Singleton, & Olson, 1993; George & Stratmann, 1952).

In intact muscle, the rate of myoglobin oxidation is highest at 5 – 7 mmHg oxygen partial pressure (Ledward, 1970). As postmortem mitochondria continue to consume oxygen (Tang et al., 2005a), myoglobin oxidation has been reported subsurface of OxyMb in the *psoas major* muscle (Limsupavanich et al., 2004, 2008). Furthermore, the depth of MetMb increases numerically during storage (Limsupavanich et al., 2004, 2008). Under low oxygen partial pressure, DeoxyMb rapidly oxidizes to MetMb (Brantley et al., 1993; George & Stratmann, 1952; Ledward, 1970). In addition, OxyMb depth decreases with greater oxygen exposure time in the *psoas major* muscle, likely due to the formation of low oxygen partial pressure subsurface (Limsupavanich et al., 2004, 2008). The changes in depth reported by Limsupavanich et al. (2004, 2008) support the SfR quantification of the loss of OxyMb and the increase in MetMb at 1- and 2-mm depths during retail display. The current study's oxygen penetration increase also supports interior myoglobin redox changes. The SfR method allows a better understanding of oxidation changes during storage.

In the current research, metmyoglobin reducing ability and oxygen consumption was determined on surface exposed to air and the interior to better understand interior discoloration. Most published studies reported metmyoglobin reducing ability and oxygen consumption of one surface. Both metmyoglobin reducing ability and oxygen consumption of surfaces exposed to air decreased with storage time. Previous research also reported that the metmyoglobin reducing ability of the retail surface decreased during retail display (Joseph et al., 2012; McKenna et al., 2005). Mancini, Seyfert, and Hunt (2008) reported greater metmyoglobin reducing ability for the interior surface than the retail surface of the *psoas major* muscle aligning with the current study. Therefore,

lower surface metmyoglobin reducing ability and oxygen consumption can promote interior meat discoloration.

CONCLUSION

An in-house needle-probe SfR spectroscopy was developed to quantify sub-surface myoglobin forms. The myoglobin forms quantified on beef *psoas major* steaks over a depth of 1 mm to 5 mm demonstrated an increase in MetMb content with storage time, while DeoxyMb content decreased in the interior. Oxygen consumption and metmyoglobin reducing ability of steaks exposed to air decreased with increased storage time. The MetMb determined by the SfR measurements at 1 mm depth correlated ($r = -0.85$) with HunterLab a^* values. However, the relationship between surface color and interior color decreased with increased depth. The current research suggests that needle-probe SfR spectroscopy would be a viable system to evaluate internal myoglobin changes which influence retail color.

Table 3.1. Proximate compositions (%) and pH of the *psoas major* steaks (n = 7) on day 0 of display

Parameter	Mean	Standard error
Protein	21.13	0.51
Moisture	73.88	1.58
Fat	5.67	2.31
pH	5.72	0.09

Table 3.2. Effects of retail display day on color attributes of *psoas major* steaks (n = 7)

Retail display day	*L**	*a**	Chroma	Hue
0	39.62^{a}	30.07^{a}	37.59^{a}	36.82^{e}
1	36.86^{b}	25.68^{b}	32.50^{b}	37.81^{de}
2	36.13^{cb}	22.68^{c}	29.28^{c}	39.40^{dc}
3	34.26^{d}	21.83^{c}	29.32^{c}	42.13^{ba}
4	38.94^{a}	16.91^{d}	22.28^{d}	40.88^{bc}
5	34.94^{cd}	15.55^{d}	21.38^{d}	43.33^{a}
	SEM = 0.93	SEM = 1.08	SEM = 1.18	SEM = 1.38

$^{a\text{-}e}$Least squares means with different letters are different ($P < 0.05$).
SEM = standard error of mean

Table 3.3 Pearson's correlation between (a) surface myoglobin forms calculated from HunterLab Miniscan spectrophotometer and surface *a** values and (b) the myoglobin forms at various depths calculated from needle probe single-fiber reflectance (SFR) spectroscopy and HunterLab MiniScan surface *a** values

(a)	Location	HunterLab DeoxyMb	HunterLab OxyMb	HunterLab MetMb
	HunterLab (Surface *a**)	-0.57*	0.96*	-0.95*

(b)	Depth (mm)	SFR DeoxyMb vs. surface *a**	SFR OxyMb vs. surface *a**	SFR MetMb vs. surface *a**
	1	0.63*	0.59*	-0.85*
	2	0.61*	0.40*	-0.78*
	3	0.64*	0.30	-0.79*
	4	0.51*	0.16	-0.62*
	5	0.34*	0.20	-0.57*

* denotes significant correlations ($P < 0.05$).

Table 3.4 Simple linear regression analysis between (a) surface myoglobin forms calculated from HunterLab Miniscan spectrophotometer and surface *a** values and (b) the myoglobin forms at various depths calculated from needle probe single-fiber reflectance (SFR) spectroscopy and HunterLab MiniScan surface *a** values the NIR percent myoglobin forms at various depths and the HunterLab spectrophotometer percent myoglobin forms and *a** values at the surface

a)	Location	HunterLab DeoxyMb	HunterLab OxyMb	HunterLab MetMb
	HunterLab (Surface *a**)	0.32*	0.93*	0.90*
b)	Depth (mm)	SFR DeoxyMb vs. surface *a**	SFR OxyMb vs. surface *a**	SFR MetMb vs. surface *a**
	1	0.40*	0.35*	0.72*
	2	0.37*	0.16*	0.62*
	3	0.41*	0.09	0.62*
	4	0.27*	0.02	0.38*
	5	0.11*	0.04	0.33*

* denotes significant regressions ($P < 0.05$).

Table 3.5 Effect of location[1] on the metmyoglobin reducing ability[2] of *psoas major* steaks (n =7) displayed for 5 d

	Retail display day		
Location	0	3	5
Interior	1.00[a]	0.99[a]	1.00[a]
Retail surface	1.00[a]	0.81[c]	0.85[b]
	SEM = 0.01		

[a-c]Least squares means with different letters are significantly different ($P < 0.05$).
[1]Location of analysis indicates as the retail surface and as the interior of the muscle.
[2]Metmyoglobin formation after submersion in sodium nitrite solution determined by K/S ratio of metmyoglobin (K/S 572 ÷ K/S525)., where a greater number indicates greater reduction.
SEM = standard error of mean

Table 3.6. Least squares means of oxygen consumption[1] (retail display day × location[2]) of *psoas major* steaks (n = 7) displayed for 5 d

	Retail display day		
Location	0	3	5
Interior	0.15[bc]	0.19[ab]	0.22[a]
Retail surface	0.15[bc]	0.13[cd]	0.09[d]
	SEM = 0.02		

[a-d]Least squares means with different letters are significantly different ($P < 0.05$).
[1]Change in oxymyoglobin formation before and after incubation for 30 minutes determined by the change in K/S ratio of oxymyoglobin (Preincubation K/S610 ÷ K/S525 – Post incubation K/S610 ÷ K/S525).
[2]Location of analysis indicates as the retail surface and as the interior of the muscle.

Table 3.7. Effect of retail display day on percent surface layer depth[1] of *psoas major* steaks (n = 7)

Retail display day	Surface layer depth (%)
0	0.00 [b]
3	32.04[a]
5	35.86[a]
	SEM = 2.34

[ab]Least squares means with different letters are significantly different ($P < 0.05$).
[1]Depth of the layer of oxymyoglobin and metmyoglobin on the oxygen exposed surface of muscle after retail display relative to the piece width. % oxygen penetration = (depth after retail / piece size) x 100
SEM = standard error of mean

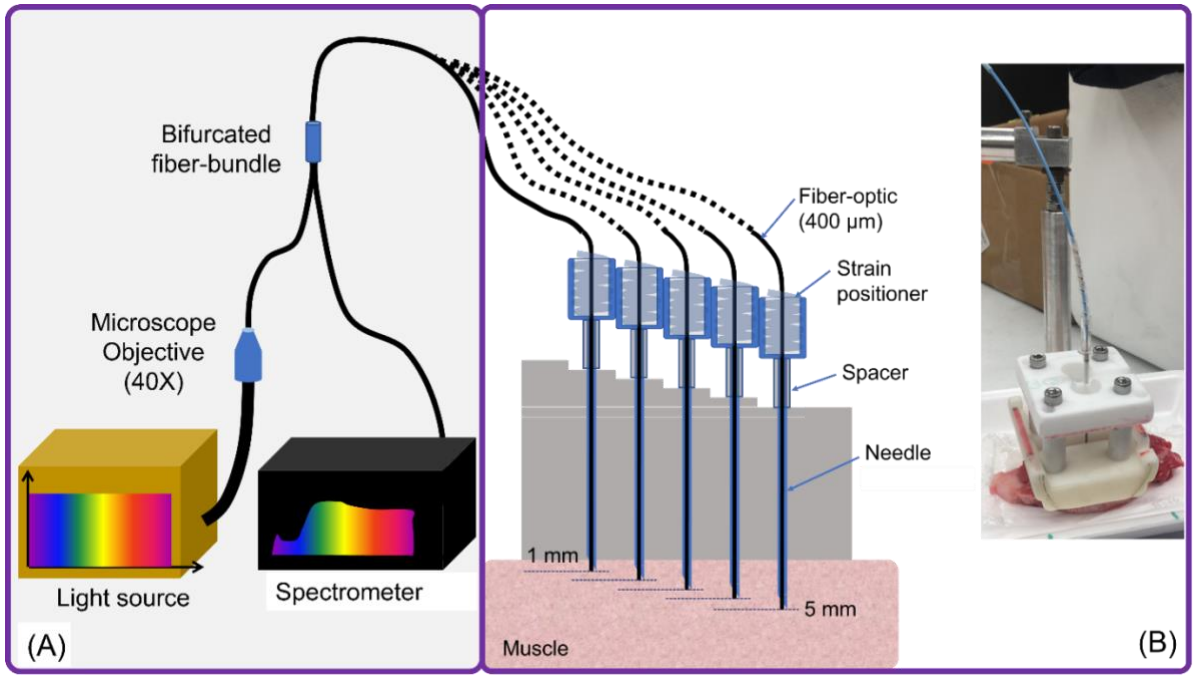

Figure 3.1. Schematic of the single-fiber-reflectance SfR fitted with a needle-probe for assessing myoglobin composition in muscle below the surface at an increment of 1 mm from a depth of 1 mm to 5 mm. (A) The illumination of a white light source was coupled to a 400 µm fiber by using a microscope objective lens. The 400 µm fiber was one branch of a bifurcated fiber bundle. The bundled side of the fiber consisting of two side-by-side placed 400 µm fibers was coupled to a 400 µm percutaneous laser disk ablation fiber of approximately 2 m length. The straight cleaved 400 µm percutaneous laser disk ablation fiber that is straight cleaved was inserted into a stylet- removed 17-gauge needle. The fiber was held in position by using a spiral wire strain squeezed into the barrel of the needle. The squeezing of the spiral wire by the barrel of the needle caused the spiral wire strain to press on the tight sleeve of the fiber to maintain the position of the fiber in the needle. The fiber's position in the needle was set to extrude approximately 0.5 mm beyond the beveled tip. A heat-shrinking tube was outfitted to the needle to be used as a spacer to control the terminal position of the needle with respect to the platform.

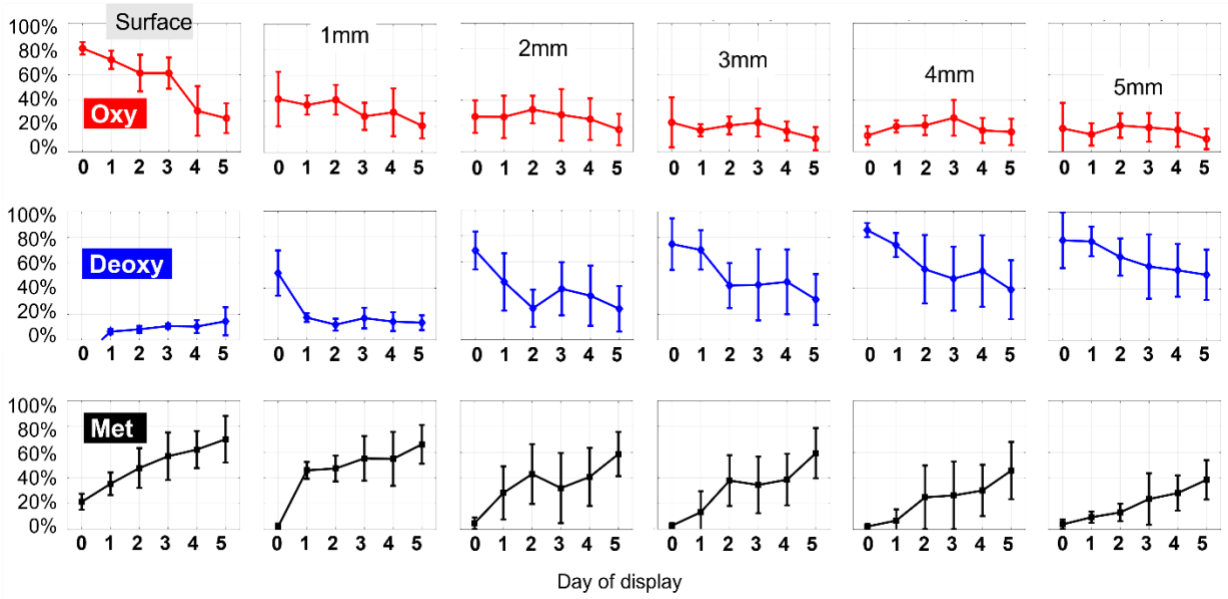

Figure 3.2. The percentage compositions of oxymyoglobin (top row), deoxymyoglobin (middle row), and metmyoglobin (bottom row) assessed on the surface of the muscle by HunterLab MiniScan (the first figure on each row) and at depths from 1 mm to 5 mm with an increment of 1 mm estimated by the needle-probe SfR. Within each subfigure, the specific form of myoglobin is plotted with the mean and standard deviation averaged for 7 samples and measured daily over days of display 0 to display 5.

CHAPTER IV

OXYGEN EXPOSURE EFFECTS ON THE BIOCHEMICAL ATTRIBUTES OF *LONGISSIMUS LUMBORUM* MUSCLE DURING RETAIL DISPLAY

ABSTRACT

Limited studies have compared the effects of oxygen exposure on biochemical properties related to color stability. The objective of this study was to evaluate the effects of oxygen exposure on the biochemical attributes of *longissimus lumborum* muscle. Steaks were (1.91 cm) sliced from USDA Low Choice beef strip loins (n = 7), packaged in PVC overwrap trays, and randomly assigned to 3 d or 6 d of retail display. During display, instrumental color was evaluated daily using a HunterLab MiniScan spectrophotometer. The display surface was considered as oxygen exposed (OE), while the interior of the steak was denoted as not exposed to oxygen (NOE). NOE surface was obtained by slicing the steak in half parallel to the previously OE surface. The NOE and OE surfaces were used to determine oxygen consumption and metmyoglobin reducing ability (metmyoglobin reducing ability). Nitrite-induced metmyoglobin reduction was used to measure metmyoglobin reducing ability, while changes in deoxymyoglobin level with vacuum were used as an indicator of oxygen consumption. The data were analyzed using the GLIMMIX procedure of SAS (SAS 9.4, SAS Institute Inc., Cary, NC) and considered significant at $P < 0.05$. NOE steak surface had greater ($P < 0.05$)

metmyoglobin reducing ability compared with OE surfaces. Oxygen exposure affected the oxygen consumption of the steaks, with the OE surfaces having lower ($P < 0.05$) oxygen consumption compared to NOE surfaces on d 6 of display. The exposure of oxygen to the muscle resulted in a decrease in activity, paralleling in decline in retail color and color stability. The OE metmyoglobin reducing ability was highly correlated ($P < 0.05$) with a^* values during retail display. In conclusion, the presence of oxygen can result in negative impacts on the shelf life of steaks; however, the non-exposed interior of muscle remains more biochemically active.

INTRODUCTION

Consumers consider meat color important to the perceived quality of the product (Holman et al., 2017). More specifically, consumers prefer to see a bright-cherry red color formed by oxymyoglobin on the surface of a steak (Carpenter et al., 2001). Oxymyoglobin can be oxidized to create metmyoglobin or discoloration on the surface of meat. At around 20% discoloration, consumers and trained panelists begin to discriminate against meat products (Hood & Riordan, 1973; Limsupavanich et al., 2008). Recently, it has been estimated surface discoloration costs the meat industry approximately $3.73 billion annually (Ramanathan et al., 2022a). Surface discoloration from metmyoglobin formation can be increased by a variety of factors including but not limited to high temperature (Brown & Mebine, 1969; Snyder & Ayres, 1961; Yin & Faustman, 2002), low pH (Apple, Sawyer, Meullenet, Yancey, & Wharton, 2011; Brown & Mebine, 1969; Yin & Faustman, 2002), increased lipid oxidation (Faustman et al., 2010; Lynch & Faustman, 2000), and low oxygen partial pressure (Brown & Mebine, 1969; George & Stratmann, 1952). Low oxygen partial pressure led to the formation of metmyoglobin

below the surface layer of oxymyoglobin in meat (Sáenz et al., 2008). This phenomenon created layers of myoglobin forms in the muscle of the visible oxymyoglobin, below surface metmyoglobin, and interior deoxymyoglobin (Limsupavanich et al., 2004, 2008). The depth of the oxymyoglobin and deoxymyoglobin layers has been reported to indicate color stability (McKenna et al., 2005; O'Keeffe & Hood, 1982). The movement of the metmyoglobin layer to the surface through oxidation of reduced myoglobin forms in aerobically packaged meat is key to consumer perception of meat products (Limsupavanich et al., 2004, 2008). The understanding of metmyoglobin layer formation is limited while research on the influence of oxygen partial pressure in packaging systems has been more extensive. Research has reported aerobic packaging types such as PVC and HiOx-MAP has greater metmyoglobin formation compared to anaerobic packaging (Lanari & Cassens, 1991; Łopacka et al., 2017; Yang et al., 2016). Therefore, oxygen conditions and oxygen penetration into muscle play a role in metmyoglobin formation on the surface and extension of color stability. Extensive research has looked to limit metmyoglobin formation on the surface of meat to extend color stability. However, the connection between oxygen exposure from retail and metmyoglobin formation subsurface on the biochemical attributes of the *longissimus lumborum* muscle indicating color stability has not been determined.

In addition to instrumental color analysis, metmyoglobin reducing ability and oxygen consumption have been reported to indicate color stability in retail (O'Keeffe & Hood, 1982; Sammel et al., 2002). Using procedures established by the American Meat Science Association Meat Color Guidelines (King et al., 2023), oxygen consumption and metmyoglobin reducing ability can be evaluated using the retail (oxygen exposed) or the

interior (non-oxygen exposed) surfaces. Research has reported using the oxygen exposed (OE) surface and the non-oxygen exposed (NOE) surface for metmyoglobin reducing ability evaluation and reported a better correlation between the OE metmyoglobin reducing ability and color stability in retail than the NOE metmyoglobin reducing ability (Mancini et al., 2008). This research demonstrates the importance of considering the oxygen exposure when evaluating biochemical attributes. Therefore, determining the surface best used to evaluate metmyoglobin reducing ability and oxygen consumption in relation to retail color stability would help to evaluate and limit metmyoglobin formation. The objectives of this study were to determine the effects of oxygen exposure in retail on the biochemical attributes of the *longissimus lumborum* muscle and evaluate the effect of oxygen exposure on parameters used to represent color stability.

MATERIALS AND METHODS

Materials

Seven USDA Low Choice strip loins (IMPS #180) were collected from a local processing facility 5 days postmortem and transported back to Oklahoma State University Food and Agricultural Products Center on ice. On d 7 postmortem, loins were removed from their packaging, and pH was measured in three locations across the loin using a probe-type pH meter (Handheld HI 99163; probe FC232; Hanna Instruments). From the anterior end, loins were faced then sliced using a meat slicer (Bizerba USA INC., Piscataway, NJ) into six 1.91-cm steaks. Steaks were randomly selected to be packaged in pairs in white Styrofoam® trays overlapped with PVC (15,500-16,275 cm^3 O_2/m^2/24 h at 23°C, E-Z Wrap Crystal Clear Polyvinyl Chloride Wrapping Film, Koch Supplies, Kansas City, MO) The packaged steaks were randomly selected for 3 d or 6 d in retail

display. One steak was used for the d 0 analysis of the NOE surface of the loins. The sixth-positioned steak was used for proximate analysis.

Proximate composition

Each steak was ground using a table-top grinder (Big Bite Grinder, 4.5 mm, fine grind, LEM) and approximately 200 g of ground meat were placed in a 140-mm sample cup. A FoodScan Lab analyzer (Serial No. 91753206; Foss, NIRsystem Inc.; Slangerupgrade, Denmark) was used to determine the percent moisture, fat, and protein for each loin by near-infrared spectrophotometry. Means of proximate composition were reported.

Retail display

White coffin style cases were used for a simulated retail display using continuous LED lighting (Philips LED lamps, 12 watts, 48 inches, color temperature = 3,500°K,54 Phillips, China) for 6 d at 2 ± 1°C. Instrumental color was evaluated every day on steaks selected for 6 days in retail using a HunterLab 4500L MiniScan EZ Spectrophotometer (2.5-cm aperture, illuminant A, and 10° standard observer angle, HunterLab Associates, Reston, VA). Three scans were taken on each steak in the package for a total of six scans per package. From the CIE a^* and b^* values, the chroma $\left[\sqrt{(a^{*2} + b^{*2})}\right]$ and hue $(\tan^{-1}(\frac{b^*}{a^*}))$ were calculated.

Oxygen exposure

Oxygen exposure was determined by the diagram described in Figure 4.1. Retail surfaces used for instrumental color analysis were considered the OE surface. The

interior of the muscle was the NOE surface. For comparison of the surfaces, steaks were bisected parallel to the retail surface to expose the NOE surface.

Lipid oxidation

On d 0, d 3, and d 6 of display, lipid oxidation was evaluated using the Thiobarbituric Acid Reactive Substances method from Denzer et al., (2022). From each sample, 3 grams of both the NOE and OE surface was removed then blended with 27 mL of trichloroacetic acid. The homogenate was filtered through a Whatman No. 42 filter paper. One mL of filtrate was combined with 1 mL of Thiobarbituric acid and heated for 10 min at 100°C then cooled for 5 min. At 532 nm, the absorbance was evaluated using a UV-Vis Spectrophotometer (UV-2600, UV-VIS Spectrophotometer, Shimadzu, Columbia, MD) and subsequently converted to mg of malondialdehyde per kg of sample.

Metmyoglobin reducing ability

On the selected day of retail, packages were removed from the display, and steaks assigned to metmyoglobin reducing ability had a rectangle, devoid of fat portion removed. The portion was cut parallel to the retail surface to create an NOE and OE surface. Both the NOE and OE surfaces were evaluated for metmyoglobin reducing ability by a modified procedure from Sammel et al. (2002). Samples were submerged in 0.3% sodium nitrite solution for 20 min to evaluate nitric oxide induced metmyoglobin reducing ability. Initial metmyoglobin formation was determined using a HunterLab 4500L MiniScan EZ Spectrophotometer with three scans on each surface. The K/S ratio of K/S572 ÷ K/S525 was used to calculate the amount of metmyoglobin formed with a greater number indicating a lower metmyoglobin formation and greater reduction.

Oxygen consumption

The same procedure to expose the OE and NOE surfaces was completed on the steak assigned to oxygen consumption. Oxygen consumption was determined by oxygen exposure of both the NOE and OE surface for 1 h at 4ºC. Samples were vacuum packaged, incubated at 30ºC for 60 min, and read using the HunterLab 4500L MiniScan EZ Spectrophotometer at 0, 30, and 60 min. The zero-time point was used for evaluating instruemntal between the NOE and OE surfaces. To determine the oxygen consumption, the change in oxymyoglobin formation during incubation was determined by the preincubation K/S610 ÷ K/S525 – post incubation K/S610 ÷ K/S525. A greater change in oxymyoglobin indicates a greater oxygen consumption.

Oxidation via oxygen consumption

Samples for both the NOE and OE surfaces were evaluated for oxidation via oxygen consumption during incubation. A HunterLab 4500L MiniScan EZ Spectrophotometer was used to evaluate samples after a bloom period for 1 h at 4ºC. The samples were read at 30 min and 60 min of incubation for metmyoglobin formation. Metmyoglobin was determined by the K/S ratio of K/S572 ÷ K/S525 at 30 min and 60 min of incubation. By evaluating metmyoglobin, the reducing capacity of samples was evaluated in the transition between oxymyoglobin to metmyoglobin to deoxymyoglobin in anaerobic conditions in addition to the oxygen consumption. A low oxygen consumption could extend the period of time in low oxygen partial pressures leading to greater oxidation of myoglobin and formation of metmyoglobin.

Oxygen penetration

Oxygen penetration was considered the area which oxygen has diffused into the muscle forming metmyoglobin and oxymyoglobin. This penetration was separated into two terms for the two different surfaces of OE and NOE. Oxygen depth was the oxymyoglobin and metmyoglobin layers of the NOE surface formed after 1 h bloom at 4ºC. A handheld caliper was used to measure the depth of oxymyoglobin and metmyoglobin three times across the surface of the steak lateral to the cut surface. Additionally, the thickness of the steak piece was measured to determine the percent oxygen depth based on the size of the steak piece. Oxygen depth measurements are further detailed in Figure 4.1.

Surface layer depth was analyzed for the NOE and OE surfaces as the depth of oxymyoglobin and metmyoglobin layers. For the OE surface, the surface layer depth was measured lateral to the retail surface. The surface layer depth of the NOE surface was analyzed after 1 h bloom at 4ºC. To expose the surface layer of the NOE surface, approximately 2 mm was sliced transversely to the cut surface to re-expose the lateral surface. At three locations, the depth was measured lateral to the cut surface. Percent surface depth was determined based on surface layer oxygen depth divided by the thickness of the steak piece.

Statistical analysis

This experiment was a split-plot design with a randomized block. The loin was considered the block and random effect. The whole plot experimental unit was the steak with the whole plot factor as the pull day in retail display. The sub-plot factor was the oxygen exposure with the experimental unit as the NOE and OE steak pieces. The fixed

effects were the pull day, oxygen exposure, and their interactions. Repeated measures were evaluated for retail display with a covariance structure of first order autoregressive based on the AICC values. PROC GLIMMIX of SAS was used to determine significant effects and interactions with a protected type III F-test. Least square means were determined with the GLIMMIX procedure and separated using the PDIFF option with a $P < 0.05$ considered significant.

Pearson's correlation and simple linear regression analysis were analyzed for the NOE and OE surface parameters and a^* values during retail display. Parameters evaluated include lipid oxidation, metmyoglobin reducing ability, oxygen consumption after 30 min, oxygen consumption after 60 min, oxidation after 30 min, oxidation after 60 min, surface layer oxygen depth, and oxygen depth of the NOE surface. Significant correlation and regression were considered with a $P < 0.05$.

RESULTS

Proximate composition, pH, and lipid oxidation

Results of proximate composition are included in Table 4.1 and align with expected composition. The mean pH for the strip loins were 5.55 indicating pH in the normal range for beef. There were no significant effects for the lipid oxidation of the steaks for all retail days and oxygen exposure (data not reported).

Retail color

Retail day had a significant effect on the L^* values, a^* values, chroma, and hue of the steaks (Table 4.2). As retail time increased, the color stability decreased represented by the decrease ($P < 0.05$) in L^* values, a^* values, and chroma. Therefore, the steaks

appeared less red and darker as retail display time increased. Hue decreased ($P < 0.05$) during retail display indicating minimal shift of the color away from true red. The limited changes in hue angle aligns with the color stability of the *longissimus lumborum* during retail display.

Metmyoglobin reducing ability

There was a significant oxygen exposure × retail day effect on the metmyoglobin reducing ability of the steaks (Table 4.3). The OE surface had a lower ($P < 0.05$) metmyoglobin reducing ability compared to the NOE surface on d 3 and d 6 of retail. There were limited changes ($P > 0.05$) in the metmyoglobin reducing ability of the NOE surface through retail display. The atmospheric oxygen conditions lead to negative impact on the metmyoglobin reducing ability of the *longissimus lumborum* during retail display which could influence the color stability.

Oxygen consumption

There was a significant oxygen exposure × retail day effect on the oxygen consumption of steaks after 30 min of incubation (Table 4.4). The NOE surface of the steaks had greater ($P < 0.05$) oxygen consumption than the OE surface on d 3 of retail display while there was no ($P > 0.05$) difference on d 6 of display. The oxygen exposure did not have a large impact on the oxygen consumption of the *longissimus lumborum*. Oxygen exposure and retail display did not have a significant impact on the oxygen consumption after 60 min.

Instrumental color of the NOE and OE surfaces

There was no difference in the *a** values after the 1 h bloom of the NOE surface and the OE surface after retail display. There was a significant decrease in bloom *a** values of the NOE surface as retail display increased (data not included).

Oxidation via oxygen consumption

Metmyoglobin formation during anaerobic incubation of NOE and OE samples indicated there was a significant retail display day and oxygen exposure effects (Table 4.5 and Table 4.6, respectively). There was less metmyoglobin formed on d 0 compared to d 3 and d 6 of display. The NOE surface had less metmyoglobin compared to the OE surface. Incubation for 60 min resulted in no significant effect of retail display day and oxygen exposure on metmyoglobin formation.

Oxygen penetration

The surface layer depth of the OE surface was measured as the visual layer of oxy- and metmyoglobin after retail display. There was a significant effect of the retail display day on the OE surface layer depth as included in Table 4.7. On d 6 of retail, there was a larger ($P < 0.05$) surface layer of oxy- and metmyoglobin compared to d 0 and d 3 of retail display. The surface layer of the NOE surface was measured after 1 h bloom at 4°C, and there was not a significant day effect on the surface layer of the NOE surface.

Oxygen depth measures the depth of the oxy- and metmyoglobin layers after 1 h bloom at 4°C of the NOE surface of the steak. There was no significant day effect on the oxygen depth of the NOE surface of the steaks.

Correlation analysis

There was a significant negative correlation between pull day and *a** values as expected (Table 4.8). The OE surface layer oxygen depth was significantly negatively correlated with the *a** values. Therefore, development of a larger oxygen penetration layer of oxymyoglobin and metmyoglobin under the retail surface correlates with a decrease in redness. There was a significant positive correlation between *a** value and NOE oxygen depth indicating a greater *a** value correlated with a larger oxygen penetration upon bloom. A significant positive correlation was reported between *a** values and OE metmyoglobin reducing ability. The decline in redness of the retail surface can be correlated with a decrease in metmyoglobin reducing ability activity of the OE surface. This provided an indication of the OE metmyoglobin reducing ability representing the color stability during retail over the NOE metmyoglobin reducing ability. However, oxygen consumption evaluated did not have high correlation with retail *a** values. The oxidation via oxygen consumption had significant positive correlation with *a** values indicating a higher value or lower metmyoglobin correlated with higher *a** values during retail display. Although traditional oxygen consumption methodology was limited in explaining changes in color of the *longissimus lumborum* muscle during retail display, the oxidation via oxygen consumption demonstrated viability. The correlation analysis demonstrates the OE and NOE surface parameters representative of the color stability of *longissimus lumborum* steaks in retail.

Regression analysis

The simple linear regression analysis evaluated the ability of parameters to predict the *a** values during retail display. There was a significant R-squared value for the NOE

oxygen depth (Table 4.9). However, the R-squared value was below 0.5 meaning the NOE depth can explain less than 50% of the variation in the *a** value. Additionally, a significant R-squared between the OE surface metmyoglobin reducing ability and *a** values demonstrated a good linear relationship between the two parameters. The ability of OE metmyoglobin reducing ability to explain the variability of the *a** values in retail made OE metmyoglobin reducing ability a good option to predict color stability. The oxidation via oxygen consumption did explain 47% of the variation in the *a** values during retail display. The R-squared value between the OE surface layer oxygen depth and *a** values was the highest indicating a strong linear relationship between the two parameters. Therefore, the OE surface layer depth can explain large portion of the variation reported in the *a** values during retail display. Overall, the OE surface color stability parameters best represented the changes in color during retail display.

DISCUSSION

Research has shown aerobic packaging is less color stable in comparison to anaerobic packaging (Griffin et al., 1982; Lavieri & Williams, 2014; Mohan et al., 2010b; Reyes et al., 2022). In addition, aerobic packaging such as PVC has more metmyoglobin formation on the surface during retail display than anaerobic vacuum packaging of beef *longissimus lumborum* steaks (Mohan et al., 2010b; Reyes et al., 2022). Development of a metmyoglobin layer underneath the oxymyoglobin layer during retail display has been reported by Limsupavanich et al. (2004) along with a decrease in *a** values during display of *longissimus lumborum* steaks. Similarly, the present study reported an increase in the surface layer depth of OE and subsequent decline in *a** values. High regression and strong negative correlation values of the retail *a** and OE surface layer depth supports the

greater penetration of oxygen during retail display as an indicator of loss of redness. In addition, greater oxygen penetration has been reported to indicate color stability (Limsupavanich et al., 2004, 2008; O'Keeffe & Hood, 1982) aligning with the OE surface layer depth representing color stability in the current study. Anaerobic vacuum packaging has been reported to have higher bloom of the *longissimus lumborum* muscle after storage compared to PVC packaging (Fu et al., 1992). The current study contrasted in the impact of oxygen on bloom as the NOE and OE surface had no difference in bloom *a** values and retail *a** values. Therefore, the oxygen penetration during retail provides insight into the color stability but has limited impact on the oxygenation of the color-stable *longissimus lumborum* muscle.

Research has revealed the oxidation of lipids and myoglobin are interconnected with increased lipid oxidation connected to increased myoglobin oxidation (Faustman et al., 2010; Lynch & Faustman, 2000). Previous research has reported greater lipid oxidation in PVC-packaged *longissimus lumborum* steaks compared to vacuum packaging with greater display time (Fu et al., 1992; Reyes et al., 2022). The present study did not indicate differences in lipid oxidation and limited changes in hue angle when *a** values declined. The lack of differences in lipid oxidation and oxygen consumption may be due to the color stability from glycolytic metabolism (McKenna et al., 2005; Seyfert et al., 2006) and increased antioxidant capacity (Joseph et al., 2012) found in the *longissimus lumborum* muscle. The limited effects of oxygen exposure on lipid oxidation and color stability are supported by the low regression and correlation values for the *a** values and lipid oxidation of both surfaces and minimal impact on oxygen consumption in the present study. The impact of atmospheric oxygen levels on

protein oxidation was more variable with some studies reporting higher protein oxidation levels (Bao & Ertbjerg, 2015) and some studies with minimal impact on protein oxidation compared to anaerobically packaged pork chops (Spanos et al., 2016). Although protein oxidation was not evaluated in the present study, the effects of protein oxidation could lead to the differences reported in metmyoglobin reducing ability based on the oxygen exposure.

The American Meat Science Association Meat Color Guidelines (King et al., 2023) recommends either the retail surface or the interior surface to be used for metmyoglobin reducing ability and oxygen consumption. Past research evaluating metmyoglobin reducing ability and oxygen consumption in relation to color stability has limited focus on the oxygen exposure and many studies do not indicate the surface used. Several studies have reported using the OE surface for metmyoglobin reducing ability (Canto et al., 2016; Joseph et al., 2012; Salim et al., 2019; Seyfert et al., 2006; Wu et al., 2020a; Wu et al., 2020b) and the NOE surface for oxygen consumption (Wu et al., 2020a; Wu et al., 2020b) in *longissimus lumborum* steaks. Studies using the NOE surface for oxygen consumption have reported a decrease in oxygen consumption during retail display for steaks (Wu et al., 2020b) while others reported no change in oxygen consumption (Wu et al., 2020a). An OE Surface to evaluate metmyoglobin reducing ability has demonstrated a decline in metmyoglobin reducing ability during retail display (Canto et al., 2016; Seyfert et al., 2006) or no change in metmyoglobin reducing ability (Salim et al., 2019; Wu et al., 2020a) for *longissimus lumborum* steaks. Some previous studies used two NOE surfaces for metmyoglobin reducing ability and oxygen consumption reporting decreased metmyoglobin reducing ability and oxygen

consumption during retail display (Abraham et al., 2017; Ke et al., 2017). By evaluating oxygen exposure in the present study, the variations in oxygen consumption and metmyoglobin reducing ability may be mitigated.

Current results indicate the potential of OE metmyoglobin reducing ability to represent changes in color stability when compared to oxygen consumption and metmyoglobin reducing ability using NOE and OE surfaces. Mancini et al. (2008) evaluated the differences between metmyoglobin reducing ability of the NOE and OE surfaces. These researchers reported the NOE portions had greater metmyoglobin reducing ability after retail display than the OE portions of *longissimus lumborum* steaks supporting results presented in the current study. This result is supported by the general loss of metmyoglobin reducing ability during retail display seen in past research (Canto et al., 2016; Seyfert et al., 2006). In addition, the NOE surface metmyoglobin reducing ability was not well correlated to the color stability in retail (Mancini et al., 2008) supporting the present results. Mancini et al. (2008) speculated the limited changes in the NOE surface metmyoglobin reducing ability could be due to lower oxygen penetration and limited photooxidation. Based on the results of the present study and the results of Mancini et al. (2008), the OE surface metmyoglobin reducing ability would represent the color stability of the *longissimus lumborum* muscle in retail compared to the metmyoglobin reducing ability of the NOE surface. To our knowledge, no study has compared the use of the NOE and OE surface on the results of oxygen consumption to develop a better understanding of the oxygen exposure as well as determine the surface representative of the retail color stability. However, the low correlation and regression reported between the changes in a^* value during display and the oxygen consumption of

both OE and NOE surfaces indicates the oxygen consumption determined by oxymyoglobin changes may not represent color stability. The oxidation via oxygen consumption of the OE surface may be a more suitable method for evaluating color stability during storage as supported by the correlation and regression results. This methodology represented reduction of formed metmyoglobin under anaerobic conditions as well as oxygen consumption of the *longissimus lumborum* as the steaks transitioned from oxymyoglobin to deoxymyoglobin via metmyoglobin. Therefore, a high oxidation via oxygen consumption indicated both low reduction capacity and low oxygen consumption increasing rapid oxidation of myoglobin. The OE oxidation via oxygen consumption and OE metmyoglobin reducing ability represented the changes in color stability of the *longissimus lumborum* during retail display better than the NOE surface. Oxygen exposure is a key attribute to consider when evaluating color stability in retail.

CONCLUSION

The *longissimus lumborum* muscle is classified as a color stable muscle, and the limited effects of oxygen exposure on the *longissimus lumborum* during retail continue to support the color stability. While oxygen exposure had a detrimental impact on the oxygen consumption and metmyoglobin reducing ability, the NOE surface reported consistent oxygen penetration and no difference in a^* values upon bloom compared to the OE surface. The new methodology of oxidation by oxygen consumption has viability to represent color changes during retail in comparison to the current oxygen consumption method. In addition, changes in the a^* values during retail display were best represented by the OE oxidation by oxygen consumption, OE surface layer depth, NOE oxygen

depth, and OE metmyoglobin reducing ability. The influence of oxygen on color stability attributes should be considered in future studies.

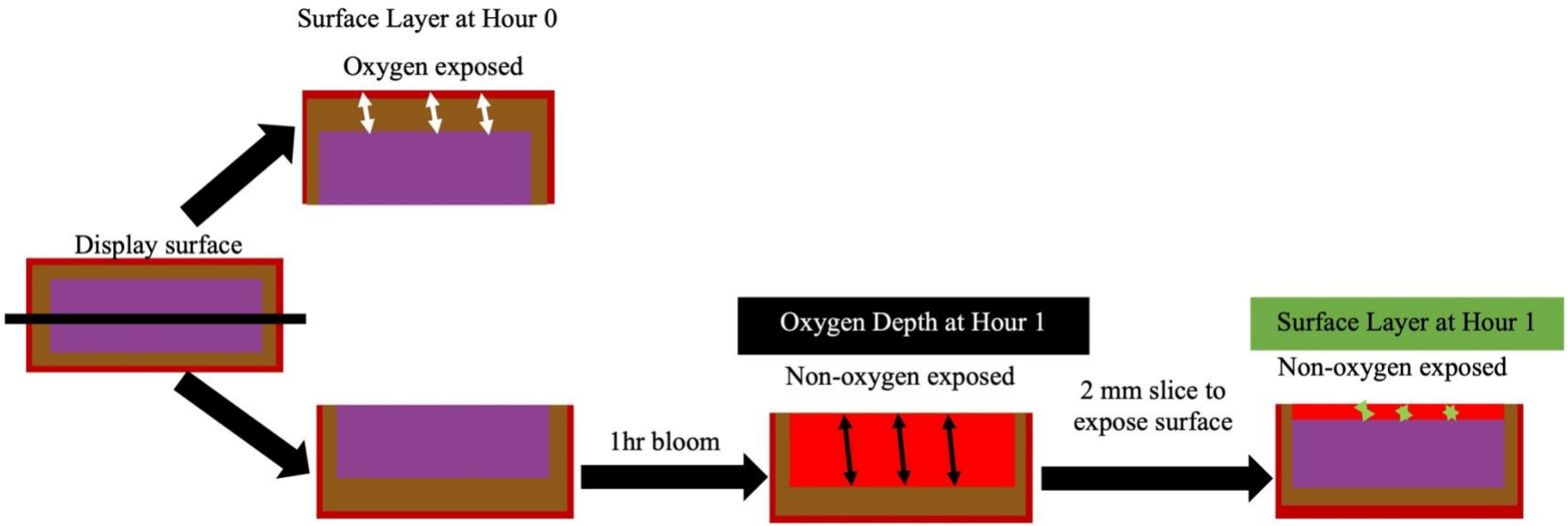

Figure 4.1. Evaluation of oxygen penetration through oxygen exposure of the oxygen exposed and non-oxygen exposed surfaces. [1]Depth of oxymyoglobin and metmyoglobin after retail display. [2]Depth of oxymyoglobin and metmyoglobin after 1 hour bloom of the lateral surface to the freshly cut NOE surface. [3]Depth of oxymyoglobin and metmyoglobin after 1 hour bloom and re-exposure of the lateral surface to evaluate oxygen penetration into the NOE surface.

Table 4.1. Proximate Composition (%) and pH least square means for the *longissimus lumborum* muscles (n = 7)

Parameter	Mean	SEM
Protein	22.57	0.10
Moisture	73.72	0.21
Fat	4.52	0.24
pH	5.55	0.01

SEM = standard error of mean

Table 4.2. Effects of retail display day on color attributes of steaks (n = 7) displayed for 6 d

Retail display day	*L**	*a**	Chroma	Hue
0	43.23^{ab}	35.36^{a}	46.79^{a}	40.89^{a}
1	43.70^{ab}	31.34^{b}	39.14^{b}	36.73^{c}
2	44.42^{a}	30.10^{c}	37.38^{c}	36.32^{d}
3	43.16^{ab}	29.84^{c}	37.12^{c}	36.51^{cd}
4	42.19^{b}	28.18^{cd}	34.97^{de}	36.32^{cd}
5	43.05^{ab}	29.02^{cd}	36.02^{cd}	36.40^{cd}
6	40.29^{c}	27.15^{e}	34.10^{e}	37.28^{b}
	SEM = 1.63	SEM = 0.59	SEM = 0.81	SEM = 0.23

$^{a-e}$Least squares means with different letters are significantly different ($P < 0.05$).
SEM = standard error of mean

Table 4.3. Effect of oxygen exposure[1] on the metmyoglobin reducing ability[2] (metmyoglobin reducing ability) of the steaks (n = 7)

	Retail display day		
Oxygen exposure	0	3	6
Non-oxygen exposed	0.92[a]	0.93[a]	0.93[a]
Oxygen exposed	0.92[a]	0.77[b]	0.76[b]
	SEM = 0.02		

[ab]Least squares means with different letters are significantly different ($P < 0.05$).
[1]Exposure of muscle to oxygen as display surface indicated as exposed or interior of the muscle as not exposed.
[2]Metmyoglobin formation after submersion in sodium nitrite solution determined by K/S ratio of metmyoglobin (K/S 572/K/S525)., where a greater number indicates greater reduction.
SEM = standard error of mean

Table 4.4. Least squares means of oxygen consumption[2] (retail display day × oxygen exposure[1]) of steaks displayed for 6 d

	Retail display day		
Oxygen exposure	0	3	6
Non-oxygen exposed	0.14[a]	0.15[a]	0.12[ab]
Oxygen exposed	0.14[a]	0.09[b]	0.12[a]
	SEM = 0.01		

[a-c]Least squares means with different letters are significantly different ($P < 0.05$).
[1]Exposure of muscle to oxygen as display surface indicated as exposed or interior of the muscle as not exposed.
[2]Change in oxymyoglobin formation before and after 30 minutes of incubation determined by the change in K/S ratio of oxymyoglobin (Preincubation K/S610/K/S525 – Post incubation K/S610/K/S525).

Table 4.5. Effect of retail display day of oxidation by oxygen consumption of steaks (n = 7) displayed for 6 d

Retail display day	Metmyoglobin[1]
0	2.04[a]
3	1.67[b]
6	1.58[b]
	SEM = 0.09

[ab]Least squares means with different letters are significantly different ($P < 0.05$).
[1]Metmyoglobin formation after anaerobic incubation determined by by K/S ratio of metmyoglobin (K/S 572 ÷ K/S525)., where a greater number indicates lower metmyoglobin.
SEM = standard error of mean

Table 4.6. Effect of oxygen exposure[1] of oxidation by oxygen consumption of steaks (n = 7) displayed for 6 d

Oxygen exposure	Metmyoglobin[2]
Non-oxygen exposed	1.86[a]
Oxygen exposed	1.67[b]
	SEM = 0.08

[ab]Least squares means with different letters are significantly different ($P < 0.05$).
[1]Exposure of muscle to oxygen as display surface indicated as exposed or interior of the muscle as not exposed.
[2]Metmyoglobin formation after anaerobic incubation determined by by K/S ratio of metmyoglobin (K/S 572 ÷ K/S525)., where a greater number indicates lower metmyoglobin.
SEM = standard error of mean

Table 4.7. Effect of retail display day on percent surface layer depth[1] of steaks (n = 7) displayed for 6 d

Retail display day	Surface layer (%) after retail
0	0.00[c]
3	60.23[b]
6	66.23[a]
	SEM = 5.82

[ab]Least squares means with different letters are significantly different ($P < 0.05$).
[1]Depth of the layer of oxymyoglobin and metmyoglobin on the oxygen exposed surface of muscle after retail display divided by size of the piece where surface layer was measured. % Surface layer = (Depth after retail / Piece size) x 100
SEM = standard error of mean

Table 4.8. Pearson's correlation between *a** values and color attributes

Parameter	Correlation
Pull day	-0.86*
Non-oxygen exposed lipid oxidation	0.14
Oxygen exposed lipid oxidation	0.16
Non-oxygen exposed metmyoglobin reducing ability	-0.12
Oxygen exposed metmyoglobin reducing ability	0.77*
Non-oxygen exposed oxygen consumption at 30 min	0.18
Oxygen exposed oxygen consumption at 30 min	0.25
Non-oxygen exposed oxygen consumption at 60 min	0.42
Oxygen exposed oxygen consumption at 60 min	0.36
Non-oxygen exposed Oxidation at 30 min	0.30
Oxygen exposed Oxidation at 30 min	0.68*
Non-oxygen exposed Oxidation at 60 min	0.24
Oxygen exposed Oxidation at 60 min	-0.09
Non-oxygen exposed surface layer oxygen depth (%)	-0.15
Oxygen exposed surface layer oxygen depth (%)	-0.83*
Non-oxygen exposed oxygen depth (%)	0.54*

*Significant correlation values indicated.

Table 4.9. Regression between *a** values and color attributes

Parameter	Regression
Non-oxygen exposed lipid oxidation	0.02
Oxygen exposed lipid oxidation	0.03
Non-oxygen exposed metmyoglobin reducing ability	0.02
Oxygen exposed metmyoglobin reducing ability	0.59*
Non-oxygen exposed oxygen consumption at 30 min	0.03
Oxygen exposed oxygen consumption at 30 min	0.06
Non-oxygen exposed oxygen consumption at 60 min	0.18
Oxygen exposed oxygen consumption at 60 min	0.13
Non-oxygen exposed Oxidation at 30 min	0.09
Oxygen exposed Oxidation at 30 min	0.47*
Non-oxygen exposed Oxidation at 60 min	0.01
Oxygen exposed Oxidation at 60 min	0.06
Non-oxygen exposed surface layer oxygen depth (%)	0.02
Oxygen exposed surface layer oxygen depth (%)	0.69*
Non-oxygen exposed oxygen depth (%)	0.29*

*Significant regression values indicated.

CHAPTER V

METABOLITE DIFFERENCES BETWEEN THE OXYGEN-EXPOSED AND NON-OXYGEN EXPOSED SURFACES OF THE *LONGISSIMUS LUMBORUM* MUSCLE

ABSTRACT

The effects of oxygen exposure on the metabolome of the beef *longissimus lumborum* have not been evaluated. Therefore, the objective of this study was to evaluate the impact of oxygen exposure on the metabolome of the *longissimus lumborum* muscle. USDA Low Choice beef strip loins were sliced into steaks (1.91-cm) and packaged in PVC overwrap trays for 3 or 6 days of retail display. The oxygen exposed (OE) surface was the display surface during retail, and the non-oxygen exposed (NOE) surface was the intact interior muscle. Instrumental color was evaluated using a HunterLab spectrophotometer. To analyze the NOE surface on d 3 and 6, steaks were sliced parallel to the OE surface to expose the NOE surface. Metmyoglobin reducing ability was determined by nitrite-induced metmyoglobin reduction. A gas chromatography-mass spectrometry was used to identify metabolites. The least square means were determined using the GLIMMIX procedure of SAS with significance at a $P < 0.05$. Metabolites were analyzed using the MetaboAnalyst 5.0. The a^* values of steaks decreased ($P < 0.05$) with display time. metmyoglobin reducing ability was greater ($P < 0.05$) in the NOE surface compared with the OE surface on d 3 and 6. The loss of succinate from d 0 to d 6 during

retail display reinforced the decline in color during display. Greater alpha-tocopherol in the NOE surface supported less oxidative changes compared to the OE surface during retail display. These results indicate the presence of oxygen can influence metabolite profile and negatively influence metmyoglobin reducing ability and color.

INTRODUCTION

Oxygenation of steaks form bright cherry red oxymyoglobin which is preferred by consumers (Carpenter et al., 2001). Oxygen binds to the sixth position of the heme group on myoglobin to form oxymyoglobin. Oxidation of the heme leads to the formation of metmyoglobin. Metmyoglobin is negatively perceived by consumers due to its Brown pigmentation (Carpenter et al., 2001) and has been reported to cost the meat industry approximately $3.73 billion annually (Ramanathan et al., 2022a). Metmyoglobin forms initially subsurface below a layer of oxymyoglobin (Limsupavanich et al., 2004, 2008). Research has reported that as time in display increases the metmyoglobin layer increases in size and rises to the surface leading to visible surface discoloration (Limsupavanich et al., 2004). Low oxygen partial pressure contributes to the formation of the metmyoglobin layer leading to an increase in the rate of metmyoglobin formation (Brown & Mebine, 1969; George & Stratmann, 1952). While low oxygen partial pressure leads to the formation of metmyoglobin, the partial pressure is created through oxygen consumption in postmortem muscle.

Oxygen is consumed by mitochondria and oxygen-consuming enzymes in postmortem muscle (Ramanathan & Mancini, 2018) leading to variation in oxygen partial pressure in muscle. Oxygen consumption can influence the oxygen penetration and diffusion. The oxygen consumption has been reported to cause the low oxygen partial

pressure subsurface causing the formation of metmyoglobin internally (O'Keeffe & Hood, 1982). Research has reported a smaller penetration result in thinner layer of oxymyoglobin and faster rise of metmyoglobin (Limsupavanich et al., 2004, 2008). Oxygen consumption has been reported to be influenced by postmortem metabolism including mitochondria (Ke et al., 2017). Specifically, mitochondrial degradation can negatively impact the oxygen consumption and lead to reactive oxygen species production (Ke et al., 2017). Furthermore, myoglobin oxidation and lipid oxidation has been linked in muscle and occur through reactive oxygen species (Faustman et al., 2010; Lynch & Faustman, 2000). Therefore, changes in oxygen consumption could influence the oxygen penetration and myoglobin oxidation. Hence, the oxygen exposure in retail could influence the oxidative state of steaks and the oxygen consumption. However, the understanding of the impact of the formation of metmyoglobin and subsequent oxidative changes on the metabolome due to oxygen exposure is limited.

In addition, the metabolome plays a role in color stability as various metabolites have been reported to influence and reduce metmyoglobin. Metmyoglobin reduction can occur through inherent enzymes present in meat such as lactate dehydrogenase (Kim et al., 2006; Kim et al., 2009), malate dehydrogenase (Mohan et al., 2010a), and NADH-dependent cytochrome b5 reductase (Arihara et al., 1995). A key role in these enzymatic pathways are malate and lactate utilization to produce NADH (Kim et al., 2006; Kim et al., 2009; Mohan et al., 2010a). NADH has been reported as an important electron donor in the reduction of metmyoglobin (Arihara et al., 1995; Brown & Snyder, 1969; Kim et al., 2006; Kim et al., 2009; Mohan et al., 2010a). Furthermore, succinate has been reported to increase electron transport mediated metmyoglobin reduction (Tang et al.,

2005b). While the connection between metabolome changes and color stability of the *longissimus lumborum* muscle during display is well understood, there is limited research on the effects of oxygen exposure on the metabolome of the *longissimus lumborum* muscle. Therefore, the objective of this study was to evaluate the effect of oxygen exposure of the retail surface compared to the interior non-oxygen exposed surface of the *longissimus lumborum* muscle on the metabolome of the *longissimus lumborum* muscle.

MATERIALS AND METHODS

Materials

From Creekstone Farms LLC (Arkansas City, KS), USDA Low Choice loins (n = 6; IMPS #173) were transported to Oklahoma State University Food and Agricultural Products Center on ice. On d 7 postmortem, pH (Hanna Instruments pH probe Handheld HI 99163; probe FC232; Hanna Instruments) was analyzed in three random locations across the loin. The face steack was removed from each loin then loins were sliced into six 1.91-cm steaks. One steak was used for d 0 analysis and the entire steak was considered NOE. Four steaks were randomly selected and paired to package in PVC (15,500-16,275 cm^3 O_2/m^2/24 h at 23°C, E-Z Wrap Crystal Clear Polyvinyl Chloride Wrapping Film, Koch Supplies, Kansas City, MO) overwrap Styrofoam® trays for retail display. Packages were assigned to either 3 or 6 d in retail display with continuous LED lighting (Philips LED lamps, 12 watts, 48 inches, color temperature = 3,500°K,54 Phillips, China). Instrumental color was measured six times on each package every day of retail display using a HunterLab 4500L MiniScan EZ Spectrophotometer (2.5-cm

aperture, illuminant A, and 10˚ standard observer angle, HunterLab Associates, Reston, VA). The remaining steak in the sixth position was used for proximate analysis.

Proximate composition

External fat was removed from one steak from each loin. Approximately 200 g from the steak was ground with a able-top grinder (Big Bite Grinder, 4.5 mm, fine grind, LEM) and analyzed with near infrared spectrophotometer (FoodScan Lab Analyzer, Serial No. 91753206; Foss, NIRsystem Inc.; Slangerupgrade, Denmark). The percent protein, fat, and moisture were determined.

Oxygen exposure

Steaks were exposed to oxygen through retail display, and the retail surface was considered OE surface (Figure 5.1). The interior muscle was considered NOE surface and was exposed on the pull days by bisecting parallel to the retail surface. On d 3 or 6, surfaces were analyzed for oxygen consumption, metmyoglobin reducing ability, and metabolomic profiling.

Oxygen consumption

The NOE and OE surfaces were exposed to oxygen 1 h at 4°C, and then packaged in vacuum packaging and incubated at 30°C for 60 min. A HunterLab spectrophotometer read the surface three times at 0, 30, and 60 min to evaluate the change in oxymyoglobin content. Using the spectra from the HunterLab, the preincubation K/S610 ÷ K/S525 – post incubation K/S610 ÷ K/S525 determined the change in oxymyoglobin content through incubation. A greater change in oxymyoglobin indicates greater oxygen consumption.

Metmyoglobin reducing ability

To evaluate metmyoglobin reducing ability, samples were submerged in 0.3% sodium nitrite for 20 min then vacuum packaged and incubated at 30°C for 2 hr. Samples were read using a HunterLab spectrophotometer before and after incubation. To determine metmyoglobin reducing ability, preincubation metmyoglobin was calculated from the K/S ratio of K/S572 ÷ K/S525 with a greater ratio indicating a greater metmyoglobin reducing ability.

Metabolomic analysis

Analysis and subsequent identification of metabolites occurred at the National Institute of Health West Coast Metabolomics Center at the University of California Davis (CA, USA). Freeze dried samples (approximately 10 mg) were stored at -80°C until analysis. To extract metabolites, 1000 µL of degassed acetonitrile/isopropanol/water mixture (3:3:2, v/v/v) was added to the samples. Samples were homogenized for 30 s and shook at 4°C for 6 min then centrifuged at 14,000 g for 2 min. Additionally, carbon 8-carbon 30 fatty acid methyl esters were added to the mixture as an internal standard. Samples were dried with nitrogen gas and derivatized with methyloxolane in pyridine and N-methyl-N(trimethylsilyl)trifluoroacetamide for trimethylsilylation of acidic protons. The remaining details about the metabolomic profiling are included in Fiehn et al. (2008).

Statistical analysis

This experiment was a split-plot design with a randomized complete block blocked by loin. The whole plot factor being the pull day in retail, and the sub-plot factor is oxygen exposure. Instrumental color analysis was evaluated as a repeated measure with

the retail day being the repeated measure. The covariance structure for the repeated measures was first order autoregressive and was selected based on the AICC values. The fixed effects were pull day, oxygen exposure and their interactions. From the GLIMMIX procedure of SAS, least square means were calculated and separated with the PDIFF option and significance was considered with a $P < 0.05$.

Metabolite profiling was evaluated using MetaboAnalyst 5.0. The metabolite peak intensities were normalized by the median, transformed by log, and scaled with Pareto scaling. To compare d 0 and d 6 metabolites as well as NOE and OE surfaces, an analysis of variance was completed to indicate the significantly different metabolites between the two groups with Fisher's LSD used to separate the abundance of specific metabolites. Significance was considered as a $P < 0.05$. Unsupervised principal component analysis (PCA) and supervised projections to latent structure-discriminant analysis (PLS-DA) were used demonstrate differences in metabolites between the pull days and oxygen exposure. Metabolites were ranked based on their importance in determining differences in oxygen exposure and pull day using the variable importance in the projection (VIP) in PLS-DA. A pathway analysis of MetaboAnalyst 5.0 established pathways impacted by significantly different metabolites.

RESULTS

Proximate composition and retail display color

The proximate composition of the strip loins is included in Table 5.1. The mean pH was 5.55 after 7 d postmortem. These results confirm the loins were in normal postmortem pH range for beef. There was a significant effect of retail display day on the

*a** values (Table 5.2). There was a decrease ($P < 0.05$) in redness with greater retail display time.

Metmyoglobin reducing ability and oxygen consumption

Metmyoglobin reducing ability and oxygen consumption were influenced by retail display and oxygen exposure (Table 5.3). The OE surface had lower ($P < 0.05$) metmyoglobin reducing ability than the NOE surface on day 3 and 6 of retail display while the oxygen consumption of the OE surface was only lower ($P < 0.05$) than the NOE on day 3. Overall, the oxygen exposure had a negative impact on the metmyoglobin reducing ability of the *longissimus lumborum* muscle in retail display and may be linked to the loss in redness during display.

Metabolomics

From the nontargeted metabolomics, 403 features were found, and of those, 149 were identified in the metabolite library. The partial least-squares discriminant analysis (PLS-DA) scores plot demonstrates the separation between the metabolite profiles of d 0 NOE, d 6 NOE, and d 6 OE surfaces (Figure 5.2). A variable importance projection analysis reported citric acid, gluconic acid, and ribonic acid as the top metabolites influencing the PLS-DA plot separation between the retail days and oxygen exposure (Figure 5.3). Additionally, KEGG pathway impact analysis was completed to evaluate the metabolic pathways associated with the differently abundant metabolites among d 0 NOE, d 6 NOE, and d 6 OE surfaces (Figure 5.4). Differently abundant metabolites were mostly associated with the TCA cycle, pentose phosphate pathway, and pentose and glucuronate interconversions.

There were thirty differently abundant ($P < 0.05$) metabolites of d 0 NOE surface relative to d 6 OE surface (Table A5.1). Twelve of the metabolites were downregulated on d 0 compared to d 6 while the remaining 18 were upregulated on d 0 NOE versus d 6 OE surface (Figure 5.5). Upregulated metabolites on d 0 included succinic acid, 4-hydroxybutric acid, creatinine, and alpha-tocopherol. Ribonic acid, citric acid, hypoxanthine, gluconic acid, and xylulose are downregulated on d 0 OE surface versus d 6 OE surface. Evaluating the effect of retail display on the metabolite profile of the NOE surface indicated 28 metabolites were differently abundant between d 0 and d 6 of display ($P < 0.05$). Of the 28, 14 metabolites were upregulated, and 14 metabolites were down regulated on d 0 compared to d 6. Stearic acid, saccharic acid, and arachidic acid were upregulated on d 0 compared to d 6 of the non-oxygen exposed surface. Furthermore, metabolites such as xylitol, xylulose, and gluconic acid were downregulated on d 0 compared to d 6. The changes in metabolome during retail display for both surfaces were very similar. The amino acid metabolism increased during display resulting in greater methionine sulfoxide, serine, and tyrosine on d 6 compared to d 0 for both surfaces.

Thirteen metabolites were identified to be differently abundant ($P < 0.05$) in the NOE surface relative to the OE surface on d 6 of retail display. Three metabolites were downregulated on the NOE surface compared to the OE surface. Metabolites such as creatinine, alpha-tocopherol, and 4-hydroxybutyric acid are upregulated while gluconic acid, citric acid, and ribonic acid are downregulated in the NOE surface compared to the OE surface.

DISCUSSION

Several studies have reported the loss of redness during retail display of the *longissimus lumborum* muscle (Abraham et al., 2017; Joseph et al., 2012). Oxygen effects on metmyoglobin reducing ability have been reported in research by Mancini et al. (2008). These researchers determined metmyoglobin reducing ability was lower for the OE surface compared to the NOE surface of the *longissimus lumborum* muscle (Mancini et al., 2008). In addition, there was strong correlation between the OE surface metmyoglobin reducing ability and the loss of redness during retail display (Mancini et al., 2008). Research on the implication of oxygen on the oxygen consumption has been more limited. Several studies have separately evaluated the NOE surface for oxygen consumption of the *longissimus lumborum* muscle during retail display and determined oxygen consumption decreases during retail display (Abraham et al., 2017; Ke et al., 2017). The *longissimus lumborum* has been categorized as a color stable muscle with greater antioxidant capacity (Joseph et al., 2012) and lower oxidative stress (Ke et al., 2017) compared to less color stable muscles such as the *psoas major* muscle. Therefore, the oxygen consumption of the *longissimus lumborum* muscle may not be impacted by the presence of oxygen. The results of the current study indicate the color stability of the *longissimus lumborum* and the limited impact of oxygen exposure on oxygen consumption.

Free amino acids have been reported to increase in the *longissimus lumborum* muscle during storage (Abraham et al., 2017; Ma et al., 2017; Mitacek et al., 2019). Postmortem proteolysis may result in the increase in free amino acids reported such as serine and tyrosine (Feidt, Petit, Bruas-Reignier, & Brun-Bellut, 1996). Tyrosine (Ma et

al., 2017; Subbaraj, Kim, Fraser, & Farouk, 2016) and serine (Mitacek et al., 2019; Subbaraj et al., 2016) have been reported to increase in the *longissimus lumborum* during storage. The connection between these amino acids and color stability is unclear. The enzyme methionine sulfoxide reductase has been reported to reduce methionine sulfoxide to methionine (Lee and Gladyshev, 2011). Meanwhile, methionine sulfoxide has been reported to be a potential biomarker of aging and disease whereas methionine has been used to create antioxidant systems in the body (Lee and Gladyshev, 2011). Wu et al. (2016) reported a strong positive correlation between *a** values and mitochondrial peptide methionine sulfoxide reductase in the *longissimus lumborum* muscle. Joseph et al. (2012) reported more methionine sulfoxide reductase and Abraham et al. (2017) reported more methionine in the color stable *longissimus lumborum* muscle over the color labile *psoas major* muscle. Furthermore, Subbaraj et al. (2016) reported higher methionine in color stable ovine meat compared to color labile. Hence, methionine and methionine sulfoxide reductase have been indicative of color stability. Therefore, the presence of methionine sulfoxide supports less color stability and more myoglobin oxidation during retail display of the muscle.

Fatty acid metabolism decreased during retail display for both the NOE and OE surfaces. Fatty acids such as stearic acid, arachidic acid, and saccharic acid decreased during display. Some studies have reported changes fatty acids in metabolomic analysis (Abraham et al., 2017; Yu et al., 2020). However, there is limited understanding of the impact of fatty acids on meat color stability. Glycerol can be formed through the breakdown of fatty acids for use in the TCA cycle (Mitacek et al., 2019) which would support the changes in fatty acids in the current study. Depletion of creatinine and

glycerol during display indicates the shift of different metabolites to glycolytic metabolism to supply energy during display similarly reported by Mitacek et al. (2019). Furthermore, creatinine had greater abundance in the NOE surface than the OE surface on d 6 of display. Creatinine is naturally present in meat and can be an indicator of meat consumption in humans (Dragsted, 2010). Creatinine content has been reported to increase with aging due to the formation of creatinine from ATP production (Mitacek et al., 2019). Furthermore, creatinine production has been reported to be higher in diseased small ruminant animals compared to healthy animals (Bozukluhan et al., 2018). In physiological conditions, creatinine will be broken down to creatine by the kidneys (Bozukluhan et al., 2018), and the creatinine metabolites methylguanidine and creatol increase in the presence of oxidants (Abramowitz, Meyer, & Hostetter, 2010). Therefore, the presence of oxygen at the retail surface and subsequent oxidative stress may lead to the breakdown and lower content of creatinine in comparison to the interior surface.

Furthermore, sugar metabolism increased during display with ribose and ribonic acid being upregulated on d 6 compared to d 0 for both surfaces. Ribonic acid increased in the *longissimus lumborum* muscle during retail display (Abraham et al., 2017). Ribose has been reported to increase with greater postmortem time in chicken as a contributor to flavor from the breakdown of IMP (Aliani, Farmer, Kennedy, Moss, & Gordon, 2013). Ribose is a component to ATP and may increase due to the ATP needs of postmortem muscle (Dhanoa & Housner, 2007). Furthermore, ribose can lead to the production of NADPH and subsequent formation of ribonic acid (Mahoney et al., 2018). Metmyoglobin reduction has been reported to occur with NADPH (Shimizu & Matsuura, 1968). Therefore, the presence of ribose could contribute to color stability of the *longissimus*

lumborum muscle on both surfaces. Furthermore, ribonic acid was reported to be greater in the OE surface than the NOE surface on day 6. Ribonic acid forms from the breakdown of ribose to create NADPH (Mahoney et al., 2018). NADPH has been reported to act in metmyoglobin reduction (Shimizu & Matsuura, 1968). Therefore, the production of NADPH on the retail surface may be important to color stability in comparison to the more oxidatively stable interior.

The changes in TCA cycle were more metabolite specific. Citric acid and aconitic acid increased during retail display for both surfaces while succinic acid decreased. Citrate can form succinate through the TCA cycle with aconitate acting as in intermediate (Krebs & Johnson, 1980). Succinate has been reported to reduce metmyoglobin through electron transport mediated metmyoglobin reduction (Tang et al., 2005b) and reverse transport metmyoglobin reduction (Belskie et al., 2015). Therefore, the changes in TCA metabolites may be due to forming succinate via citric and aconitic acid to stabilize the color of the *longissimus lumborum* during retail display. Abraham et al. (2017) reported greater citric acid in the *longissimus lumborum* with greater display time but did not indicate oxygen specific effects. Citric acid can be metabolized to form succinate (Krebs & Johnson, 1980). Succinate has been reported to be part of metmyoglobin reduction (Tang et al., 2005b). The accumulation of citric acid at the surface may be due to the increased demands for reduction of metmyoglobin by production of succinate from citrate Therefore, a greater abundance of citric acid on the OE surface may relate to the oxidative changes occurring at the surface.

4-hydroxybutyric acid has been reported as a neurotransmitter in the brain and active in mitochondria (Bourguignon et al., 1988; Caputo, Vignoli, Maremmani,

Bernardi, & Zoli, 2009; Gibson & Nyhan, 1989). In the mitochondria, oxidation of 4-hydroxybutyric acid can form succinic acid (Caputo et al., 2009; Gibson & Nyhan, 1989). As succinate has been used to reduce metmyoglobin, the presence of greater 4-hydroxybutyric acid in the NOE surface may indicate the use of 4-hydroxybutyric acid on the exposed surface to form succinate. Therefore, the NOE would have the ability to maintain color stability.

After death, ATP production continued to occur in beef for an additional 24 hours (Matarneh, England, Scheffler, & Gerrard, 2017). As ATP production decreased with postmortem time, ADP accumulated in excess and from the breakdown of ADP through purine metabolism, hypoxanthine was formed (Matarneh et al., 2017). Hypoxanthine has been reported to increase with aging (Ma et al., 2017) and postmortem time (Yu et al., 2020) supporting the increase during retail display. Hypoxanthine has been reported to increase the formation of a reactive oxygen species superoxide anion as well as decrease the activity of antioxidant enzymes responding to oxidative stress (Mesquita Casagrande et al., 2013; Rodrigues et al., 2014). Therefore, the increased presence of hypoxanthine during retail display could indicate the increased presence of reactive oxygen species and oxidative stress during retail display on both NOE and OE surfaces.

Propylene glycol can contribute to propionate metabolism by forming substrates for the TCA cycle (Zhang et al., 2020a). This process has been reported to occur in negative energy balance conditions in dairy cattle (Zhang et al., 2020a). Therefore, the high energy demanded postmortem could influence the production of propylene glycol. The lower presence of propylene glycol in the exterior may relate to its breakdown to support the production of TCA metabolites such as succinate (Zhang et al., 2020a). On

the surface, succinate production would contribute to metmyoglobin reduction (Tang et al., 2005b) while the interior propylene glycol may remain high due to lower oxidative changes. Overall, the greater presence of propylene glycol on the retail surface could indicate activity to limit metmyoglobin.

Glycolate has been reported to be present in humans and can form glyoxylate and subsequently oxalate (Booth, Conners, Rumsby, & Brady, 2006; Fry & Richardson, 1979). The reduction of glyoxylate to glycolate occurs by lactate dehydrogenase or glyoxylate reductase via consumption of NADH in the muscle to prevent the accumulation of glyoxylate which can be highly reactive (Booth et al., 2006; Mdluli, Booth, Brady, & Rumsby, 2005). Glyoxylate addition has been reported to increase reactive oxygen species leading to apoptosis of cells through effecting membrane potential of the mitochondria (Patra, Ghosh, Alam, & Murmu, 2018). Therefore, the presence of greater glycolate may indicate prevention of reactive glyoxylate formation in the NOE portion of muscle and limited oxidative changes.

Pyrazines have been reported as flavor compounds in beef which increase with cooking temperature and age of the product (Wall, Kerth, Miller, & Alvarado, 2019; Watanabe et al., 2015). The formation of pyrazines occurs through the condensation of amino acids (Mortzfeld, Hashem, Vranková, Winkler, & Rudroff, 2020). However, research specific to the implications of 2,5-dihydroxypyrazine on changes in muscle biochemistry has not been reported.

Isothreonic acid is a product of ascorbate metabolism produced by ascorbic acid oxidation (Arun et al., 2018). A greater formation of isothreonic acid was reported in mice brain under oxidative stress from greater reactive oxygen species (Arun et al.,

2018). Furthermore, isothreonic acid content was greater in obese women under oxidative stress on the surface (Ruebel et al., 2019). Therefore, the oxidation of ascorbic acid may be due to response and prevention of further oxidative stress. Furthermore, ascorbic acid has been reported to reduce metmyoglobin *in vitro* (Tomoda, Tsuji, Matsukawa, Takeshita, & Yoneyama, 1978; Tsukahara & Yamamoto, 1983; Vestling, 1942). Furthermore, ascorbic acid has been reported to extend color stability of beef (Sanchez-Escalante, Djenane, Torrescano, Beltran, & Roncales, 2001, 2003) and lamb (Andres, Petron, Adamez, Lopez, & Timon, 2017) during retail display. Therefore, the greater formation of isothreonic acid may indicate the use of ascorbic acid to extend color stability of the NOE surface.

Alpha-tocopherol or vitamin E is an antioxidant which has been demonstrated to increase meat color stability when fed to cattle (Chan et al., 1995). More specifically, dietary vitamin E has decreased the myoglobin and lipid oxidation in beef (Faustman et al., 1998). This may be due to the presence of tocopherol influences the mitochondrial proteome and decreases enzymes involved in oxidative phosphorylation and possibly minimizing oxidative stress (Zhai et al., 2019). Hence, the greater tocopherol content in the NOE surface may be due to limited oxygen presence and reduced oxidative stress in comparison to the OE surface.

Gluconic acid is part of glycolytic metabolism and formed through the degradation of glucose (Bankar, Bule, Singhal, & Ananthanarayan, 2009; Kornecki et al., 2020). The increase in gluconic acid on the exposed surface could relate to increased glycolytic metabolites. Xylitol has been reported to be lower in the NOE surface of the *longissimus lumborum* muscle. Furthermore, xylitol is a product of pentose phosphate

pathway from the consumption of NADH and breakdown of xylose (Aguer, Piccolo, Fiehn, Adams, & Harper, 2017). Past research has reported a greater xylitol content in mice with an overexpression of proteins minimizing oxidative damage (Aguer et al., 2017). Therefore, in the present study, the presence of greater xylitol on the OE surface could indicate the response to oxidative stress induced by oxygen during retail display and the use of NADH and xylose to limit damage.

CONCLUSION

The oxygen exposure during retail display had negative implications on color stability compared to the interior of muscle. Specifically, oxygen consumption and metmyoglobin reducing ability decreased with oxygen exposure indicating the negative effects of oxygen on biochemical attributes of the *longissimus lumborum* muscle. Oxygen exposure influences the metabolome of the *longissimus lumborum* during retail display. The exposed surface represented more changes in response to oxidative stress and use of metabolites to form NADH and extend color stability. Therefore, the oxygen exposure is important to consider when evaluating the biochemical properties of muscle in storage.

Table 5.1. Proximate Composition (%) and pH least square means for the *longissimus lumborum* muscles (n = 6)

Parameter	Mean	SEM
Protein	22.53	0.29
Moisture	73.59	0.59
Fat	4.66	0.66
pH	5.55	0.03

SEM = standard error of mean

Table 5.2. Effects of retail display day on color attributes of steaks (n = 6) displayed for 6 d

Retail display day	*a**
0	35.24^{a}
1	31.41^{b}
2	30.36^{c}
3	29.72^{cd}
4	28.00^{e}
5	28.94^{d}
6	27.12^{e}
	SEM = 0.72

$^{a-e}$Least squares means with different letters are significantly different ($P < 0.05$).

SEM = standard error of mean

Table 5.3. Least squares means of oxygen consumption[1] and metmyoglobin reducing ability[2] (retail display day × oxygen exposure[3]) of steaks (n = 6)

		Retail display day		
Parameter	Oxygen exposure	0	3	6
Oxygen consumption	Non-oxygen exposed	0.14[a]	0.15[a]	0.12[ab]
SEM = 0.02	Oxygen exposed	0.14[a]	0.09[b]	0.12[a]
Metmyoglobin reducing ability	Non-oxygen exposed	0.92[a]	0.94[a]	0.95[a]
SEM = 0.02	Oxygen exposed	0.92[a]	0.76[b]	0.75[b]

[ab]Least squares means with different letters are significantly different ($P < 0.05$).

[1]Change in oxymyoglobin formation before and after 30 minutes of incubation determined by the change in K/S ratio of oxymyoglobin (Preincubation K/S610/K/S525 – Post incubation K/S610/K/S525).

[2]Metmyoglobin formation after submersion in sodium nitrite solution determined by K/S ratio of metmyoglobin (K/S 572/K/S525)., where a greater number indicates greater reduction.

[3]Exposure of muscle to oxygen as display surface indicated as oxygen exposed or interior of the muscle as non-oxygen exposed.

SEM = standard error of mean

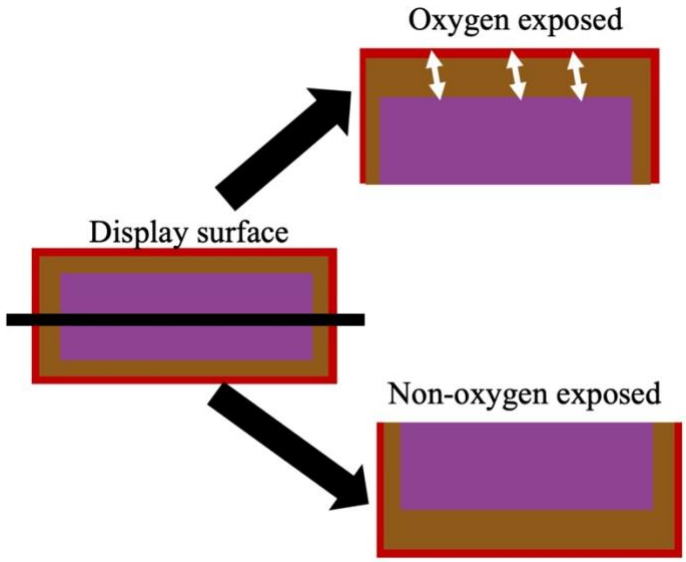

Figure 5.1. Evaluation of oxygen penetration through oxygen exposure of the oxygen exposed and non-oxygen exposed surfaces

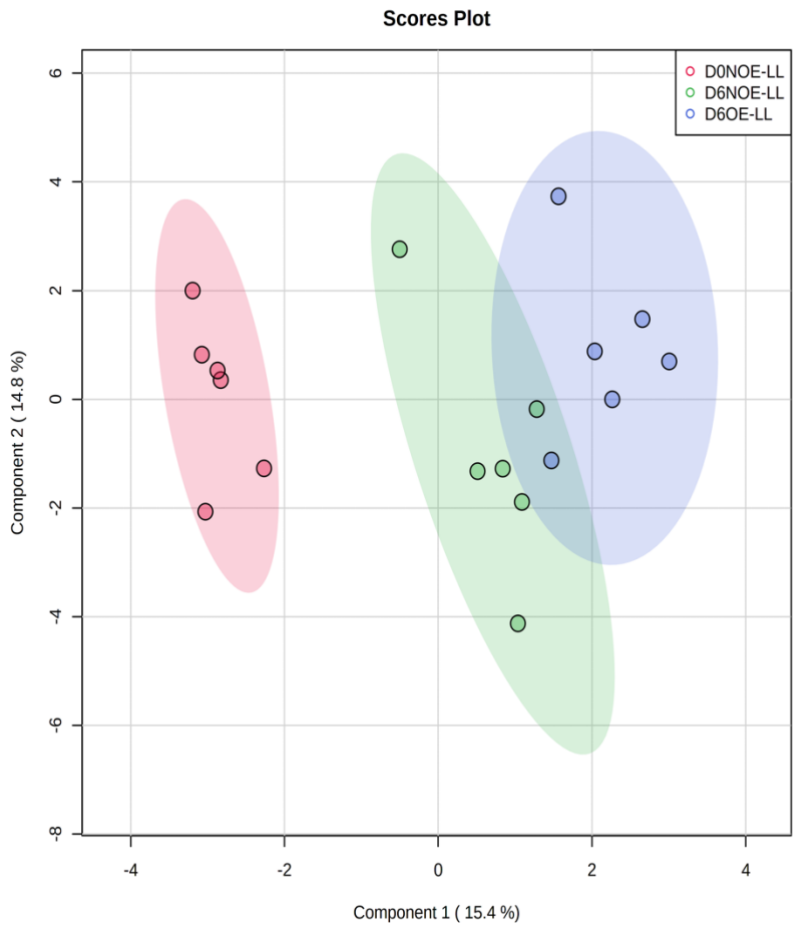

Figure 5.2. Partial least-squares discriminant analysis of metabolites present in surfaces

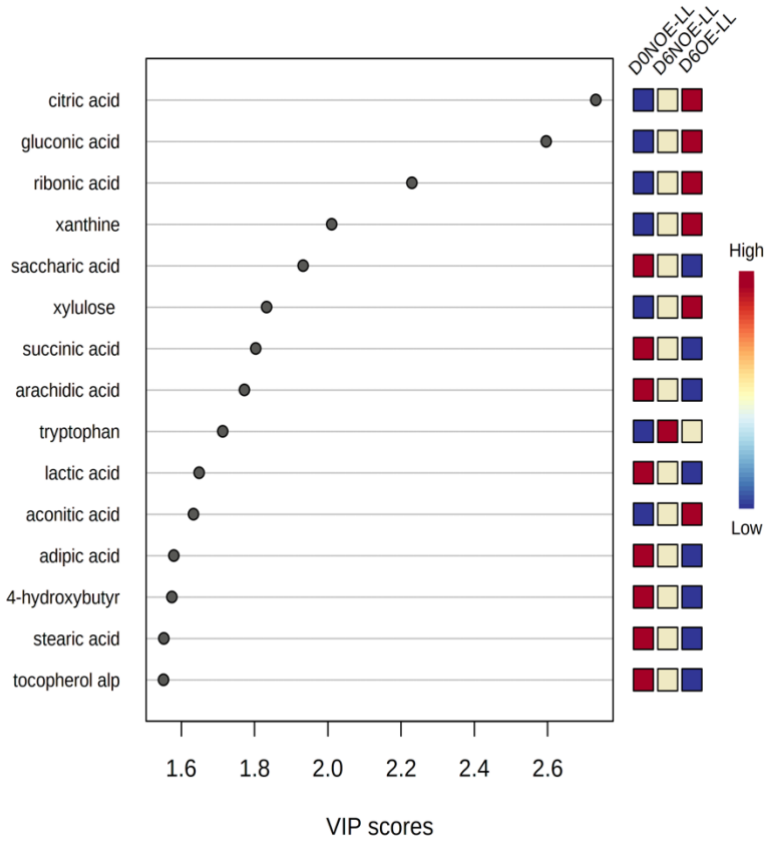

Figure 5.3. Important features identified by PLS-DA analysis of oxygen exposure of the *longissimus lumborum* muscle in retail display. A variable importance projection (VIP) is a measure of a variable importance in PLS-DA model. The VIP score indicates the contribution a variable makes to the model. A greater value denotes more importance.

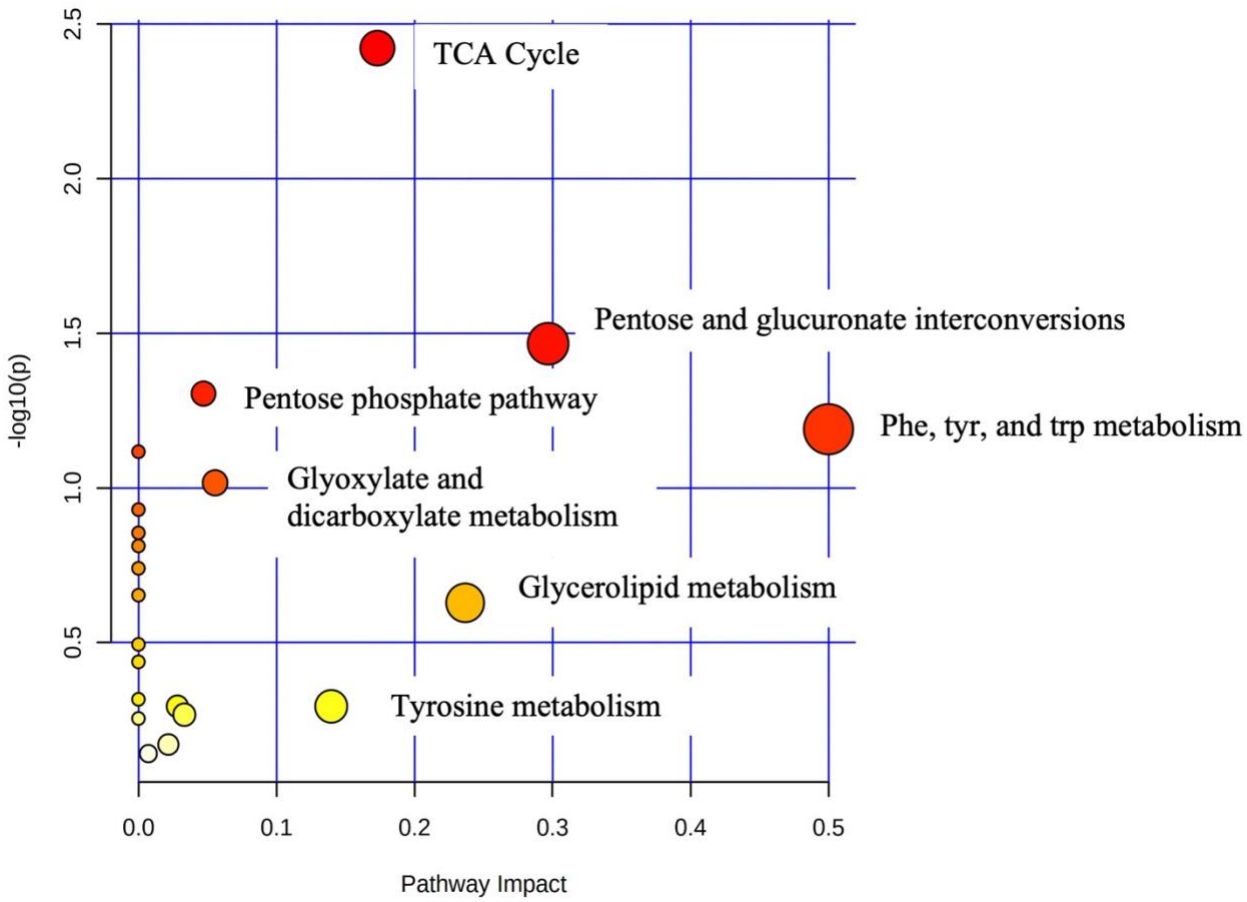

Figure 5.4. KEGG pathway analysis to determine biological process and metabolic pathways that are associated with the metabolites in *longissimus lumborum* muscle during retail display. X-axis represents the impact of the pathway, and the y-axis is the -log(*P*-value). The dot color is based on the *P*-value, and the dot size is based on the pathway impact values.

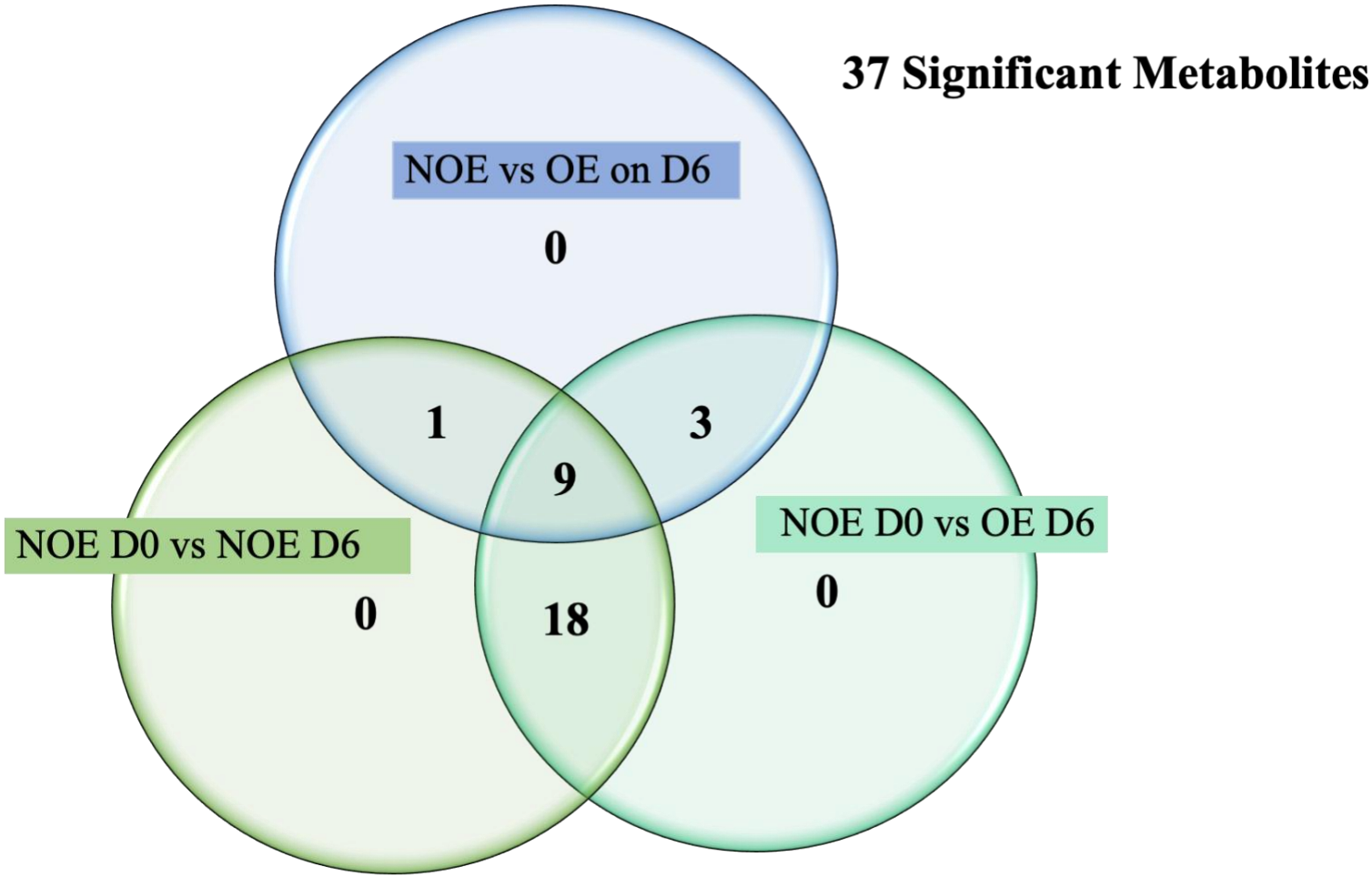

Figure 5.5. Separation of the significantly differentially abundant metabolites for the non-oxygen (NOE) surface on d 0, NOE surface on d 6, and oxygen exposed (OE) surface on d 6 of the *longissimus lumborum* muscle during retail display

CHAPTER VI

IMPACT OF OXYGEN EXPOSURE ON THE *LONGISSIMUS LUMBORUM, PSOAS MAJOR*, AND *SEMITENDINOSUS* MUSCLES DURING RETAIL DISPLAY

ABSTRACT

Oxymyoglobin leads to a bright-cherry red pigment on the surface of meat which is preferred by consumers. Oxidation of ferrous myoglobin leads to formation of metmyoglobin and discoloration. Myoglobin is prone to oxidation at a low (5-7 mmHg) oxygen partial pressure. Hence, meat discoloration starts from the interior and spreads to the surface. In aerobic packaging, the retail surface develops discoloration over time. However, the connection between oxygen exposure of the retail surface and internal discoloration has not been clear. The objective of this study was to evaluate the effects of oxygen exposure on the biochemical attributes of *longissimus lumborum , psoas major ,* and *semitendinosus* muscles. USDA Low Choice short loins and eye of rounds (5 d postmortem) were purchased from a commercial packing facility. Steaks were sliced (1.91 cm) from USDA Low Choice beef strip loins (n = 7), tenderloins (n = 7), and eye of rounds (n = 7). Steaks were packaged in pairs in PVC overwrap trays, and randomly assigned to 3 or 6 days in retail display. Instrumental color was evaluated every day of retail display using a HunterLab MiniScan spectrophotometer. On d 0, one steak was used to analyze the muscles for oxygen consumption, metmyoglobin reducing ability,

and lipid oxidation on a freshly cut non-oxygen exposed (NOE) surface. For d 3 and d 6, the retail surface was considered oxygen exposed (OE), while interior muscle was denoted as NOE. To analyze the two surfaces, steaks were sliced parallel to the OE surface to expose the NOE surface. On d 3 and d 6, oxygen consumption and metmyoglobin reducing ability were evaluated for the NOE and the OE surfaces. The amount of metmyoglobin formed was evaluated after nitrite submersion for analysis of metmyoglobin reducing ability, and oxygen consumption was determined as oxymyoglobin formation in vacuum packaging after 30 min and 60 min. The GLIMMIX procedure of SAS was used to determine the least square means of 7 replicates. Least square means were separated using the PDIFF option with a $P < 0.05$ considered significant. All three muscles decreased in a^* values ($P < 0.05$) with retail display with the *psoas major* having the lowest ($P < 0.05$) a^* followed by the *longissimus lumborum* and then the *semitendinosus* on d 6 of display. The NOE surface had greater ($P < 0.05$) metmyoglobin reducing ability compared to the OE surface on d 3 and d 6 for all muscles. The OE surface of the *psoas major* had lower ($P < 0.05$) oxygen consumption at 30 min compared to the NOE surface on d 3 and d 6 of retail display. Both the NOE surface of the *psoas major* and *semitendinosus* muscles had greater ($P < 0.05$) oxygen consumption at 60 min than the OE surfaces on d 3 and d 6 of display. The exposure to oxygen resulted in a decrease in metmyoglobin reducing ability and oxygen consumption aligning with a decline in retail color. In conclusion, oxygen exposure can negatively impact color stability while the non-exposed interior of muscle remains more biochemically active.

INTRODUCTION

Consumers prefer to see bright-cherry red steaks in the retail case as they associate the red color with freshness and wholesomeness (Carpenter et al., 2001). Even so, the red color of oxymyoglobin oxidizes in the display case forming discoloration on the surface as metmyoglobin. The formation of metmyoglobin or surface discoloration is negatively perceived by consumers (Carpenter et al., 2001), and recently, discoloration in beef steaks has been reported to cost $3.73 billion annually (Ramanathan et al., 2022a). Many factors can influence the formation of metmyoglobin such as muscle type and oxygen partial pressure.

Metmyoglobin formation rapidly occurred under low oxygen partial pressure (5 – 7 mmHg) in intact steaks such as the oxygen conditions in poorly sealed vacuum packaging (George & Stratmann, 1952; Ledward, 1970). In muscle, a low oxygen partial pressure occurred below the surface oxymyoglobin layer creating an internal layer of metmyoglobin (Limsupavanich et al., 2004, 2008). During retail, the oxidation of myoglobin rises from the interior layer to the surface creating visible surface discoloration and metmyoglobin (Limsupavanich et al., 2004, 2008). Research on the development of internal metmyoglobin is limited. Furthermore, the impact of internal metmyoglobin on color stability is not well understood. As oxygen plays a role in the development of internal and subsequent surface metmyoglobin, it would be valuable to enhance the understanding of the impact of oxygen on the color stability of meat such as influence on the oxygen consumption and metmyoglobin reducing ability.

Oxygen plays a key role in the formation of surface metmyoglobin through differences in oxygen penetration, diffusion, and oxygen consumption dependent on

muscle type (O'Keeffe & Hood, 1982). Muscle type impacts the color stability of steaks in retail through metabolic differences impacting use and penetration of oxygen. The *psoas major* muscle has mostly red fibers with an oxidative metabolism while the *longissimus lumborum* and *semitendinosus* have a glycolytic metabolism due to having more white fibers (Hunt and Hedrick, 1977). From differences in fiber type, research has reported differences in the proteome (Joseph et al., 2012) and metabolome (Abraham et al., 2017; Yu et al., 2020) which impact the color stability. The *psoas major* has been categorized as color-labile muscle while the *longissimus lumborum* and *semitendinosus* muscles were reported as color stable (McKenna et al., 2005; Seyfert et al., 2007). Metmyoglobin formed more rapidly in the *psoas major* muscle compared to *longissimus lumborum* muscle due to the *psoas major* muscle having greater oxidative metabolism compared to the *longissimus lumborum* muscle (McKenna et al., 2005; O'Keeffe & Hood, 1982). Furthermore, the differences in metabolome and proteome impact the lipid oxidation, oxygen consumption, and metmyoglobin reducing ability in relation to color stability due to different responses to oxidative stress (Joseph et al., 2012; Ke et al., 2017; McKenna et al., 2005). The *psoas major* muscle has been shown to have increased lipid oxidation compared to the *longissimus lumborum* contributing to the oxidation of myoglobin (Canto et al., 2016; Joseph et al., 2012; Ke et al., 2017). Such that, the *longissimus lumborum* muscle retained higher oxygen consumption and metmyoglobin reducing ability during storage compared to the *psoas major* muscle increasing color stability of the *longissimus lumborum* compared to the *psoas major* (Abraham et al., 2017; Ke et al., 2017). As oxygen can act as a prooxidant, oxygen exposure could influence the oxidative state of lipids and proteins in muscle during retail display.

However, limited research has evaluated the effects of oxygen exposure in retail on the color stability of the *longissimus lumborum*, *psoas major*, and *semitendinosus* muscles. Therefore, the first objective of this study was to determine the effects of oxygen exposure in retail on the biochemical attributes of the *longissimus lumborum*, *psoas major*, and *semitendinosus* muscles.

Based on the American Meat Science Association Meat Color Guidelines (King et al., 2023), the color stability attributes of oxygen consumption and metmyoglobin reducing ability can be evaluated using the retail surface or interior surface of the muscle. Past research has varied in the surface used for evaluation of metmyoglobin reducing ability and oxygen consumption with limited research considering the impact of oxygen exposure. Therefore, establishing the impact of oxygen exposure and the best method to evaluate color stability would allow for more consistent and comparable methodology in future research for different muscle types. In addition, understanding how oxygen exposure influences color stability analysis and the role oxygen plays in oxidative changes of myoglobin would help to determine methods to extend color stability.

MATERIALS AND METHODS

Materials

USDA Low-Choice short loins (n = 7; IMPS #173) and *semitendinosus* (n = 7; IMPS #171C) were collected from a commercial processing plant 5 d postmortem and transported back on ice to Oklahoma State University Food and Agriculture Products Center. The muscles were held till 7 d postmortem then the *psoas major* muscle was separated from the *longissimus lumborum*. The Hanna Instruments pH probe (Handheld HI 99163; probe FC232; Hanna Instruments) was used to measure pH in three locations

across the muscles. A face steak was removed from each muscle. Each muscle was sliced from the anterior end into six 1.91-cm steaks. Four steaks were randomly selected and packaged in pairs in white polystyrene trays with PVC overwrap (15,500-16,275 cm^3 O_2/m^2/24 h at 23°C, E-Z Wrap Crystal Clear Polyvinyl Chloride Wrapping Film, Koch Supplies, Kansas City, MO) trays. In the pairs, one steak was used for lipid oxidation, oxygen consumption, and oxygen penetration analysis while the other steak was used for metmyoglobin reducing ability and metabolomic samples. The remaining steak was used as the d 0 non-oxygen exposed (NOE) surface analysis. The sixth steak was used for proximate composition analysis.

Proximate composition

Approximately 200 g of each muscle were ground using a table-top grinder (Big Bite Grinder, 4.5 mm, fine grind, LEM) and pressed into 140-mm sample cup. An AOAC-approved near-infrared spectrophotometer (FoodScan Lab Analyzer, Serial No. 91753206; Foss, NIRsystem Inc.; Slangerupgrade, Denmark) determined the percent protein, fat, and moisture of each muscle.

Retail display

Packaged steaks were placed in a simulated retail display held at 2 ± 1°C for 6 d under continuous LED lighting (Philips LED lamps, 12 watts, 48 inches, color temperature = 3,500°K,54 Phillips, China). Packaged steaks were randomly selected for either 3 or 6 days in display. A HunterLab 4500L MiniScan EZ Spectrophotometer (2.5-cm aperture, illuminant A, and 10° standard observer angle, HunterLab Associates, Reston, VA) was used to determine instrumental color every day of retail for steaks held

for 6 d. For each package, six readings were taken with three readings per steak in the package. The CIE a^* and b^* values were used to calculate hue $(\tan^{-1}(\frac{b^*}{a^*}))$ and chroma $\left[\sqrt{(a^{*^2} + b^{*^2})}\right]$. A larger hue value indicates greater discoloration while a larger chroma represents greater red intensity. Reflectance from 400-700 nm was used to determine K/S ratios at 474, 525, 572, and 610 using the equation $K/S = (1 - R)^2 \div 2R$. These K/S ratios were used to determine metmyoglobin reducing ability and oxygen consumption.

Oxygen exposure

Figure 6.1 provides a representation of the analysis of the oxygen exposure. The surface from the retail display was the oxygen exposed (OE) surface while the interior or intact muscle was the NOE surface. To separate the two surfaces, the muscles were sliced parallel to the display surface exposing the NOE surface for analysis. Oxygen exposure was evaluated for lipid oxidation, metmyoglobin reducing ability, and oxygen consumption.

Lipid oxidation

Three grams of each surface was removed from the steaks on d 0, 3, and 6 of display and blended with 27 mL of trichloroacetic acid. The homogenous mixture was filtered using a Whatman No. 42 filter paper then one mL of filtrate was combined with 1 mL of Thiobarbituric acid. The solution was heated for 10 min at 100°C then cooled for 5 min. Absorbance was evaluated using a UV-Vis Spectrophotometer (UV-2600, UV-VIS Spectrophotometer, Shimadzu, Columbia, MD) at 532 nm and converted to mg of malondialdehyde per kg of sample.

Metmyoglobin reducing ability

metmyoglobin reducing ability was determined by submerging both surfaces in 0.3% sodium nitrite at 25ºC for 20 min. After 20 min, samples were removed, blotted dry, and vacuum packaged. Each sample was read three times using the HunterLab 4500L MiniScan EZ Spectrophotometer and then incubated for 2 h at 30ºC. Samples were read in triplicate after incubation. From the spectra, the K/S ratio of K/S572 ÷ K/S525 was used to determine the amount of metmyoglobin formed after submersion. A greater ratio indicates greater metmyoglobin reduction.

Oxygen consumption

Both the OE and NOE surfaces were exposed to oxygen at 4ºC for 1 h then vacuum packaged. The surfaces were read in triplicate using the HunterLab 4500L MiniScan EZ Spectrophotometer and incubated at 30ºC for 60 min where samples were analyzed after 30 and 60 min. The change in oxymyoglobin was determined using the preincubation K/S610 ÷ K/S525 – post incubation K/S610 ÷ K/S525. A greater change in oxymyoglobin indicates a greater oxygen consumption.

Oxidation via oxygen consumption

On both the NOE and OE surfaces, metmyoglobin formation was evaluated during anaerobic incubation at 30ºC. In anaerobic conditions, oxymyoglobin is converted to deoxymyoglobin through an intermediary of metmyoglobin. Metmyoglobin is reduced to deoxymyoglobin in meat with high reducing capacity. Oxygen consumption leads to the formation of low oxygen partial pressure ideal for the formation of deoxymyoglobin and further limits metmyoglobin formation. As display time increases, metmyoglobin

reducing capacity could be limited in addition to further oxidation of myoglobin with limited oxygen consumption resulting in ideal oxygen conditions for deoxymyoglobin oxidation. Therefore, oxidation by oxygen consumption would evaluate reduction and oxygen consumption of the samples. A HunterLab 4500L MiniScan EZ Spectrophotometer read samples after 30 min and 60 min of incubation to determine metmyoglobin formation on the NOE and OE surfaces. Metmyoglobin content was determined by the K/S ratio of K/S572 ÷ K/S525. A higher number indicates a lower metmyoglobin content.

Oxygen penetration

Oxygen depth was considered the oxymyoglobin and metmyoglobin layer formed on the lateral to the NOE surface as seen in Figure 6.1. Oxygen depth was analyzed on the NOE after 1 h bloom at 4ºC. The depth was determined using a handheld caliper to measure the oxygen depth in three locations across the section. The depth was calculated based relating to the width of the steak piece where the measurements were taken place.

Surface layer depth was considered for both the OE and NOE surface. The OE surface layer depth was the depth of oxymyoglobin and metmyoglobin layer from the oxygen exposure during retail on the OE surface. The NOE surface layer depth was the depth of the oxymyoglobin and metmyoglobin layer formed after 1 h bloom at 4ºC and slicing transverse (approximately 2 mm) to the NOE surface to re-expose the penetration from bloom. The surface layer depth was measured in three locations across the lateral surface to the NOE or OE surface. Percent surface layer depth was calculated as the surface layer relative to the width of the piece size × 100 for both surfaces.

Statistical analysis

The experimental design was a split-split plot design within a completely randomized block design. The loin was considered the block and random effect. The whole plot was the muscle. The subplot was the packaged steaks in retail display for 3 or 6 days with the pull day as the subplot factor. The sub-subplot factor was the oxygen exposure of the muscle surfaces. The fixed effects were the muscle, pull day, oxygen exposure, and their interactions. Retail display day was a repeated measure for the retail color analysis with a covariance structure of first order Toeplitz structure with homogenous variances selected based on the AICC values. Least square means were determined using the GLIMMIX procedure of SAS (SAS 9.4, SAS Institute Inc., Cary, NC). The PDIFF option was used to separate significant least square means with a nominal level of significance at 0.05.

Both Pearson's correlation and regression were analyzed for the muscles pooled and for each muscle type. The correlation and simple linear regression analysis of the NOE and OE surfaces evaluated the relationship between a^* values from retail display on d 0, d 3 and d 6, and the parameters analyzed on the NOE surface including lipid oxidation, metmyoglobin reducing ability, oxygen consumption after 30 min, oxygen consumption after 60 min, oxygen depth, oxidation by oxygen consumption, and surface layer oxygen depth. The OE parameters of lipid oxidation, metmyoglobin reducing ability, oxygen consumption after 30 min, oxygen consumption after 60 min, oxidation by oxygen consumption, and surface layer depth were analyzed for their relationship with a^* values on d 0, d 3, and d 6 of retail display using correlation and simple linear

regression. A *P*-value less than 0.05 was considered significant correlation and simple linear regression.

RESULTS

pH and proximate composition

The *psoas major* muscle had a greater ($P < 0.05$) pH than both the *longissimus lumborum* and *semitendinosus* muscles (Table 1). The *semitendinosus* muscle had a higher ($P < 0.05$) moisture content and lower ($P < 0.05$) fat content compared to the *psoas major* and *longissimus lumborum* muscles (Table 6.1).

Retail color

There was a significant retail display day × muscle effect on the instrumental color attributes including L^* values, a^* values, chroma and hue (Table 6.2). On d 0, the L^* values of the *longissimus lumborum* and the *psoas major* muscles were not significantly different ($P > 0.05$). The *semitendinosus* was lighter ($P < 0.05$) than both the *longissimus lumborum* and the *psoas major* on d 0 and d 6. By the end of retail display, the *longissimus lumborum* and the *psoas major* muscles were similar ($P > 0.05$) in L^* values. The *longissimus lumborum* and the *psoas major* muscles became darker ($P < 0.05$) with display time while the *semitendinosus* muscle remained unchanged ($P > 0.05$). All muscles decreased ($P < 0.05$) in a^* values and chroma values with retail display time. On d 6 of retail display, the *psoas major* muscle had lower ($P < 0.05$) a^* and chroma compared to the *semitendinosus* and *longissimus lumborum* muscles. The *semitendinosus* muscle was redder ($P < 0.05$; greater a^* values and chroma) than the *longissimus lumborum* muscle on d 6 of retail display. Hue angle represents the deviation of color

from the true red color. Therefore, greater hue angle values indicate greater surface discoloration during display. The *semitendinosus* muscle did not change ($P > 0.05$) in hue angle values throughout retail display. The *psoas major* muscle increased ($P < 0.05$) in hue values from d 0 to d 6 of display indicating an increase in surface discoloration. The *psoas major* muscle had greater ($P < 0.05$) hue values compared to the *semitendinosus* and *longissimus lumborum* muscles on d 6 of retail display. The *longissimus lumborum* had smaller ($P < 0.05$) hue values compared to the *semitendinosus* muscle on d 6 of retail display.

Metmyoglobin reducing ability

There was a significant retail day × oxygen exposure interaction on the metmyoglobin reducing ability (Table 6.3). There was no change ($P > 0.05$) in metmyoglobin reducing ability for the NOE surface during retail display. The metmyoglobin reducing ability of the OE surface decreased ($P < 0.05$) from d 0 to d 6. The NOE surface had greater ($P < 0.05$) metmyoglobin reducing ability compared to the OE surface on d 3 and d 6 of display.

Lipid oxidation

There was a significant muscle effect and retail day × oxygen exposure interaction on the lipid oxidation (Table 6.4 and Table 6.5, respectively). The *longissimus lumborum* muscle had less ($P < 0.05$) lipid oxidation compared to the *psoas major* muscle while the lipid oxidation of the *semitendinosus* was not significantly different from the lipid oxidation of the *longissimus lumborum* and *psoas major* muscles. The OE surface has greater ($P < 0.05$) lipid oxidation compared to NOE surface on d 6 of retail display. There was no ($P > 0.05$) difference in lipid oxidation between the two surfaces on d 3.

Oxygen consumption

The oxygen consumption was determined by the change in oxymyoglobin during incubation at 30 and 60 min. After a 30-min incubation, there was a significant retail day × muscle × oxygen exposure effect on the oxygen consumption (Table 6.6). The NOE surface had no change ($P > 0.05$) in oxygen consumption from d 0 to d 6 for each muscle. The oxygen consumption of the OE surface of *longissimus lumborum* and *semitendinosus* did not change ($P > 0.05$) from d 0 to d 6 during retail display. The *longissimus lumborum* had significantly lower oxygen consumption than the *semitendinosus* for both the NOE and OE surfaces on d 6 whereas the OE surface of the *psoas major* and *longissimus lumborum* were not different ($P > 0.05$) on d 6. The OE surface of the *psoas major* muscle decreased ($P < 0.05$) in oxygen consumption from d 0 to d 6 of retail display. At the end of display, the OE surface of the *psoas major* had lower ($P < 0.05$) oxygen consumption than the NOE surfaces of the *psoas major*. The NOE surface of the *semitendinosus* muscle had greater ($P < 0.05$) oxygen consumption than the NOE surface of the *psoas major* and *longissimus lumborum* muscles at the start of display. There was no impact of oxygen exposure ($P > 0.05$) for the oxygen consumption of the *longissimus lumborum* and *semitendinosus* on d 6.

There was a significant retail day × muscle × oxygen exposure effect on the oxygen consumption after 60 min of incubation (Table 6.7). There were no differences ($P > 0.05$) among the three muscles of the NOE surface on d 0 of display. The oxygen consumption of the NOE and OE surface of the *semitendinosus* muscle decreased ($P < 0.05$) from d 0 to d 6 of display. The OE surface of the *psoas major* muscle decreased ($P < 0.05$) in oxygen consumption from d 0 to d 6 of display while the NOE surface of the

psoas major muscle remained unchanged ($P > 0.05$) in oxygen consumption. The OE surface of the *psoas major* and *semitendinosus* muscles had lower ($P < 0.05$) oxygen consumption than the NOE surface on d 3 and d 6.

Oxidation via oxygen consumption

Metmyoglobin formation during 30 min of anaerobic incubation was affected ($P < 0.05$) by retail day × oxygen exposure interaction (Table 6.8). The metmyoglobin formation increased ($P < 0.05$) for the OE during retail display while the NOE surface remained stable. At 30 min of incubation, there was a significant muscle × retail display day effect on the metmyoglobin formation during anaerobic incubation (Table 6.9). The *semitendinosus* muscle was stable ($P > 0.05$) during retail display while both the *longissimus lumborum* and *psoas major* increased ($P < 0.05$) in metmyoglobin formation during display. Specifically, the *longissimus lumborum* had lower ($P < 0.05$) metmyoglobin at d 0 compared to the *semitendinosus* and *psoas major* muscles. On d 3 and d 6, the *psoas major* muscle had greater ($P < 0.05$) metmyoglobin formation than the *longissimus lumborum* and *semitendinosus* muscles. Additionally, there was a significant muscle × oxygen exposure on the oxidation via oxygen consumption (Table 6.10). The *longissimus lumborum* had the lower ($P < 0.05$) metmyoglobin formation on the NOE and OE surfaces than the *semitendinosus* and *psoas major* muscles. The OE surface of the *semitendinosus* had lower ($P < 0.05$) metmyoglobin formed than the *psoas major* muscle during incubation. Overall, the OE surface of each muscle had greater ($P < 0.05$) metmyoglobin formation than the NOE surface of each muscle. The oxygen exposure negatively impacted the color stability of the muscles during retail display.

After 60 min of incubation, metmyoglobin formation was significantly affected by retail day × oxygen exposure (Table 6.11) and muscle × oxygen exposure (Table 6.12). The NOE surface had no change ($P > 0.05$) in metmyoglobin content with retail display. The OE surface on d 0 had lower ($P < 0.05$) metmyoglobin formation than d 3 and d 6 of display. There was no difference ($P > 0.05$) in the metmyoglobin formation on the NOE surface of the different muscles. The metmyoglobin formation on the OE surface was lower ($P < 0.05$) for the *longissimus lumborum* than the *psoas major* muscle during incubation. The OE surface of the *psoas major* and *longissimus lumborum* had greater ($P < 0.05$) metmyoglobin formation than the NOE surface during incubation. Therefore, the OE surface had lower stability compared to the NOE surface during display and for the *longissimus lumborum* and *psoas major* muscles after 60 min of incubation.

Oxygen penetration

Surface layer depth

The surface layer was the layer formed on the surface and below composed of oxy- and metmyoglobin. The surface layer depth was determined for the OE surface after retail and the NOE surface after bloom. There was a significant retail day × muscle effect on the OE surface layer depth (Table 6.13). The *longissimus lumborum* muscle had greater ($P < 0.05$) surface layer oxygen depth on d 3 than the *psoas major* muscle. On d 6, *longissimus lumborum* and *semitendinosus* muscles had similar ($P > 0.05$) surface layer oxygen depths while the layer in both the *longissimus lumborum* and *semitendinosus* was significantly smaller in the *psoas major* muscle. Additionally, the surface layer was measured on the NOE surface after 1 h bloom and after slicing

transverse to the NOE surface to re-expose the penetration. There was a significant muscle effect on the NOE surface layer depth after 1 h of bloom (Table 6.14). The *longissimus lumborum* had a larger ($P < 0.05$) layer than the *semitendinosus* and *psoas major* muscles.

Oxygen depth

The oxygen depth was measured after 1 h bloom of the non-exposed surface as the depth of oxy- and metmyoglobin. There was a significant retail display day effect on the oxygen depth (Table 6.15). The oxygen depth decreased ($P < 0.05$) with retail display time indicating a decrease in oxygen penetration with increased display time.

Correlation analysis

There are significant Pearson's correlation values between the color parameters and *a** values for all muscles as well as the *psoas major*, *longissimus lumborum*, and *semitendinosus* muscles, individually (Table 6.16). For all the muscles pooled, there was significant strong negative correlation between the pull day and the *a** values as expected since the *a** values decreased with more time in display. A moderate negative correlation ($P < 0.05$) was reported between *a** values and OE lipid oxidation as well as OE surface layer oxygen depth. This correlation indicates the negative implications of oxygen exposure on lipid oxidation are linked to the decline in redness in retail display. Additionally, the increase in oxygen penetration and resulting increase in the layer of metmyoglobin and oxymyoglobin during retail aligns with a decrease in *a** values during retail display. There were positive ($P < 0.05$) correlations between *a** values and NOE oxygen depth, OE oxygen consumption at 30 min and 60 min, OE metmyoglobin reducing ability, NOE oxidation at 30 min and 60 min, and OE oxidation at 30 min and

60 min. Low positive significant correlations were reported for OE oxygen consumption at 30 min, and NOE oxidation at 30 min and 60 min. The OE metmyoglobin reducing ability and OE oxygen consumption at 60 min were moderately ($P < 0.05$) positively correlated with *a** values indicating the methodology could be used across multiple muscles. The NOE oxygen depth and OE oxidation at 60 min was strongly ($P < 0.05$) positively correlated with *a** values. Therefore, the ability for oxygen to penetrate muscles aligns with color changes in retail display. In addition, the oxidation of myoglobin under anaerobic conditions and subsequent low reduction aligns with changes in retail color stability across muscles. The highest correlation ($P < 0.05$) reported with *a** values was with OE oxidation at 30 min of incubation. Therefore, the high oxidation of myoglobin and low reduction of metmyoglobin during anaerobic storage aligned best the *a** changes during retail display for the muscles.

OE lipid oxidation and OE surface layer depth were negatively correlated ($P < 0.05$) with the *a** values of the *psoas major* muscle during retail display. The correlation between *a** values and OE surface layer depth of the *psoas major* muscle was strongly ($P < 0.05$) negative. Therefore, a smaller *a** value was reported with greater penetration during retail display. The oxidation via oxygen consumption of the NOE surface at 60 min and OE surface at 30 and 60 min of anaerobic incubation was significantly correlated with *a** values of the *psoas major* during retail display. The OE oxidation had high positive ($P < 0.05$) correlation with *a** values during display with a low metmyoglobin formed during incubation aligned with low *a** values in display. Therefore, the inability to reduce metmyoglobin anaerobically aligned with the loss of redness during retail. A positive correlation ($P < 0.05$) was reported between the *a** values and OE metmyoglobin

reducing ability as well as OE oxygen consumption at 30 min and 60 min. The OE oxygen consumption at 60 min had a stronger correlation with *a** values than the OE oxygen consumption at 30 min. A lower metmyoglobin reducing ability and oxygen consumption of the OE surface correlated with lower *a** values during display. Thereby, the OE surface of the color stability parameters better aligns with the loss of redness during display for the *psoas major* muscle. Oxygen exposure and subsequent bloom of the NOE surface was strongly ($P < 0.05$) correlated with the *a** values in retail. A greater penetration of the NOE aligned with the *a** values indicating the oxygen penetration as a good indicator of retail color for the *psoas major* muscle. Overall, the ability for oxygen penetration during retail display and bloom was well aligned with *a** values.

Significant strong negative correlations were reported between the OE surface layer depth and *a** values for the *longissimus lumborum* muscle. The negative correlation between the OE surface layer oxygen depth and *a** values in retail display indicates a greater depth of oxymyoglobin and metmyoglobin align with a decrease in *a** values. A moderate positive ($P < 0.05$) correlation was reported between NOE oxygen depth and the *a** values of the *longissimus lumborum* muscle. Therefore, the greater oxygen penetration of the NOE surface upon blooming demonstrates a greater *a** value in retail display. The oxidation via oxygen consumption of the oxygen consumption surface after 30 min of incubation was positively correlated ($P < 0.05$) with *a** values during display. The OE metmyoglobin reducing ability was strongly positively correlated ($P < 0.05$) with *a** values during retail display for the *longissimus lumborum* muscle. Therefore, greater reducing capacity of the OE surface aligned well with the changes in retail color for the *longissimus lumborum* muscle.

For the *semitendinosus* muscle, there were significant negative correlations between *a** values and OE surface layer oxygen depth. Therefore, a greater depth resulted in lower *a** values. The NOE oxidation via oxygen consumption was negatively correlated ($P < 0.05$) with *a** values during display. Therefore, on the NOE surface of the *semitendinosus*, the greater metmyoglobin formation during anaerobic conditions the higher *a** values in retail display which may be influenced by the muscle-specific color stability of the *semitendinosus*. The OE and NOE metmyoglobin reducing ability, OE oxygen consumption at 30 min, and OE oxidation at 30 min and 60 min were positively correlated ($P < 0.05$) with *a** values. The OE metmyoglobin reducing ability and OE oxidation at 30 min and 60 min had larger correlation values than the NOE metmyoglobin reducing ability and OE oxygen consumption at 30 min. The use of the OE surface for the metmyoglobin reducing ability and oxidation via oxygen consumption align with the changes in retail color. Therefore, the color stability of the OE surface aligned with the *a** values reported in retail display. Overall, there were muscle specific parameters and surfaces which had a strong relationship with *a** values. Therefore, the oxygen exposure should be considered when evaluating muscle specific color stability. The parameters of OE metmyoglobin reducing ability, OE surface layer depth, and NOE oxygen depth align well with color changes for all muscles and should be considered when comparing muscles in future research.

Regression analysis

The regression analysis on the pooled muscles indicated a significant R-squared value between *a** values and OE lipid oxidation, OE metmyoglobin reducing ability, OE oxygen consumption at 30 min and 60 min, OE oxidation at 30 and 60 min, NOE

oxidation at 30 and 60 min, OE surface layer oxygen depth, and NOE oxygen depth (Table 6.16). However, the linear relationships were not strong with the highest R-squared value of 0.63 reported for the OE oxidation at 30 min. For the *psoas major* muscle, the same parameters were indicated to have significant R-squared values as the pooled muscles analysis except NOE oxidation at 30 min. OE oxidation at 30 min and 60 min had high R-squared values indicating strong linear relationship between the oxidation and the *a** values. NOE oxygen depth had a good linear relationship with *a** values of the *psoas major*. OE metmyoglobin reducing ability, OE oxidation at 30 min, and OE surface layer oxygen depth had a strong linear relationship with the *a** values of the *longissimus lumborum*. Furthermore, NOE oxygen depth had a significant R-squared value, but the linear relationship would not be considered good based on the value. Therefore, the OE surface parameters better represent changes in *a** values during retail display for the *longissimus lumborum* muscle. The *semitendinosus* muscle had a strong linear relationship of *a** values and OE metmyoglobin reducing ability, and a good linear relationship with the OE surface layer oxygen depth and OE oxidation at 30 min. Although NOE metmyoglobin reducing ability, OE oxygen consumption at 30 min and 60 min, and NOE oxidation at 30 and 60 min were reported to have significant R-squared values with *a** values, the low values indicate the ability of NOE metmyoglobin reducing ability, OE oxygen consumption at 30 min and 60 min to explain the variability in *a** values of the *semitendinosus* would be low. Overall, OE surface layer oxygen depth and OE metmyoglobin reducing ability would act as a good predictor of the *a** values in retail for the *psoas major*, *longissimus lumborum*, and *semitendinosus* muscles based on the regression analysis.

DISCUSSION

Previous research has demonstrated the greater color stability of the *longissimus lumborum* over the *psoas major* muscle during storage (Abraham et al., 2017; Ke et al., 2017; McKenna et al., 2005; O'Keeffe & Hood, 1982). The *semitendinosus* muscle has been reported to have similar color stability to the *longissimus lumborum* muscle and greater color stability than the *psoas major* muscle (Seyfert et al., 2006). More specifically, the *semitendinosus* muscle had greater lightness (higher L^* values) compared to the *longissimus lumborum* and *psoas major* muscles during retail display while the *semitendinosus* and *longissimus lumborum* had similar redness by the end of retail display (Seyfert et al., 2006). The present study supports the color stability of the *longissimus lumborum* and *semitendinosus* over the *psoas major* muscle during retail display.

The muscle-specific influence of oxygen exposure has been reported using different packaging methods. The use of anaerobic vacuum packaging for storage demonstrated no differences among the *longissimus lumborum*, *psoas major*, and *semitendinosus* in redness (Liu et al., 2014), metmyoglobin content (Liu et al., 2014), and oxymyoglobin content (Mohan et al., 2010b). Therefore, the anaerobic conditions allowed for similar color stability amongst the muscles. The *psoas major* muscle in HiOx-MAP has been reported to have lower a^* values compared to the *longissimus lumborum* in HiOx-MAP (Liu et al., 2014; Suman, Mancini, Ramanathan, & Konda, 2009). Furthermore, the *longissimus lumborum* packaged in HiOx-MAP has been reported to be higher in oxymyoglobin (Mohan et al., 2010b) and lower in metmyoglobin (Liu et al., 2014) compared to the *psoas major* in HiOx-MAP. The *semitendinosus* on the

other hand has less oxymyoglobin than the *longissimus lumborum* and greater oxymyoglobin than the *psoas major* in HiOx-MAP conditions (Mohan et al., 2010b). Therefore, the oxygen in packaging can have muscle specific effects which supports effects of oxygen exposure reported in the present study.

Oxygen exposure influenced the muscles in differently during retail display which may be connected to the primary metabolism present in each muscle. The *longissimus lumborum* and *semitendinosus* muscles have mostly glycolytic metabolism while the *psoas major* has primarily oxidative (Hunt & Hedrick, 1977; Yu et al., 2019). Furthermore, mitochondrial content has been reported to be greater in *psoas major* muscle than *longissimus lumborum* muscle as the *psoas major* has been categorized as a more oxidative muscle (Ke et al., 2017). The *psoas major* muscle has greater oxygen consumption with a more rapid decline than the *longissimus lumborum* muscle supported by the greater mitochondrial content and oxidative metabolism of the *psoas major* muscle (Abraham et al., 2017; Ke et al., 2017). Research has reported greater oxidative stress in the *psoas major* than the *longissimus lumborum* muscle during storage (Joseph et al., 2012; Ke et al., 2017). The *psoas major* muscle has faster mitochondrial degradation than the *longissimus lumborum* muscle increasing the oxidative stress (Ke et al., 2017). Mitochondrial degradation increases the release of free radicals and formation of reactive oxygen species leading to oxidation of lipids and proteins (Bekhit et al., 2013; Ke et al., 2017; Ramanathan et al., 2020a). In support, the *longissimus lumborum* muscle has been reported to have greater antioxidant capacity and better sustainment of antioxidant mechanism which would limit the effects of reactive oxygen species and subsequent oxidation (Joseph et al., 2012; Ke et al., 2017). These factors can limit oxidative changes

from free radicals and reactive oxygen species extending color stability of the *longissimus lumborum* compared to the *psoas major*. The negative implications of oxygen exposure on color stability may relate to differences in response to oxidative stress of the muscle sin retail display. More specifically, the decrease in oxygen consumption and increased oxidation reported for the OE surface of the *psoas major* may be related to its greater susceptibility to oxidative stress (Ke et al., 2017) and presence of oxygen to form free radicals. The correlation between the OE oxygen consumption and OE oxidation and *a** values in retail display demonstrate a greater or retained oxygen consumption along with lower oxidation strongly related to greater color stability in the *longissimus lumborum* muscle supporting muscles with lower oxidative changes in retail display were more color stable. Furthermore, lipid oxidation has been reported to be higher in the *psoas major* than the *longissimus lumborum* (Canto et al., 2016; Joseph et al., 2012; Ke et al., 2017) and *semitendinosus* (McKenna et al., 2005) during storage as reported in the current study. Oxygen presence during display could further increase lipid oxidation due to the prooxidant activity of oxygen resulting in higher oxidation on the surface compared to the interior (Faustman et al., 2010). With greater lipid oxidation, myoglobin oxidation increases influencing the color stability of the retail surface (Faustman et al., 2010). This is further supported by the negative correlation between the *a** values and the OE lipid oxidation for all muscles. Therefore, the susceptibility of muscles to oxidative stress aligns with the negative impact of oxygen on oxidative states of lipids and myoglobin.

Oxygen penetration in previous research has evaluated the formation and depth of oxymyoglobin during storage. Research has reported a greater oxygen penetration and

larger oxymyoglobin depth in the *longissimus lumborum* muscle compared to the *psoas major* muscle during storage (McKenna et al., 2005; O'Keeffe & Hood, 1982) as reported in the present study in the change of the surface layer depth. The *semitendinosus* had numerically larger penetration than the *psoas major* and *longissimus lumborum* by the end of storage (McKenna et al., 2005) unlike the surface layer depth results in the current manuscript. Correlation analysis reported a greater surface layer depth on the OE surface correlated with a smaller *a** value in the present study for all muscles. McKenna et al. (2005) reported increased penetration with greater retail time which supports the greater depth as *a** values decreased during retail in the present study. However, past research has reported the color stable *longissimus lumborum* muscle having greater depth and higher *a** values than the *psoas major* muscle in display indicating a positive relationship (Limsupavanich et al., 2004). Past research indicated the oxygen penetration increased during storage as indicated by a greater depth of oxymyoglobin for both the *longissimus* and *psoas major* muscles (Joseph et al., 2012; McKenna et al., 2005; O'Keeffe & Hood, 1982). However, oxymyoglobin layer was reported to decrease with increased oxygen exposure for the *psoas major* muscle whereas the *longissimus* muscle had limited changes (Limsupavanich et al., 2004, 2008). Research reported a maximum penetration was achieved by 7 d of storage then decreased from 7 d to 14 d of storage for *longissimus* steaks (Lu et al., 2020). Furthermore, Joseph et al. (2012) reported greater penetration in the *psoas major* than the *longissimus* during display and attributed the greater penetration due to longer display of 9 d to the previously reported 5 d. Therefore, the oxygen penetration may achieve a maximum during a shorter retail display then decrease with greater retail time influencing the relationship between oxygen penetration and color

stability. The variation in oxygen penetration reported here compared to past research may be in the methodology. Oxygen penetration was considered zero initially as steaks had not been oxygen exposed. Additionally, metmyoglobin and oxymyoglobin depths were considered in combination whereas past research has focused solely on oxymyoglobin formation. Metmyoglobin layer depth has reported to increase with greater oxygen exposure for both the *longissimus* and *psoas major* muscles (Limsupavanich et al., 2004, 2008). The results of the present study support the previous muscle specific knowledge about oxygen penetration and demonstrates a strong relationship between penetration during retail and color stability.

Limited research has reported oxygen penetration differences upon blooming of steaks during retail display. In consistent with the present study, the oxymyoglobin depth upon blooming was reported to increase with greater postmortem time in the *longissimus* and *psoas major* muscles (O'Keeffe & Hood, 1982). The differences may be due to the difference in methodology as the present study did not bind the samples with plates to limit oxygen exposure. Furthermore, oxymyoglobin depth was reported to be greater in the *longissimus* compared to the *psoas major* after blooming (O'Keeffe & Hood, 1982) supporting the differences reported in NOE surface layer depth. Anaerobic systems have been reported to have higher bloom in *longissimus* steaks compared to PVC packaging (Fu et al., 1992). Therefore, the results presented in the current manuscript supports greater penetration correlated with a greater a^* value. Therefore, increased diffusion of oxygen during bloom indicated the color stability in retail display.

The Meat Color Measurement Guidelines do not indicate a specific surface for evaluating metmyoglobin reducing ability and oxygen consumption (King et al., 2023).

Previous studies reported NOE surface of the *longissimus* and *psoas major* decreased in oxygen consumption and metmyoglobin reducing ability during display (Ke et al., 2017). The OE surface of the *longissimus*, *psoas major*, and *semitendinosus* muscles reported similar decrease in metmyoglobin reducing ability during display (Canto et al., 2016; Joseph et al., 2012; Seyfert et al., 2006). Therefore, both surfaces have been used to evaluate metmyoglobin reducing ability and oxygen consumption connections to meat color. The retail surface metmyoglobin reducing ability and oxygen consumption has higher correlation with changes in color stability during display for color stable and color labile muscles. Therefore, oxygen exposure should be considered when evaluating metmyoglobin reducing ability and oxygen consumption. Muscle type had limited impact on the differences in metmyoglobin reducing ability in comparison to oxygen exposure in the present study. Previous research has reported the higher metmyoglobin reducing ability in the *longissimus lumborum* over the *psoas major* during retail display (Abraham et al., 2017; Joseph et al., 2012). The *semitendinosus* has been reported to have intermediate metmyoglobin reducing ability compared to the *longissimus* (higher metmyoglobin reducing ability) and *psoas major* (lower metmyoglobin reducing ability) muscles (Seyfert et al., 2006). The presence of oxygen may be more muscle specific in its effects on oxygen consumption and lipid oxidation compared to metmyoglobin reducing ability due to differences in muscle type and changes due to oxidative stress. Mancini et al. (2008) reported lower metmyoglobin reducing ability of the OE surface than the NOE surface for both the *longissimus lumborum* and *psoas major* muscles. Both surfaces were reported to have greater metmyoglobin reducing ability in the *longissimus lumborum* muscle compared to the *psoas major* (Mancini et al., 2008). The inconsistency with the

present study may be due to differences in the calculation of metmyoglobin reducing ability.

The Meat Color Measurement Guidelines indicate to calculate both metmyoglobin reducing ability and oxygen consumption based off percentage changes in myoglobin forms on the surface of samples (King et al., 2023). However, to evaluate the percent forms, 100% standards need to be made especially when comparing different muscle types. With this additional step, there can be an increase variability in results and methods. By using $\frac{K}{S}$ ratios, standards do not need to be made which can improve the accuracy and allow for better comparisons across studies. The OE surface of the metmyoglobin reducing ability and oxygen consumption were better correlated with a^* changes during retail display than NOE surface metmyoglobin reducing ability and oxygen consumption. However, the relationship with oxygen consumption was heavily dependent on muscle. In addition, oxidation of myoglobin via oxygen consumption was reported in the present study to relate to the color stability in retail display. Oxygen consumption analysis depends on the conversion to deoxymyoglobin or the loss of oxymyoglobin (King et al., 2023). With oxidized myoglobin from retail display, anerobic conditions may lead to little-to-no metmyoglobin reduction or further oxidation as low oxygen partial pressures were achieved. As oxygen consumption decreased, deoxymyoglobin oxidized more readily with extended periods at low oxygen partial pressure (George & Stratmann, 1952). In addition, a lower metmyoglobin reduction would lead to greater metmyoglobin formation under low oxygen partial pressure. The combination of low oxygen consumption and low reduction results in greater metmyoglobin which would represent in the oxidation by oxygen consumption

parameter. Therefore, the methodology presented in oxidation via oxygen consumption demonstrated the implications of oxygen consumption via oxidation. The oxidation by oxygen consumption with the OE surface reported good relationship with all muscles and would be a viable option to evaluate color stability. Therefore, the use of OE would be best to evaluate all color parameters, and the use of $\frac{K}{S}$ ratios allow for more consistent evaluation of color specifically the use of ratios to evaluate the oxidation by oxygen consumption.

CONCLUSION

Oxygen exposure has muscle specific impacts on the color stability and oxidative changes during retail display. The results of the present study support the importance of considering oxygen exposure when evaluating color stability parameters. More specifically, the study indicates the use of the exposed or retail surface for evaluation of metmyoglobin reducing ability and oxygen consumption for color stable and color labile muscles. Oxidation by oxygen consumption is a new methodology which demonstrates promise to relate to color stability of different muscles during retail display. In addition, oxygen penetration plays a key role in color stability and should be considered. Future studies should evaluate oxygen penetration more specifically based on myoglobin form as subsurface changes from oxygen exposure influence color stability.

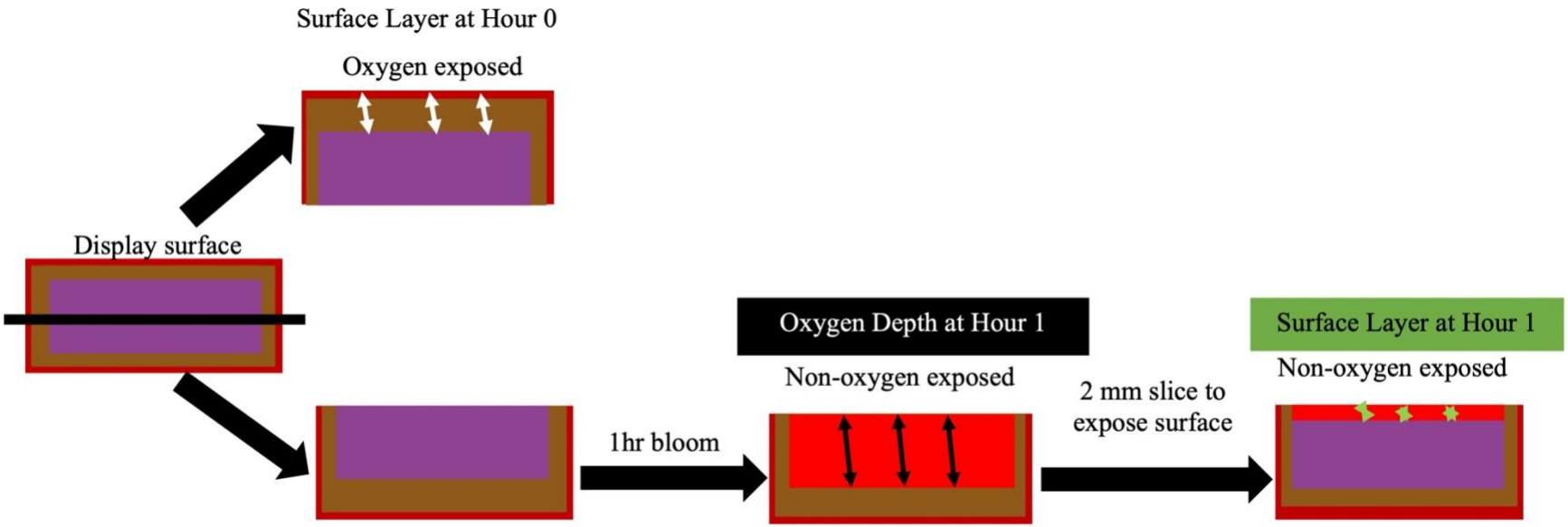

Figure 6.1. Evaluation of oxygen penetration through oxygen exposure of the oxygen exposed and non-oxygen exposed surfaces. [1]Depth of oxymyoglobin and metmyoglobin after retail display. [2]Depth of oxymyoglobin and metmyoglobin after 1 hour bloom of the lateral surface to the freshly cut NOE surface. [3]Depth of oxymyoglobin and metmyoglobin after 1 hour bloom and re-exposure of the lateral surface to evaluate oxygen penetration into the NOE surface.

Table 6.1. Proximate Composition (%) and pH least square means for the three muscles (n = 7)

Parameter	*Longissimus lumborum*	*Psoas major*	*Semitendinosus*	SEM
Protein	22.58	22.54	22.66	0.25
Moisture	73.72[b]	74.59[ab]	75.94[a]	0.52
Fat	4.52[a]	4.42[a]	2.78[b]	0.56
pH	5.55[b]	5.65[a]	5.50[b]	0.03

[ab]Least squares means with different letters are significantly different ($P < 0.05$).

SEM = standard error of mean

Table 6.2. Least squares means of color attributes (muscle × retail display day) of steaks (n = 7) displayed for 6 d

		Retail display day						
Parameter	Muscle	0	1	2	3	4	5	6
*L**	*Longissimus lumborum*	43.05^{def}	43.61^{de}	44.40^{d}	43.22^{def}	42.29^{defgh}	43.22^{def}	40.52^{ghi}
	Psoas major	42.31^{defg}	43.16^{def}	41.92^{defgh}	40.79^{fgh}	39.97^{hi}	41.58^{efgh}	38.35^{i}
SEM = 1.42	*Semitendinosus*	49.78^{ab}	49.83^{ab}	49.85^{ab}	48.23^{c}	48.24^{c}	51.07^{a}	49.50^{b}
*a**	*Longissimus lumborum*	36.37^{a}	32.01^{bcd}	30.11^{cde}	29.33^{h}	27.35^{f}	27.78^{f}	25.81^{gh}
	Psoas major	33.92^{ab}	28.97^{ef}	27.08^{fg}	24.37^{i}	22.08^{i}	21.96^{i}	18.42^{j}
SEM = 1.00	*Semitendinosus*	35.52^{a}	32.40^{bc}	31.38^{bcde}	31.62^{bcde}	29.61^{def}	31.73^{bcde}	30.70^{cde}
Chroma	*Longissimus lumborum*	47.91^{a}	39.91^{de}	37.44^{efg}	36.55^{fg}	34.03^{hij}	34.64^{gh}	32.67^{ij}
	Psoas major	44.31^{bc}	36.45^{fgh}	34.36^{ghi}	31.24^{j}	28.72^{k}	28.99^{k}	25.26^{l}
SEM = 1.18	*Semitendinosus*	47.48^{ab}	41.86^{cd}	40.64^{d}	41.21^{cd}	38.60^{de}	41.31^{cd}	40.46^{de}
Hue	*Longissimus lumborum*	40.82^{bcd}	36.67^{gh}	36.21^{h}	36.39^{h}	36.21^{h}	36.30^{h}	37.25^{fgh}
	Psoas major	39.96^{bcd}	37.39^{fgh}	38.05^{efgh}	38.83^{defg}	39.96^{bcd}	41.14^{bc}	43.59^{a}
SEM = 0.87	*Semitendinosus*	41.53^{ab}	39.26^{cdef}	39.44^{cdef}	39.91^{bcde}	39.93^{bcde}	39.84^{bcde}	40.67^{bcd}

$^{a-l}$Least squares means with different letters are significantly different ($P < 0.05$).

SEM = standard error of mean

Table 6.3. Effect of day × oxygen exposure[1] on the metmyoglobin reducing ability[2] of the steaks (n = 7)

	Retail display day		
Oxygen exposure	0	3	6
NOE	0.93[a]	0.94[a]	0.92[a]
OE	0.93[a]	0.77[b]	0.76[b]
	SEM = 0.01		

[ab]Least squares means with different letters are significantly different ($P < 0.05$).

[1]Exposure of muscle to oxygen with retail display surface indicated as oxygen exposed (OE) or interior of the muscle as non-oxygen exposed (NOE).

[2]Metmyoglobin formation after submersion in sodium nitrite solution determined by K/S ratio of metmyoglobin (K/S 572 ÷ K/S525)., where a greater number indicates greater reduction.

SEM = standard error of mean

Table 6.4. Effect of muscle on lipid oxidation of the steaks (n = 7) during retail display

Muscle	Lipid oxidation (mg MDA/kg)
Longissimus lumborum	0.35[b]
Psoas major	0.48[a]
Semitendinosus	0.43[ab]
SEM = 0.04	

[ab]Least squares means with different letters are significantly different ($P < 0.05$).

SEM = standard error of mean

Table 6.5. Least squares means of lipid oxidation (day × oxygen exposure[1]) of steaks (n = 7) displayed for 6 d

	Retail display day		
Oxygen exposure	0	3	6
NOE	0.42[b]	0.38[b]	0.39[b]
OE	0.42[b]	0.39[b]	0.53[a]
	SEM = 0.04		

[ab]Least squares means with different letters are significantly different ($P < 0.05$).

SEM = standard error of mean

[1]Exposure of muscle to oxygen with retail display surface indicated as oxygen exposed (OE) or interior of the muscle as non-oxygen exposed (NOE).

Table 6.6. Least squares means of oxygen consumption[1] (day × muscle × oxygen exposure[2]) after 30 min of incubation of steaks (n = 7) displayed for 6 d

		Retail display day		
Oxygen exposure	Muscle	0	3	6
NOE	*Longissimus lumborum*	0.14^{abx}	0.15^{axy}	0.12^{bx}
	Psoas major	0.15^{ax}	0.18^{awx}	0.17^{aw}
	Semitendinosus	0.20^{aw}	0.20^{aw}	0.19^{aw}
OE	*Longissimus lumborum*	0.14^{ax}	0.09^{bz}	0.12^{ax}
	Psoas major	0.15^{ax}	0.15^{ay}	0.10^{bx}
	Semitendinosus	0.20^{aw}	0.18^{awx}	0.18^{aw}
			SEM = 0.01	

[ab]Least squares means with different letters in a row are significantly different ($P < 0.05$).

[w-z]Least squares means with different letters in a column are significantly different ($P < 0.05$).

[1]Change in oxymyoglobin formation before and after 30 minutes of incubation determined by the change in K/S ratio of oxymyoglobin (Preincubation K/S610 ÷ K/S525 – Post incubation K/S610 ÷ K/S525).

[2]Exposure of muscle to oxygen with retail display surface indicated as oxygen exposed (OE) or interior of the muscle as non-oxygen exposed (NOE).

SEM = standard error of mean

Table 6.7. Least squares means of oxygen consumption[1] (day × muscle × oxygen exposure[2]) after 60 min of incubation of steaks (n = 7) displayed for 6 d

		Retail display day		
Oxygen exposure	Muscle	0	3	6
NOE	*Longissimus lumborum*	0.19^{aw}	0.19^{aw}	0.16^{bw}
	Psoas major	0.18^{aw}	0.16^{awx}	0.16^{aw}
	Semitendinosus	0.17^{aw}	0.14^{abx}	0.11^{bx}
OE	*Longissimus lumborum*	0.19^{aw}	0.18^{awx}	0.18^{aw}
	Psoas major	0.18^{aw}	0.09^{by}	0.09^{bx}
	Semitendinosus	0.17^{aw}	0.04^{bz}	0.05^{by}
			SEM = 0.02	

[ab]Least squares means with different letters in a row are significantly different ($P < 0.05$).

[w-z]Least squares means with different letters in a column are significantly different ($P < 0.05$).

[1]Change in oxymyoglobin formation before and after 60 minutes of incubation determined by the change in K/S ratio of oxymyoglobin (Preincubation K/S610 ÷ K/S525 – Post incubation K/S610 ÷ K/S525).

[2]Exposure of muscle to oxygen with retail display surface indicated as oxygen exposed (OE) or interior of the muscle as non-oxygen exposed (NOE).

SEM = standard error of mean

Table 6.8. Least squares means of oxidation[1] via oxygen consumption (day × oxygen exposure[2]) after 30 min of incubation of steaks (n = 7) displayed for 6 d

	Retail display day		
Oxygen exposure	0	3	6
NOE	1.73[a]	1.65[a]	1.69[a]
OE	1.73[a]	1.37[b]	1.21[c]
	SEM = 0.06		

[ab]Least squares means with different letters are significantly different ($P < 0.05$).

SEM = standard error of mean

[1]Metmyoglobin formation after 30 min of anaerobic incubation determined by by K/S ratio of metmyoglobin (K/S 572 ÷ K/S525)., where a greater number indicates lower metmyoglobin.

[2]Exposure of muscle to oxygen with retail display surface indicated as oxygen exposed (OE) or interior of the muscle as non-oxygen exposed (NOE).

Table 6.9. Least squares means of oxidation[1] via oxygen consumption (day × muscle) after 30 min of incubation of steaks (n = 7) displayed for 6 d

	Retail display day		
Muscle	0	3	6
Longissimus lumborum	2.04[a]	1.67[b]	1.58[b]
Psoas major	1.58[b]	1.32[c]	1.21[c]
Semitendinosus	1.57[b]	1.56[b]	1.55[b]
	SEM = 0.08		

[a-e]Least squares means with different letters are significantly different ($P < 0.05$).

[1]Metmyoglobin formation after 30 min of anaerobic incubation determined by K/S ratio of metmyoglobin (K/S 572 ÷ K/S525)., where a greater number indicates lower metmyoglobin.

SEM = standard error of mean

Table 6.10. Least squares means of oxidation[1] via oxygen consumption (muscle × oxygen exposure[2]) after 60 min of incubation of steaks (n = 7) displayed for 6 d

	Oxygen exposure	
Muscle	NOE	OE
Longissimus lumborum	1.86[a]	1.67[b]
Psoas major	1.58[bc]	1.15[d]
Semitendinosus	1.64[b]	1.49[c]
	SEM = 0.07	

[a-e]Least squares means with different letters are significantly different ($P < 0.05$).

[1]Metmyoglobin formation after 30 min of anaerobic incubation determined by by K/S ratio of metmyoglobin (K/S 572 ÷ K/S525)., where a greater number indicates lower metmyoglobin.

SEM = standard error of mean

Table 6.11. Least squares means of oxidation[1] via oxygen consumption (day × oxygen exposure[2]) after 60 min of incubation of steaks (n = 7) displayed for 6 d

	Retail display day		
Oxygen exposure	0	3	6
NOE	1.74[a]	1.66[a]	1.72[a]
OE	1.74[a]	1.38[b]	1.31[b]
	SEM = 0.07		

[ab]Least squares means with different letters are significantly different ($P < 0.05$).

SEM = standard error of mean

[1]Metmyoglobin formation after 60 min of anaerobic incubation determined by by K/S ratio of metmyoglobin (K/S 572 ÷ K/S525)., where a greater number indicates lower metmyoglobin.

[2]Exposure of muscle to oxygen with retail display surface indicated as oxygen exposed (OE) or interior of the muscle as non-oxygen exposed (NOE).

Table 6.12. Least squares means of oxidation[1] via oxygen consumption (muscle × oxygen exposure[2]) of steaks (n = 7) displayed for 6 d

	Oxygen exposure	
Muscle	NOE	OE
Longissimus lumborum	1.77[a]	1.64[b]
Psoas major	1.68[ab]	1.33[c]
Semitendinosus	1.66[ab]	1.46[bc]
	SEM = 0.07	

[a-e]Least squares means with different letters are significantly different ($P < 0.05$).

[1]Metmyoglobin formation after 60 min of anaerobic incubation determined by K/S ratio of metmyoglobin (K/S 572 ÷ K/S525)., where a greater number indicates lower metmyoglobin.

SEM = standard error of mean

Table 6.13. Effect of muscle × day on the percent surface layer oxygen depth[1] of the oxygen exposed surface of steaks (n = 7) after retail display

	Retail display day		
Muscle	0	3	6
Longissimus lumborum	0.00[e]	60.23[ab]	66.43[a]
Psoas major	0.00[e]	42.19[cd]	39.67[d]
Semitendinosus	0.00[e]	52.81[bc]	57.55[ab]
		SEM = 4.69	

[a-e]Least squares means with different letters are significantly different ($P < 0.05$).

[1]Depth of the layer of oxymyoglobin and metmyoglobin on the oxygen exposed surface of muscle after retail display divided by size of the piece where surface layer was measured. % Surface layer = (Depth after retail ÷ Piece size) x 100

SEM = standard error of mean

Table 6.14. Effect of muscle on the percent surface layer oxygen depth[1] after an hour of bloom at 4°C of the non-oxygen exposed surface of steaks (n = 7) displayed for 6 d

Muscle	Surface layer oxygen depth (%) after 1 h bloom
Longissimus lumborum	35.65[a]
Psoas major	18.95[b]
Semitendinosus	22.74[b]
	SEM = 3.94

[ab]Least squares means with different letters are significantly different ($P < 0.05$).

[1]Depth of layer of oxymyoglobin and metmyoglobin on the surface of muscle not exposed to oxygen after an hour bloom at 4°C and slicing 2 mm to re-expose surface layer divided by size of the piece where surface layer was measured. % Surface layer = (Depth after 1 h bloom ÷ Piece size) x 100

SEM = standard error of mean

Table 6.15. Effect of retail display day on the percent oxygen depth[1] after an hour of bloom at 4°C of the non-oxygen exposed surface of steaks (n = 7) displayed for 6 d

Retail display day	Oxygen Depth (%)
0	100.00[a]
3	85.17[b]
6	72.89[c]
	SEM = 4.23

[a-c]Least squares means with different letters are significantly different ($P < 0.05$).

[1]Depth of layer of oxymyoglobin and metmyoglobin gained after an hour bloom at 4°C divided by size of the piece where oxygen depth was measured. Oxygen depth (%) = ((Depth after 1 h bloom) ÷ Piece size) x 100

SEM = standard error of mean

Table 6.16. Pearson's correlation between *a** values and color attributes

Parameter	All muscles	*Psoas major*	*Longissimus*	*Semitendinosus*
Pull day	-0.66*	-0.88*	-0.86*	-0.76*
Non-oxygen exposed lipid oxidation	-0.16	-0.27	0.14	0.36
Oxygen exposed lipid oxidation	-0.42*	-0.55*	0.16	-0.23
Non-oxygen exposed metmyoglobin reducing ability	0.09	0.29	-0.12	0.53*
Oxygen exposed metmyoglobin reducing ability	0.55*	0.69*	0.77*	0.81*
Non-oxygen exposed oxygen consumption at 30 min	-0.09	0.007	0.18	0.12
Oxygen exposed oxygen consumption at 30 min	0.31*	0.71*	0.25	0.49*
Non-oxygen exposed oxygen consumption at 60 min	0.07	-0.39	0.42	0.42
Oxygen exposed oxygen consumption at 60 min	0.60*	0.45*	0.36	0.50*
Non-oxygen exposed oxidation at 30 min	0.26*	0.28	0.30	-0.45*
Oxygen exposed oxidation at 30 min	0.80*	0.92*	0.68*	0.68*
Non-oxygen exposed oxidation at 60 min	0.26*	0.47*	0.24	-0.32*
Oxygen exposed oxidation at 60 min	0.67*	0.86*	-0.09	0.60*
Non-oxygen exposed surface layer oxygen depth (%)	0.05	-0.007	-0.15	0.05
Oxygen exposed surface layer oxygen depth (%)	-0.45*	-0.72*	-0.83*	-0.73*
Non-oxygen exposed oxygen depth (%)	0.69*	0.81*	0.54*	0.43

*Significant correlation values indicated.

Table 6.17. Simple linear regression values between *a** values and color attributes

Parameter	All muscles	*Psoas major*	*Longissimus*	*Semitendinosus*
Non-oxygen exposed lipid oxidation	0.03	0.07	0.02	0.13
Oxygen exposed lipid oxidation	0.18*	0.31*	0.03	0.05
Non-oxygen exposed metmyoglobin reducing ability	0.008	0.08	0.02	0.28*
Oxygen exposed metmyoglobin reducing ability	0.31*	0.48*	0.59*	0.65*
Non-oxygen exposed oxygen consumption at 30 min	0.01	0.0001	0.03	0.01
Oxygen exposed oxygen consumption at 30 min	0.09*	0.50*	0.06	0.24*
Non-oxygen exposed oxygen consumption at 60 min	0.005	0.15	0.18	0.17
Oxygen exposed oxygen consumption at 60 min	0.36*	0.21*	0.13	0.25*
Non-oxygen exposed oxidation at 30 min	0.07*	0.08	0.09	0.20*
Oxygen exposed oxidation at 30 min	0.63*	0.85*	0.47*	0.46*
Non-oxygen exposed oxidation at 60 min	0.07*	0.22*	0.01	0.10
Oxygen exposed oxidation at 60 min	0.45*	0.74*	0.06	0.36*
Non-oxygen exposed surface layer oxygen depth (%)	0.002	0.00	0.02	0.002
Oxygen exposed surface layer oxygen depth (%)	0.20*	0.52*	0.69*	0.53*
Non-oxygen exposed oxygen depth (%)	0.48*	0.66*	0.29*	0.18

*Significant regression values indicated.

CHAPTER VII

INFLUENCE OF OXYGEN EXPOSURE ON THE METABOLOME OF THE *LONGISSIMUS LUMBORUM*, *PSOAS MAJOR*, AND *SEMITENDINOSUS* MUSCLES DURING RETAIL DISPLAY

ABSTRACT

The color stability of muscles varies depending on the dominant metabolism present. A predominant oxidative metabolism such as that found in the *psoas major* has been reported to have less color stability in comparison to a dominant glycolytic metabolism in the *longissimus lumborum* and *semitendinosus* muscles. These variations in metabolism also influence the muscle-specific response to oxidative stress. However, the influence of oxygen in relation to the color stability and the oxidative changes of specific muscles has not been determined. Therefore, the objective of the current study was to determine the influence of oxygen exposure on the metabolome of the *longissimus lumborum*, *psoas major*, and *semitendinosus* muscles. USDA Low-Choice eye of rounds, strip loins, and tenderloins were processed and sliced into 1.91-cm steaks and packaged into PVC overwrap trays. Steaks were placed into a retail display for 6 d, and instrumental color was determined using a HunterLab spectrophotometer daily. To evaluate oxygen exposure, the steaks were sliced parallel to retail surface (oxygen

exposed; OE) to expose the non-oxygen exposed (NOE) surface. Steaks were analyzed for oxygen exposure on d 0, 3, and 6 including oxygen consumption, metmyoglobin reducing abilitymetmyoglobin reducing ability, and metabolomics. Metabolites were identified using a gas-chromatography-mass spectrometry. Retail data was analyzed using the GLIMMIX procedure of SAS while metabolites were analyzed with MetaboAnalyst 5.0 using a KEGG pathway analysis and projections to latent structure-discriminant analysis (PLS-DA). For all muscles, the *a** values decreased ($P < 0.05$) during display time. The NOE surface had greater ($P < 0.05$) metmyoglobin reducing ability than the OE surface. On d 6, the OE surface of the *psoas major* had lower ($P < 0.05$) oxygen consumption than the NOE surface. Furthermore, the OE surface of the *longissimus lumborum* and *semitendinosus* had greater ($P < 0.05$) oxygen consumption than the OE surface of the *psoas major* at the end of display. The PLSDA plot indicated the separation of the metabolite profiles for the NOE and OE surfaces of each muscle. Fumarate was greater ($P < 0.05$) in abundance in the NOE surface than the OE surface of the *psoas major* and *semitendinosus* muscles supporting the greater metmyoglobin reducing ability in the NOE surface. In addition, the *semitendinosus* and *longissimus lumborum* muscles had greater ($P < 0.05$) fumarate than the *psoas major* muscles. Mannose-6-phosphate was more abundant ($P < 0.05$) in the OE surface of the *longissimus lumborum* and *semitendinosus* muscles than the OE surface of the *psoas major* as well as greater ($P < 0.05$) abundance in the NOE surface of the *psoas major* muscle compare with the OE surface of the *psoas major*. As a marker of lysosomal enzyme transport, the differences in mannose-6-phosphate could indicate the greater enzymatic activity of the color stable muscles and NOE surface. Furthermore, the glycolytic metabolites present in

the *semitendinosus* and *longissimus lumborum* support their color stability over the *psoas major* muscle. The KEGG pathway analysis supports the TCA cycle and pentose phosphate pathway influencing color stability in relation to oxygen exposure. In conclusion, oxygen exposure has muscle-specific implications on the metabolome and subsequent biochemical activity.

INTRODUCTION

Oxygen allows for the bloom of steaks with the binding of oxygen to myoglobin to form consumer-preferred bright red oxymyoglobin (Carpenter et al., 2001). Oxygen penetration and diffusion will influence retail color of steaks (O'Keeffe and Hood, 1982). Oxygen partial pressure within muscle can impact the oxidation of oxymyoglobin. Low oxygen partial pressure results in rapid oxidation of oxymyoglobin and formation of brown metmyoglobin (George and Stratmann, 1952). Low oxygen partial pressure can be formed through oxygen consumption in postmortem muscle by the mitochondria and oxygen-consuming enzymes (Tang et al., 2005a). This oxygen consumption can lead to development of layers of different forms of myoglobin in the interior of intact steaks (Limsupavanich et al., 2004, 2008). From the presence of oxygen, an oxymyoglobin layer is on the surface and a subsurface layer of metmyoglobin (Limsupavanich et al., 2004, 2008). A greater oxygen consumption will decrease oxygen penetration leading to a shallow layer of oxymyoglobin (Bendall and Taylor, 1972; O'Keeffe and Hood, 1982). With time, metmyoglobin rises to the surface, and with a thinner layer of oxymyoglobin, metmyoglobin will rise faster (Limsupavanich et al., 2004, 2008). Metmyoglobin is negatively perceived by consumers (Carpenter et al., 2001) and can lead to the loss of $3.73 billion annually due to discarded and discounted product (Ramanathan et al.,

2022a). Lipid oxidation can influence myoglobin oxidation (Lynch and Faustman, 2000; Faustman et al., 2010). However, oxidative changes and oxygen consumption are muscle specific.

Oxygen consumption, lipid oxidation, and color stability are influenced by muscle type. Muscles with greater type I fibers have more oxidative metabolism while muscles with greater type IIb fibers have more glycolytic metabolism (Hunt and Hedrick, 1977). Oxidative muscles such as the *psoas major* have lower color stability (O'Keeffe and Hood, 1982; McKenna et al., 2005) and increased lipid oxidation (Joseph et al., 2012; Canto et al., 2016; Ke et al., 2017) compared to more glycolytic muscles such as the *longissimus lumborum* . In addition, the *semitendinosus* muscle is considered a color stable muscle with primarily a glycolytic metabolism (McKenna et al., 2005). The *longissimus lumborum* has more TCA metabolites such as succinate which have been reported to contribute to metmyoglobin reduction and increased color stability compared to the *psoas major* (Abraham et al., 2018). Metabolomic research on the color stability of *semitendinosus* muscle has been more limited. The *psoas major* has greater mitochondrial content (Ke et al., 2017; Abraham et al., 2018) and lower antioxidant capacity in the proteome (Joseph et al., 2012) compared to the *longissimus lumborum* muscle which influences oxygen consumption and oxidative changes. The *psoas major* has been reported to have greater oxygen consumption initially and faster degradation of mitochondria and oxygen consumption than the *longissimus lumborum* muscle. This has led to a smaller oxygen penetration with a thinner oxymyoglobin layer and faster discoloration in the *psoas major* compared to *longissimus lumborum* muscles (Limsupavanich et al., 2004, 2008). Although there is a connection between oxygen

consumption and oxygen penetration, there is little knowledge on impact of oxygen exposure in retail on the oxidative changes and subsequent oxidation influence on the metabolome.

These differences in metabolome and proteome have been indicated to influence color stability differences between the *longissimus lumborum* and *psoas major*. Comparisons of these muscles will allow for a comparison of color stability and implications of postmortem muscle metabolism. Therefore, the current study evaluates the metabolomic differences among the *longissimus lumborum*, *psoas major*, and *semitendinosus* muscles during retail display and the effects of oxygen exposure on the metabolome of all three muscles.

MATERIALS AND METHODS

Materials and processing

Six USDA Low Choice short loins (n = 6; IMPS #173) and *semitendinosus* (n = 6; IMPS #171C) were selected 5 d postmortem from Creekstone Farms LLC. As selection of muscles took place during COVID-19, animal effect was not controlled between the short loins and eye of rounds. Muscles were transported to Oklahoma State University Food and Agricultural Products Center on ice and held till 7 d postmortem in dark storage at 4°C. On d 7, the *psoas major* and *longissimus lumborum* muscles were separated. pH was evaluated on all three muscles using Hanna Instruments pH probe in three locations across the muscles (Handheld HI 99163; probe FC232; Hanna Instruments). First, each muscle was faced then muscles were sliced into six 1.91-cm steaks starting from the anterior end. Steaks were randomly assigned to be packaged in pairs for retail display

with the most posterior steak used for proximate analysis and the remaining steak used for d 0 analysis. On d 0, the entire steak was considered non-oxygen exposed surface. Steaks in retail display were analyzed on d 3 or d 6 with one steak analyzed for oxygen consumptionand the other steak analyzed for metmyoglobin reducing ability and metabolomics.

Proximate composition

One steak from each muscle was ground using a table-top grinder (Big Bite Grinder, 4.5 mm, fine grind, LEM). Proximate composition was determined using an AOAC-approved near-infrared spectrophotometer (FoodScan Lab Analyzer, Serial No. 91753206; Foss, NIRsystem Inc.; Slangerupgrade, Denmark). Percent protein, fat, and moisture were reported.

Retail display

Paired steaks were packaged in Styrofoam® PVC overwrap (15,500-16,275 cm^3 $O_2/m^2/24$ h at 23°C, E-Z Wrap Crystal Clear Polyvinyl Chloride Wrapping Film, Koch Supplies, Kansas City, MO) trays and placed in simulated retail display with continuous LED lighting (Philips LED lamps, 12 watts, 48 inches, color temperature = 3,500°K,54 Phillips, China). Instrumental color was evaluated every day using a HunterLab 4500L MiniScan EZ Spectrophotometer (2.5-cm aperture, illuminant A, and 10° standard observer angle, HunterLab Associates, Reston, VA) with each package read six times. CIE *a** values were reported.

Oxygen exposure

The retail surface of the steak was considered the OE surface for analysis on d 3 and 6 while the NOE surface was the interior portion of the steaks. To expose the NOE surface for analysis, steaks were cut parallel to the retail surface. Both surfaces were analyzed for metmyoglobin reducing ability, oxygen consumption, and metabolomics.

Oxygen consumption

Oxygen consumption was determined by blooming the samples for 1 h at 4°C and subsequently incubating at 30°C in vacuum packaging for 60 min. Three HunterLab spectrophotometer readings were taken every 30 min to determine the oxygen consumption. From the spectra data, the change in oxymyoglobin was determined by K/S ratios of preincubation K/S610 / K/S525 – post incubation K/S610 / K/S525.

Metmyoglobin reducing ability

Nitrite-induced metmyoglobin reducing ability was determined by the submersion of samples in 0.3% sodium nitrite for 20 min. Metmyoglobin formation was determined using the K/S ratio of K/S572 / K/S525 from the spectra of the HunterLab 4500L MiniScan EZ Spectrophotometer. A greater number indicates a greater metmyoglobin reduction.

Metabolomic analysis

The National Institute of Health West Coast Metabolomics Center (University of California Davis, CA, USA) analyzed the metabolite samples and identified the metabolites. Ten milligrams of sample were freeze-dried and stored at -80°C until analysis. Extraction of metabolites occurred with 1000 µL of degassed

acetonitrile/isopropanol/water mixture (3:3:2, v/v/v) and was homogenized for 30 s and shook for 6 min at 4°C. The mixture was centrifuged for 2 min at 14,000 g. An internal standard of carbon 8-carbon 30 fatty acid methyl esters were added. Nitrogen-dried samples were derivatized with methyloxolane in pyridine and N-methyl-N(trimethylsilyl)trifluoroacetamide for trimethylsilylation of acidic protons. Further details included in Fiehn et al. (2008) were used in the steps for metabolomic profiling.

Statistical analysis

This experiment was a split-split plot design with the whole plot factor being the muscle. The muscles were blocked by loin. The sub-plot factor and sub-plot factor is pull day and oxygen exposure respectively. Repeated measures were used for the instrumental color analysis with the retail day being the repeated measure. The covariance structure for the repeated measures was first order Toeplitz structure with homogenous variancesand was selected based on the AICC values. Muscle, pull day, oxygen exposure, and their interactions were considered fixed effects. The GLIMMIX procedure of SAS was used to determine the least square means, and the least square means were separated with the PDIFF option and significance was considered with a $P < 0.05$.

MetaboAnalyst 5.0 was utilized to evaluate the metabolites of the three muscles. Data filtering was based on the interquantile range. The data were normalized by the median, transformed by log, and scaled with Pareto scaling. The comparison of d 0 and d 6 metabolites as well as NOE and OE surfaces of each muscle used a fold change analysis. Fold change analysis indicated the significantly different metabolites between the two groups with a fold change threshold of 2.0. To compare the three muscles, an ANOVA analysis with Fisher's LSD post hoc analysis indicated the significantly

different metabolites among the three muscles. Two of the three muscles were compared using a similar fold change analysis previously mentioned. Supervised projections to latent structure-discriminant analysis (PLS-DA) were used to identify different metabolites between the groups of muscles, days, and oxygen exposure. The variable importance in the projection (VIP) in PLS-DA was used to rank metabolites based on their importance in discriminating differences among muscles, days, and oxygen exposure. The VIP was determined to select metabolites with scores greater than 1. Additionally, pathway analysis of MetaboAnalyst 5.0 established pathways impacted by significantly different metabolites.

RESULTS

Proximate composition

Proximate composition of the muscles demonstrated the no differences in fat and protein content (Table 7.1). The *longissimus lumborum* muscle had lower moisture content ($P < 0.05$) compared to the *semitendinosus* muscle. The *psoas major* had higher pH ($P < 0.05$) than the *semitendinosus* and *longissimus lumborum* muscles.

Retail display color

As display time increased, all muscles decreased ($P < 0.05$) in a^* values (Table 7.2). Initially, all muscles had similar ($P > 0.05$) redness in retail display. By the end of retail display, the *psoas major* had the lowest redness followed by the *longissimus lumborum* and the *semitendinosus* had the greatest redness.

Metmyoglobin reducing ability

There was a significant day × oxygen exposure effect on the metmyoglobin reducing ability (Table 7.3). The NOE surface had no change ($P > 0.05$) in metmyoglobin reducing ability during retail display. The OE surface decreased ($P < 0.05$) in metmyoglobin reducing abilityfrom day 0 to day 3 in retail display then remained constant. On days 3 and 6, the NOE surface had higher ($P > 0.05$) metmyoglobin reducing ability than the OE surface.

Oxygen consumption

There was a significant day × muscle × oxygen exposure interaction on the oxygen consumption at 30 min and 60 min (Table 7.4). There were no differences in muscle-specific oxygen consumption at 30 min at day 0. The NOE surface of the *psoas major* did not change ($P > 0.05$) during retail display while the NOE surface of the *longissimus lumborum* and *semitendinosus* surfaces decreased ($P < 0.05$) in oxygen consumption at 30 min. The OE surface of all muscles decreased ($P < 0.05$) in oxygen consumption at 30 min during retail display. At the end of retail display, the OE surface of the *psoas major* and *semitendinosus* had significantly lower oxygen consumption at 30 min than the NOE surface. The NOE surface of *semitendinosus* had lower ($P < 0.05$) oxygen consumption than the NOE surface of *longissimus lumborum* and *psoas major* on day 6. The OE surface of the *longissimus lumborum* had greater ($P < 0.05$) oxygen consumption at 30 min than the same surface of the *semitendinosus* and *psoas major* on day 6.

The oxygen consumption of the NOE surface *psoas major* and *semitendinosus* at 60 min did not change ($P > 0.05$) from day 0 to day 6 of retail display. The OE surface of

the *psoas major* and *longissimus lumborum* decreased ($P < 0.05$) during retail display. On day 0, the *semitendinosus* had greater ($P < 0.05$) oxygen consumption than the *psoas major* and *longissimus lumborum*. At the end of retail display, there was no significant effect of oxygen exposure on the oxygen consumption of *semitendinosus* and *longissimus lumborum*. The *psoas major* NOE surface had greater ($P < 0.05$) oxygen consumption than the OE surface of the *psoas major*. Both surfaces of the *semitendinosus* muscle had greater ($P < 0.05$) oxygen consumption than both surfaces of the *longissimus lumborum* muscle.

Metabolomics

Four hundred and three features were identified in the GC-MS nontargeted analysis, and from those, 149 known compounds were identified in the metabolite library. Select differently abundant metabolites were reported in Table 7.5.

Metabolome profile of the psoas major

The PLS-DA scores plot demonstrates the difference between d 0 NOE surface and OE and OE d 6 surfaces of the *psoas major* muscle (Figure 7.1a). The metabolite profiles of the NOE and OE surfaces of the *psoas major* on d 6 were not separated. From the variable importance projection analysis, gluconic acid, ribonic acid, and fumaric acid were indicated as the most important metabolites influencing the separation from retail days in the PLS-DA plot (Figure 7.1b). Twenty-nine metabolites were found to be differently abundant ($P < 0.05$) among the d 0 OE, d 6 OE, and d6 NOE surfaces of the *psoas major* muscle (Figure 7.2). Metabolites such as hypoxanthine, citric acid, gluconic acid, xylose are upregulated on d 6 versus d 0 of the NOE surface whereas adenosine-5-monophosphate, succinic acid, glucose, and creatinine were downregulated on d 6

compared with d 0 of the NOE surface. Ribonic acid, citric acid, and gluconic acid were downregulated on d 0 compared with d 6 of the OE surface while succinic acid, glucose, and fumaric acid were upregulated on d 0. There were seven metabolites of the *psoas major* significantly influenced by oxygen exposure (Table 7.1A). Fumaric acid, mannos-6-phosphate, ribose, glucose, and salicylic acid were upregulated on the NOE surface compared with the OE surface. The metabolites 3-hydroxybutyric acid and lactamide were upregulated on the OE surface in comparison to the NOE surface. From the pathway analysis, differently abundant metabolites were reported to be associated with the TCA cycle, pentose phosphate pathway, arginine biosynthesis, and pentose and glucoronate interconversions (Figure 7.3).

Metabolome profile of the semitendinosus

Based on the groupings in the PLS-DA plot, there are differences between the metabolite profiles of the d 0 NOE surface, d 6 OE surface, and d 6 NOE surface of the *semitendinosus* muscle during retail display (Figure 7.4a). There were 21 metabolites determined as significantly different among the three surfaces of the *semitendinosus* (Table A7.2). The variable importance projection analysis (Figure 7.4b) demonstrated citric acid, xanthine, succinic acid, and aconitic acid as the top metabolites contributing to the separation of metabolite profiles reported in the PLS-DA plot. Of the identified metabolites, twenty metabolites were differently abundant ($P < 0.05$) on the NOE surface on d 0 relative to d 6 of retail display (Figure 7.5). Upregulated metabolites of d 0 NOE surface included succinic acid, fumaric acid, and arachidonic acid. Citric acid, gluconic acid, and aconitic acid were some of the down regulated metabolites on d 0 NOE surface relative to d 6 NOE surface. Twenty metabolites were differently abundant ($P < 0.05$) on

d 0 OE surface relative to d 6 OE surface with downregulated metabolites on d 0 comprising aconitic acid, citric acid, and ribose. Upregulated metabolites of d 0 OE surface compared to d 6 OE surface included succinic acid, fumaric acid, and 3-hydroxybutyric acid. The evaluation of the metabolite profiles of OE relative to NOE surfaces indicated 14 metabolites with different abundance ($P < 0.05$). Succinic acid and gluconic acid were downregulated while citric acid and aconitic acid were upregulated in OE surface compared to NOE surface. Metabolite profile differences in d 0 NOE, d 6 NOE, and d 6 OE surfaces were mostly associated with TCA cycle, pentose phosphate pathway, alanine, aspartic acid, and glutamic acid metabolism, and glyoxylate and dicarboxylate metabolism (Figure 7.6) based on the KEGG pathway analysis.

Comparison of muscles

On d 6, the metabolite profile for the NOE surfaces of the three muscles indicated separation in the PLS-DA plot between *longissimus lumborum* and *psoas major* as well as *longissimus lumborum* and *semitendinosus* profiles (Figure 7.7a). There was little separation between the *psoas major* and *semitendinosus* profiles of the NOE surface. Thirty-two metabolites were significantly different among the three muscles NOE surfaces (Table A7.3). From the VIP analysis, inosine-5-monophosphate, gluconic acid, and methionine influenced the separation of the PLS-DA plots of the three muscles (Figure 7.7b). Metabolites such as hypoxathine, ribonic acid, and gluconic acids were upregulated in the *psoas major* compared with the *longissimus lumborum* and *semitendinosus* muscles whereas threonic acid, glucose, and creatinine were downregulated in comparison to *longissimus lumborum* and *semitendinosus* muscles. 4-hydroxybutyric acid was differently abundant ($P < 0.05$) among the three muscles on d 6

NOE surface with greater abundance in the *longissimus lumborum* than the *psoas major* and the *semitendinosus* muscle. A KEGG pathway analysis indicated the pentose phosphate pathway, TCA cycle, and purine metabolism as the metabolisms mostly associated with the significantly different metabolites (Figure 7.8).

There were thirty significantly different metabolites among the OE surface of the three muscles (Table A7.4). The PLS-DA plot demonstrates a separation in metabolite profiles of the d 6 OE surface of the three muscles (Figure 7.9a). Based on the VIP analysis, inosine-5-monophosphate and mannitol greatly influenced the separation among muscles in the PLS-DA plot (Figure 7.9b). Inosine-5-monophosphate had greater abundance in the OE surface of *longissimus lumborum* muscle compared with the OE surfaces of *psoas major* and the *semitendinosus* muscles (Table 7.9). Gluconic acid was upregulated in the *psoas major* OE surface followed by the OE surface of *longissimus lumborum* and then the OE surface of the *semitendinosus*. Lysine, isoleucine, phenylalanine were upregulated in the *longissimus lumborum* muscle and downregulated in the *psoas major* muscle and the *semitendinosus* muscles on the OE surface. The KEGG pathway analysis reported the pentose phosphate pathway, purine metabolism, and phenylalanine, tyrosine, and tryptophan metabolisms as mostly associated with the significantly different metabolites (Figure 7.10).

DISCUSSION

Color stability between the *psoas major* and *longissimus lumborum* has been connected to differences in muscle fiber types. With a greater number of oxidative fibers than the *longissimus lumborum* (Hunt & Hedrick, 1977; Yu et al., 2019), the *psoas major* has a more oxidative metabolism and less color stable (O'Keeffe and Hood, 1982;

McKenna et al., 2005). Furthermore, a greater number of oxidative fibers means the *psoas major* has more mitochondria and faster degradation of mitochondria leading to lower oxygen consumption than the *longissimus lumborum* (O'Keeffe and Hood, 1982; Abraham et al., 2017; Ke et al., 2017) as reported here. The more rapid degradation of mitochondria can lead to production of reactive oxygen species and increased oxidative stress in the *psoas major* than the *longissimus lumborum* (Ke et al., 2017). These same attributes could contribute to the negative influence of oxygen on the oxygen consumption of the *psoas major*. Previous research has reported less metmyoglobin reducing ability in the *psoas major* compared to the *longissimus lumborum* muscle (McKenna et al., 2005; Joseph et al., 2012; Abraham et al., 2017; Ke et al., 2017) and the *semitendinosus* muscle (Nair et al., 2018). Although the present study does not indicate these differences, oxygen exposure had a negative influence on the metmyoglobin reducing ability which may relate to changes in the metabolome.

Previous research has reported the conversion of fumaric acid to malic acid leading to the generation of NADH (Mitacek et al., 2019). In support, fumaric acid was reported to increase in parallel with an increase in malic acid *longissimus lumborum* muscles early postmortem (England et al., 2018). Therefore, the presence of fumaric acid in greater abundance on the NOE surface of the *semitendinosus* and *psoas major* muscles supports the greater reducing capacity of the NOE surface. Furthermore, the loss of fumaric acid during aging of the *longissimus lumborum* muscle supports the decline in fumaric acid during display reported in the present study (Mitacek et al., 2019). The greater abundance of fumaric acid in both surfaces of the *longissimus lumborum* muscle compared with the *psoas major* muscle aligns with the color stability of the muscles as

the *longissimus lumborum* muscle has been reported to be more color stable than the *psoas major* muscle (Abraham et al., 2017; Yu et al., 2019).

From citrate, aconitic acid is formed leading to the production of succinic acid (Krebs and Johnson, 1980). Succinate is utilized as part of the electron-transport mediated metmyoglobin reduction (Tang et al., 2005b) and reverse transport metmyoglobin reduction (Belskie et al., 2015). In the present study, the more color-stable *longissimus lumborum* and *semitendinosus* muscles had greater succinic acid in comparison to the *psoas major* muscle on d 6. Hence, the formation of citric acid and aconitic acid during retail display in the *longissimus lumborum* and *semitendinosus* muscles supports the greater production of succinate and increased color stability. In support, previous research reported the *longissimus lumborum* muscle having greater succinic acid than the *psoas major* muscle (Abraham et al., 2017; Yu et al., 2019). Lastly, the greater abundance of citric acid on the retail surface of the *longissimus lumborum* and *semitendinosus* muscles compared with the interior surface may indicate the need for reduction of metmyoglobin by production of succinate from citrate. Furthermore, loss of succinate during retail display supports the decline in redness of all three muscles.

Ribose and ribonic acid increased in the *longissimus lumborum* and *psoas major* muscles during retail display indicating an increase in sugar metabolism with greater retail time. Greater postmortem time of chicken has reported an increase in ribose (Aliani et al., 2013). Ribose is a component to ATP and may increase due to the ATP needs of postmortem muscle (Dhanoa and Housner, 2007). Furthermore, the *longissimus lumborum* muscle increased in ribonic acid during retail display (Abraham et al., 2017) paralleling with the increase reported in the present study. By the breakdown of ribose,

ribonic acid and NADPH are formed (Mahoney et al., 2018). As NADPH can be used for metmyoglobin reduction (Shimizu and Matsuura, 1968), the increased presence of ribose and ribonic acid during retail display could indicate the demand for metmyoglobin reducing pathways. Past research reported ribonic acid was greater in the *psoas major* muscle than the *longissimus lumborum* muscle on d 7 of retail display (Abraham et al., 2017) aligning with the findings of the current study. Therefore, the demand for NADPH could be greater in the *psoas major* muscle than the *longissimus lumborum* muscle to allow for metmyoglobin reduction. Ribose content was not reported to vary between the *psoas major* and *longissimus lumborum* muscles in the present study. The NOE surface had greater ribose in the *psoas major* muscle and less ribonic acid in the *longissimus lumborum* muscle compared to the OE surface supporting the need for NADPH production on the retail surface to increase reducing capacity in comparison to the more biochemically and oxidatively stable interior.

The pentose phosphate pathway has been reported to play a role in color stability of pork (Welzenbach et al., 2016). Metabolites such as ribulose-5-phosphate and ribose-5-phosphate in the pentose phosphate pathway may impact the color stability and oxygen effects. Abraham et al. (2017) reported greater abundance of ribose-5-phosphate in the *psoas major* compared with the *longissimus lumborum* as found in the OE surface of the *psoas major* in this work whereas the opposite was found in the NOE surface. Furthermore, ribulose-5-phosphate was reported to decrease during retail display of the *psoas major* as well as be in lower abundance in the NOE surface of the *psoas major* compared with the *longissimus lumborum* in the present study. These changes may be an indication of the formation of ribose in the *psoas major* muscle. However, the role these

metabolites associated with the pentose phosphate pathway may play in color stability is unclear at this time.

Glycolytic metabolites such as fructose-6-phosphate, glucose-6-phosphate, and glucose were more abundant in the glycolytic *longissimus lumborum* and *semitendinosus* than the oxidative *psoas major* muscle. Similarly, research has reported lower galactose-6-phosphate in the less glycolytic (Zerouala and Stickland, 1991; Ramanathan et al., 2020b) dark-cutting beef compared to normal-pH beef (Ramanathan et al., 2020b; Kiyimba et al., 2021). Fructose was indicated to be in greater abundance in the *longissimus lumborum* than the *psoas major* muscle during retail display (Abraham et al., 2017) as reported in the present study. Furthermore, fructose can be broken down in the presence of ATP to form fructose-6-phosphate and NADH (Khitan and Kim, 2013). NADH has been reported to reduce metmyoglobin (Brown and Snyder, 1969; Denzer et al., 2020). Galactose-6-phosphate can also be converted to fructose-6-phosphate through the pentose phosphate pathway (Grapov et al., 2019). Therefore, the greater presence of fructose, galactose-6-phosphate, and fructose-6-phosphate in the NOE surface of the *longissimus lumborum* compared to the NOE surface of the *psoas major* may relate to the greater color stability of the *longissimus lumborum*.

Research has reported mitochondrial reactive oxygen species (Kajihara et al., 2017) and oxidative stress in the presence of low glucose conditions in endothelial cells (Wang et al., 2012). Therefore, the lower glucose on the OE surface of the *psoas major* muscle may be indicative of oxidative stress. Furthermore, the lack of effect of oxygen on the glucose levels *longissimus lumborum* muscle supports the greater susceptibility of the *psoas major* to oxidative stress. (Ke et al., 2017). The presence of lactamide has been

suggested to indicate a decrease in glycolysis and increase in gluconeogenesis (Wei et al., 2018; Yan et al., 2020). Therefore, the greater presence of lactamide on the OE surface and during retail supports the decreased presence of glucose in the *psoas major*.

Mannose-6-phosphate may play a role in the oxidative stability of postmortem muscle. Mannose-6-phosphate is a marker for lysosome enzyme transport (Hoflack et al., 1987; Westlund et al., 1991; Coutinho et al., 2012). Hence, the greater presence of mannose-6-phosphate in the OE surface of *longissimus lumborum* and *semitendinosus* compared to the *psoas major* may indicate the greater enzyme activity in the more glycolytic muscles. Similarly, dark-cutting beef which have greater number of oxidative fibers than normal-pH beef was reported to have less mannose-6-phosphate than normal-pH beef (Ramanathan et al., 2020b). Furthermore, Ke et al. (2017) reported greater oxidative stress and less reducing activity in the *psoas major* over the *longissimus lumborum*. The presence of oxygen in the *psoas major* resulted in lower mannose-6-phosphate which may indicate a decrease in enzyme activity due to oxygen. Steaks from the *longissimus lumborum* in vacuum packaging had higher metmyoglobin reducing ability compared to steaks packaged in HiOx-MAP and PVC (Ramanathan et al., 2011) in support of the decline in enzyme activity due to oxygen.

Creatinine has been reported to increase with wet aging as a source for ATP production (Mitacek et al., 2019). Creatinine can be broken down by the kidneys (Bozukluhan et al., 2018) creating methylguandine and creatol when oxidants are present (Abramowitz et al., 2010). Hence, a lower content in the OE surface of the *longissimus lumborum* muscle and supporting the less creatinine in the more oxidative *psoas major* muscle. Guanosine was in greater abundance in color-stable ovine muscles compared to

color labile muscles (Subbaraj et al., 2016). Similarly, the current study found the color-labile *psoas major* with less guanosine compared to the color-stable *longissimus lumborum* on both surfaces.

Methionine can create antioxidant systems while methionine sulfoxide has been indicated as a marker of aging (Lee and Gladyshev, 2011). Methionine sulfoxide reductase reduces methionine sulfoxide to methionine (Lee and Gladyshev, 2011). In postmortem muscle, there has been a strong positive correlation between *a** values and mitochondrial peptide methionine sulfoxide reductase in the *longissimus lumborum* muscle (Wu et al., 2016). Contrary to the present study, greater methionine sulfoxide reductase (Joseph et al., 2012) and methionine (Abraham et al., 2017) were reported in the *longissimus lumborum* muscle than the *psoas major* muscle. However, the greater presence of methionine sulfoxide in the *semitendinosus* and *longissimus lumborum* on both surfaces may relate to declining retail color.

Two neurotransmitters were different among the three muscles. 4-aminobutyric acid (GABA) had greater abundance in the OE surface of the *longissimus lumborum* and *semitendinosus* muscles compared with the OE surface of the *psoas major* muscles. Research on dark-cutting beef has reported greater GABA in dark-cutting *longissimus lumborum* over normal-pH *longissimus lumborum* muscle (Ramanathan et al., 2020b). Although dark-cutting beef has more oxidative fibers aligning closer to the *psoas major*, the greater GABA content in the *longissimus lumborum* and *semitendinosus* muscles may be due to the formation of succinate through the oxidation of GABA (Jakobs et al., 1993; Kleppner and Tobin, 2002; Ravasz et al., 2017) to increase color stability. A second mitochondrial neurotransmitter (Bourguignon et al., 1988; Gibson and Nyhan, 1989;

Caputo et al., 2009) 4-hydroxybutyric acid (GHB) was found in greater abundance in the NOE surface of the *longissimus lumborum* muscle compared to the NOE surface of the *psoas major* muscle. Through oxidation, GHB can form succinic acid in the mitochondria (Gibson and Nyhan, 1989; Caputo et al., 2009). Hence, the presence of greater GHB in the *longissimus lumborum* supports greater color stability. Furthermore, the greater abundance of GHB in the interior of the *longissimus lumborum* compared to the retail surface indicates more biochemical activity.

3-hydroxybutyric acid has a role in fatty acid metabolism as well as a regulatory factor (Mierziak et al., 2021). In mammalian liver mitochondria, 3-hydroxybutyrate dehydrogenase breaks down 3-hydroxybutyrate to form acetoacetate and NADH (Bruss, 2008). However, concentrations of the enzyme have been reported to be lower in ruminants than other species (Nielsen and Fleischer, 1969), which may lead to more 3-hydroxybutyrate to reach surrounding tissues (Bruss, 2008). 3-hydroxybutyric acid could be acting as an antioxidant for reactive oxygen species, inhibit the production of mitochondrial reactive oxygen species, and promote antioxidant defenses (Rojas-Morales et al., 2020). Therefore, the greater presence on the OE surface of the *psoas major* may be in response to oxidative stress compared to the NOE surface.

Nucleoside metabolism varied based on the muscle and oxygen exposure. Metabolites such as hypoxanthine, inosine, and inosine-5-phophate were varied among the three muscles. Hence, the nucleoside metabolism was influenced by muscle type. Previous research by Abraham et al. (2017) reported variations in hypoxanthine between the *longissimus lumborum* and *psoas major*. Furthermore, uridine is part of the production of uracil for RNA (Zhang et al., 2020b). Uridine production may indicate the

increase in nucleoside metabolism due to low-ATP conditions (Yamamoto et al., 2002). Hence, the lack of difference between the *longissimus lumborum* and *psoas major* on the retail surface may indicate the energy demands of an OE surface compared to the NOE surface. Furthermore, the higher uridine in the NOE surface of the *psoas major* may indicate the metabolic energy differences between the *longissimus lumborum* and *psoas major*. The relation of these differences to color stability is unclear. In glycolytic muscles, threonate has been reported to be higher than in oxidative muscles of mice acting as an antioxidant (Fernando et al., 2019). These results support the lower threonate content reported in the *psoas major* compared with the *longissimus lumborum* and *semitendinosus*. Hence, the variations among the three muscles supports the color stability of more glycolytic muscles over more oxidative muscles.

CONCLUSION

Oxygen exposure from the retail settings has implications on the color stability of muscles. Oxygen consumption and metmyoglobin reducing ability were negatively influenced by oxygen exposure. More specifically, the oxygen consumption of the *psoas major* was more negatively influenced by the oxygen exposure than the *longissimus lumborum* and *semitendinosus* supporting the known color-stability of each muscle. The metabolome of the *longissimus lumborum* and *semitendinosus* indicate greater color stability than the *psoas major* as well as a more biochemically active interior compared with the retail surface. Furthermore, shifts in the metabolome of the *psoas major* muscle provides evidence of the negative implications of oxygen on the color-stability of the oxidative muscle. Oxygen is an important factor to consider when evaluating differences in color stability.

Table 7.1. Proximate Composition (%) and pH least square means for the three muscles (n = 6)

Parameter	*Longissimus lumborum*	*Psoas major*	*Semitendinosus*	SEM
Protein	22.53	22.42	22.60	0.36
Moisture	73.59^{b}	74.42^{ab}	75.99^{a}	0.73
Fat	4.66	4.51	2.80	0.83
pH	5.55^{b}	5.65^{a}	5.51^{b}	0.04

^{ab}Least squares means with different letters are significantly different ($P < 0.05$).
SEM = standard error of mean

Table 7.2. Least squares means of color attributes (muscle × retail display day) of steaks (n = 6) displayed for 6 d

		Retail display day						
Parameter	Muscle	0	1	2	3	4	5	6
*a**	*Longissimus lumborum*	36.14^{a}	32.03^{bc}	30.37^{cde}	29.14^{edfg}	27.08^{ghi}	27.66^{fghi}	25.89^{hi}
	Psoas major	33.81^{ab}	29.39^{cdefg}	27.82^{efgh}	25.12^{i}	22.93^{j}	23.02^{j}	19.39^{k}
SEM = 1.59	*Semitendinosus*	35.40^{a}	32.10^{bc}	31.03^{bcd}	31.27^{bcd}	29.26^{defg}	31.28^{bcd}	30.23^{cdef}

$^{a\text{-}l}$Least squares means with different letters are significantly different ($P < 0.05$).
SEM = standard error of mean

Table 7.3. Effect of day × oxygen exposure[1] on the metmyoglobin reducing ability[2] (metmyoglobin reducing ability) of the steaks (n = 6)

	Retail display day		
Oxygen exposure	0	3	6
Non-oxygen exposed	0.93[a]	0.94[a]	0.92[a]
Oxygen exposed	0.93[a]	0.77[b]	0.76[b]
	SEM = 0.01		

[ab]Least squares means with different letters are significantly different ($P < 0.05$).
[1]Exposure of muscle to oxygen as display surface indicated as oxygen exposed or interior of the muscle as non-oxygen exposed.
[2]Metmyoglobin formation after submersion in sodium nitrite solution determined by K/S ratio of metmyoglobin (K/S 572/K/S525)., where a greater number indicates greater reduction.
SEM = standard error of mean

Table 7.4. Least squares means of oxygen consumption (day × muscle × oxygen exposure[1]) of steaks (n = 6) displayed for 6 d

			Retail display day		
Parameter	**Oxygen exposure**	**Muscle**	**0**	**3**	**6**
Oxygen consumption at 30 minutes[2]					
	Non-oxygen exposed	*Longissimus lumborum*	0.19^{aw}	0.19^{abw}	0.16^{bwx}
		Psoas major	0.18^{aw}	0.15^{awx}	0.15^{awx}
SEM = 0.02		*Semitendinosus*	0.17^{aw}	0.15^{abw}	0.12^{bxy}
	Oxygen exposed	*Longissimus lumborum*	0.19^{aw}	0.18^{aw}	0.17^{aw}
		Psoas major	0.18^{aw}	0.11^{bx}	0.10^{byz}
		Semitendinosus	0.18^{aw}	0.04^{by}	0.05^{bz}
Oxygen consumption at 60 minutes[3]					
	Non-oxygen exposed	*Longissimus lumborum*	0.14^{aby}	0.15^{ax}	0.12^{by}
		Psoas major	0.15^{ay}	0.17^{axy}	0.16^{ax}
SEM = 0.01		*Semitendinosus*	0.20^{ax}	0.20^{ay}	0.19^{ax}
	Oxygen exposed	*Longissimus lumborum*	0.14^{ay}	0.09^{bz}	0.12^{aby}
		Psoas major	0.15^{ay}	0.14^{ax}	0.11^{by}
		Semitendinosus	0.20^{ax}	0.18^{axy}	0.18^{ax}

[ab]Least squares means with different letters in a row are significantly different ($P < 0.05$).
[w-z]Least squares means with different letters in a column are significantly different ($P < 0.05$).
[1]Exposure of muscle to oxygen as display surface indicated as oxygen exposed or interior of the muscle as non-oxygen exposed.
[2]Change in oxymyoglobin formation before and after 30 minutes incubation determined by the change in K/S ratio of oxymyoglobin (Preincubation K/S610/K/S525 – Post incubation K/S610/K/S525).
[3]Change in oxymyoglobin formation before and after 60 minutes incubation determined by the change in K/S ratio of oxymyoglobin (Preincubation K/S610/K/S525 – Post incubation K/S610/K/S525).
SEM = standard error of mean

Table 7.5. Differently abundant metabolites among the three muscles[1], during display of the individual muscles[2], and the surfaces of the individual muscles[3]

			Surface[1]		NOE[2]	OE[2]	Day 6[3]
Functional role	Metabolites	Muscles	OE	NOE	Display effect	Display effect	Oxygen effect
Neurotransmitter	4-hydroxybutyric acid	LL	NS	High	NS	Decreasing	NOE
		PM	NS	Low	NS	NS	NS
		ST	NS	Intermediate	NS	NS	NS
TCA Cycle	citric acid	LL	NS	NS	Increasing	Increasing	OE
		PM	NS	NS	Increasing	Increasing	NS
		ST	NS	NS	Increasing	Increasing	OE
	fumaric acid	LL	High	High	NS	NS	NS
		PM	Low	Low	Decreasing	Decreasing	NOE
		ST	High	High	Decreasing	Decreasing	NOE
	succinic acid	LL	NS	High	Decreasing	Decreasing	NS
		PM	NS	Low	Decreasing	Decreasing	NS
		ST	NS	High	Decreasing	Decreasing	NOE
Amino acid metabolism	creatinine	LL	NS	High	Decreasing	Decreasing	NOE
		PM	NS	Low	Decreasing	Decreasing	NS
		ST	NS	High	NS	NS	NS
Glycolysis	gluconic acid	LL	Intermediate	Intermediate	Increasing	Increasing	OE
		PM	High	High	Increasing	Increasing	NS
		ST	Low	Low	Increasing	Increasing	NOE
	glucose	LL	Intermediate	Intermediate	NS	NS	NS
		PM	Low	Low	Decreasing	Decreasing	NOE

Purine metabolism	guanosine	ST	High	High	NS	NS	NS
		LL	High	High	NS	NS	NS
		PM	Low	Low	NS	NS	NS
	hypoxanthine	ST	Intermediate	High	NS	NS	NS
		LL	Low	Low	Increasing	Increasing	NS
		PM	High	High	Increasing	Increasing	NS
	inosine 5-monophosphate	ST	Intermediate	Low	NS	NS	NS
		LL	High	High	NS	NS	NS
		PM	Low	Low	NS	NS	NS
Sugar metabolism	mannose-6-phosphate	ST	Low	Intermediate	NS	NS	NS
		LL	High	NS	NS	NS	NS
		PM	Low	NS	Decreasing	Decreasing	NOE
	ribose	ST	High	NS	NS	NS	NS
		LL	Low	Low	Increasing	Increasing	NS
		PM	Low	Low	Increasing	Increasing	NOE
	ribonic acid	ST	High	High	Increasing	Increasing	NOE
		LL	Intermediate	Low	Increasing	Increasing	OE
		PM	High	High	Increasing	Increasing	NS
	xylulose	ST	Low	Low	NS	NS	NS
		LL	NS	NS	Increasing	Increasing	NS
		PM	NS	NS	Increasing	Increasing	NS
Amino acid metabolism	methionine	ST	NS	NS	Increasing	Increasing	NOE
		LL	High	NS	NS	NS	NS
		PM	High	NS	NS	NS	NS

Pentose phosphate pathway	methionine sulfoxide	ST	Low	NS	NS	NS	NS
		LL	NS	NS	Increasing	Increasing	NS
		PM	NS	NS	NS	NS	NS
	ribose-6-phosphate	ST	NS	NS	Increasing	Increasing	NOE
		LL	Low	High	NS	NS	NS
		PM	High	Intermediate	NS	NS	NS
		ST	Intermediate	Low	NS	NS	NS

[1]Differently abundant metabolites among the *longissimus lumborum (LL), psoas major (PM)* and *semitendinosus (ST)* muscles for the NOE and OE surfaces separately. High indicates the muscle with the greatest abundance of the metabolite.
[2]Differently abundant metabolites between day 0 and day 6 of retail display for each separate muscle and surface. Increasing indicates the abundance increased during display.
[3]Differently abundant metabolites between the NOE and OE surface for each separate muscle on day 6 of display. NOE indicates the non-oxygen exposed surface had greater abundance than the oxygen-exposed surface.

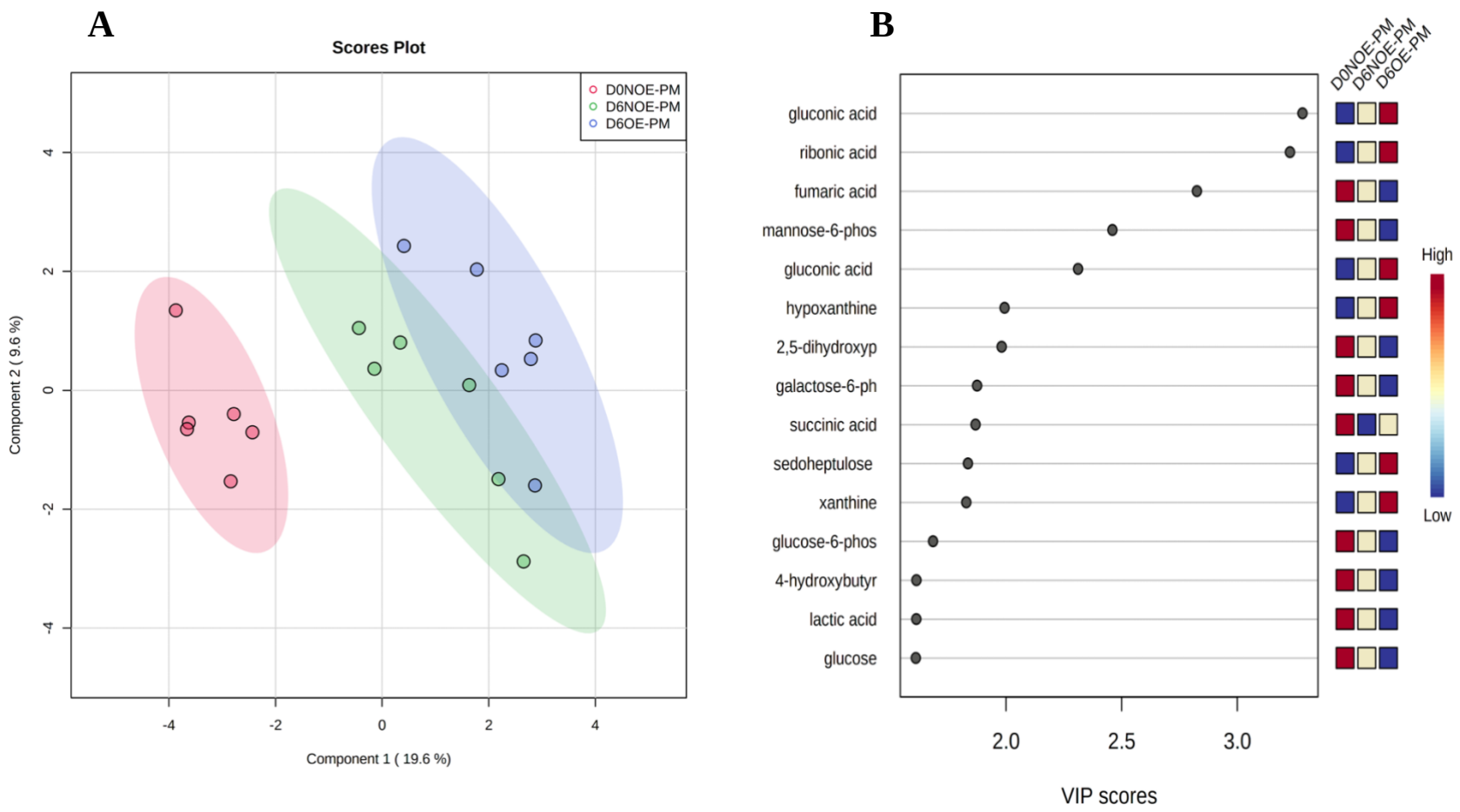

Figure 7.1. (A) Partial least-squares discriminant analysis of metabolites present in surfaces of the *psoas major* muscle. (B) Important features identified by PLS-DA analysis of oxygen exposure of the *psoas major* muscle in retail display. A variable importance projection (VIP) is a measure of a variable importance in PLS-DA model. The VIP score indicates the contribution a variable makes to the model. A greater value denotes more importance.

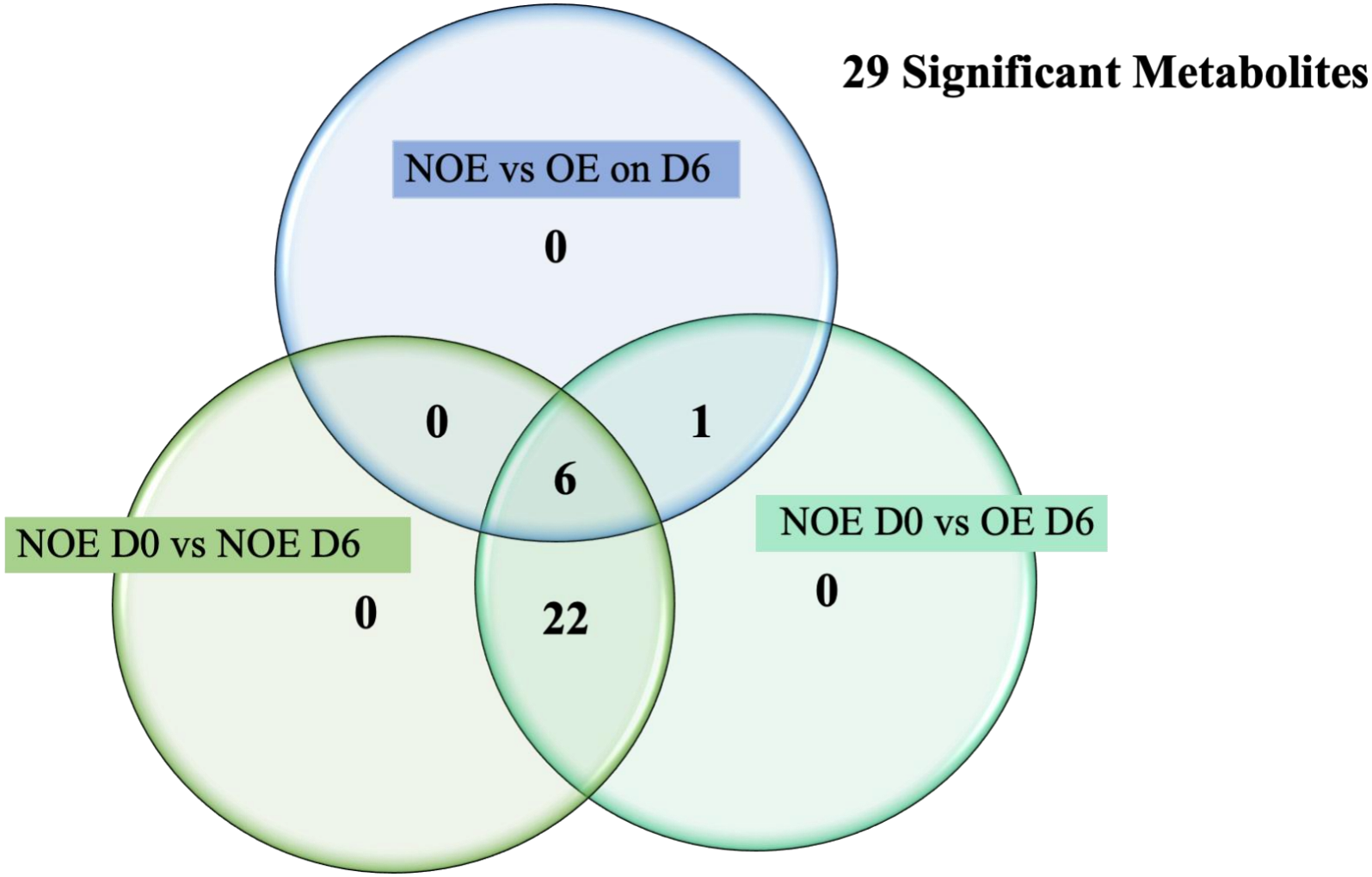

Figure 7.2. Separation of the significantly differentially abundant metabolites for the non-oxygen (NOE) surface on d 0, NOE surface on d 6, and oxygen exposed (OE) surface on d 6 of the *psoas major* muscle during retail display.

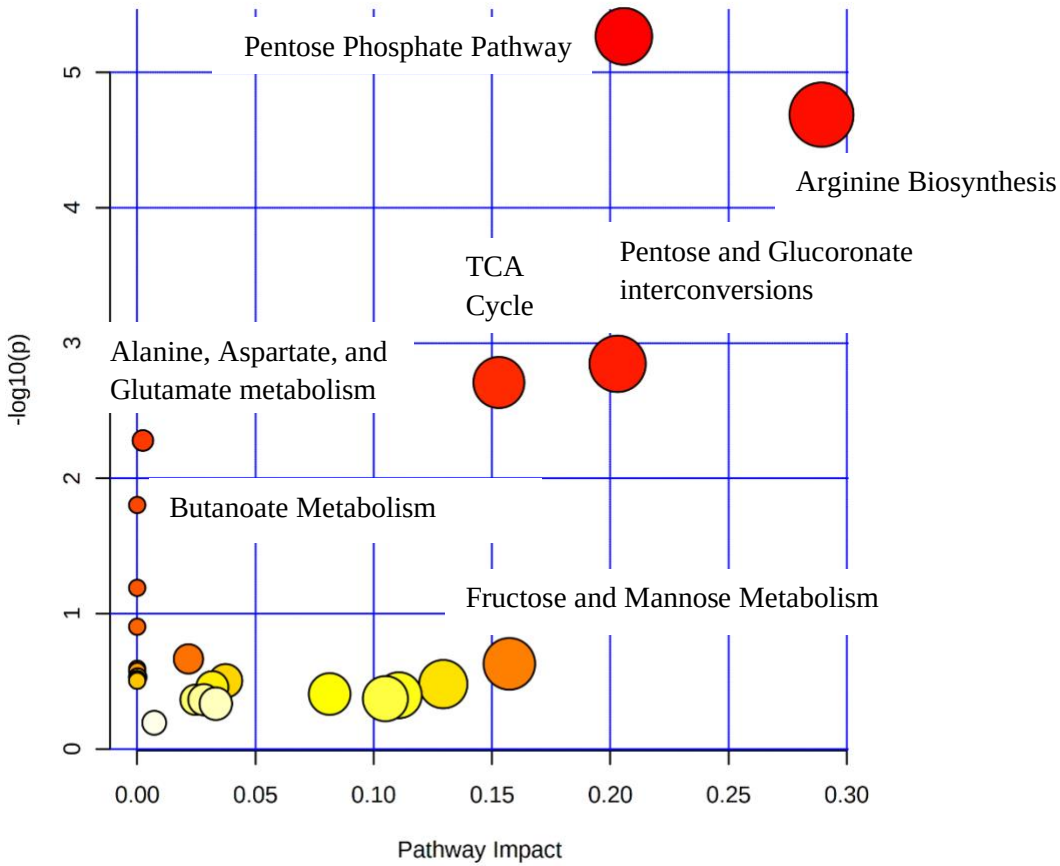

Figure 7.3. KEGG pathway analysis to determine biological process and metabolic pathways that are associated with the metabolites in *psoas major* muscle during retail display. X-axis represents the impact of the pathway, and the y-axis is the -log(*P*-value). The dot color is based on the *P*-value, and the dot size is based on the pathway impact value.

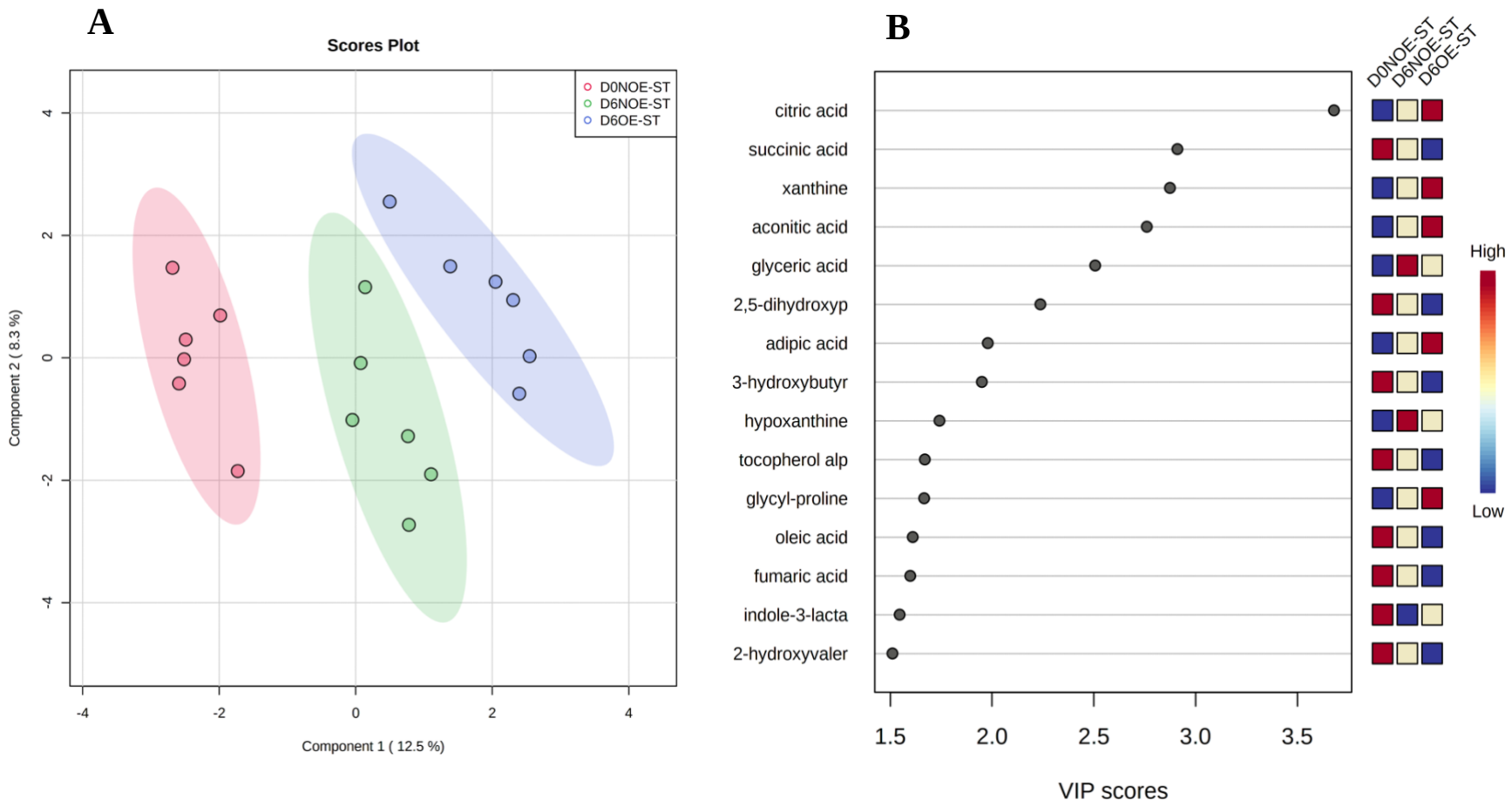

Figure 7.4. (A) Partial least-squares discriminant analysis of metabolites present in surfaces of the *semitendinosus* muscle. (B) Important features identified by PLS-DA analysis of oxygen exposure of the *semitendinosus* muscle in retail display. A variable importance projection (VIP) is a measure of a variable importance in PLS-DA model. The VIP score indicates the contribution a variable makes to the model. A greater value denotes more importance.

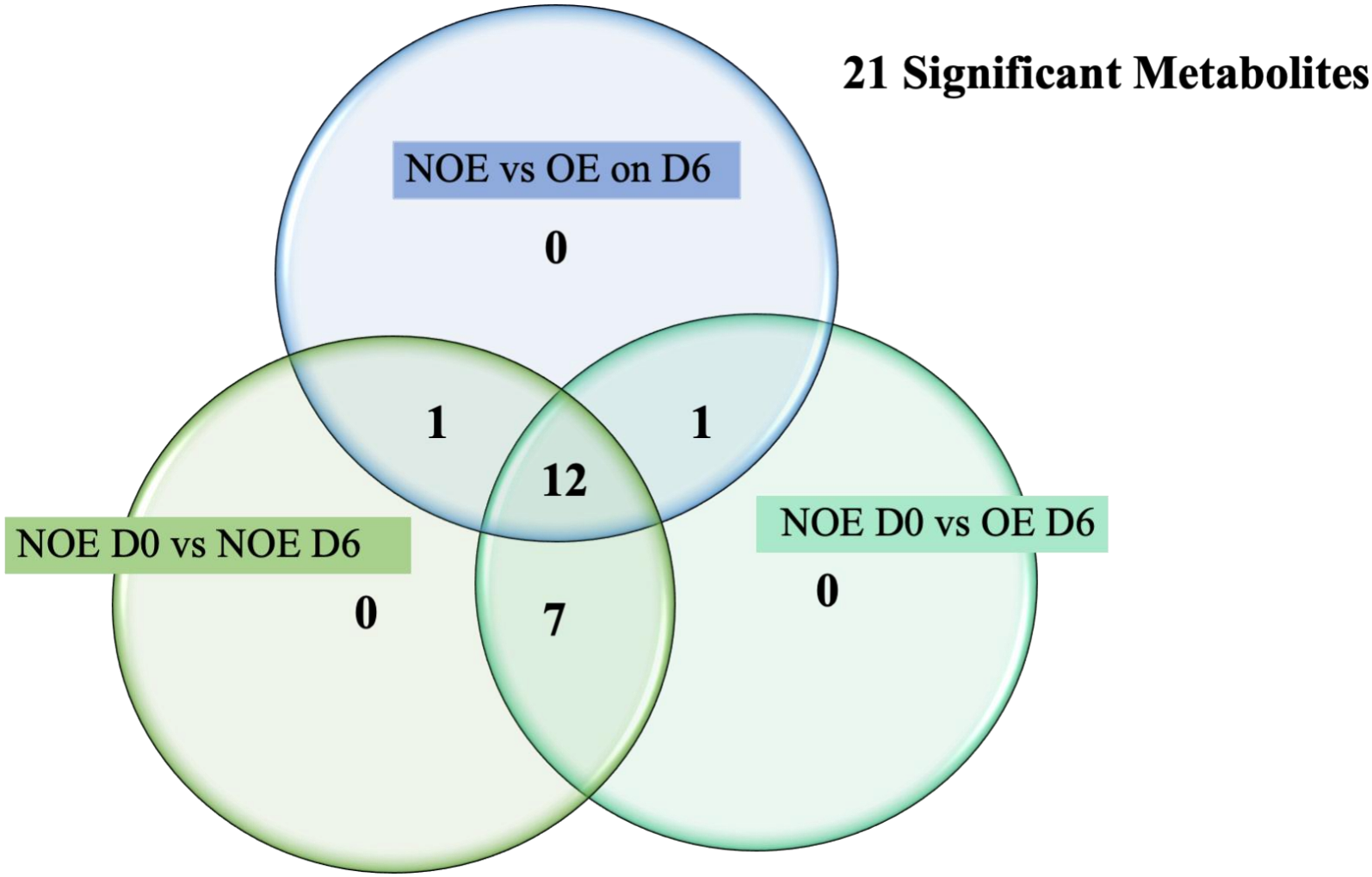

Figure 7.5. Separation of the significantly differentially abundant metabolites for the non-oxygen (NOE) surface on d 0, NOE surface on d 6, and oxygen exposed (OE) surface on d 6 of the *semitendinosus* muscle during retail display.

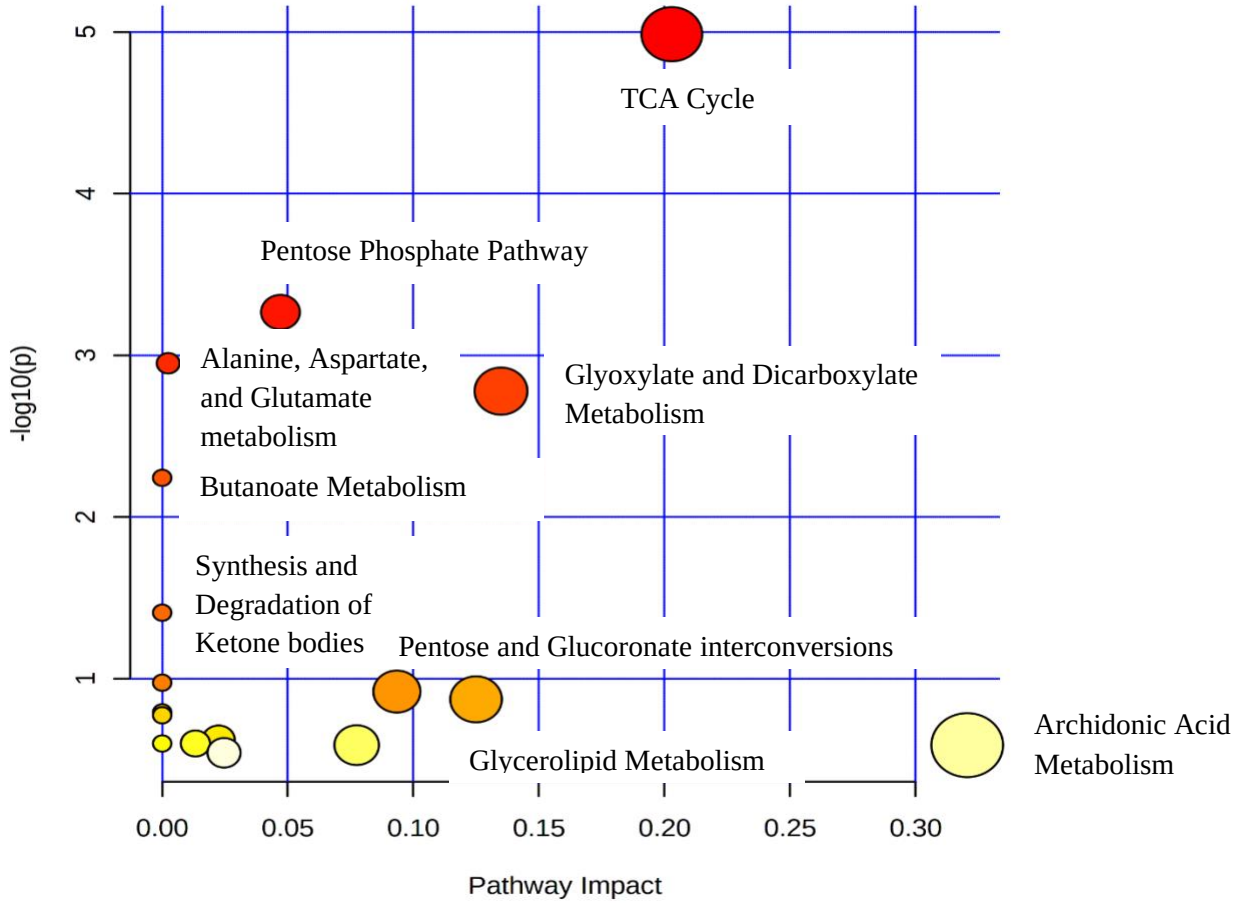

Figure 7.6. KEGG pathway analysis to determine biological process and metabolic pathways that are associated with the metabolites in *semitendinosus* muscle during retail display. X-axis represents the impact of the pathway, and the y-axis is the -log(*P*-value). The dot color is based on the *P*-value, and the dot size is based on the pathway impact values.

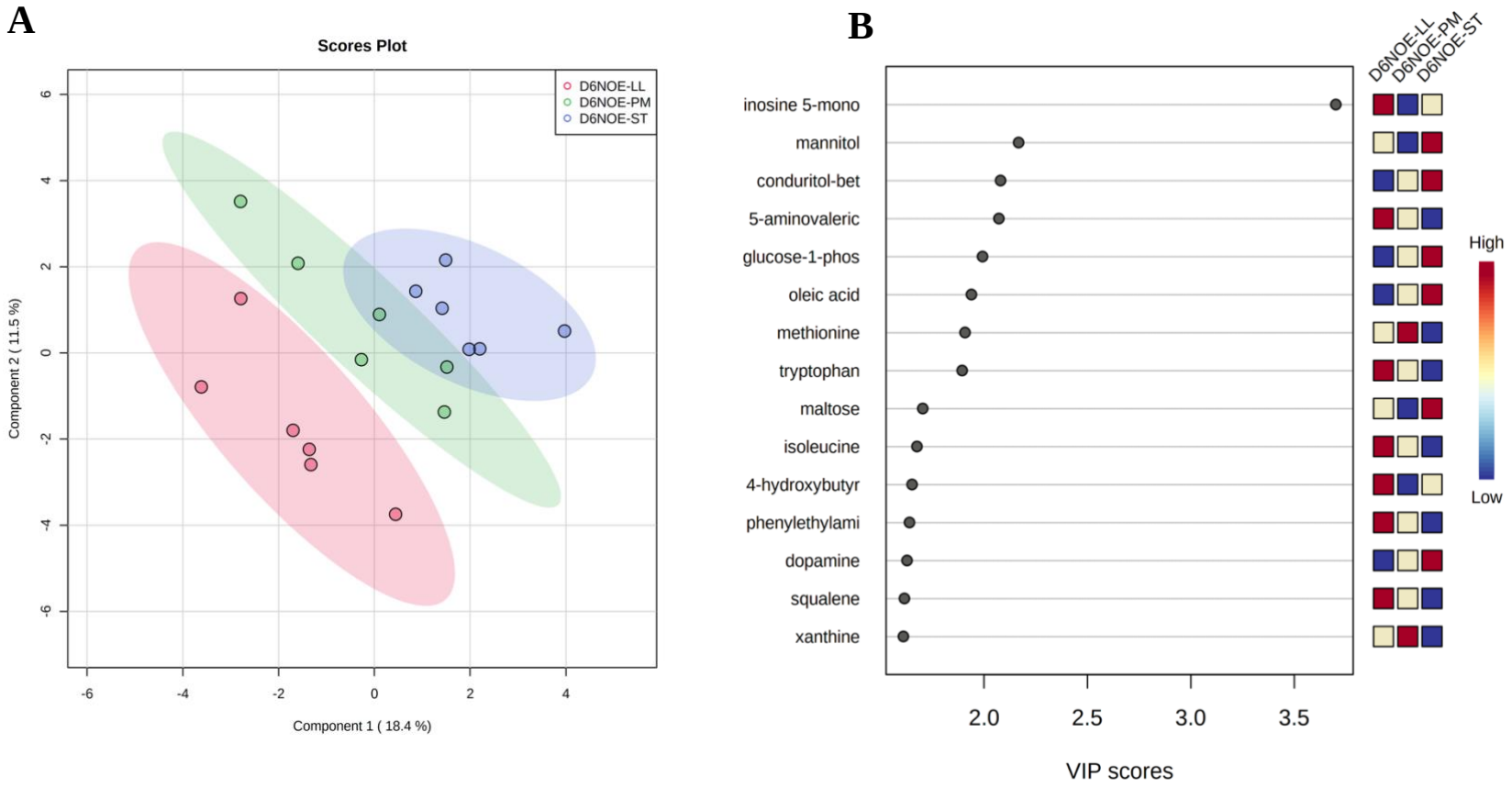

Figure 7.7. (A) Partial least-squares discriminant analysis of metabolites present in non-oxygen exposed (NOE) surfaces of the *semitendinosus*, *psoas major*, and *longissimus lumborum* muscles. (B) Important features identified by PLS-DA analysis of the non-oxygen exposed surface of the *longissimus lumborum*, *semitendinosus*, and *psoas major* muscles in retail display. A variable importance projection (VIP) is a measure of a variable importance in PLS-DA model. The VIP score indicates the contribution a variable makes to the model. A greater value denotes more importance.

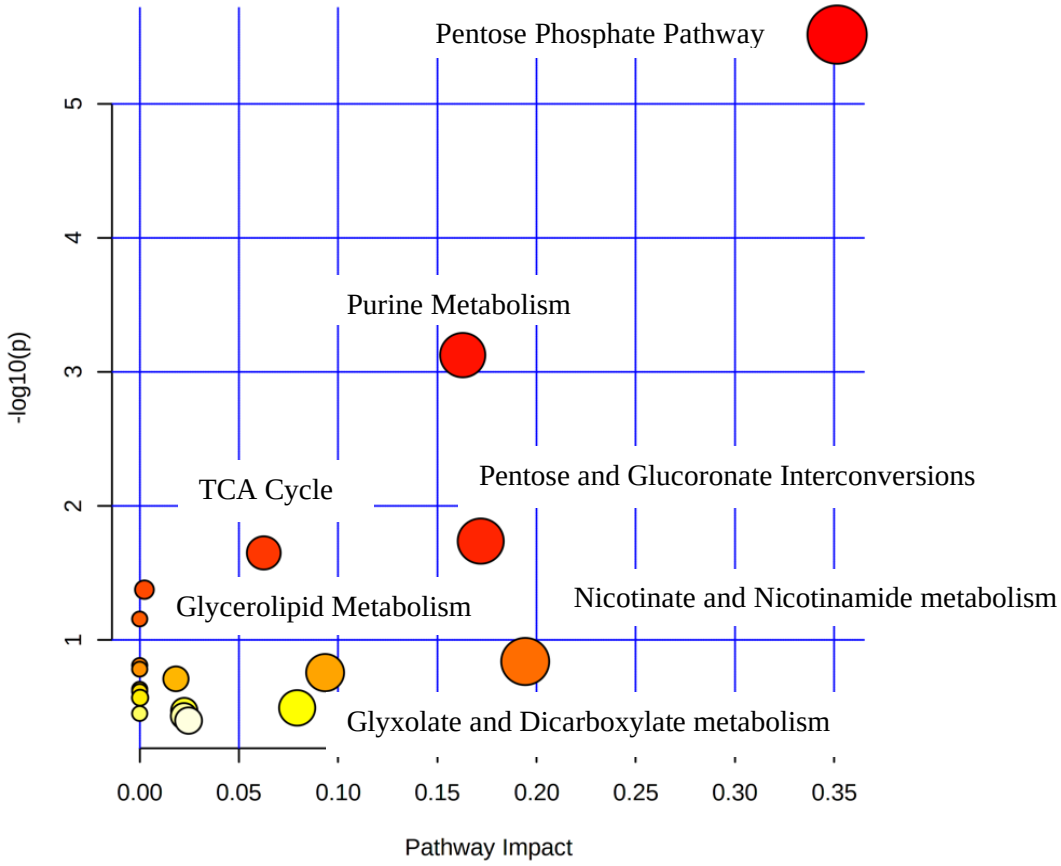

Figure 7.8. KEGG pathway analysis to determine biological process and metabolic pathways that are associated with the metabolites in the NOE surface of the *longissimus lumborum*, *psoas major*, and *semitendinosus* muscle during retail display. X-axis represents the impact of the pathway, and the y-axis is the -log(*P*-value). The dot color is based on the *P*-value, and the dot size is based on the pathway impact values.

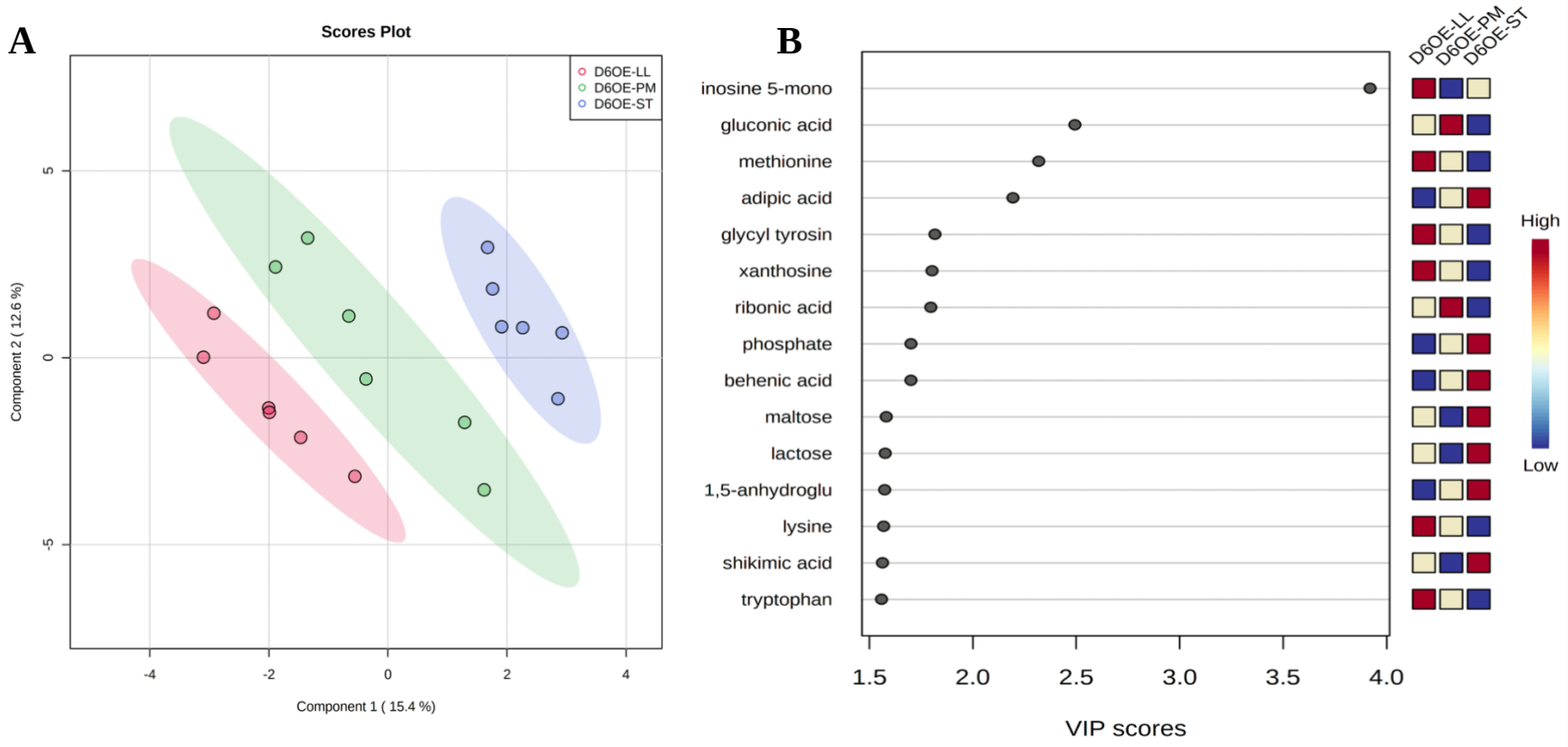

Figure 7.9. (A) Partial least-squares discriminant analysis of metabolites present in oxygen exposed (OE) surfaces of the *semitendinosus*, *psoas major*, and *longissimus lumborum* muscles. (B) Important features identified by PLS-DA analysis of the oxygen exposed (OE) surface of the *longissimus lumborum*, *semitendinosus*, and *psoas major* muscles in retail display. A variable importance projection (VIP) is a measure of a variable importance in PLS-DA model. The VIP score indicates the contribution a variable makes to the model. A greater value denotes more importance.

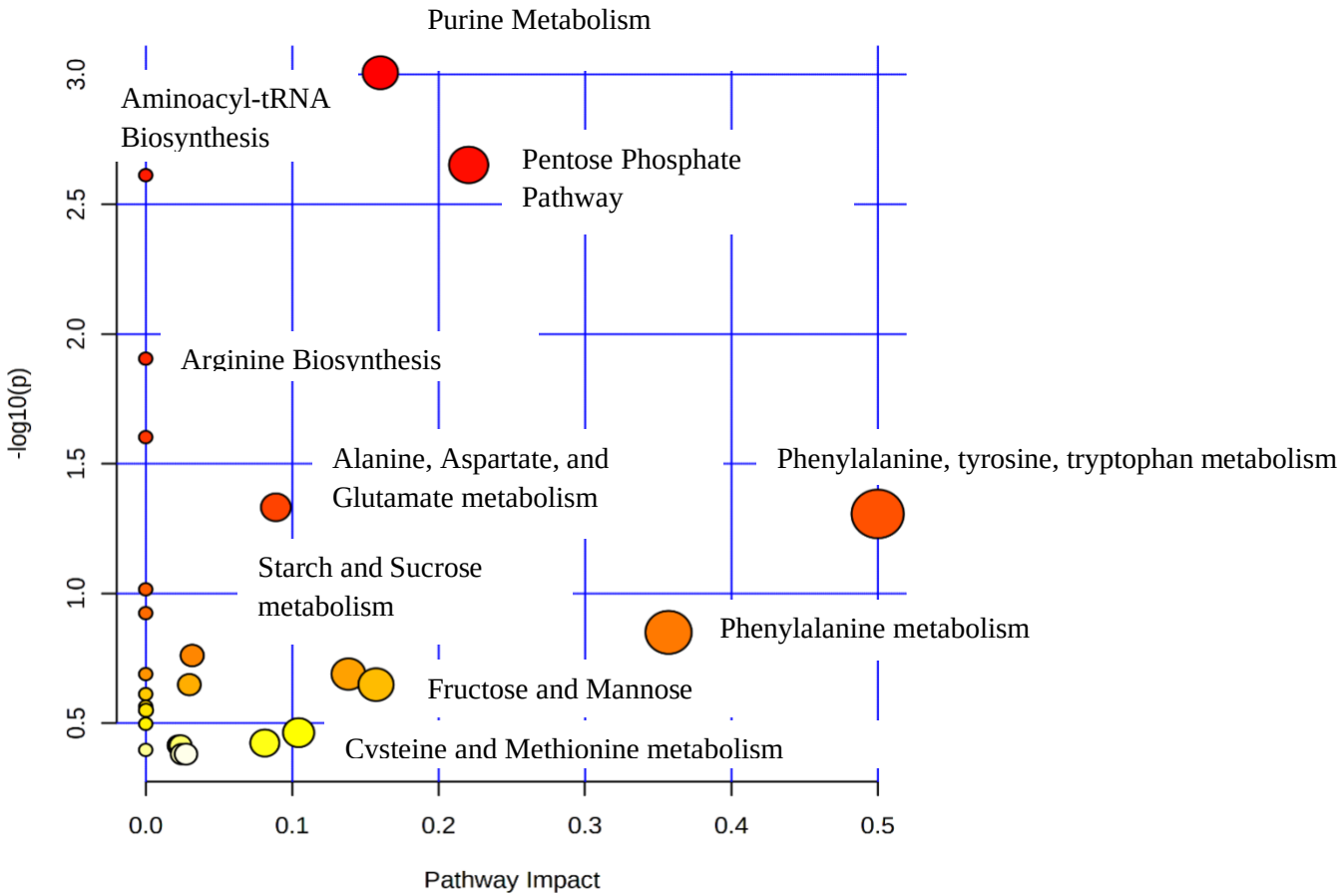

Figure 7.10. KEGG pathway analysis to determine biological process and metabolic pathways that are associated with the metabolites in the OE surface of the *longissimus lumborum*, *psoas major*, and *semitendinosus* muscle during retail display. X-axis represents the impact of the pathway, and the y-axis is the -log(*P*-value). The dot color is based on the *P*-value, and the dot size is based on the pathway impact values.

CHAPTER VIII

CONCLUSION

Oxygen is critical for the development of oxymyoglobin on the surface of beef steaks and providing an appealing appearance to consumers. However, oxygen also plays a key role in the oxidation of lipids and proteins leading to surface discoloration. As myoglobin oxidation occurs internally prior to surface discoloration, the knowledge gained on the transition from interior oxidation to surface discoloration is important to predicting color stability. Furthermore, understanding the impact of oxygen exposure on various parameters related to meat color helps to better predict color stability. Oxygen exposure led to muscle-specific metabolome changes and loss of metmyoglobin reducing ability and oxygen consumptionduring retail storage. Hence, oxygen exposure should be a factor included in analysis of color stability as well as muscle-specific changes.

REFERENCES

Abraham, A., Dillwith, J. W., Mafi, G. G., VanOverbeke, D. L., & Ramanathan, R. (2017). Metabolite Profile Differences between Beef Longissimus and Psoas Muscles during Display. *Meat and Muscle Biology, 1*(1). doi: 10.22175/mmb2016.12.0007

Abramowitz, M. K., Meyer, T. W., & Hostetter, T. H. (2010). Chapter 18 - The Pathophysiology of Uremia. In J. Himmelfarb & M. H. Sayegh (Eds.), *Chronic Kidney Disease, Dialysis, and Transplantation (Third Edition)* (pp. 251-264). Philadelphia: W.B. Saunders.

Aguer, C., Piccolo, B. D., Fiehn, O., Adams, S. H., & Harper, M.-E. (2017). A novel amino acid and metabolomics signature in mice overexpressing muscle uncoupling protein 3. *The FASEB Journal, 31*(2), 814-827. doi: 10.1096/fj.201600914R

Aliani, M., Farmer, L. J., Kennedy, J. T., Moss, B. W., & Gordon, A. (2013). Post-slaughter changes in ATP metabolites, reducing and phosphorylated sugars in chicken meat. *Meat Science, 94*(1), 55-62. doi: 10.1016/j.meatsci.2012.11.032

Andres, A. I., Petron, M. J., Adamez, J. D., Lopez, M., & Timon, M. L. (2017). Food by-products as potential antioxidant and antimicrobial additives in chill stored raw lamb patties *Meat Science, 129*, 62-70. doi: 10.1016/j.meatsci.2017.02.013

. Apple, J. K., Sawyer, J. T., Meullenet, J. F., Yancey, J. W., & Wharton, M. D. (2011). Lactic acid enhancement can improve the fresh and cooked color of dark-cutting beef. *Journal of Animal Science, 89*(12), 4207-4220. doi: 10.2527/jas.2011-4147

Arihara, K., Cassens, R. G., Greaser, M. L., Luchansky, J. B., & Mozdziak, P. E. (1995). Localization of metmyoglobin-reducing enzyme (NADH-cytochrome b5 reductase) system components in bovine skeletal muscle. *Meat Science, 39*(2), 205-213. doi: 10.1016/0309-1740(94)p1821-c

Arun, P., Rittase, W. B., Wilder, D. M., Wang, Y., Gist, I. D., & Long, J. B. (2018). Defective methionine metabolism in the brain after repeated blast exposures might contribute to increased oxidative stress. *Neurochemistry International, 112*, 234-238. doi: 10.1016/j.neuint.2017.07.014

Ashmore, C. R., Parker, W., & Doerr, L. (1972). Respiration of Mitochondria Isolated from Dark-Cutting Beef: Postmortem Changes. *Journal of Animal Science, 34*(1), 46-48. doi: 10.2527/jas1972.34146x

Bankar, S. B., Bule, M. V., Singhal, R. S., & Ananthanarayan, L. (2009). Glucose oxidase — An overview. *Biotechnology advances, 27*(4), 489-501. doi: 10.1016/j.biotechadv.2009.04.003

Bao, Y., & Ertbjerg, P. (2015). Relationship between oxygen concentration, shear force and protein oxidation in modified atmosphere packaged pork. *Meat Science, 110*, 174-179. doi: 10.1016/j.meatsci.2015.07.022

Bao, Y., Puolanne, E., & Ertbjerg, P. (2016). Effect of oxygen concentration in modified atmosphere packaging on color and texture of beef patties cooked to different temperatures. *Meat Science, 121*, 189-195. doi: 10.1016/j.meatsci.2016.06.014

Baron, C. P., & Andersen, H. J. (2002). Myoglobin-induced lipid oxidation. A review. *Journal of Agricultural and Food Chemistry, 50*(14), 3887-3897. doi: 10.1021/jf011394w

Bekhit, A. E.-D. A., Hopkins, D. L., Fahri, F. T., & Ponnampalam, E. N. (2013). Oxidative Processes in Muscle Systems and Fresh Meat: Sources, Markers, and Remedies: Oxidative processes in muscle systems and fresh meat. *Comprehensive reviews in food science and food safety, 12*(5), 565-597. doi: 10.1111/1541-4337.12027

Belskie, K. M., Van Buiten, C. B., Ramanathan, R., & Mancini, R. A. (2015). Reverse electron transport effects on NADH formation and metmyoglobin reduction. *Meat Science, 105*, 89-92. doi: 10.1016/j.meatsci.2015.02.012

Bendall, J. R., and A. A. Taylor. 1972. Consumption of oxygen by the muscles of beef animals and related species. II. Consumption of oxygen by post-rigor muscle. J Sci Food Agric 23(6):707-719. doi: 10.1002/jsfa.2740230606

Bertram, H. C., & Andersen, H. J. (2007). NMR and the water-holding issue of pork.. *Journal of Animal Breeding and Genetics, 124 Suppl 1*(s1), 35-42. doi: 10.1111/j.1439-0388.2007.00685.x

Booth, M. P. S., Conners, R., Rumsby, G., & Brady, R. L. (2006). Structural Basis of Substrate Specificity in Human Glyoxylate Reductase/Hydroxypyruvate Reductase. *Journal of Molecular Biology, 360*(1), 178-189. doi: 10.1016/j.jmb.2006.05.018

Bourguignon, J. J., Schoenfelder, A., Schmitt, M., Wermuth, C. G., Hechler, V., Charlier, B., & Maitre, M. (1988). Analogues of gamma-hydroxybutyric acid. Synthesis

and binding studies. *Journal of medicinal chemistry, 31*(5), 893-897. doi: 10.1021/jm00400a001

Bozukluhan, K., Merhan, O., Ibrahim, H., Öğün, M., Atakişi, E., Kızıltepe, S., & Gökce, G. (2018). *Determination of Some Acute Phase Proteins , Biochemical Parameters and Oxidative Stress in Sheep with Naturally Infected Sheeppox Virus*.

Brantley, R. E., Jr., Smerdon, S. J., Wilkinson, A. J., Singleton, E. W., & Olson, J. S. (1993). The mechanism of autooxidation of myoglobin. *Journal of biological chemistry, 268*(10), 6995-7010.

Brown, R., Capozzi, F., Cavani, C., Cremonini, M., Petracci, M., & Placucci, G. (2000). Relationships between 1H NMR Relaxation Data and Some Technological Parameters of Meat: A Chemometric Approach. *Journal of Magnetic Resonance, 147*(1), 89-94. doi: 10.1006/jmre.2000.2163

Brown, W., & Mebine, L. (1969). Autoxidation of oxymyoglobins. *Journal of biological chemistry, 244*(24), 6696-6701.

Brown, W., & Snyder, H. (1969). Nonenzymatic reduction and oxidation of myoglobin and hemoglobin by nicotinamide adenine dinucleotides and flavins. *Journal of biological chemistry, 244*(24), 6702-6706.

Bruss, M. L. 2008. Chapter 4 - Lipids and Ketones. In: J. J. Kaneko, J. W. Harvey and M. L. Bruss, editors, Clinical Biochemistry of Domestic Animals (Sixth Edition). Academic Press, San Diego. p. 81-115.

Canto, A., Costa-Lima, B. R. C., Suman, S. P., Monteiro, M. L. G., Viana, F. M., Salim, A., . . . Conte-Junior, C. A. (2016). Color attributes and oxidative stability of

longissimus lumborum and psoas major muscles from Nellore bulls. *Meat Science, 121*, 19-26. doi: 10.1016/j.meatsci.2016.05.015

Caputo, F., Vignoli, T., Maremmani, I., Bernardi, M., & Zoli, G. (2009). Gamma hydroxybutyric acid (GHB) for the treatment of alcohol dependence: a review. *International Jounral of Environmental Research and Public Health, 6*(6), 1917-1929. doi: 10.3390/ijerph6061917

Carpenter, C. E., Cornforth, D. P., & Whittier, D. (2001). Consumer preferences for beef color and packaging did not affect eating satisfaction. *Meat Science, 57*(4), 359-363. doi: 10.1016/s0309-1740(00)00111-x

Cecarini, V., Gee, J., Fioretti, E., Amici, M., Angeletti, M., Eleuteri, A. M., & Keller, J. N. (2007). Protein oxidation and cellular homeostasis: Emphasis on metabolism. *Biochimica Biophysica Acta (BBA) - Molecular Cell Research, 1773*(2), 93-104. doi: 10.1016/j.bbamcr.2006.08.039

Celi, P. (2011). Oxidative Stress in Ruminants. In L. Mandelker & P. Vajdovich (Eds.), *Studies on Veterinary Medicine* (pp. 191-231). Totowa, NJ: Humana Press.

Celi, P., & Gabai, G. (2015). Oxidant/Antioxidant Balance in Animal Nutrition and Health: The Role of Protein Oxidation. *Frontiers in Veterinary Science, 2*, 48. doi: 10.3389/fvets.2015.00048

Chan, W. K. M., Hakkarainen, K., Faustman, C., Schaefer, D. M., Scheller, K. K., & Liu, Q. (1995). Color Stability and Microbial Growth Relationships in Beef as Affected by Endogenous α-Tocopherol. *Journal of Food Science, 60*(5), 966-971. doi: 10.1111/j.1365-2621.1995.tb06272.x

Chen, C., Zhang, J., Guo, Z., Shi, X., Zhang, Y., Zhang, L., . . . Han, L. (2020). Effect of oxidative stress on AIF-mediated apoptosis and bovine muscle tenderness during postmortem aging. *Journal of Food Science, 85*(1), 77-85. doi: 10.1111/1750-3841.14969

Consolo, N. R. B., Rosa, A. F., Barbosa, L., Maclean, P. H., Higuera-Padilla, A., Colnago, L. A., & Titto, E. A. L. (2021). Preliminary study on the characterization of Longissimus lumborum dark cutting meat in Angus x Nellore crossbreed cattle using NMR-based metabolomics. *Meat Science, 172*, 108350. doi: 10.1016/j.meatsci.2020.108350

Coutinho, M. F., M. J. Prata, and S. Alves. 2012. Mannose-6-phosphate pathway: A review on its role in lysosomal function and dysfunction. Molecular Genetics and Metabolism 105(4):542-550. doi: 10.1016/j.ymgme.2011.12.012

Cui, H., Kong, Y., & Zhang, H. (2012). Oxidative stress, mitochondrial dysfunction, and aging. *Journal of Signal Transduction, 2012*, 646354. doi: 10.1155/2012/646354

de Groot, B., Zuurbier, C. J., & van Beek, J. H. (1999). Dynamics of tissue oxygenation in isolated rabbit heart as measured with near-infrared spectroscopy. *American Journal of Physiology, 276*(5), H1616-1624. doi: 10.1152/ajpheart.1999.276.5.H1616

Denzer, M., Mowery, C., Comstock, H., Maheswarappa, N. B., Mafi, G. G., VanOverbeke, D. L., & Ramanathan, R. (2020). Characterization of the Cofactors Involved in Non-enzymatic Metmyoglobin/Methemoglobin Reduction In Vitro. *Meat and Muscle Biology, 4*(1). doi: 10.22175/mmb.9507

Denzer, M., Mafi, G., VanOverbeke, D., & Ramanathan, R. (2022). Repackaging Nitrite-Embedded Dark-Cutting Steak in Aerobic Polyvinyl Chloride Film Decreases Surface Redness. *Meat and Muscle Biology, 5*(1), 1-12. doi: 10.22175/mmb.12944

Dhanoa, T. S., & Housner, J. A. (2007). Ribose: More than a simple sugar? *Current sports medicine reports, 6*(4), 254-257. doi: 10.1007/s11932-007-0041-8

Dragsted, L. O. (2010). Biomarkers of meat intake and the application of nutrigenomics. *Meat Science, 84*(2), 301-307. doi: 10.1016/j.meatsci.2009.08.028

England, E. M., Matarneh, S. K., Mitacek, R. M., Abraham, A., Ramanathan, R., Wicks, J. C., . . . Gerrard, D. E. (2018). Presence of oxygen and mitochondria in skeletal muscle early postmortem. *Meat Science, 139*, 97-106. doi: 10.1016/j.meatsci.2017.12.008

English, A. R., Mafi, G. G., VanOverbeke, D. L., & Ramanathan, R. (2016a). Effects of extended aging and modified atmospheric packaging on beef top loin steak color. *Journal of Animal Science, 94*(4), 1727-1737. doi: 10.2527/jas.2015-0149

English, A. R., Wills, K. M., Harsh, B. N., Mafi, G. G., VanOverbeke, D. L., & Ramanathan, R. (2016b). Effects of aging on the fundamental color chemistry of dark-cutting beef. *Journal of Animal Science, 94*(9), 4040-4048. doi: 10.2527/jas.2016-0561

Faustman, C., & Cassens, R. G. (1990). The Biochemical Basis for Discoloration in Fresh Meat: A Review. *Journal of Muscle Foods, 1*(3), 217-243. doi: 10.1111/j.1745-4573.1990.tb00366.x

Faustman, C., Chan, W. K., Schaefer, D. M., & Havens, A. (1998). Beef color update: the role for vitamin E. *Journal of Animal Science, 76*(4), 1019-1026. doi: 10.2527/1998.7641019x

Faustman, C., Sun, Q., Mancini, R., & Suman, S. P. (2010). Myoglobin and lipid oxidation interactions: mechanistic bases and control. *Meat Science, 86*(1), 86-94. doi: 10.1016/j.meatsci.2010.04.025

Feidt, C., Petit, A., Bruas-Reignier, F., & Brun-Bellut, J. (1996). Release of free amino-acids during ageing in bovine meat. *Meat Science, 44*(1), 19-25. doi: 10.1016/S0309-1740(96)00088-5

Fernando, R., C. Drescher, S. Deubel, T. Jung, M. Ost, S. Klaus, T. Grune, and J. P. Castro. 2019. Low proteasomal activity in fast skeletal muscle fibers is not associated with increased age-related oxidative damage. *Experimental Gerontology, 117*:45-52. doi: https://doi.org/10.1016/j.exger.2018.10.018

Filho, I. T. M. D. P., Nguyen, N. M. B. S., Jivani, R. B. S., Terner, J. P., Romfh, P. B. S. M. B. A., Vakhshoori, D. P., & Ward, K. R. M. D. (2016). Oxygen saturation monitoring using resonance Raman spectroscopy. *The Journal of surgical research, 201*(2), 425-431. doi: 10.1016/j.jss.2015.12.001

Fry, D. W., & Richardson, K. E. (1979). Isolation and characterization of glycolic acid dehydrogenase from human liver. *Biochimica et Biophysica Acta (BBA) - Enzymology, 567*(2), 482-491. doi: 10.1016/0005-2744(79)90134-7

Fu, A.-H., Molins, R. A., & Sebranek, J. G. (1992). Storage Quality Characteristics of Beef Rib Eye Steaks Packaged in Modified Atmospheres. *Journal of Food Science, 57*(2), 283-287. doi: 10.1111/j.1365-2621.1992.tb05477.x

Gagaoua, M., Hughes, J., Terlouw, E. M. C., Warner, R. D., Purslow, P. P., Lorenzo, J. M., & Picard, B. (2020). Proteomic biomarkers of beef colour. *Trends in Food Science & Technology, 101*, 234-252. doi: 10.1016/j.tifs.2020.05.005

Gao, X.-g., Wang, Z.-y., Tang, M.-t., Ma, C.-w., & Dai, R.-t. (2014). Comparsion of the Effects of Succinate and NADH on Postmortem Metmyoglobin Redcutase Activity and Beef Colour Stability. *Journal of Integrative Agriculture, 13*(8), 1817-1826. doi: 10.1016/s2095-3119(14)60754-1

George, P., & Stratmann, C. J. (1952). The oxidation of myoglobin to metmyglobin by oxygen. 2. The relation between the first order rate constant and the partial pressure of oxygen. *Biochemical Journal, 51*(3), 418-425. doi: 10.1042/bj0510418

Gibson, K. M., & Nyhan, W. L. (1989). Metabolism of [U-14C]-4-hydroxybutyric acid to intermediates of the tricarboxylic acid cycle in extracts of rat liver and kidney mitochondria. *European Journal of Drug Metabolism and Pharmacokinet, 14*(1), 61-70. doi: 10.1007/bf03190843

Giustarini, D., Dalle-Donne, I., Tsikas, D., & Rossi, R. (2009). Oxidative stress and human diseases: Origin, link, measurement, mechanisms, and biomarkers. *Critical Reviews in Clinical Laboratory Sciences, 46*(5-6), 241-281. doi: 10.3109/10408360903142326

Grapov, D., O. Fiehn, C. Campbell, C. J. Chandler, D. J. Burnett, E. C. Souza, G. A. Casazza, N. L. Keim, J. W. Newman, G. R. Hunter, J. R. Fernandez, W. T. Garvey, C. L. Hoppel, M. E. Harper, and S. H. Adams. 2019. Exercise plasma metabolomics and xenometabolomics in obese, sedentary, insulin-resistant

women: impact of a fitness and weight loss intervention. *American Journal of Physiology – Endocrinology and Metabolism, 317*(6):E999-e1014. doi: 10.1152/ajpendo.00091.2019

Griffin, D. B., Savell, J. W., Smith, G. C., Vanderzant, C., Terrell, R. N., Lind, K. D., & Galloway, D. E. (1982). Centralized Packaging of Beef Loin Steaks with Different Oxygen-Barrier Films: Physical and Sensory Characteristics. *Journal of Food Science, 47*(4), 1059-1069. doi: 10.1111/j.1365-2621.1982.tb07621.x

Guttmann, R. P., & Johnson, G. V. W. (1998). Oxidative Stress Inhibits Calpain Activity in Situ *. *Journal of Biological Chemistry*, *273*(21), 13331-13338. doi: 10.1074/jbc.273.21.13331

Hawkins, N., Denzer, M., Mafi, G., Pfeiffer, M., Hunt, M. C., Mancini, R., & Ramanathan, R. 2021. Comparison of Myoglobin Quantification Methods. Presented at the 2021 Reciprocal Meats Conference in Reno, NV. *Meat and Muscle Biology, 6*(2): 54-55. doi: 10.22175/mmb.13203

Hoflack, B., K. Fujimoto, and S. Kornfeld. 1987. The interaction of phosphorylated oligosaccharides and lysosomal enzymes with bovine liver cation-dependent mannose 6-phosphate receptor. Journal of Biological Chemistry 262(1):123-129. doi: 10.1016/S0021-9258(19)75897-9

Holman, B., Collins, D., Kilgannon, A., & Hopkins, D. (2018). The effect of technical replicate (repeats) on Nix Pro Color Sensor™ measurement precision for meat: A case-study on aged beef colour stability. *Meat Science, 135,* 42-45. doi: 10.1016/j.meatsci.2017.09.001

Holman, B., Diffey, S., Logan, B., Mortimer, S., & Hopkins, D. (2021). Nix Pro Color Sensor Comparison to HunterLab MiniScan for Measuring Lamb Meat Colour and Investigation of Repeat Measures, Illuminant and Standard Observer Effects. *Food Analytical Methods, 14*(4), 697-705. doi: 10.1007/s12161-020-01914-0

Holman, B., & Hopkins, D. (2019). A comparison of the Nix Colour Sensor Pro™ and HunterLab MiniScan™ colorimetric instruments when assessing aged beef colour stability over 72 h display. *Meat Science, 147*, 162-165. doi: 10.1016/j.meatsci.2018.09.009

Holman, B., van de Ven, R., Mao, Y., Coombs, C., & Hopkins, D. (2017). Using instrumental (CIE and reflectance) measures to predict consumers' acceptance of beef colour. *Meat Science, 127*, 57-62. doi: 10.1016/j.meatsci.2017.01.005

Hood, D. E. (1980). Factors affecting the rate of metmyoglobin accumulation in pre-packaged beef. *Meat Science, 4*(4), 247-265. doi: https://doi.org/10.1016/0309-1740(80)90026-1

Hood, D. E., & Riordan, E. B. (1973). Discolouration in pre-packaged beef: measurement by reflectance spectrophotometry and shopper discrimination. *International Journal of Food Science & Technology, 8*(3), 333-343. doi: 10.1111/j.1365-2621.1973.tb01721.x

Hunt, M. C., & Hedrick, H. B. (1977). Profile of Fiber Types and Related Properties of Five Bovine Muscles. *Journal of Food Science, 42*(2), 513-517. doi: 10.1111/j.1365-2621.1977.tb01535.x

HunterLab. Lightweight Portable Color Reader: Miniscan EZ 4500. Retrieved September 5, 2022, from https://www.hunterlab.com/en/products/portable-spectrophotometers/miniscan-ez-4500/

Jakobs, C., J. Jaeken, and K. M. Gibson. 1993. Inherited disorders of GABA metabolism. *Journal of Inherited Metabolic Disease, 16*(4):704-715. doi: 10.1007/BF00711902

Jayasingh, P., Cornforth, D. P., Brennand, C. P., Carpenter, C. E., & Whittier, D. R. (2002). Sensory Evaluation of Ground Beef Stored in High-oxygen Modified Atmosphere Packaging. *Journal of Food Science, 67*(9), 3493-3496. doi: 10.1111/j.1365-2621.2002.tb09611.x

Jeong, J. Y., Hur, S. J., Yang, H. S., Moon, S. H., Hwang, Y. H., Park, G. B., & Joo, S. T. (2009). Discoloration characteristics of 3 major muscles from cattle during cold storage. *Journal of Food Science, 74*(1), C1-5. doi: 10.1111/j.1750-3841.2008.00983.x

Jeremiah, L. E., & Gibson, L. L. (2001). The influence of packaging and storage time on the retail properties and case-life of retail-ready beef. *Food Research International, 34*(7), 621-631. doi: 10.1016/s0963-9969(01)00080-1

Jia, X., Hildrum, K. I., Westad, F., Kummen, E., Aass, L., & Hollung, K. (2006). Changes in Enzymes Associated with Energy Metabolism during the Early Post Mortem Period in Longissimus Thoracis Bovine Muscle Analyzed by Proteomics. *Journal of proteome research, 5*(7), 1763-1769. doi: 10.1021/pr060119s

Joseph, P., Suman, S. P., Rentfrow, G., Li, S., & Beach, C. M. (2012). Proteomics of muscle-specific beef color stability. *Journal of Agricultural and Food Chemistry, 60*(12), 3196-3203. doi: 10.1021/jf204188v

Kajihara, N., D. Kukidome, K. Sada, H. Motoshima, N. Furukawa, T. Matsumura, T. Nishikawa, and E. Araki. 2017. Low glucose induces mitochondrial reactive oxygen species via fatty acid oxidation in bovine aortic endothelial cells. *Journal of Diabetes Investigation, 8*(6):750-761. doi: 10.1111/jdi.12678

Kanick, S. C., van der Leest C., Djamin, R. S., Janssens, A. M., Hoogsteden, H. C,, Sterenborg, H. J., Amelink, A., & Aerts, . JG. (2010). Characterization of mediastinal lymph node physiology in vivo by optical spectroscopy during endoscopic ultrasound-guided fine needle aspiration. *Journal of Thoracic Oncology*, 5(7), 981-987. doi: 10.1097/jto.0b013e3181ddbc0e

Ke, Y., Mitacek, R. M., Abraham, A., Mafi, G. G., VanOverbeke, D. L., DeSilva, U., & Ramanathan, R. (2017). Effects of Muscle-Specific Oxidative Stress on Cytochrome c Release and Oxidation-Reduction Potential Properties. *Journal of Agricultural and Food Chemistry*, *65*(35), 7749-7755. doi: 10.1021/acs.jafc.7b01735

Khitan, Z., and D. H. Kim. 2013. Fructose: a key factor in the development of metabolic syndrome and hypertension. *Journal of Nutritional Metabolism, 2013,* 682673. doi: 10.1155/2013/682673

Kim, Y. H., Huff-Lonergan, E., Sebranek, J. G., & Lonergan, S. M. (2010). High-oxygen modified atmosphere packaging system induces lipid and myoglobin oxidation

and protein polymerization. *Meat Science, 85*(4), 759-767. doi: 10.1016/j.meatsci.2010.04.001

Kim, Y. H., Hunt, M. C., Mancini, R. A., Seyfert, M., Loughin, T. M., Kropf, D. H., & Smith, J. S. (2006). Mechanism for lactate-color stabilization in injection-enhanced beef. *Journal of Agricultural and Food Chemistry, 54*(20), 7856-7862. doi: 10.1021/jf061225h

Kim, Y. H., Keeton, J. T., Smith, S. B., Berghman, L. R., & Savell, J. W. (2009). Role of lactate dehydrogenase in metmyoglobin reduction and color stability of different bovine muscles. *Meat Science, 83*(3), 376-382. doi: 10.1016/j.meatsci.2009.06.009

King, D. A., Hunt, M. C., Barbut, S., Claus, J. R., Cornforth, D. P., Joseph, P., . . . Weber, M. (2023). American Meat Science Association Guidelines for Meat Color Measurement. *Meat and Muscle Biology, 6*(4).

Kirchofer, K. S., Calkins, C. B., & Gwartney, B. L. (2002). Fiber-type composition of muscles of the beef chuck and round. *Journal of Animal Science, 80*(11), 2872-2878. doi: 10.2527/2002.80112872x

Kiyimba, F., Hartson, S. D., Rogers, J., VanOverbeke, D. L., Mafi, G. G., & Ramanathan, R. (2021). Changes in glycolytic and mitochondrial protein profiles regulates postmortem muscle acidification and oxygen consumption in dark-cutting beef. *Journal of Proteomics*, *232*, 104016. doi: 10.1016/j.jprot.2020.104016

Kleppner, S. R., and A. J. Tobin. 2002. GABA. In: V. S. Ramachandran, editor, Encyclopedia of the Human Brain. Academic Press, New York. p. 353-367.

Koizumi, C., & Brown, W. (1972). A peroxidative mechanism for the nonenzymatic reduction of metmyoglobin. *Biochimica Biophysica Acta (BBA), 264*(1), 17-24. doi: 10.1016/0304-4165(72)90112-2

Kornecki, J. F., Carballares, D., Tardioli, P. W., Rodrigues, R. C., Berenguer-Murcia, Á., Alcántara, A. R., & Fernandez-Lafuente, R. (2020). Enzyme production of d-gluconic acid and glucose oxidase: Successful tales of cascade reactions. *Catalysis science & technology, 10*(17), 5740-5771. doi: 10.1039/d0cy00819b

Krebs, H. A., & Johnson, W. A. (1980). The role of citric acid in intermediate metabolism in animal tissues. *The FEBS Letters, 117*(S1), K2-K10. doi: 10.1016/0014-5793(80)80564-3

Krzywicki, K. (1982). The determination of haem pigments in meat. *Meat Science, 7*(1), 29-36. doi: 10.1016/0309-1740(82)90095-X

Lagerstedt, A., Lundstrom, K., & Lindahl, G. (2011). Influence of vacuum or high-oxygen modified atmosphere packaging on quality of beef M. longissimus dorsi steaks after different ageing times. *Meat Science, 87*(2), 101-106. doi: 10.1016/j.meatsci.2010.08.010

Lanari, M. C., & Cassens, R. G. (1991). Mitochondrial Activity and Beef Muscle Color Stability. *Journal of Food Science, 56*(6), 1476-1479. doi: 10.1111/j.1365-2621.1991.tb08619.x

Lavieri, N., & Williams, S. K. (2014). Effects of packaging systems and fat concentrations on microbiology, sensory and physical properties of ground beef stored at 4±1°C for 25days. *Meat Science, 97*(4), 534-541. doi: 10.1016/j.meatsci.2014.02.014

Lawson, M., Denzer, M., Mafi, G., & Ramanathan, R. 2020. Novel probe-type oxygen sensor to measure oxygen consumption in beef steaks. *Meat and Muscle Biology, 5*(2): 135-136. doi: 10.22175/mmb.11683

Ledward, D. A. (1970). Metmyoglobin Formation in Beef Stored in Carbon Dioxide Enriched and Oxygen Depleted Atmospheres. *Journal of Food Science, 35*(1), 33-37. doi: 10.1111/j.1365-2621.1970.tb12362.x

Lee, B. C., & Gladyshev, V. N. (2011). The biological significance of methionine sulfoxide stereochemistry. *Free Radical Biology and Medicine, 50*(2), 221-227. doi: 10.1016/j.freeradbiomed.2010.11.008

Legako, J. F., Brooks, J. C., O'Quinn, T. G., Hagan, T. D. J., Polkinghorne, R., Farmer, L. J., & Miller, M. F. (2015). Consumer palatability scores and volatile beef flavor compounds of five USDA quality grades and four muscles. *Meat Science, 100*, 291-300. doi: 10.1016/j.meatsci.2014.10.026

Lenaz, G. (1998). Role of mitochondria in oxidative stress and ageing. *Biochimica Biophysica Acta (BBA), 1366*(1-2), 53-67. doi: 10.1016/s0005-2728(98)00120-0

Limbo, S., Torri, L., Sinelli, N., Franzetti, L., & Casiraghi, E. (2010). Evaluation and predictive modeling of shelf life of minced beef stored in high-oxygen modified atmosphere packaging at different temperatures. *Meat Science, 84*(1), 129-136. doi: 10.1016/j.meatsci.2009.08.035

Limsupavanich, R., Kropf, D., Hunt, M. C., Boyle, E., Boyle, D., & Loughin, T. (2004). Dynamics of myoglobin layer change during display of color-stable and color-labile beef muscles. Presented at the 2004 International Congress of Meat Science and Technology in Helinski, Finland. Source: www.icomst.helsinki.fi/Digicomst

Limsupavanich, R., Kropf, D., Hunt, M. C., Boyle, E., Boyle, D., & Loughin, T. (2008). Myoglobin layer depth, surface myoglobin and visual colour-life of beef Longissimus and Psoas major steaks from various postmortem times. Presented at the 2008 International Congress of Meat Science and Technology in Cape Town, South Africa. Source: www.icomst.helsinki.fi/Digicomst

Liu, C., Wei, Q., Li, X., Han, D., Liu, J., Huang, F., & Zhang, C. (2022). Proteomic analyses of mitochondrial damage in postmortem beef muscles. *Journal of the Science of Food and Agriculture, n/a*(n/a). doi: 10.1002/jsfa.11767

Liu, C., & Xiong, Y. L. (2015). Oxidation-initiated myosin subfragment cross-linking and structural instability differences between white and red muscle fiber types. *Journal of Food Science, 80*(2), C288-297. doi: 10.1111/1750-3841.12749

Liu, C., Zhang, Y., Yang, X., Liang, R., Mao, Y., Hou, X., . . . Luo, X. (2014). Potential mechanisms of carbon monoxide and high oxygen packaging in maintaining color stability of different bovine muscles. *Meat Science, 97*(2), 189-196. doi: 10.1016/j.meatsci.2014.01.027

Łopacka, J., Półtorak, A., & Wierzbicka, A. (2017). Effect of reduction of oxygen concentration in modified atmosphere packaging on bovine M. Longissimus lumborum and M. gluteus medius quality traits. *Meat Science, 124*, 1-8. doi: 10.1016/j.meatsci.2016.10.004

Lu, X., Cornforth, D. P., Carpenter, C. E., Zhu, L., & Luo, X. (2020). Effect of oxygen concentration in modified atmosphere packaging on color changes of the M. Longissimus thoraces et lumborum from dark cutting beef carcasses. *Meat Science, 161*, 107999. doi: 10.1016/j.meatsci.2019.107999

Lund, M. N., Heinonen, M., Baron, C. P., & Estévez, M. (2011). Protein oxidation in muscle foods: A review. *Molecular nutrition & food research, 55*(1), 83-95. doi: 10.1002/mnfr.201000453

Lund, M. N., Lametsch, R., Hviid, M. S., Jensen, O. N., & Skibsted, L. H. (2007). High-oxygen packaging atmosphere influences protein oxidation and tenderness of porcine longissimus dorsi during chill storage. *Meat Science, 77*(3), 295-303. doi: 10.1016/j.meatsci.2007.03.016

Lynch, M. P., & Faustman, C. (2000). Effect of aldehyde lipid oxidation products on myoglobin. *Journal of Agricultural and Food Chemistry, 48*(3), 600-604. doi: 10.1021/jf990732e

Ma, D., Kim, Y. H. B., Cooper, B., Oh, J. H., Chun, H., Choe, J. H., . . . Min, B. (2017). Metabolomics Profiling to Determine the Effect of Postmortem Aging on Color and Lipid Oxidative Stabilities of Different Bovine Muscles. *Journal of Agricultural and Food Chemistry, 65*(31), 6708-6716. doi: 10.1021/acs.jafc.7b02175

Mahoney, D. E., Hiebert, J. B., Thimmesch, A., Pierce, J. T., Vacek, J. L., Clancy, R. L., . . . Pierce, J. D. (2018). Understanding D-Ribose and Mitochondrial Function. *Advances in Bioscience and Clinical Medicine, 6*(1), 1-5. doi: 10.7575/aiac.abcmed.v.6n.1p.1

Malheiros, J. M., Braga, C. P., Grove, R. A., Ribeiro, F. A., Calkins, C. R., Adamec, J., & Chardulo, L. A. L. (2019). Influence of oxidative damage to proteins on meat tenderness using a proteomics approach. *Meat Science, 148*, 64-71. doi: 10.1016/j.meatsci.2018.08.016

Mancini, R. A., & Ramanathan, R. (2014). Effects of postmortem storage time on color and mitochondria in beef. *Meat Science, 98*(1), 65-70. doi: 10.1016/j.meatsci.2014.04.007

Mancini, R. A., Ramanathan, R., Suman, S. P., Dady, G., & Joseph, P. (2011). Effects of succinate on ground beef color and premature browning. *Meat Science, 89*(2), 189-194. doi: 10.1016/j.meatsci.2011.04.016

Mancini, R. A., Seyfert, M., & Hunt, M. C. (2008). Effects of data expression, sample location, and oxygen partial pressure on initial nitric oxide metmyoglobin formation and metmyoglobin-reducing-activity measurement in beef muscle. *Meat Science, 79*(2), 244-251. doi: 10.1016/j.meatsci.2007.09.008

Matarneh, S. K., England, E. M., Scheffler, T. L., & Gerrard, D. E. (2017). Chapter 5 - The Conversion of Muscle to Meat. In F. Toldra´ (Ed.), *Lawrie´s Meat Science (Eighth Edition)* (pp. 159-185): Woodhead Publishing.

McKenna, D. R., Mies, P. D., Baird, B. E., Pfeiffer, K. D., Ellebracht, J. W., & Savell, J. W. (2005). Biochemical and physical factors affecting discoloration characteristics of 19 bovine muscles. *Meat Science, 70*(4), 665-682. doi: 10.1016/j.meatsci.2005.02.016

Mdluli, K., Booth, M. P. S., Brady, R. L., & Rumsby, G. (2005). A preliminary account of the properties of recombinant human Glyoxylate reductase (GRHPR), LDHA and LDHB with glyoxylate, and their potential roles in its metabolism. *Biochimica et Biophysica Acta (BBA) - Proteins and Proteomics, 1753*(2), 209-216. doi: 10.1016/j.bbapap.2005.08.004

Mesquita Casagrande, A. C., Wamser, M. N., de Lima, D. D., Pereira da Cruz, J. G., Wyse, A. T., & Dal Magro, D. D. (2013). In vitro stimulation of oxidative stress by hypoxanthine in blood of rats: prevention by vitamins e plus C and allopurinol. *Nucleosides Nucleotides Nucleic Acids*, *32*(1), 42-57. doi: 10.1080/15257770.2012.760043

Mierziak, J., M. Burgberger, and W. Wojtasik. 2021. 3-Hydroxybutyrate as a Metabolite and a Signal Molecule Regulating Processes of Living Organisms. *Biomolecules*, *11*(3)doi: 10.3390/biom11030402

Mikkelsen, A., & Skibsted, L. H. (1992). Kinetics of enzymatic reduction of metmyoglobin in relation to oxygen activation in meat products. *Zeitschrift fr Lebensmittel-Untersuchung und -Forschung*, *194*(1), 9-16. doi: 10.1007/bf01191032

Mitacek, R. M., Ke, Y., Prenni, J. E., Jadeja, R., VanOverbeke, D. L., Mafi, G. G., & Ramanathan, R. (2019). Mitochondrial Degeneration, Depletion of NADH, and Oxidative Stress Decrease Color Stability of Wet-Aged Beef Longissimus Steaks. *Journal of Food Science*, *84*(1), 38-50. doi: 10.1111/1750-3841.14396

Moczkowska, M., Poltorak, A., Montowska, M., Pospiech, E., & Wierzbicka, A. (2017). The effect of the packaging system and storage time on myofibrillar protein degradation and oxidation process in relation to beef tenderness. *Meat Science*, *130*, 7-15. doi: 10.1016/j.meatsci.2017.03.008

Mohan, A., Hunt, M. C., Barstow, T. J., Houser, T. A., Bopp, C., & Hueber, D. M. (2010b). Effects of fibre orientation, myoglobin redox form, and postmortem

storage on NIR tissue oximeter measurements of beef longissimus muscle. *Meat Science, 84*(1), 79-85. doi: 10.1016/j.meatsci.2009.08.024

Mohan, A., Hunt, M. C., Barstow, T. J., Houser, T. A., & Hueber, D. M. (2010). Near-infrared oximetry of three post-rigor skeletal muscles for following myoglobin redox forms. *Food Chemistry, 123*(2), 456-464. doi: 10.1016/j.foodchem.2010.04.068

Mohan, A., Hunt, M. C., Barstow, T. J., Houser, T. A., & Muthukrishnan, S. (2010). Effects of malate, lactate, and pyruvate on myoglobin redox stability in homogenates of three bovine muscles. *Meat Science, 86*(2), 304-310. doi: 10.1016/j.meatsci.2010.04.030

Mohan, A., Muthukrishnan, S., Hunt, M. C., Barstow, T. J., & Houser, T. A. (2010a). Kinetics of myoglobin redox form stabilization by malate dehydrogenase. *Journal of Agricultural and Food Chemistry, 58*(11), 6994-7000. doi: 10.1021/jf100639n

Moreira, L. F. P. P., Ferrari, A. C., Moraes, T. B., Reis, R. A., Colnago, L. A., & Pereira, F. M. V. (2016). Prediction of beef color using time-domain nuclear magnetic resonance (TD-NMR) relaxometry data and multivariate analyses. *Magnetic resonance in chemistry, 54*(10), 800-804. doi: 10.1002/mrc.4456

Mortzfeld, F. B., Hashem, C., Vranková, K., Winkler, M., & Rudroff, F. (2020). Pyrazines: Synthesis and Industrial Application of these Valuable Flavor and Fragrance Compounds. *Biotechnology Journal, 15*(11), 2000064. doi: 10.1002/biot.202000064

Nair, M. N., Li, S., Beach, C. M., Rentfrow, G., & Suman, S. P. (2018). Changes in the Sarcoplasmic Proteome of Beef Muscles with Differential Color Stability during

Postmortem Aging. *Meat and Muscle Biology, 2*(1). doi: 10.22175/mmb2017.07.0037

Nielsen, N. C., and S. Fleischer. 1969. 3-Hydroxybutyrate Dehydrogenase: Lack in Ruminant Liver Mitochondria. *Science, 166*(3908):1017-1019. doi: doi:10.1126/science.166.3908.1017

Nerimetla, R., Krishnan, S., Mazumder, S., Mohanty, S., Mafi, G. G., VanOverbeke, D. L., & Ramanathan, R. (2017). Species-Specificity in Myoglobin Oxygenation and Reduction Potential Properties. *Meat and Muscle Biology, 1*(1). doi: 10.22175/mmb2016.10.0003

Nix Color Sensor. (2022, August 16). Nix Pro 2 Color Sensor. Retrieved September 5, 2022, from https://www.nixsensor.com/nix-pro/

Ocean Insights. Retrieved September 4, 2022, from https://www.oceaninsight.com/products/systems/sensors/neofox-gt/?qty=1

O'Keeffe, M., & Hood, D. E. (1982). Biochemical factors influencing metmyoglobin formation on beef from muscles of differing colour stability. *Meat Science, 7*(3), 209-228. doi: 10.1016/0309-1740(82)90087-0

Ouali, A., Gagaoua, M., Boudida, Y., Becila, S., Boudjellal, A., Herrera-Mendez, C. H., & Sentandreu, M. A. (2013). Biomarkers of meat tenderness: Present knowledge and perspectives in regards to our current understanding of the mechanisms involved. *Meat Science, 95*(4), 854-870. doi: 10.1016/j.meatsci.2013.05.010

Patra, T., Ghosh, P., Alam, N., & Murmu, N. (2018). Supra-physiological concentration of glyoxylate inhibits proliferation of human colon cancer cells through oxidative stress. *Life Sciences, 207*, 80-89. doi: 10.1016/j.lfs.2018.05.047

Piao, D., Borron, H., Hawxby, A., Wright, H., & Rubin, E. M. (2018). Effects of capsule on surface diffuse reflectance spectroscopy of the subcapsular parenchyma of a solid organ. *Journal of Biomedical Optics*, *23*(12), 1-23. doi: 10.1117/1.JBO.23.12.121602

Piao, D., Denzer, M., Mafi, G., & Ramanathan, R. (2022). Daily Quantification of Myoglobin Forms on Beef Longissimus Lumborum Steaks Over 7 Days of Display by Near-infrared Diffuse Reflectance Spectroscopy. *Meat and Muscle Biology*, *5*(1). doi: 10.22175/mmb.12562

Piao, D., McKeirnan, K. L., Sultana, N., Breshears, M. A., Zhang, A., & Bartels, K. E. (2014). Percutan. eous single-fiberreflectancespectroscopy of canine intervertebral disc: is there a potential for in situ probing of mineral degeneration? *Lasers in Surgery & Medicine*, *46(6)*, 508-519. doi: 10.1002/lsm.22261.

Piao, D., Sultana, N., Holyoak, G. R., Ritchey, J. W., Wall, C. R., Murray, J. K., & Bartels, K. E. (2015). In vivo assessment of diet-induced rat hepatic steatosis development by percutaneous single-fiberspectroscopy detects scattering spectral changes due to fatty infiltration. *Journal of Biomedical Optics*, *20*(11), 117002. doi: 10.1117/1.JBO.20.11.117002.

Piao, D., McKeirnan, K., Jiang, Y., Breshears, M. A., & Kenneth E. Bartels, K. E. (2012). A low-cost needle-based single-fiber reflectance spectroscopy method to probe scattering changes associated with mineralization in intervertebral discs in chondrodystrophoid canine species – A pilot study. *Photonics & Lasers in Medicine 1*, 103-115. https://doi.org/10.1515/plm-2012-0006

Ramanathan, R., Hunt, M. C., Mancini, R. A., Nair, M. N., Denzer, M. L., Suman, S. P., & Mafi, G. G. (2020c). Recent Updates in Meat Color Research: Integrating Traditional and High-Throughput Approaches. *Meat and Muscle Biology, 4*(2). doi: 10.22175/mmb.9598

Ramanathan, R., Kiyimba, F., Gonzalez, J., Mafi, G., & DeSilva, U. (2020b). Impact of Up- and Downregulation of Metabolites and Mitochondrial Content on pH and Color of the Longissimus Muscle from Normal-pH and Dark-Cutting Beef. *Journal of Agricultural and Food Chemistry, 68*(27), 7194-7203. doi: 10.1021/acs.jafc.0c01884

Ramanathan, R., Lambert, L., Nair, M., Morgan, B., Feuz, R., Mafi, G., & Pfeiffer, M. (2022a). Economic Loss, Amount of Beef Discarded, Natural Resources Wastage, and Environmental Impact Due to Beef Discoloration. *Meat and Muscle Biology, 6*(1), 1-8. doi: 10.22175/mmb.13218

Ramanathan, R., & Mancini, R. (2018). Role of Mitochondria in Beef Color: A Review. *Meat and Muscle Biology, 2*(1), 309-320. doi: 10.22175/mmb2018.05.0013

Ramanathan, R., & Mancini, R. A. (2010). Effects of pyruvate on bovine heart mitochondria-mediated metmyoglobin reduction. *Meat Science, 86*(3), 738-741. doi: 10.1016/j.meatsci.2010.06.014

Ramanathan, R., Mancini, R. A., & Dady, G. A. (2011). Effects of pyruvate, succinate, and lactate enhancement on beef longissimus raw color. *Meat Science, 88*(3), 424-428. doi: 10.1016/j.meatsci.2011.01.021

Ramanathan, R., Mancini, R. A., Joseph, P., & Suman, S. P. (2013). Bovine mitochondrial oxygen consumption effects on oxymyoglobin in the presence of

lactate as a substrate for respiration. *Meat Science, 93*(4), 893-897. doi: 10.1016/j.meatsci.2012.12.005

Ramanathan, R., Mancini, R. A., & Konda, M. K. R. (2010). Effect of Lactate Enhancement on Myoglobin Oxygenation of Beef Longissimus Steaks Overwrapped in Pvc and Stored at 4c. *Journal of Muscle Foods, 21*(4), 669-684. doi: 10.1111/j.1745-4573.2010.00212.x

Ramanathan, R., Mancini, R. A., & Konda, M. R. (2009). Effects of lactate on beef heart mitochondrial oxygen consumption and muscle darkening. *Journal of Agricultural and Food Chemistry, 57*(4), 1550-1555. doi: 10.1021/jf802933p

Ramanathan, R., Mancini, R. A., Konda, M. R., Bailey, K., More, S., & Mafi, G. G. (2022b). Evaluating the failure to bloom in dark-cutting and lactate-enhanced beef longissimus steaks. *Meat Science, 184*, 108684. doi: 10.1016/j.meatsci.2021.108684

Ramanathan, R., Mancini, R. A., & Maheswarappa, N. B. (2010). Effects of lactate on bovine heart mitochondria-mediated metmyoglobin reduction. *Journal of Agricultural and Food Chemistry, 58*(9), 5724-5729. doi: 10.1021/jf1002842

Ramanathan, R., Mancini, R. A., Suman, S. P., & Beach, C. M. (2014). Covalent binding of 4-hydroxy-2-nonenal to lactate dehydrogenase decreases NADH formation and metmyoglobin reducing ability. *Journal of Agricultural and Food Chemistry, 62*(9), 2112-2117. doi: 10.1021/jf404900y

Ramanathan, R., Mancini, R. A., Suman, S. P., & Cantino, M. E. (2012b). Effects of 4-hydroxy-2-nonenal on beef heart mitochondrial ultrastructure, oxygen

consumption, and metmyoglobin reduction. *Meat Science, 90*(3), 564-571. doi: 10.1016/j.meatsci.2011.09.017

Ramanathan, R., Mancini, R. A., Van Buiten, C. B., Suman, S. P., & Beach, C. M. (2012a). Effects of pyruvate on lipid oxidation and ground beef color. *Journal of Food Science, 77*(8), C886-892. doi: 10.1111/j.1750-3841.2012.02814.x

Ramanathan, R., Nair, M. N., Hunt, M. C., & Suman, S. P. (2019). Mitochondrial functionality and beef colour: A review of recent research. *South African Journal of Animal Science, 49*(1), 9-19. doi: 10.4314/sajas.v49i1.2

Ramanathan, R., Suman, S. P., & Faustman, C. (2020a). Biomolecular Interactions Governing Fresh Meat Color in Post-mortem Skeletal Muscle: A Review. *Journal of Agricultural and Food Chemistry, 68*(46), 12779-12787. doi: 10.1021/acs.jafc.9b08098

Ravasz, D., G. Kacso, V. Fodor, K. Horvath, V. Adam-Vizi, and C. Chinopoulos. 2017. Catabolism of GABA, succinic semialdehyde or gamma-hydroxybutyrate through the GABA shunt impair mitochondrial substrate-level phosphorylation. *Neurochemistry Intrernattional, 109,* 41-53. doi: 10.1016/j.neuint.2017.03.008

Reyes, T. M., Wagoner, M. P., Zorn, V. E., Coursen, M. M., Wilborn, B. S., Bonner, T., . . . Sawyer, J. T. (2022). Vacuum Packaging Can Extend Fresh Color Characteristics of Beef Steaks during Simulated Display Conditions. *Foods, 11*(4). doi: 10.3390/foods11040520

Richards, M. P. (2013). Redox reactions of myoglobin. *Antioxidants & redox signaling, 18*(17), 2342-2351. doi: 10.1089/ars.2012.4887

Rodrigues, A. F., Roecker, R., Junges, G. M., de Lima, D. D., da Cruz, J. G., Wyse, A. T., & Dal Magro, D. D. (2014). Hypoxanthine induces oxidative stress in kidney of rats: protective effect of vitamins E plus C and allopurinol. *Cell Biochemistry and Function, 32*(4), 387-394. doi: 10.1002/cbf.3029

Rodríguez, G., Kim, Y. H., Faget, S., Rosazza, C., & Keeton, J. T. (2011). Lactate-mediated enzymatic reduction of metmyoglobin in vitro. *Food Chemistry, 125*(2), 732-735. doi: 10.1016/j.foodchem.2010.08.069

Rojas-Morales, P., J. Pedraza-Chaverri, and E. Tapia. 2020. Ketone bodies, stress response, and redox homeostasis. *Redox Biology 29*, 101395. doi: 10.1016/j.redox.2019.101395

Rowe, L. J., Maddock, K. R., Lonergan, S. M., & Huff-Lonergan, E. (2004). Oxidative environments decrease tenderization of beef steaks through inactivation of μ-calpain1. *Journal of Animal Science, 82*(11), 3254-3266. doi: 10.2527/2004.82113254x

Ruebel, M. L., Piccolo, B. D., Mercer, K. E., Pack, L., Moutos, D., Shankar, K., & Andres, A. (2019). Obesity leads to distinct metabolomic signatures in follicular fluid of women undergoing in vitro fertilization. *American Journal of Physiology-Endocrinology and Metabolism, 316*(3), E383-E396. doi: 10.1152/ajpendo.00401.2018

Sáenz, C., Hernández, B., Alberdi, C., Alfonso, S., & Diñeiro, J. M. (2008). A multispectral imaging technique to determine concentration profiles of myoglobin derivatives during meat oxygenation. *European Food Research and Technology, 227*(5), 1329-1338. doi: 10.1007/s00217-008-0848-4

Salim, A., Suman, S. P., Canto, A., Costa-Lima, B. R. C., Viana, F. M., Monteiro, M. L. G., . . . Conte-Junior, C. A. (2019). Muscle-specific color stability in fresh beef from grain-finished Bos indicus cattle. *Asian-Australas Journal of Animal Science, 32*(7), 1036-1043. doi: 10.5713/ajas.18.0531

Sammel, L. M., Hunt, M. C., Kropf, D. H., Hachmeister, K. A., & Johnson, D. E. (2002). Comparison of Assays for Metmyoglobin Reducing Ability in Beef Inside and Outside Semimembranosus Muscle. *Journal of Food Science, 67*(3), 978-984. doi: 10.1111/j.1365-2621.2002.tb09439.x

Sanchez-Escalante, A., Djenane, D., Torrescano, G., Beltran, J. A., & Roncales, P. (2001). The effects of ascorbic acid, taurine, carnosine and rosemary powder on colour and lipid stability of beef patties packaged in modified atmosphere. *Meat Science, 58*(4), 421-429. doi: 10.1016/s0309-1740(01)00045-6

Sanchez-Escalante, A., Djenane, D., Torrescano, G., Beltran, J. A., & Roncales, P. (2003). Antioxidant Action of Borage, Rosemary, Oregano, and Ascorbic Acid in Beef Patties Packaged in Modified Atmosphere. *Journal of Food Science, 68*(1), 339-344. doi: 10.1111/j.1365-2621.2003.tb14162.x

Sastre, J., Pallardó, F. V., & Viña, J. (2003). The role of mitochondrial oxidative stress in aging. *Free Radical Biology and Medicine, 35*(1), 1-8. doi: 10.1016/s0891-5849(03)00184-9

Sawyer, J. T., Apple, J. K., Johnson, Z. B., Baublits, R. T., & Yancey, J. W. (2009). Fresh and cooked color of dark-cutting beef can be altered by post-rigor enhancement with lactic acid. *Meat Science, 83*(2), 263-270. doi: 10.1016/j.meatsci.2009.05.008

Schmitt, J. M., & Kumar, G. (1998). Optical scattering properties of soft tissue: a discrete particle model. *Applied Optics, 37*(13), 2788-2797. doi: 10.1364/ao.37.002788

Seyfert, M., Mancini, R. A., Hunt, M. C., Tang, J., & Faustman, C. (2007). Influence of carbon monoxide in package atmospheres containing oxygen on colour, reducing activity, and oxygen consumption of five bovine muscles. *Meat Science, 75*(3), 432-442. doi: 10.1016/j.meatsci.2006.08.007

Seyfert, M., Mancini, R. A., Hunt, M. C., Tang, J., Faustman, C., & Garcia, M. (2006). Color stability, reducing activity, and cytochrome c oxidase activity of five bovine muscles. *Journal of Agricultural and Food Chemistry, 54*(23), 8919-8925. doi: 10.1021/jf061657s

Shimizu, C., & Matsuura, F. (1968). Purification and Some Properties of "Methemoglobin Reductase". *Agricultural and Biological Chemistry, 32*(5), 587-592. doi: 10.1080/00021369.1968.10859100

Snyder, H. E., & Ayres, J. C. (1961). The Autoxidation of Crystallized Beef Myoglobin. *Journal of Food Science, 26*(5), 469-474. doi: 10.1111/j.1365-2621.1961.tb00391.x

Spanos, D., Tørngren, M. A., Christensen, M., & Baron, C. P. (2016). Effect of oxygen level on the oxidative stability of two different retail pork products stored using modified atmosphere packaging (MAP). *Meat Science, 113*, 162-169. doi: 10.1016/j.meatsci.2015.11.021

Subbaraj, A. K., Kim, Y. H., Fraser, K., & Farouk, M. M. (2016). A hydrophilic interaction liquid chromatography-mass spectrometry (HILIC-MS) based

metabolomics study on colour stability of ovine meat. *Meat Science, 117*, 163-172. doi: 10.1016/j.meatsci.2016.02.028

Suman, S. P., Mancini, R. A., Ramanathan, R., & Konda, M. R. (2009). Effect of lactate-enhancement, modified atmosphere packaging, and muscle source on the internal cooked colour of beef steaks. *Meat Sci, 81*(4), 664-670. doi: 10.1016/j.meatsci.2008.11.007

Sun, T., & Piao, D. (2022). Diffuse photon remission associated with the center-illuminated-area-detection geometry: Part I, an approach to the steady-state model. *Applied Optics, 61*(31), 9143-9153. doi: 10.1364/AO.468342

Sun, T., Piao, D., Yu, L., & Murari, K. (2021). Diffuse photon-remission associated with single-fiber geometry may be a simple scaling of that collected over the same area when under centered-illumination. *Optics Letters, 46*(19), 4817-4820. doi: 10.1364/OL.433233

Tang, J., Faustman, C., & Hoagland, T. A. (2006). Krzywicki Revisited: Equations for Spectrophotometric Determination of Myoglobin Redox Forms in Aqueous Meat Extracts. *Journal of Food Science, 69*(9), C717-C720. doi: 10.1111/j.1365-2621.2004.tb09922.x

Tang, J., Faustman, C., Hoagland, T. A., Mancini, R. A., Seyfert, M., & Hunt, M. C. (2005a). Postmortem oxygen consumption by mitochondria and its effects on myoglobin form and stability. *Journal of Agricultural and Food Chemistry, 53*(4), 1223-1230. doi: 10.1021/jf048646o

Tang, J., Faustman, C., Mancini, R. A., Seyfert, M., & Hunt, M. C. (2005b). Mitochondrial reduction of metmyoglobin: dependence on the electron transport

chain. *Journal of Agricultural and Food Chemistry, 53*(13), 5449-5455. doi: 10.1021/jf050092h

Tapp, W. N., Yancey, J. W. S., & Apple, J. K. (2011). How is the instrumental color of meat measured? *Meat Science, 89*(1), 1-5. doi: 10.1016/j.meatsci.2010.11.021

Taylor, A. A., & MacDougall, D. B. (1973). Fresh beef packed in mixtures of oxygen and carbon dioxide. *International Journal of Food Science & Technology, 8*(4), 453-461. doi: 10.1111/j.1365-2621.1973.tb01732.x

Tomoda, A., Tsuji, A., Matsukawa, S., Takeshita, M., & Yoneyama, Y. (1978). Mechanism of methemoglobin reduction by ascorbic acid under anaerobic conditions. *Journal of biological chemistry, 253*(20), 7240-7243.

Tsukahara, K., & Yamamoto, Y. (1983). Kinetic studies on the reduction of metmyoglobins by ascorbic acid. *Journal of Biochemistry, 93*(1), 15-22. doi: 10.1093/oxfordjournals.jbchem.a134149

Vestling, C. S. (1942). The reduction of methemoglobin by ascorbic acid. *Journal of biological chemistry., 143*(2), 439.

Wackerbarth, H., Kuhlmann, U., Tintchev, F., Heinz, V., & Hildebrandt, P. (2009). Structural changes of myoglobin in pressure-treated pork meat probed by resonance Raman spectroscopy. *Food Chemistry, 115*(4), 1194-1198. doi: 10.1016/j.foodchem.2009.01.027

Wall, K. R., Kerth, C. R., Miller, R. K., & Alvarado, C. (2019). Grilling temperature effects on tenderness, juiciness, flavor and volatile aroma compounds of aged ribeye, strip loin, and top sirloin steaks. *Meat Science, 150*, 141-148. doi: 10.1016/j.meatsci.2018.11.009

Wang, J., A. Alexanian, R. Ying, T. J. Kizhakekuttu, K. Dharmashankar, J. Vasquez-Vivar, D. D. Gutterman, and M. E. Widlansky. 2012. Acute Exposure to Low Glucose Rapidly Induces Endothelial Dysfunction and Mitochondrial Oxidative Stress. *Arteriosclerosis, Thrombosis, and Vascular Biology, 32*(3):712-720. doi: doi:10.1161/ATVBAHA.111.227389

Watanabe, A., Kamada, G., Imanari, M., Shiba, N., Yonai, M., & Muramoto, T. (2015). Effect of aging on volatile compounds in cooked beef. *Meat Science, 107*, 12-19. doi: 10.1016/j.meatsci.2015.04.004

Wei, X., Q. Yin, H. Zhao, Y. Cao, C. Cai, and J. Yao. 2018. Metabolomics for the Effect of Biotin and Nicotinamide on Transition Dairy Cows. *Journal of Agricultural and Food Chemistry 66*(22):5723-5732. doi: 10.1021/acs.jafc.8b00421

Welzenbach, J., C. Neuhoff, C. Looft, K. Schellander, E. Tholen, and C. Große-Brinkhaus. 2016. Different Statistical Approaches to Investigate Porcine Muscle Metabolome Profiles to Highlight New Biomarkers for Pork Quality Assessment. *PLoS One, 11*(2):e0149758. doi: 10.1371/journal.pone.0149758

Westlund, B., N. M. Dahms, and S. Kornfeld. 1991. The bovine mannose 6-phosphate/insulin-like growth factor II receptor. Localization of mannose 6-phosphate binding sites to domains 1-3 and 7-11 of the extracytoplasmic region. *Journal of Biological Chemistry, 266*(34):23233-23239.

Wills, K. M., Mitacek, R. M., Mafi, G. G., VanOverbeke, D. L., Jaroni, D., Jadeja, R., & Ramanathan, R. (2017). Improving the lean muscle color of dark-cutting beef by aging, antioxidant-enhancement, and modified atmospheric packaging. *Journal of Animal Science, 95*(12), 5378-5387. doi: 10.2527/jas2017.1967

Wilson, J. R., Mancini, D. M., McCully, K., Ferraro, N., Lanoce, V., & Chance, B. (1989). Noninvasive detection of skeletal muscle underperfusion with near-infrared spectroscopy in patients with heart failure. *Circulation (New York, N.Y.), 80*(6), 1668-1674. doi: 10.1161/01.CIR.80.6.1668

Wrobel, T. P., Piergies, N., Pieta, E., Kwiatek, W., Paluszkiewicz, C., Fornal, M., & Grodzicki, T. (2018). Erythrocyte heme-oxygenation status indicated as a risk factor in prehypertension by Raman spectroscopy. *Biochimica et biophysica acta. Molecular basis of disease, 1864*(11), 3659-3663. doi: 10.1016/j.bbadis.2018.07.006

Wu, S., Han, J., Liang, R., Dong, P., Zhu, L., Hopkins, D. L., . . . Luo, X. (2020a). Investigation of muscle-specific beef color stability at different ultimate pHs. *Asian-Australas Journal of Animal Science, 33*(12), 1999-2007. doi: 10.5713/ajas.19.0943

Wu, S., Luo, X., Yang, X., Hopkins, D. L., Mao, Y., & Zhang, Y. (2020b). Understanding the development of color and color stability of dark cutting beef based on mitochondrial proteomics. *Meat Science, 163,* 108046. doi: 10.1016/j.meatsci.2020.108046

Wu, W., Yu, Q.-Q., Fu, Y., Tian, X.-J., Jia, F., Li, X.-M., & Dai, R.-T. (2016). Towards muscle-specific meat color stability of Chinese Luxi yellow cattle: A proteomic insight into post-mortem storage. *Journal of Proteomics, 147,* 108-118. doi: 10.1016/j.jprot.2015.10.027

Xiong, Y., Chen, M., Warner, R. D., & Fang, Z. (2020). Incorporating nisin and grape seed extract in chitosan-gelatine edible coating and its effect on cold storage of fresh pork. *Food Control, 110,* 107018. doi: 10.1016/j.foodcont.2019.107018

Yamamoto, T., Y. Moriwaki, J. Cheng, S. Takahashi, Z. Tsutsumi, T. Ka, and T. Hada. 2002. Effect of inosine on the plasma concentration of uridine and purine bases. *Metabolism, 51*(4):438-442. doi: 10.1053/meta.2002.31322

Yan, L., B. M. Rust, and M. J. Picklo. 2020. Plasma Metabolomic Changes in Mice With Time-restricted Feeding-attenuated Spontaneous Metastasis of Lewis Lung Carcinoma. *Anticancer Research, 40*(4):1833-1841. doi: 10.21873/anticanres.14137

Yang, X., Wu, S., Hopkins, D. L., Liang, R., Zhu, L., Zhang, Y., & Luo, X. (2018). Proteomic analysis to investigate color changes of chilled beef longissimus steaks held under carbon monoxide and high oxygen packaging. *Meat Science, 142,* 23-31. doi: 10.1016/j.meatsci.2018.04.001

Yang, X., Zhang, Y., Luo, X., Zhang, Y., Zhu, L., Xu, B., . . . Liang, R. (2022). Influence of oxygen concentration on the fresh and internal cooked color of modified atmosphere packaged dark-cutting beef stored under chilled and superchilled conditions. *Meat Science, 188,* 108773. doi: 10.1016/j.meatsci.2022.108773

Yang, X., Zhang, Y., Zhu, L., Han, M., Gao, S., & Luo, X. (2016). Effect of packaging atmospheres on storage quality characteristics of heavily marbled beef longissimus steaks. *Meat Science, 117,* 50-56. doi: 10.1016/j.meatsci.2016.02.030

Yin, M. C., & Faustman, C. (2002). Influence of temperature, pH, and phospholipid composition upon the stability of myoglobin and phospholipid: A liposome

model. *Journal of Agricultural and Food Chemistry, 41*(6), 853-857. doi: 10.1021/jf00030a002

Yu, Q., Tian, X., Shao, L., Li, X., & Dai, R. (2019). Targeted metabolomics to reveal muscle-specific energy metabolism between bovine longissimus and psoas major during early postmortem periods. *Meat Science, 156*, 166-173. doi: 10.1016/j.meatsci.2019.05.029

Yu, Q., Tian, X., Shao, L., Li, X., & Dai, R. (2020). Mitochondria changes and metabolome differences of bovine longissimus and psoas major during 24 h postmortem. *Meat Science, 166*, 108112. doi: 10.1016/j.meatsci.2020.108112

Yu, Q., Tian, X., Shao, L., Xu, L., Dai, R., & Li, X. (2018). Label-free proteomic strategy to compare the proteome differences between longissimus and psoas major muscles during early postmortem periods. *Food Chemistry, 269*, 427-435. doi: 10.1016/j.foodchem.2018.07.040

Yu, Q., Wu, W., Tian, X., Jia, F., Xu, L., Dai, R., & Li, X. (2017). Comparative proteomics to reveal muscle-specific beef color stability of Holstein cattle during post-mortem storage. *Food Chemistry, 229*, 769-778. doi: 10.1016/j.foodchem.2017.03.004

Zakrys, P. I., Hogan, S. A., O'Sullivan, M. G., Allen, P., & Kerry, J. P. (2008). Effects of oxygen concentration on the sensory evaluation and quality indicators of beef muscle packed under modified atmosphere. *Meat Science, 79*(4), 648-655. doi: 10.1016/j.meatsci.2007.10.030

Zerouala, A. C., and N. C. Stickland. 1991. Cattle at risk for dark-cutting beef have a higher proportion of oxidative muscle fibres. *Meat Science, 29*(3):263-270. doi: 10.1016/0309-1740(91)90055-U

Zhai, C., Djimsa, B. A., Prenni, J. E., Woerner, D. R., Belk, K. E., & Nair, M. N. (2020). Tandem mass tag labeling to characterize muscle-specific proteome changes in beef during early postmortem period. *Journal of Proteomics, 222*, 103794. doi: 10.1016/j.jprot.2020.103794

Zhai, C., Peckham, K., Belk, K. E., Ramanathan, R., & Nair, M. N. (2019a). Carbon Chain Length of Lipid Oxidation Products Influence Lactate Dehydrogenase and NADH-Dependent Metmyoglobin Reductase Activity. *Journal of Agricultural and Food Chemistry, 67*(48), 13327-13332. doi: 10.1021/acs.jafc.9b05634

Zhai, C., Suman, S. P., Nair, M. N., Li, S., Luo, X., Beach, C. M., . . . Shike, D. W. (2019b). Supranutritional supplementation of vitamin E influences mitochondrial proteome profile of post-mortem longissimus lumborum from feedlot heifers. *South African Journal of Animal Science, 48*(6), 1140-1147. doi: 10.4314/sajas.v48i6.18

Zhang, F., Nan, X., Wang, H., Zhao, Y., Guo, Y., & Xiong, B. (2020a). Effects of Propylene Glycol on Negative Energy Balance of Postpartum Dairy Cows. *Animals (Basel), 10*(9). doi: 10.3390/ani10091526

Zhang, Y., S. Guo, C. Xie, and J. Fang. (2020b). Uridine Metabolism and Its Role in Glucose, Lipid, and Amino Acid Homeostasis. *Biomed Research International,* 2020:7091718. doi: 10.1155/2020/7091718

Zhu, J., Liu, F., Li, X., & Dai, R. (2009). Effect of succinate sodium on the metmyoglobin reduction and color stability of beef patties. *Journal of Agricultural and Food Chemistry, 57*(13), 5976-5981. doi: 10.1021/jf900958p

APPENDICES

APPENDIX – CHAPTER III

Appendix: Examples of spectral fitting for the estimation of myoglobin composition are given in Figure A1. Each of the three spectral profiles acquired by the needle-probe SfR spectroscopy (marked by blue line) is overlapped with fitted spectrum (red dot). The (A) corresponds to a sample presenting more oxygyMb, the (B) corresponds to a sample presenting more depxyMb, and the (C) corresponds to a sample presenting more MetMb.

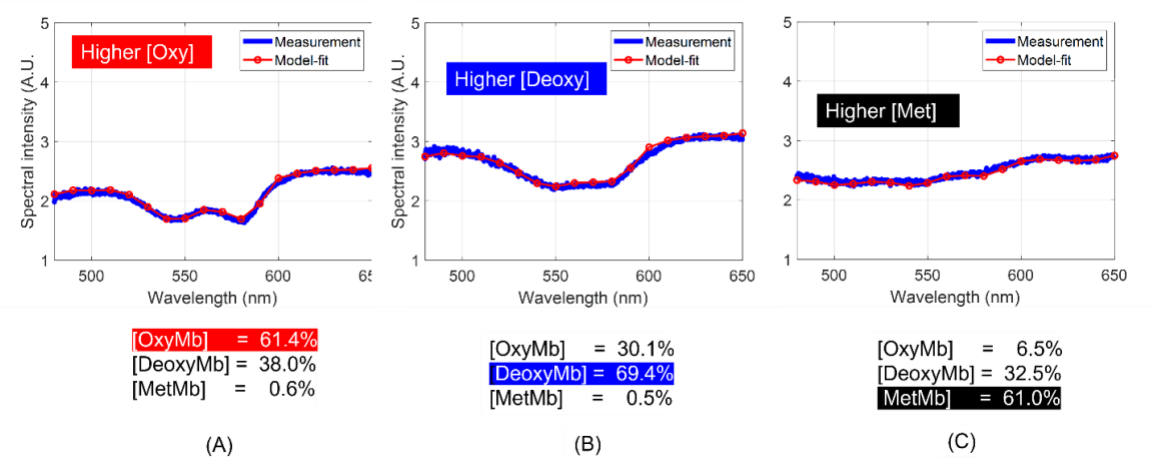

Figure A3.1. Representative results of the model fitting to the spectral profile obtained by the needle-probe SfR. (A). The SfR profile indicated a higher oxymyoglobin composition of the muscle. The fitted spectral profile corresponded to fitting resulted in [OxtMb] of 61.4%, [DeoxyMb] of 38.0% and [MetMb] of 0.6%. (B). The SfR profile indicated a higher deoxymyoglobin composition of the muscle. The fitted spectral profile corresponded to fitting resulted in [OxtMb] of 30.1%, [DeoxyMb] of 69.4% and [MetMb] of 0.5%. (C). The SfR profile indicated a higher metmyoglobin composition of the muscle. The fitted spectral spectral profile corresponded to fitting resulted in [OxtMb] of 6.5%, [DeoxyMb] of 32.5% and [MetMb] of 61.0%.

APPENDIX – CHAPTER V

Table A5.1. Metabolites differentially abundant in non-oxygen exposed (NOE) and oxygen exposed (OE) surfaces[1] of the *longissimus lumborum* during d 0 and 6 of display

Functional role	Metabolite	FDR	P-value	NOE		OE		Day 6	
				Day 0	Day 6	Day 0	Day 6	NOE	OE
Pentose and glucuronate interconversions	xylulose	0.01	0	Down	Up	Down	Up	NS	
	xylitol	0.04	0.001	Down	Up	NS		Up	Down
Pentose phosphate pathway	gluconic acid	0.04	0.001	Down	Up	Down	Up	Down	Up
Fatty acid metabolism	stearic acid	0.05	0.003	Up	Down	Up	Down	NS	
	saccharic acid	0.1	0.012	Up	Down	Up	Down	NS	
	arachidic acid	0.16	0.03	Up	Down	Up	Down	Up	Down
	hexadecylglycerol	0.1	0.013	Up	Down	Up	Down	NS	
	1-monopalmitin	0.09	0.007	Up	Down	Up	Down	NS	
	glycerol	0.07	0.004	Up	Down	Up	Down	NS	
TCA cycle	citric acid	0.04	0.001	Down	Up	Down	Up	Down	Up
	aconitic acid	0.09	0.007	Down	Up	Down	Up	NS	
	succinic acid	0.15	0.027	Up	Down	Up	Down	NS	
Amino acid metabolism	benzoic acid	0.05	0.002	Up	Down	Up	Down	NS	
	methionine sulfoxide	0.15	0.025	Down	Up	Down	Up	NS	
	serine	0.15	0.027	Down	Up	Down	Up	NS	
	tyrosine	0.16	0.034	Down	Up	Down	Up	NS	
Sugar metabolism	ribose	0.13	0.018	Down	Up	Down	Up	NS	
	ribonic acid	0.14	0.022	Down	Up	Down	Up	Down	Up
Ascorbate metabolism	isothreonic acid	0.05	0.003	Down	Up	Down	Up	Up	Down
Steroid hormone biosynthesis	cholesterol	0.05	0.003	Up	Down	Up	Down	NS	
Oxidative phosphorylation	creatinine	0.07	0.005	Up	Down	Up	Down	Up	Down
Purine metabolism	hypoxanthine	0.09	0.008	Down	Up	Down	Up	NS	

Pyrazine metabolism	2,5-dihydroxypyrazine	0.09	0.009	Up	Down	Up	Down	Up	Down
Collagen metabolism	glycylproline	0.1	0.01	Down	Up	Down	Up	NS	
Antioxidant	alpha-tocopherol	0.1	0.012	NS		Up	Down	Up	Down
Neurotransmitter	4-hydroxybutyric acid	0.1	0.012	NS		Up	Down	Up	Down
Propionate metabolism	Propylene glycol	0.14	0.021	Up	Down	Up	Down	Up	Down
Glyoxylate and dicarboxylate metabolism	glycolic acid	0.16	0.033	NS		Up	Down	Up	Down
	adipic acid	0.16	0.03	Up	Down	Up	Down	NS	
	terephthalic acid	0.2	0.043	Up	Down	Up	Down	Up	Down
	2-hydroxyvaleric acid	0.2	0.044	Up	Down	Up	Down	NS	

[1]Exposure of muscle to oxygen as display surface indicated as oxygen exposed (OE) or interior of the muscle as non-oxygen exposed (NOE).

APPENDIX – CHAPTER VII

Table A7.1. Differentially abundant metabolites of the *psoas major* muscle during retail display

Functional role	Metabolite	FDR	P-value	NOE		OE		Day 6	
				Day 0	Day 6	Day 0	Day 6	NOE	OE
Purine metabolism	hypoxanthine	0.0002	0.0000	Down	Up	Down	Up	NS	
	adenosine-5-monophosphate	0.08	0.01	Up	Down	Up	Down	NS	
TCA cycle	fumaric acid	0.06	0.002	Up	Down	Up	Down	Up	Down
	succinic acid	0.08	0.004	Up	Down	Up	Down	NS	
	mannose-6-phosphate	0.08	0.01	Up	Down	Up	Down	Up	Down
	citric acid	0.19	0.04	Down	Up	Down	Up	NS	
Pentose phosphate pathway	gluconic acid	0.004	0.0001	Down	Up	Down	Up	NS	
	gluconic acid lactone	0.08	0.01	Down	Up	Down	Up	NS	
	sedoheptulose 7-phosphate	0.08	0.01	Down	Up	Down	Up	NS	
	ribulose-5-phosphate	0.13	0.02	Up	Down	Up	Down	NS	
	ribose	0.17	0.03	Down	Up	Down	Up	Up	Down
Amino acid metabolism	urea	0.06	0.002	Up	Down	Up	Down	NS	
	creatinine	0.07	0.003	Up	Down	Up	Down	NS	
	citrulline	0.10	0.01	Down	Up	Down	Up	NS	
	2-hydroxyvaleric acid	0.13	0.02	Up	Down	Up	Down	NS	
	ornithine	0.14	0.02	Down	Up	Down	Up	NS	
	serotonin	0.16	0.03	Down	Up	Down	Up	NS	
Sugar metabolism	ribonic acid	0.06	0.001	Down	Up	Down	Up	NS	
	xylulose	0.10	0.01	Down	Up	Down	Up	NS	
	xylose	0.24	0.05	Down	Up	Down	Up	NS	
Fatty acid metabolism	3-hydroxybutyric acid	0.10	0.01	Up	Down	Up	Down	Down	Up
	myo-inositol	0.17	0.03	Up	Down	Up	Down	NS	
Pyrazine metabolism	2,5-dihydroxypyrazine	0.06	0.003	Up	Down	Up	Down	NS	
Steroid biosynthesis	cholesterol	0.08	0.01	Up	Down	Up	Down	NS	

Oxidative phosphorylation	pyrophosphate	0.08	0.01	Up	Down	Up	Down	NS	
Pyruvate metabolism	lactamide	0.17	0.03	Up	Down	Up	Down	Down	Up
Glycolysis	Glucose	0.17	0.03	Up	Down	Up	Down	Up	Down

Table A7.2. Differentially abundant metabolites of the *semitendinosus* muscle during retail display

Functional role	Metabolite	FDR	P-value	NOE		OE		Day 6	
				Day 0	Day 6	Day 0	Day 6	NOE	OE
TCA cycle	succinic acid	0.02	0.0001	Up	Down	Up	Down	Up	Down
	citric acid	0.02	0.0002	Down	Up	Down	Up	Down	Up
	aconitic acid	0.07	0.002	Down	Up	Down	Up	Down	Up
	fumaric acid	0.18	0.01	Up	Down	Up	Down	Up	Down
Pentose phosphate pathway	glyceric acid	0.07	0.002	Down	Up	Down	Up	NS	
	ribose	0.11	0.005	Down	Up	Down	Up	Up	Down
	gluconic acid	0.32	0.05	Down	Up	Down	Up	Up	Down
Fatty acid metabolism	3-hydroxybutyric acid	0.11	0.01	Up	Down	Up	Down	Up	Down
	ethanolamine	0.22	0.02	Up	Down	Up	Down	Down	Up
	arachidonic acid	0.32	0.04	Up	Down	Up	Down	NS	
	1-monostearin	0.32	0.04	Up	Down	NS	Down	Down	Up
	glycerol-alpha-phosphate	0.32	0.05	Up	Down	Up	Down	NS	
Amino acid metabolism	glycyl-proline	0.11	0.01	Down	Up	Down	Up	NS	
	methionine sulfoxide	0.24	0.02	Down	Up	Down	Up	Up	Down
	indole-3-lactate	0.32	0.04	Up	Down	Up	Down	NS	
Sugar metabolism	xylulose	0.24	0.02	Down	Up	Down	Up	Up	Down
	maltose	0.32	0.04	NS	Down	Up	Down	Down	Up
	N-acetylmannosamine	0.32	0.05	Down	Up	Down	Up	NS	
Pyrazine metabolism	2,5-dihydroxypyrazine	0.04	0.0009	Up	Down	Up	Down	Up	Down
Glycolysis	hexadecylglycerol	0.24	0.02	Up	Down	Up	Down	NS	
BACTERIA	adipic acid	0.32	0.03	Down	Up	Down	Up	Down	Up

Table A7.3. Differentially abundant metabolites among the *longissimus lumborum*, *semitendinosus*, and *psoas major* muscles for the non-oxygen exposed surface on day 6 of display

Functional role	Metabolite	FDR	P-value	Muscles		
				Longissimus lumborum	*Psoas major*	*Semitendinosus*
Purine metabolism	inosine 5-monophosphate	0.01	0.0001	High	Low	Intermediate
	inosine	0.07	0.003	High	Low	High
	guanosine	0.16	0.01	High	Low	High
	hypoxanthine	0.20	0.04	Low	High	Low
Fatty acid metabolism	1-monopalmitin	0.04	0.001	Low	High	Intermediate
	oleic acid	0.20	0.04	Low	High	High
	heptadecanoic acid	0.20	0.04	Low	High	Low
Sugar metabolism	ribonic acid	0.07	0.003	Low	High	Low
	xylitol	0.10	0.01	High	Low	High
	ribose	0.16	0.01	Low	Low	High
	galactose-6-phosphate	0.18	0.02	High	Low	High
	fructose-6-phosphate	0.18	0.02	Intermediate	Low	High
	fructose	0.19	0.02	Intermediate	Low	High
Amino acid metabolism	glycyl-glycine	0.16	0.01	High	Low	Intermediate
	5-aminovaleric acid	0.18	0.02	High	Low	Low
	creatinine	0.20	0.03	High	Low	High
	glyceric acid	0.20	0.04	High	Low	High
TCA Cycle	succinic acid	0.18	0.02	High	Low	High
	fumaric acid	0.18	0.02	High	Low	High
Glycolysis	gluconic acid	0.07	0.003	Intermediate	High	Low
	hexadecylglycerol	0.21	0.046	Low	High	Low
	glucose	0.21	0.046	Intermediate	Low	High

Pentose phosphate pathway	ribose-5-phosphate	0.19	0.03	High	Intermediate	Low
	ribulose-5-phosphate	0.21	0.04	Intermediate	Low	High
Ascorbate metabolism	isothreonic acid	0.08	0.004	High	Low	High
	threonic acid	0.20	0.04	High	Low	High
Neurotransmitter	4-hydroxybutyric acid	0.07	0.003	High	Low	Intermediate
Pyrazine metabolism	2,5-dihydroxypyrazine	0.19	0.02	High	Low	High
Pyrimidine Metabolism	uridine	0.20	0.03	High	Low	High
Nicotinate and nicotinamide metabolism	nicotinamide	0.21	0.049	High	Low	Intermediate

Table A7.4. Differentially abundant metabolites among the *longissimus lumborum*, *semitendinosus*, and *psoas major* muscles for the oxygen exposed surface on day 6 of display

Functional role	Metabolite	FDR	P-value	Muscles		
				Longissimus lumborum	*Psoas major*	*Semitendinosus*
Pentose phosphate pathway	gluconic acid	0.01	0.0001	Intermediate	High	Low
	ribose-5-phosphate	0.07	0.002	Low	High	Intermediate
	ribose	0.18	0.02	Low	Low	High
	phosphate	0.22	0.04	Low	Intermediate	High
Sugar metabolism	mannose-6-phosphate	0.07	0.002	High	Low	High
	ribonic acid	0.09	0.004	Intermediate	High	Low
	xylonolactone	0.22	0.03	Low	Low	High
	3,6-anhydro-D-galactose	0.22	0.04	Low	Low	High
	lactose	0.23	0.047	Low	Low	High
Purine metabolism	inosine 5-monophosphate	0.01	0.0002	High	Low	Low
	hypoxanthine	0.07	0.002	Low	High	Intermediate
	guanosine	0.14	0.01	High	Low	Intermediate
Amino acid metabolism	urea	0.14	0.01	Intermediate	Low	High
	methionine	0.18	0.02	High	High	Low
	lysine	0.22	0.03	High	Low	Low
	4-aminobutyric acid	0.23	0.04	High	Low	High
	isoleucine	0.23	0.047	High	Low	Low
	phenylalanine	0.23	0.050	High	Low	Low
Fatty acid metabolism	squalene	0.14	0.01	Low	High	Low
	behenic acid	0.16	0.01	Low	High	High
	1-monopalmitin	0.22	0.03	Low	High	Intermediate
	2-monoolein	0.23	0.04	Low	High	Low

Glycolysis	hexadecylglycerol	0.18	0.02	Low	High	Low
	glucose	0.22	0.03	Intermediate	Low	High
	glucose-6-phosphate	0.23	0.04	High	Low	High
Pyrazine metabolism	2,5-dihydroxypyrazine	0.16	0.01	High	Low	High
TCA Cycle	fumaric acid	0.22	0.03	High	Low	High
Pyrimidine metabolism	uridine	0.23	0.045	Low	Low	High

VITA

Morgan Denzer

Candidate for the Degree of

Doctor of Philosophy

Dissertation: CHARACTERIZING THE ROLE OF OXYGEN IN BEEF DISCOLORATION

Major Field: Food Science

Biographical:

Education:

Completed the requirements for the Doctor of Philosophy in Food Science at Oklahoma State University, Stillwater, Oklahoma in May 2023.

Completed the requirements for the Master of Science in Food Science at Oklahoma State University, Stillwater, Oklahoma in 2020.

Completed the requirements for the Bachelor of Science in Food Science at Iowa State University, Ames, IA in 2018.

Experience:

Oklahoma Section IFT Student Representative 2021-2023, OSU Graduate Teaching Assistant 2018-2023, OSU Meat Quiz Bowl Coach 2019-2021, Kemin Industries Research and Development Intern 2018

Professional Memberships:

American Society of Animal Science, American Meat Science Association, Institute of Food Technologists